CHEMOMETRIC APPROACHES IN THE EVALUATION OF TRACE METALS IN COMMERCIALLY RAISED TILAPIA AND PRELIMINARY HEALTH RISK ASSESSMENT OF ITS CONSUMPTION

LOW KAH HIN

FACULTY OF SCIENCE
UNIVERSITY OF MALAYA
KUALA LUMPUR

2012

CHEMOMETRIC APPROACHES IN THE EVALUATION OF TRACE METALS IN COMMERCIALLY RAISED TILAPIA AND PRELIMINARY HEALTH RISK ASSESSMENT OF ITS CONSUMPTION

LOW KAH HIN

THESIS SUBMITTED IN FULFILMENT OF
THE REQUIREMENT FOR THE DEGREE
OF DOCTOR OF PHILOSOPHY

DEPARTMENT OF CHEMISTRY
FACULTY OF SCIENCE
UNIVERSITY OF MALAYA
KUALA LUMPUR

2012

UNIVERSITI MALAYA

ORIGINAL LITERARY WORK DECLARATION

Name of Candidate: **LOW KAH HIN** (I.C/Passport No: **790914-07-5447**)

Registration/Matric No: **SHC 070034**

Name of Degree: **DOCTOR OF PHILOSOPHY**

Title of Project Paper/Research Report/Dissertation/Thesis ("this Work"):

CHEMOMETRIC APPROACHES IN THE EVALUATION OF TRACE METALS IN COMMERCIALLY RAISED TILAPIA AND PRELIMINARY HEALTH RISK ASSESSMENT OF ITS CONSUMPTION

Field of Study: **ANALYTICAL CHEMISTRY & CHEMOMETRIC**

I do solemnly and sincerely declare that:

(1) I am the sole author/writer of this Work;
(2) This Works is original;
(3) Any use of any work in which copyright exists was done by way of fair dealing and for permitted purposes and any except or extract from, or reference to or reproduction of any copyright work has been disclosed expressly and sufficiently and the title of the Work and its authorship have been acknowledged in this Work;
(4) I do not have any actual knowledge nor do I ought reasonably to know that the making of this work constitutes an infringement of any copyright work;
(5) I hereby assign all and every rights in the copyright to this Work to the University of Malaya ("UM"), who henceforth shall be owner of the copyright in this Work and that any reproduction or use in any form or by any means whatsoever is prohibited without the written consent of UM having been first had and obtained;
(6) I am fully aware that if in the course of making this Work I have infringed any copyright whether intentionally or otherwise, I may be subject to legal action or any other action as may be determined by UM.

Candidate's Signature Date: **23 JULY 2012**

Subscribed and solemnly declared before,

Witness's Signature Date:

Name: **PROF. DR. SHARIFUDDIN MD. ZAIN**
Designation: **PROFESSOR**
DEPARTMENT OF CHEMISTRY
UNIVERSITY OF MALAYA
50603 KUALA LUMPUR, MALAYSIA

ABSTRACT

The aims of this study are to evaluate the presence of trace metals in aquacultural samples using chemometric methods and to assess the safety of their consumption. In this work, chemometric techniques have been utilized to improve the analysis of metal content in commercially raised tilapia. In the method development phase, multivariate calibration techniques involving principal component regression and partial least squares were employed to establish a simple spectrophotometric method for the simultaneous determination of Cu^{2+}, Ni^{2+} and Zn^{2+} in water samples in the presence of 1-(2-thiazolylazo)-2-naphthol as chromogenic reagent. In general, no significant difference in analytical performance was observed between the models as both exhibit high reliability. Unfortunately, the proposed alternative did not work well with other sample matrices. Consequently, the use of microwave accelerated reaction system with appropriate reagent mixture for quantitative matrix decomposition and its effective combination with certain determination techniques were then investigated by experimental design. In the preliminary study, fractional factorial design was utilized to evaluate the main effects of addition of HNO_3, H_2O_2, HCl and H_2O in microwave assisted digestion of fish muscle certified reference material. Significant losses of analytes via the vessel pressure regulating mechanism were observed, particularly for Hg under the designed condition. In this regard, digestion using a lesser amount sample and reagent was put forward for investigation with two-stage experimental designs. Initially, a Plackett-Burman design was carried out to estimate the main effects of the added reagents and the influence of microwave settings. The most significant microwave parameters were further evaluated by Box–Behnken design, while others were kept constant. The influence of different parameters vary according to the metal element, thus the working conditions for their simultaneous determination were

established as a compromise within the optimum region found for each targeted element. Good agreement was observed between measured and certified values. In the assessment phase, the optimized microwave assisted digestion-inductively coupled plasma-mass spectrometry procedure was successfully applied for the determination of trace metal content in muscle, liver and gill tissues of red tilapia (*Oreochromis spp*) sampled from three different aquaculture sites in Jelebu, Negeri Sembilan. With the aid of pattern recognition techniques such as principal component analysis and its varimax rotation, it is not only possible to visualize the distribution pattern of metals in different organs as well as clustering tendencies of tilapia samples according to production sites but also to identify their corresponding relationships. For safety evaluation, the metal concentrations in the edible muscles were compared with the established legal limits and reasonable maximum exposures were simulated using the Monte Carlo algorithm.

ABSTRAK

Tujuan kajian ini adalah untuk melanjutkan penggunaan kaedah kimometrik dalam analisis logam-logam surih dalam sampel akuakutur dan menilaikan tahap keselamatan pengambilan sampel tersebut. Dalam fasa pembangunan kaedah, teknik penentukuran multivariat yang melibatkan regresi komponen utama dan kaedah separa kuasa dua terkercil telah diusahakan untuk membina satu model spektrofotometrik yang ringkas bagi penentuan serentak Cu^{2+}, Ni^{2+} dan Zn^{2+} dalam sampel air dengan kehadiran of 1-(2-tiazolilazo)-2-naftol sebagai kromogen. Secara umumnya, tiada perbezaan yang ketara dilihat dalam prestasi analisis antara model tersebut, kedua-duanya memamerkan kebolehpercayaan yang tinggi. Namun, alternatif yang dicadangkan ini tidak sesuai dengan matriks selain daripada air. Oleh itu, penggunaan sistem gelombang-mikro bersama campuran reagen yang sesuai bagi penguraian matriks secara kuantitatif dan kesannya dikaji dengan teknik rekabentuk eksperimen. Dalam kajian awal, rekabentuk faktorial pecahan digunakan untuk menyaisat kesan-kesan utama penambahan HNO_3, H_2O_2, HCl dan H_2O dalam pencernaan tisu ikan rujukan di bawah gelombang-mikro. Didapati bahawa kehilangan analit yang ketara, terutamanya Hg, berlaku melalui mekanisme pengawalan tekanan di bawah keadaan yang direkabentukan. Dalam hal ini, pencernaan yang melibatkan jumlah sampel dan reagen yang lebih kecil telah dikemukakan untuk siasatan secara rekabentuk eksperimen dua-peringkat. Di peringkat awal, rekabentuk Plackett-Burman digunakan untuk menganggar kesan utama penambahan reagen dan pengaruh parameter kawalan sistem gelombang-mikro. Parameter kawalan sistem gelombang-mikro yang paling ketara dievaluasi di peringkat selanjutnya dengan rekabentuk Box-Behnken, manakala yang lain dikekalkan. Didapati bahawa kesannya adalah bergantung kepada jenis unsur. Dengan itu proses optimasi dalam penentuan sesrentak menjadi isu kompromi antara setiap unsur sasaran. Persetujuan yang baik antara nilai-nilai yang diukur dan yang disahkan telah diperhati.

ABSTRAK

Dalam fasa penilaian, kaedah percernaan gelombang-mikro digabungkan bersama spektrometer massa-plasma gandeng induktif yang dioptimalkan telah diaplikasi dalam penentuan serentak kandungan logam-logam surih dalam sampel tisu otot, hati dan insang ikan tilapia merah (*Oreochromis spp*) dari tiga tapak akuakultur di Jelebu , Negeri Sembilan. Dengan bantuan teknik pengecaman corak seperti analisis komponen utama dan putaran varimax, gambaran corak taburan logam-logam dalam organ yang berlainan dapat diperolehi. Pengelompokan sampel tilapia berdasarkan tapak pengeluaran dan hubungan sepadan antara mereka juga dapat dilihat. Untuk menilai tahap keselamatan konsumi, kepekatan logam pada otot-otot yang boleh dimakan dibandingkan dengan had-had yang dibenarkan dan pendedahan maksimum yang munasabah juga disimulasi dengan algoritma Monte Carlo.

ACKNOWLEDGEMENTS

This thesis marks the culmination of a series of rather extraordinary trails and tribulation in my life. Therefore, it would not be complete without acknowledging my appreciation to all those whom have helped me grow academically, professionally and personally.

Foremost, I would like to express my deep and sincere gratitude to Prof. Dr. Sharifuddin Md. Zain for being an outstanding supervisor. His constant encouragement, unwavering support and stimulating suggestions have paved the way for the present thesis. His continuous guidance helped me a lot throughout the research and writing, particular in editing and improving the manuscripts as well as the drafts of this thesis enthusiastically.

I also wish to express my warm and sincere thanks to Prof. Dr. Mhd. Radzi Abas for being an excellent professor. His wide knowledge and experiences have been of great value for me. His constructive and enlightening advice on the analytical section have provided a good basis for the present thesis.

My sincere appreciation goes to Prof. Dr. Mustafa Ali Mohd., Prof. Dr. Tan Guan Huat, Prof. Dr. Misni Misran, Assoc. Prof. Dr. Lo Kong Mun and Assoc. Prof. Dr. Nor Kartini Abu Bakar for their insightful comments, inspired discussion and lending hand in instrumental analysis.

I wish to acknowledge the driver Mr. Din Mat Nor and Mr. Kaharudin Md. Salleh together with his colleagues from Freshwater Fisheries Research Division, Fisheries Research Institute, Glami Lemi for their guidance and assistance during the sampling in Jelebu. I am also grateful to Mr. Saharudin Zainal and Ms. Siti Jariani Mohd. Jani for being helpful in ICP-MS analysis.

I also owe my sincere thanks to fellow lab-mates in Environmental Research Laboratory particularly Tay Kheng Soo, Mohd. Firdaus Kamaruddin, Nur Aaainaa Syafini Mohd. Radzi, Mohd. Shahrul Mohd. Nazir and Keivan Nemati for simulating discussion, sharing experiences/knowledge and assistance in running the experiments.

Finally yet important, an endless gratitude goes to my family especially my wife Teo Yin Yin for having faith in me and being there in moments of need. To those whom I may have inadvertently left out, I wish to express my sincere and honest gratitude.

Lastly, I am deeply indebted not only to my scholarship sponsors University Malaya and Ministry of Higher Education Malaysia but also Ministry of Science, Technology and Innovation, Malaysia (ScienceFund 16-02-03-6020) and University Malaya (FS313-2008C and PS143-2007B) for their financial support and funding of this study.

TABLE OF CONTENTS

	Page
ABSTRACT	**ii**
ACKNOWLEDGEMENTS	**vi**
TABLE OF CONTENTS	**viii**
LIST OF FIGURES	**xv**
LIST OF TABLES	**xix**
LIST OF SYMBOLS AND ABBREVIATIONS	**xxi**
LIST OF PUBLICATIONS	**xxvi**
1 INTRODUCTION	**1**
1.1 Background of Target Species	1
1.2 Risk Assessment	3
1.2.1 Human Health Risk Assessment Methodology	4
1.2.1.1 Hazard Identification	5
1.2.1.2 Exposure Assessment and Analysis	5
1.2.1.3 Toxicity Assessment	6
1.2.1.4 Human Health Risk Characterization	7
1.2.2 Deterministic and Probabilistic Assessments	7
1.3 Target Analytes	9
1.4 Analytical Techniques and Methodology	11
1.4.1 Sample Preparation	11
1.4.2 Elemental Analysis Techniques	12

				Page
1.5			**Chemometrics**	13
	1.5.1		***Experimental Design***	13
		1.5.1.1	*Full Factorial Designs*	15
		1.5.1.2	*Fractional Factorial Designs*	16
		1.5.1.3	*Plackett-Burman Designs*	17
		1.5.1.4	*Box–Behnken Designs*	18
	1.5.2		***Pattern Recognition***	19
		1.5.2.1	*Exploratory Data Analysis*	20
		1.5.2.2	*Discrimination and Classification*	21
		1.5.2.3	*Multivariate Regression and Prediction*	22
1.6			**Objectives of Research**	23
1.7			**The Conceptual Framework**	24
2			**LITERATURE REVIEW**	**25**
2.1			**Profile Summaries for Hazardous Metals**	25
	2.1.1		***Arsenic***	27
	2.1.2		***Cadmium***	30
	2.1.3		***Lead***	32
	2.1.4		***Mercury***	34
	2.1.5		***Selenium***	36
	2.1.6		***Other Metals***	38
2.2			**Analytical Options for Metal Analysis**	
	2.2.1		***Flame Atomic Absorption Spectrometry***	39
	2.2.2		***Inductively Coupled Plasma-Mass Spectrometry***	43

			Page
2.2.3		***UV-Visible Spectrophotometric***	48
2.3		**Application of Chemometric Tools**	50
2.3.1		***Multivariate Calibrations in Spectrophotometric Metal Analysis***	50
	2.3.1.1	*Principal Component Regression*	51
	2.3.1.2	*Partial Least Squares*	52
2.3.2		***Experimental Designs in Microwave Assisted Sample Preparation***	53
2.3.3		***Pattern Recognition on Multielemental Dataset***	54
3		**SPECTROPHOTOMETRIC DETERMINATION OF METAL IONS USING MULTIVARIATE CALIBRATIONS**	**56**
3.1		**Introduction**	56
3.1.1		***Background of Thiazolylazo Dye***	56
3.1.2		***Multivariate Calibrations***	58
3.2		**Materials and Methods**	60
3.2.1		***Instrumentation***	60
3.2.2		***Reagents and Standard Materials***	60
	3.2.2.1	*Ammonium Acetate Stock Solution*	60
	3.2.2.2	*TAN Stock Solution*	60
	3.2.2.3	*Triton X-100 Stock Solution*	61
	3.2.2.4	*Calibration and Validation Standard Solutions*	61
3.2.3		***Cleaning***	62
3.2.4		***Calibration and Validation Set Design***	62

3.3		**Results and Discussion**	64
	3.3.1	***PLS and PCR***	65
	3.3.2	***Analytical Figures of Merit***	74
	3.3.3	***Application on Spiked Samples***	77
	3.3.4	***Influence of pH***	80
	3.3.5	***Influence of Ammonium Acetate***	80
	3.3.6	***Influence of Surfactants***	80
	3.3.7	***Influence of Foreign Ions***	81
	3.3.8	***Stability of Samples***	82
4	**PRELIMINARY EVALUATION OF REAGENT EFFECT ON FISH METAL RECOVERIES BY MAD-FAAS**		**83**
4.1		**Introduction**	83
	4.1.1	***Background of Sample Preparation***	83
	4.1.2	***Closed-Vessel Microwave Assisted Digestion***	84
4.2		**Materials and Methods**	87
	4.2.1	***Instrumentation***	87
	4.2.1.1	*Flame Atomic Absorption Spectrometer*	87
	4.2.1.2	*Cold Vapour Atomic Absorption Spectrometer*	87
	4.2.1.3	*Microwave Accelerated Reaction System*	88
	4.2.2	***Reagents and Standard Materials***	90
	4.2.3	***Experimental Design***	90
4.3		**Results and Discussion**	92
	4.3.1	***Analysis of Effects***	94

Page

4.3.1.1 Main Effect of HNO_3 95

4.3.1.2 Main Effects of Addition of Other Reagents 97

4.3.2 Models Check 97

5 OPTIMIZATION OF MAD CONDITION FOR TRACE METAL ANALYSIS BY ICP-MS **101**

5.1 Introduction 101

5.1.1 Microwave Settings and Conditions 102

5.1.2 Evaluation of MAD Performance 103

5.1.2.1 Two-Stage Experimental Design 103

5.1.2.2 Optimization of Multiple Elements 104

5.2 Materials and Methods 105

5.2.1 Instrumentation 105

5.2.1.1 ICP-MS 105

5.2.2.2 Microwave Assisted Digestion 105

5.2.2 Reagent and Standard Materials 106

5.2.2.1 Acids and Reagents 106

5.2.2.2 Calibration Standards 106

5.2.2.3 Internal Standards 106

5.2.2.4 Gaseous 107

5.2.2.5 Certified Reference Materials 107

5.2.3 Experimental 107

5.2.3.1 Cleaning 107

5.2.3.2 Experimental Design 108

			Page
5.3		**Results and Discussion**	109
	5.3.1	***ICP-MS Tuning***	109
	5.3.2	***Sample size in MAD***	114
	5.3.3	***2-level Plackett-Burman design***	115
	5.3.3.1	*Evaluation of Digestion Completeness*	117
	5.3.3.2	*Main Effects of Microwave Setting*	118
	5.3.3.2	*Main Effects of Reagent Addition*	120
	5.3.4	***Box Behnken Design***	122
6	**EVALUATION OF TRACE METALS IN AQUACULTURE RED TILAPIA AND PRELIMINARY HEALTH RISK ASSESSMENT**		**137**
6.1		**Introduction**	137
	6.1.2	***Background of Sampling Site***	139
6.2		**Materials and Methods**	140
	6.2.1	***Reagent and Standard Materials***	140
	6.2.2	***Cleaning and Decontamination***	140
	6.2.3	***Sample Collection and Preparation***	140
	6.2.3.1	*Field Sampling*	140
	6.2.2.2	*Sample Preprocessing*	141
	6.2.2.3	*Microwave Assisted Digestion*	142
	6.2.3	**Validation of Microwave Sample Preparation Method**	144
	6.2.4	**ICP-MS Analysis**	144

			Page
6.3		**Results and Discussion**	146
	6.3.1	***Morphometric Data***	146
	6.3.2	***Distribution of Metals in Red Tilapia***	150
	6.3.2.1	*Metal Concentrations in the Liver*	150
	6.3.2.2	*Metal Concentrations in the Gills*	150
	6.3.2.3	*Metal Concentrations in the Muscles*	151
	6.3.3	***Principal Component Analysis***	158
	6.3.3.1	*Metal Distribution Pattern among Tissues*	158
	6.3.3.2	*Metal Distribution Pattern among Sampling Sites*	168
	6.3.4	***Preliminary Human Health Risks Assessment***	173
	6.3.4.1	*Non-carcinogenic Risk Assessment*	174
	6.3.4.2	*Potential Arsenic Carcinogenic Risk*	182
7		**CONCLUSION**	**185**
8		**REFERENCES**	**187**

LIST OF FIGURES

		Page
Figure 1.1	Conceptual illustration of risk measures	3
Figure 1.2	The human health risk assessment process (Asante-Duah, 1998)	4
Figure 1.3	Conceptual illustration of the Monte Carlo simulation procedure	8
Figure 1.4	Geometrical and symbolic representations of a full factorial design for three factors	15
Figure 1.5	Geometrical illustration of fractional factorial design for three factors	16
Figure 1.6	Geometrical illustration of Box-Behnken design for three factors (Esbensen *et al.*, 2004)	18
Figure 1.7	Schematic of graphical representation of data	19
Figure 1.8	The conceptual framework	
Figure 2.1	Schematic illustration of atomization processes in FAAS	40
Figure 2.2	Schematic diagram of FAAS	40
Figure 2.3	Schematic illustration of ionization process in ICP-MS (Agilent, 2005a)	44
Figure 2.4	Schematic diagram of ICP-MS (Agilent, 2005a)	45
Figure 2.5	Schematic diagram of UV-Visible Spectrophotometer	48
Figure 2.6	Conceptual illustration of PCA matrix transformation	55
Figure 3.1	Schematic illustration of the equilibrium between the forms of TAN	57
Figure 3.2	Molecular structure for Triton-X 100 where x = 9-10	61
Figure 3.3	Conceptual illustration of multivariate calibration and prediction	63

		Page
Figure 3.4	Proposed structure of TAN-metal complexes	64
Figure 3.5	Zero order spectra of blank, 0.30 ppm of Cu^{2+}, Ni^{2+} and Zn^{2+} with excess TAN at pH 6.7 in 0.4 % Triton X-100	65
Figure 3.6	Conceptual illustration of bias/variance tradeoff in predictive modeling	66
Figure 3.7	Plot of RMSEC vs. number of factors for PLS model	68
Figure 3.8	Plot of RMSEP vs. number of factors for PLS model	68
Figure 3.9	Plot of RMSEC vs. number of PCs for PCR model	69
Figure 3.10	Plot of RMSEP vs. number of PCs for PCR model	69
Figure 3.11	First three loadings for both PLS and PCR models	73
Figure 3.12	Both PLS and PCR raw regression coefficients for each component using three factors/PCs	73
Figure 4.1	Schematic diagram of a typical microwave accelerated reaction system	85
Figure 4.2	Schematic diagram of CVAAS measurement by reducing vapourization	88
Figure 4.3	Reproducibility and variability check with replicates	91
Figure 4.4	Self-regulating pressure release mechanism	93
Figure 4.5	Curvature test with center sample	98
Figure 4.6	Estimated response surface and contour plots	100
Figure 5.1	Schematic of a temperature-controlled spray chamber	113
Figure 5.2	Combined Pareto chart	118
Figure 5.3	Estimated response surface and contour plots for Cr	124
Figure 5.4	Estimated response surface and contour plots for Fe	125
Figure 5.5	Estimated response surface and contour plots for Cu	126

		Page
Figure 5.6	Estimated response surface and contour plots for Zn	127
Figure 5.7	Estimated response surface and contour plots for As	128
Figure 5.8	Estimated response surface and contour plots for Hg	129
Figure 5.9	Estimated response surface and contour plots for Pb	130
Figure 6.1	The map of sampling sites showing Glami Lemi (A), Pertang (B) and Kg. Geylang (C) at the Jelebu area	139
Figure 6.2	Probabilistic metal distributions in tilapias from GL, PT and KG	155
Figure 6.3	Molecular structure of arsenobetaine	157
Figure 6.4	Scree graph for PCA with 11 metal variables	160
Figure 6.5	Plot of total explained variance vs. number of PCs for PCA	160
Figure 6.6	Correlation loadings plot for first two PC	162
Figure 6.7	Scores plot of PC1 against PC2. First letters G, P and S donate the different sampling sites (Glami Lemi, Pertang, and Kampung Geylang repectively); second letters M, L, and G refer to different organ (muscles, liver and gills)	164
Figure 6.8	PCA bi-plot for all samples. First letters G, P and S donate the different sampling sites (Glami Lemi, Pertang, and Kampung Geylang repectively); second letters M, L, and G refer to different organ (muscles, liver and gills)	165
Figure 6.9	Varimax-rotated PCA bi-plot for all samples. First letters G, P and S donate the different sampling sites (Glami Lemi, Pertang, and Kampung Geylang repectively); second letters M, L, and G refer to different organ (muscles, liver and gills)	167
Figure 6.10	Unrotated PCA bi-plot for liver samples	168
Figure 6.11	Varimax-rotated PCA bi-plot for liver samples	169

		Page
Figure 6.12	Unrotated PCA bi-plot for gill samples	171
Figure 6.13	Varimax-rotated PCA bi-plot for gill samples	171
Figure 6.14	Unrotated PCA bi-plot for muscle samples	172
Figure 6.15	Varimax-rotated PCA bi-plot for muscle samples	173

LIST OF TABLES

		Page
Table 1.1	An eight-run Plackett Burman design matrix with seven factors	17
Table 3.1	Total explained calibration variance using first three factors/PCs	67
Table 3.2	Calibration results for both PLS and PCR models	71
Table 3.3	Validation results for both PLS and PCR models	72
Table 3.4	Analytical figures of merit for PLS and PCR models	77
Table 3.5	Intraday validation of Cu^{2+}, Ni^{2+} and Zn^{2+} in spiked tap water	78
Table 3.6	Interday validation of Cu^{2+}, Ni^{2+} and Zn^{2+} in spiked tap water	79
Table 3.7	Tolerance ratios for foreign ions in the determination of 0.30 ppm of Cu^{2+}, Ni^{2+} and Zn^{2+} mixture	82
Table 4.1	AAS instrumental parameters	87
Table 4.2	Factors and levels used in factorial design	89
Table 4.3	Design matrix and the results of the two-level fractional factorial design	89
Table 4.4	Estimates of effect on metal recovery based on fractional factorial design	96
Table 4.5	Analysis of variance of Fe linear model	99
Table 5.1	Parameters and levels used in multivariate design	108
Table 5.2	ICP-MS operating conditions	109
Table 5.3	Summary of analyte masses, analytical conditions and method detection limits for studied elements	111
Table 5.4	Design matrix and the results of the two-level Plackett-Burman design	116

		Page
Table 5.5	Estimated optimum microwave setting and working condition for multi-element analysis	123
Table 5.6	Analysis of certified reference materials	132
Table 5.7	Comparison of MAD recoveries with literature reports	135
Table 6.1	Analysis of riverine water certified reference material	144
Table 6.2	Analysis of sludge and sediment certified reference materials	145
Table 6.3	Biometric parameters for tilapia from different sampling site	146
Table 6.4	Metal concentrations in freeze dried Tilapia tissues	148
Table 6.5	Total metal concentrations in tilapia muscle and permissible limits	152
Table 6.6	Percent explained variance for PCA	159
Table 6.7	The first two unrotated loadings	161
Table 6.8	Parameters and their distributions for risk estimation	176
Table 6.9	Log-normal distribution of trace metals in dried tilapia muscles from different production sites	177
Table 6.10	Probabilistic estimation of reasonable maximum exposures and non-carcinogenic risks associated with consumption of red tilapias	179
Table 6.11	Probabilistic estimation of As exposures and cancer risks associated with consumption of red tilapia	184

LIST OF SYMBOLS AND ABBREVIATIONS

$\|\ \|$	Norm
β_0	Regression Coefficient for Intercept
β_k	Regression Coefficient for *k*th Variable
χ_k	Ratio of Effective Species to Total Content of *k*th Metal
ε	Instrumental Noise
γ	Analytical Sensitivity
λ_j	Eigenvalue for *j*th Principal Component
AAS	Atomic Absorption Spectrometry
A-D	Anderson-Darling
AES	Atomic Emissions Spectrometer
$a_{k,j}$	Loading for *k*th Variable on *j*th Principal Component
ANN	Artificial Neural Network
ANOVA	Analysis of Variance
AT	Averaging Time
ATSDR	Agency for Toxic Substances and Disease Registry
AU	Absorbance Units
BBD	Box–Behnken Design
BFD	Blackfoot Disease
b_k	Vector of Final Regression Coefficients for the *k*th Wavelength
BW	Body Weight
C_0	Number of Central Point Replicates
$\hat{c}_i$	Predicted Concentration of *i*th Sample
c_i	Reference Concentration of *i*th Sample

CCD	Central Composite Design
CD_k	Concentration for the *k*th Metal on Dried Basis
CF	Condition Factor
CID	Collisionally Induced Dissociation
CMC	Critical Micelle Concentration
cps	Counts per Second
CR	Carcinogenic Risk
CRC	Collision/Reaction Cell
CVAAS	Cold-Vapour Atomic Absorption Spectrometer
CW_k	Concentration for the *k*th Metal on Wet Basis
DF	Degrees of Freedom
DL	Detection Limit
DMA	Direct Mercury Analyzer
DoE	Design of Experiment
DOF	Department of Fisheries of Malaysia
EC	Commission Regulations of the European Union
ED	Exposure Duration
EDA	Exploratory Data Analysis
EF	Exposure Frequency
E_k	Exposure of *k*th metal
ETAAS	Electrothermal Atomic Absorption Spectrometer
f	Degree of Fractionality
FA	Factor Analysis
FAAS	Flame Atomic Absorption Spectrometry
FAO	Food and Agriculture Organization of the United Nations
FFD	Factional Factorial Design

FIR	Fish Ingestion Rate
FOM	Figures of Merit
GFAAS	Graphite Furnace Atomic Absorption Spectrometer
GIFT	Genetically Improved Farmed Tilapia
GI_k	Gastrointestinal Absorption Factor for *k*th Metal
GL	Glemi Lemi
HI	Hazard Index
HOIE	High Order Interaction Effect
HQ	Hazard Quotient
HR	High Resolution
HSI	Hepatosomatic Index
ICP	Inductively Coupled Plasma
IRIS	Integrated Risk Information System
ISTD	Internal Standard
K	Number of variables
KED	Kinetic Energy Discrimination
KG	Kg. Geylang
K-S	Kolmogorov-Smirnov
L	Designed Levels
l	Length of Sample
LOD	Limit of Detection
LOQ	Limit of Quantification
m	Weight of Sample
m/z	Mass to Charge Ratio
MAD	Microwave Assisted Digestion
MAE	Microwave Assisted Extraction

MC	Monte Carlo
MDL	Method Detection Limit
MLR	Multiple Linear Regression
MPI	Metal Pollution Index
MRL	Minimum Risk Level
MS	Mass Spectrometer
MS	Mean Squares
N	Number of Experiment Runs
n	The Number of Sample
N.D.	Not Detected
NOAEL	No Observed Adverse Effects Level
NRCC	National Research Council Canada
OES	Optical Emissions Spectrometer
ORS	Octopole Reaction System
PBD	Plackett-Burman Design
PC	Principal Component
PCA	Principal Component Analysis
PCR	Principal Component Regression
PFA	Perfluoroalkoxy
PLS	Partial Least Squares
ppm	Parts per Million
PT	Pertang
PTFE	Polytetrafluoroethylene
PTWI	Provisional Tolerable Weekly Intake
PVC	Polyvinyl Chloride
QSAR	Quantitative Structure-Activity Relationship

R	Correlation Coefficient
RF	Radio Frequency
RfD	Reference Dose
RMSEC	Root Mean Square Error of Calibration
RMSEP	Root Mean Square Error of Validation
RP-HPLC	Reverse Phase-High Performance Liquid Chromatography
RSD	Relative Standard Deviation
RSM	Response Surface Methodology
SEC	Standard Errors of Calibration
SEN	Sensitivity
SEP	Standard Errors of Performance
SF	Slope Factor
SS	Sum of Squares
Std Err	Standard Error
TAN	1-(2'-thiazolylazo)-2-naphthol
$t_{i,j}$	Scores on *j*th PC for *i*th Sample
UPW	Ultra Pure Water
USDHHS	United States Department of Health and Human Services
USEPA	United State Environmental Protection Agency
USFDA	United States Food and Drug Administration
USNAS	United States National Academy of Science
UV	Ultraviolet
w	Water content
WHO	World Health Organization
$Z_{i,k}$	Transformed data of *k*th variable for *i*th sample

LIST OF PUBLICATIONS

1. Low, K.H., Zain, S.M., Abas, M.R., Misran, M. and Ali Mohd, M. (2009). Simultaneous spectrophotometric determination of copper, nickel, and zinc using 1-(2-thiazolylazo)-2-naphthol in the presence of triton x-100 using chemometric methods. *J. Korean Chem. Soc.* **53 (6)**, 717-716.

2. Low, K.H., Zain, S.M., Abas, M.R. and Ali Mohd, M. (2009). Evaluation of closed vessel microwave digestion of fish muscle with various solvent combinations using fractional factorial design. *A.S.M. Sc. J.* **3(1)**, 71-76.

3. Low, K.H., Zain, S.M. and Abas, M.R. (2011). Evaluation of metal concentrations in red tilapia (*Oreochromis spp*) from three sampling sites in Jelebu, Malaysia using principal component analysis. *Food Anal. Methods* **4(3)**, 276-285.

4. Low, K.H., Zain, S.Md. & Abas, M.R. (2012). Evaluation of microwave assisted digestion condition for the determination of metals in fish samples by inductively coupled plasma mass spectrometry using experimental design. *Int. J. Environ. Anal. Chem.* **92(10)**, 1161-1175.

1 INTRODUCTION

1.1 Background of Target Species

The importance of fish as a source of food has been well documented in the scientific literature for many regions of the world. As the human population continues to grow, many developing countries including Malaysia extend their focus towards aquaculture fishery due to its nutritional value and economical as well as social importance. According to the Malaysian Annual Fisheries Statistics (2008), the aquaculture sector showed a production increase of 32% compared to 2007, which accounted for more than 20% of total fisheries output in the country (DOF, 2008). Although the capture fisheries remain the major source of fish production, aquaculture production yields valuable species for both domestic and export markets.

Among the aquaculture fisheries food supply, cichlidae/tilapia (*Oreochromis spp*) which is native to Africa is one of the top ten species that have been introduced and farmed extensively in many parts of Asia and some Pacific Island countries, with high expansion rate in terms of production quantity. This may be due to the good characteristics of tilapia such as rapid growth, large size, palatability, adaptability on a wide range of water conditions and food types, tolerance to stocking density and easy breeding without special hatchery technology. These characteristics allow rapid production of commercial size fish which meets the market demands (Nandlal and Pickering, 2004). For these reasons the tilapia is commonly termed as the "aquatic chicken". Moreover, introduction of the genetically improved farmed tilapia (GIFT) strain, which has a wide body conformation, under a collaborative programme with the World Fish Centre in 2001 enhanced the tilapia productivity of commercial culture in Malaysia.

Since tilapia culture requires minimal management and energy input, it has become a promising business which accounted for more than a third of the total freshwater aquaculture production in Malaysia. In addition, it has been reported that besides China, Malaysia is a country where the domestic market for tilapia is stronger than the export market. Prices in the country are about 10% higher than the world import prices (Josupeit, 2008). Consequently, this industry has involved many fish farmers and commercial companies operating with several types of culture practices and systems. These include low-tech earthen ponds to more expensive concrete tanks depending upon local circumstances. Among them, open flow through culture systems are common and require minimal operating cost due to the accessibility of riverine water supply.

As recorded in the Malaysian Annual Fisheries Statistics (2008), the production of tilapia was about 36 kilotonnes per year with an estimated wholesale value of more than 62 million USD (DOF, 2008). Majority of them were red tilapias which accounted for roughly 76% of the total tilapia production compared to black tilapia. In this regard, nearly 63% of total red tilapia production were harvested from freshwater ponds, 17% from freshwater cages, 15% from ex-mining pool and 5% from concrete tank. In most cases, these intensive aquaculture facilities increasingly rely on water from river or estuary (that are prone to external pollution) for fish cultivation, application of metal-based antifoulants, and heavy input of formulated metal-enriched fish feeds (Sapkota *et al.*, 2008). In some instances, animal entrails are also utilized in the aquaculture environment. All these can lead to elevated levels of metal in aquacultured tilapia. As a result, potential food safety and human health risks associated with metals intake through consumption of commercially farmed tilapia have attracted considerable attention ([Liu *et al.*, 2010] and [Liao *et al.*, 2008]).

1.2 Risk Assessment

There is no single definition of risk that is accepted universally. It can be considered as the likelihood of an undesirable adverse threat posed by hazardous substance or situation. In fact, it is often conceptually estimated by mathematical functions which take into account the probability and severity of occurrence (Figure 1.1). To some extent, the preventative factors are involved as well. For instance, human health risk measures may correspond to probability for a chemical to cause adverse consequences on exposed population over a specified time period.

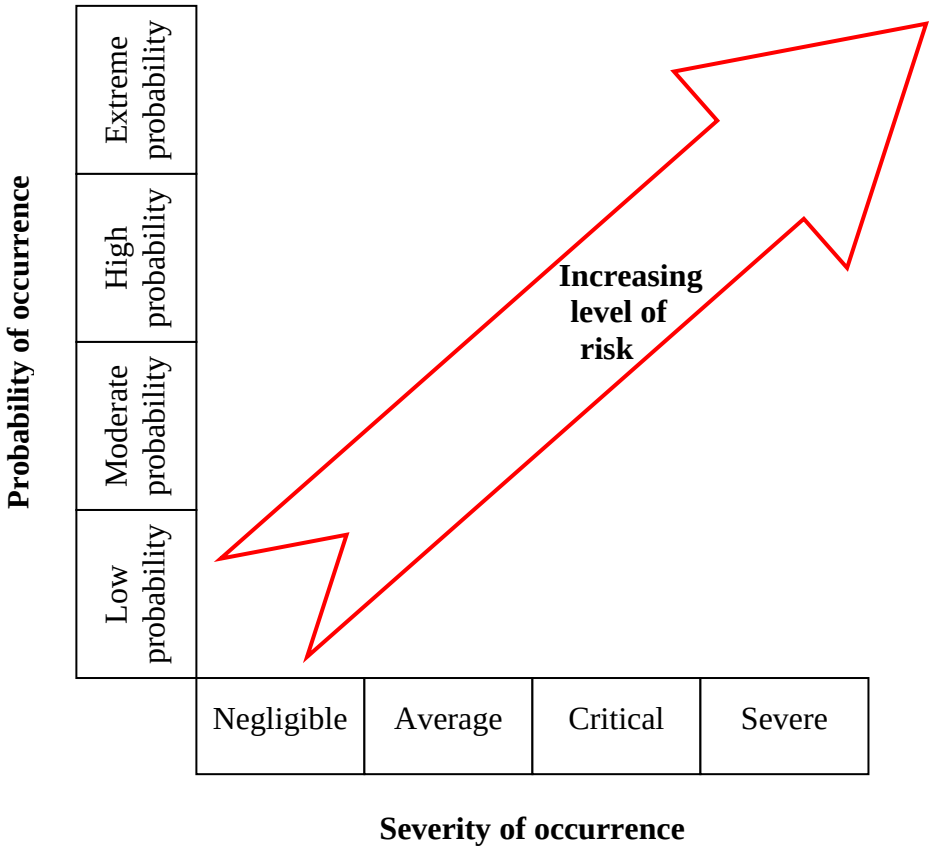

Figure 1.1 Conceptual illustration of risk measures

1.2.1 Human Health Risk Assessment Methodology

Human health risk assessment can be regarded as a process that seeks to characterize the potential adverse health impacts resulting from human exposure to hazardous substances that are present in the environment. Thus, those corresponding risks may be quantified by identifying the relevant sources and consequences as well as estimating their magnitude, the timing of those consequences and their frequencies of occurrence. In general, human health risk assessment process usually consists of a hazard identification/data collection and data evaluation in the preliminary phase followed by exposure assessment along with toxicity assessment, then risk characterization process takes place in the subsequent phase (Figure 1.2).

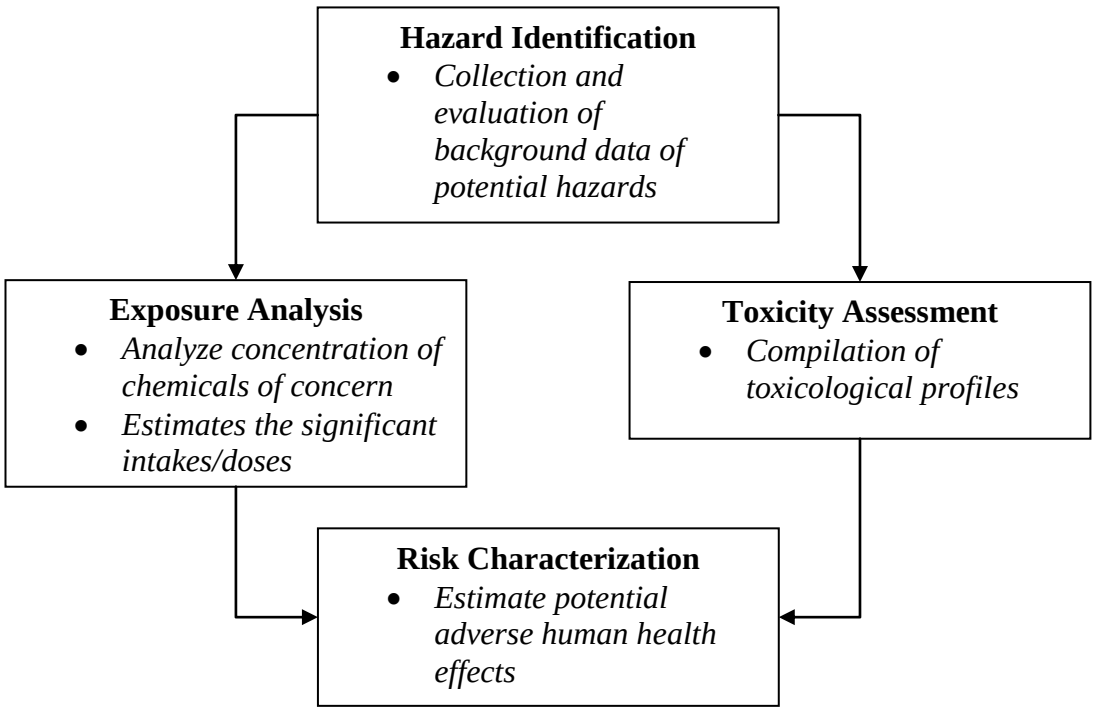

Figure 1.2 The human health risk assessment process (Asante-Duah, 1998).

1.2.1.1 Hazard Identification

Identification of applicable hazards and their possible consequences on human is a decisive process in order to quantify the resulting health risk credibly. For that reason, human health risk assessments commonly start with hazard identification involving a qualitative evaluation of the presence of undesired chemicals with potential to cause harm. This process gathers and analyzes background data that are related to the specific chemical substances of concern based on their hazardous characteristics and is usually conducted as a part of literature review (Wells, 1996). Hence, profile summaries for targeted analytes concerning current study are covered in the next chapter.

1.2.1.2 Exposure Assessment and Analysis

The process of exposure assessment and analysis is to deduce from the available information the likely human intake of chemical substances of concern. Quantitative exposure assessment provides numerical estimates of the rates at which chemicals are absorbed by the targeted receptors using a combination of mathematical and logical statements. Quantitatively analyzing the relevant chemical species is one of the major issues of the ultimate validity of the human health risk assessment (USEPA, 2000a).

In view of this, quantitative determination of those targeted analytes requires reliable analytical method so as to ensure consistency and comparability of the obtained results. This means, the laboratory procedures including sample handling and analysis should display adequate technical merit, sensitivity, data quality and also cost efficiency to a certain extent. For that reason, evaluation of analytical performance is one of the major concerns of this study.

1.2.1.3 Toxicity Assessment

Basically, toxicity assessment is concerned with compiling toxicological profiles for the chemicals of potential concern that can be subsequently used as a basis for estimating the safe threshold doses. It typically involves quantitative evaluation of toxicity information and characterization of exposure-response relationship that concern the incidence of health impacts on the targeted receptors subjected to dose of the chemical substances administered or received. These data often rely on the extrapolated results of experimental animal studies for human health assessment purposes.

In order to facilitate health risk assessments, decision-making and regulatory activities, such information can be derived from appropriate standard toxicology references and existing chemical-specific toxicological profiles. According to available literature, the common practice in facilitating the assessment is by adopting the consistent toxicological data from the Integrated Risk Information System (IRIS) by United States Environmental Protection Agency (USEPA) and also the Agency for Toxic Substances and Disease Registry (ATSDR) under United States Department of Health and Human Services (USDHHS).

1.2.1.4 Human Health Risk Characterization

Human health risk characterization consists of evaluating plausible incidence of hazardous impacts to the exposed population via chemicals of potential concern. In general, the associated risks are quantitatively derived through an integration of exposure and toxicological profiles. Typically, hazard quotient (*HQ*)/hazard index (*HI*) and carcinogenic risk (CR) set by USEPA are widely applied to define the non-carcinogenic hazards and potential cancer risks associated with exposure to a variety of chemicals. In this context, the non-carcinogenic risk is estimated using the systemic toxicity concept of reference dose (*RfD*) which is defined as the maximum level of a chemical that can be tolerated by the human body without experiencing chronic effects. On the other hand, the incremental lifetime cancer risk is expressed based on the upper-bound of the lifetime probability of a carcinogenic exposure-response function called the cancer slope factor (*SF*).

1.2.2 Deterministic and Probabilistic Assessments

Human health risks can be quantitatively estimated according to experimental data and modeling assumptions either via deterministic or stochastic assessments. The deterministic assessment based on single values such as the average to characterize each parameter in the exposure model is the most common practice. However in most cases, due to time and cost constraints, only a limited proportion of in-situ data can be analyzed in a study which may lead to an unrealistic over-estimate and somewhat assertive conclusion as a consequence of using single point estimates in the risk assessment process (Jang *et al.*, 2009).

On the other hand, probabilistic approach that uses a statistical distribution to describe the probability of occurrence provides a sensible improvement to deterministic

approach. Since a probability distribution of possible values is considered for each input parameter in the exposure model, it can be used to propagate the uncertainty of parameters owing to inherent natural variability. In this regard, probabilistic method provides greater information and thus results in a quantitative assessment that is more realistic despite its increased complexity over deterministic approach. Typically, the use of Monte Carlo (MC) simulation methods for stochastic estimation has received growing attention in recent times because of their robustness. In general, MC simulation involves assigning a joint probability distribution using randomly generated scenarios repeatedly in order to approximate the full range of possible outcome (Figure 1.3).

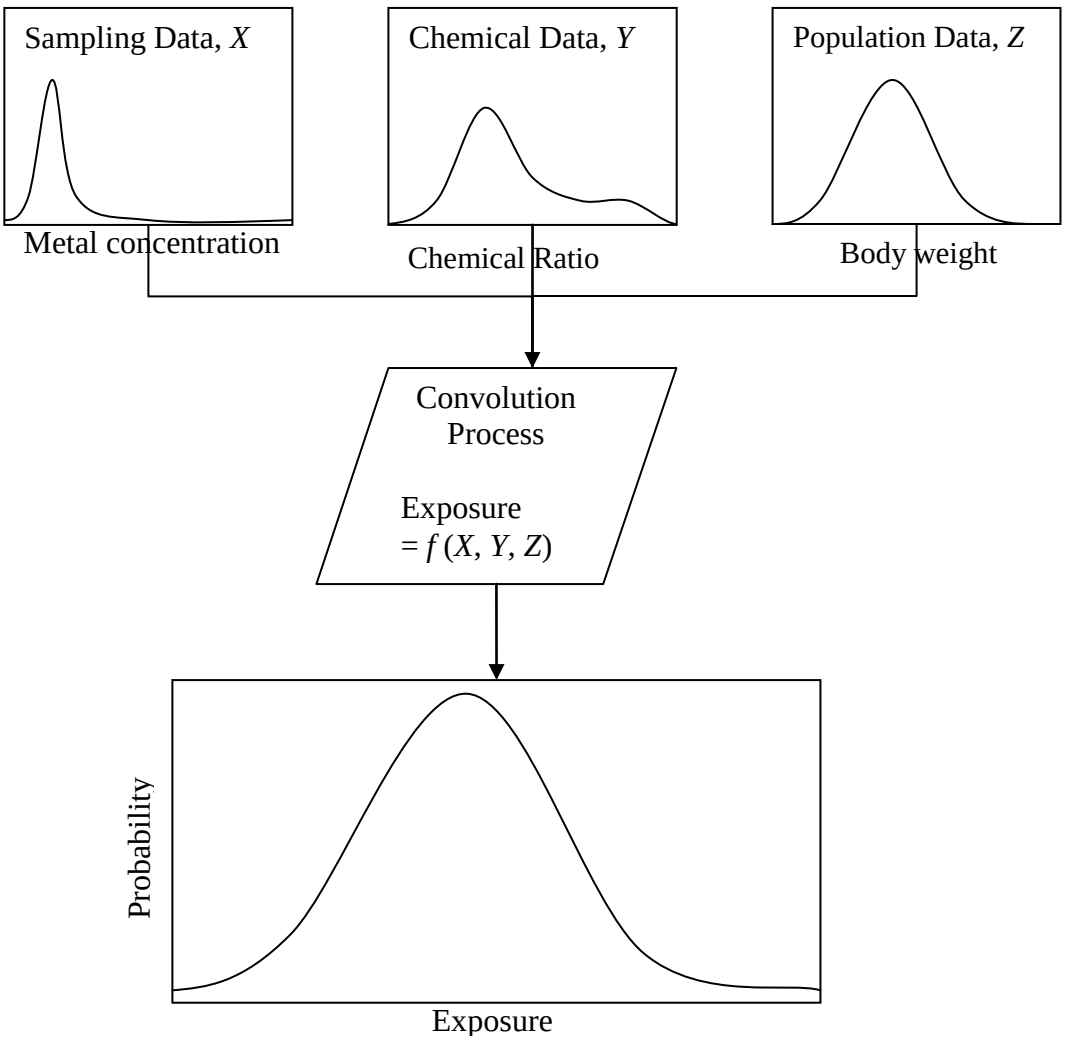

Figure 1.3 Conceptual illustration of the Monte Carlo simulation procedure

1.3 Target Analytes

Metal species are widespread in the environment as a consequence of both natural and anthropogenic processes. In aquaculture environments, additional sources of metals may come from metal-enriched fish feeds as well as metal-based antifoulants that are used to control the build-up of fouling organisms (Sapkota *et al.*, 2008). Furthermore, a host of metals may well be derived from various alloys in pumps, pipes and other applicable machinery in the surroundings. These metal species can be mobilized from the environment and accumulated in the biota in water, and are subsequently transferred to humans through the food chain. Under certain conditions, part of them can be biologically accumulated in the tissues at concentration levels thousands of times higher than those in the feed and/or water body due to the metals' capacity to form complexes with organic substances (Türkmen *et al.*, 2005). Eventually, dietary intake of these bioconcentrated and/or biomagnified species poses potential health risk.

The oral ingestion is considered a primary route of metal intoxication, with the toxicity of each metal species differing significantly and certain species are biologically essential. It is suggested that metals such as arsenic, cadmium, lead and mercury could be possibly classified as potentially toxic. They can be noxious even in trace levels resulting from multiple exposures over a significant period of time. Copper, iron, manganese, selenium and zinc are essential metals that play vital roles in biological systems, while cobalt, nickel, vanadium could be regarded as probably essential (Uluözlü *et al.*, 2007). Nevertheless, the essential and/or probably essential metals could probably introduce deleterious effects if their intake was excessive (Celik and Oehlenschlager, 2007). Some of these metal species tend to accumulate in fatty tissues of fish and others selectively bind with muscle tissues. Thus, it is suggested that intake of those lipophilic species may be reduced by removing the fat, skin, and viscera before

consuming the fish. However, the exposure to other bioaccumulative species in the flesh cannot be controlled by such trimming. Thus, monitoring and risk assessment programmes are essential to assure the balance between benefit and risk of fish ingestion.

1.4 Analytical Techniques and Methodology

Elemental analysis of trace metals is very important for routine monitoring, risk assessment and regulation. From the public viewpoint, there is a necessity to determine the metal content especially those toxic metals in commercially available fishes which are mainly consumed by human (Sures *et al.*, 1995). To assure the ultimate validity of analytical results, application of an appropriate sample preparation procedure and its effective combination with determination methods are of major importance (Balcerzak, 2002). As a rule of thumb, for accurate elemental analysis of metals, mechanical sample preparation is usually required in order to completely transfer analytes of concern into solution so that they can be quantitatively introduced to the determination step. Despite the importance of this step, few innovations had been made in sample dissolution methods.

1.4.1 Sample Preparation

In the analysis process, sample preparation procedure is always considered to be one of the most critical steps. This is due to the fact that most of the regularly used techniques for the determination of metals in environmental often require matrix dissolution so as to avoid interference from associated organic matters. The relevant organic matters in a sample matrix are usually removed by some form of oxidation processes which depends on the targeted metals and the nature of the sample.

At present, there are a wide variety of sample pretreatment techniques for fish matrices that have been published. These include dry/wet ashing with various reagents and conventional heating procedures, closed/open vessel microwave assisted digestion (MAD) and bomb dissolution ([Reis *et al.*, 2008], [Hseu, 2004], [Tüzen, 2003] and [Sures *et al.*, 1995]). Depending on the analytical task, several factors should be

considered for sample preparation. These include sample homogeneity, completeness of matrix decomposition and solution of analytes, level of possible losses and contamination, compatibility of the analytical technique, reproducibility, handling and processing time, economic significances such as equipment cost, reagent consumption, labour, and others ([Momen *et al.*, 2007] and [Soylak *et al.*, 2007]).

1.4.2 Elemental Analysis Techniques

There are a number of mature and effective end-determination methods that could be performed for elemental analysis on sample solutions. In the early days, gravimetric, volumetric and colorimetric techniques were widely employed. In recent studies, the most common practices involve instrumental analysis and spectrometry techniques such as basic flame atomic absorption spectrometry (FAAS), the more superior inductively coupled plasma-mass spectrometry (ICP-MS) and alternative spectrophotometry measurements based on various chromogenic reagents. Selecting the most appropriate tool for quantification of metal elements sometimes appear to be a daunting task, since there seems to be considerable overlap of their capabilities. However, based on the requirements of analytical performance and available resources, it is possible to assess relative strengths and weaknesses of each of these techniques. These will be treated in more detail in the next chapter.

1.5 Chemometrics

Chemometrics is characterized mainly by the application of multivariate methods to efficiently extract useful information from chemical measurements. It is an application driven discipline which is mainly applied to address both descriptive and predictive problems related to chemical data. In descriptive analyses, the latent structures in the data could be studied; while data are modeled to estimate the desired properties of the targeted systems via the predictive analyses.

One of the earlier application areas and original driving forces of chemometrics has been in the food and agriculture industries. Thereby, many of the earliest chemometricians were applied statisticians by training; where there was a tradition of development of multivariate statistics within highly regarded food and/or agricultural research institutes (Brereton, 2003a). The early applications mostly involved multivariate classification. However, the applications have diversified substantially over the years, partly due to the research interests and partly due to the economic driving forces. Most of their applications reported in academic literatures are often related to both experimental design and the interpretation of multivariate data.

1.5.1 Experimental Design

Experimental planning and design have a direct influence on the information gained from the system under study. Experimental design consists of a series of experiments under various experimental conditions, for instance, as in this study, possible microwave assisted digestion (MAD) conditions. Statistically designing what data to collect and how it is to be collected offers greater possibilities of extracting useful information with least experimental efforts compared to ad hoc and other classical approaches. With appropriate experimental designs through the establishment of

mathematical models, it is possible to assess the statistical significance of the effects related to the factors being investigated as well as to evaluate the effects of their interaction. In order words, precise models constructed under designed experiments are efficient in drawing helpful conclusions.

The two main applications of experimental design are screening and optimization. From screening design, the controllable factors that significantly affect the experiment outcomes can be identified; while the optimal conditions for an experiment can also be estimated through response surface methodology. The option ultimately depends on the objectives of the study and the number of factors to be investigated and also relies on the available resources and stage of the study. The common approach is to commence with a simple screening design that includes those suspicious inputs that may impact the experiment outcomes, since confirming the most significant factors is usually the goal in the early stage. Once the key factors have been identified, a response surface design for simultaneous optimization of their levels is employed to attain the best performance conditions.

The screening designs often encompass linear effect designs that have relatively few design levels, for instance, two-level factional fractorial designs (FFDs) and two-level Plackett-Burman designs (PBDs). Response surface designs at higher levels such as full factorial designs, central composite designs (CCDs) and Box–Behnken designs (BBDs) can also be used to provide more detailed information with a more complex model which will lead to the optimal response values.

1.5.1.1 Full Factorial Designs

The most basic design matrix that is commonly used is a full factorial design which mulls over every possible combination of conditions at defined levels. This enables the study of all possible interactions in addition to the main effect that are associated with the designed factors and their levels. For instance, Figure 1.4 illustrate a two-level full factorial design that considers three controllable factors X_1, X_2 and X_3, where combinations are put together by varying each of them from a low (-) to high (+) level in a systematic order. Each point in the cube in Figure 1.4 represents an experimental condition listed in the table next to it.

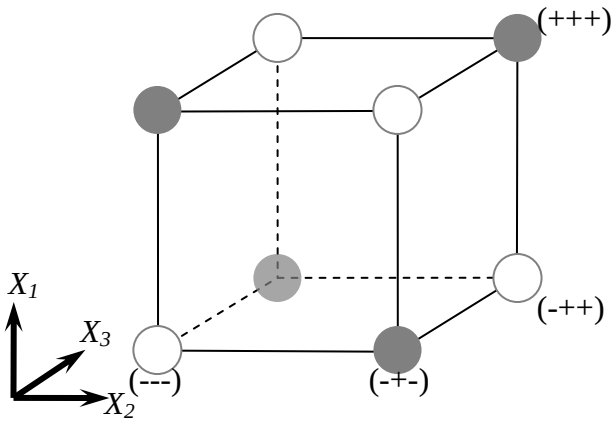

No	X_1	X_2	X_3
1	-	-	-
2	-	-	+
3	-	+	-
4	-	+	+
5	+	-	-
6	+	-	+
7	+	+	-
8	+	+	+

Figure 1.4 Geometrical and symbolic representations of a full factorial design for three factors

Full Factorial designs are appropriate for both screening and optimization techniques, but the minimum experimental trails required increases geometrically with the number of designed factors as well as the experimental levels. This is due to the fact that the number of necessary experimental runs, N is proportional to L^K, where K is the number of designed factors and L is the experimental level. As a consequence, time, cost and difficulty of control also increase in order to gather sufficient amount of information in this design.

1.5.1.2 Fractional Factorial Designs

Fractional factorial designs (FFDs) can be considered as reduced experimental plans that can provide substantial information, especially in the initial stage of study. It is prescribed as a purposely selected subset of a full factorial design which allows estimation of the desired effects from a limited number of runs depending on the resolution of the design. In *L*-level FFDs, the number of experimental runs is calculated by the expression $N = L^{K-f}$, where *K* is the number of variables, *f* indicates the degree of fractionality and *L* donates the designed levels. As a result, the number of runs can be reduced by *L* factor in any case relative to full factorial designs. For example, Figure 1.5 shows a geometrical representation of a two-level FFD, where the experimental runs required is trimmed down to half compared to Figure 1.4.

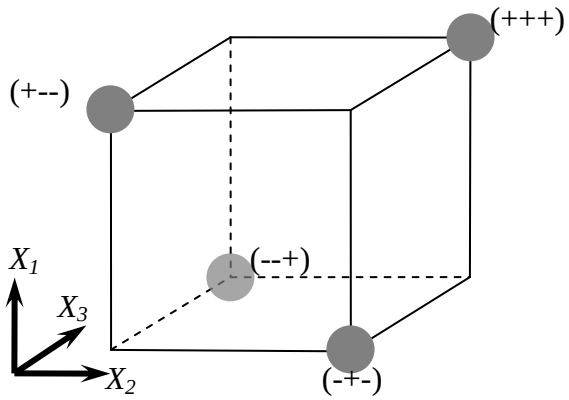

Figure 1.5 Geometrical illustration of fractional factorial design for three factors

However, confounding, which is the natural consequence for performing fewer runs, where some effects cannot be studied independently of each other, will occur. Therefore, applying a FFD involves a major assumption that high order interactions are not significant so that main effects of the designed factors can still be computed. Fortunately, these considerable interactions are not common.

1.5.1.3 Plackett-Burman Designs

The well known two-level Plackett-Burman designs (PBDs) introduced by R.L. Plackett and J.P. Burman in 1946 enables the screening of the main effects associated with *K* number of designed factors with no more than *K* + 4 experimental runs. This means, with an eight-run PBD, up to seven factors can be studied; with a twelve-run design, up to eleven factors; with a sixteen-run design up to fifteen factors, and with a twenty-run design, up to nineteen factors and so on (Table 1.1).

Table 1.1 An eight-run Plackett Burman design matrix with seven factors

No	X_1	X_2	X_3	X_4	X_5	X_6	X_7
1	-	+	-	+	+	+	-
2	+	-	+	+	+	-	-
3	-	+	+	+	-	-	+
4	+	+	+	-	-	+	-
5	+	+	-	-	+	-	+
6	+	-	-	+	-	+	+
7	-	-	+	-	+	+	+
8	-	-	-	-	-	-	-

They have demonstrated that full factorial designs could be fractionalized in different ways to give such matrices that the *N* is a multiple of 4 rather than a power of 2 (Plackett and Burman, 1946). Thus, the resulting design matrix might be identical to a factional factorial design in some cases. Due to its simplicity and relatively low cost, the designs are widely employed early in the experimental sequence to investigate whether there is any significant variation by estimating the main influence of controllable factors. However, the main drawback is that it does not allow the evaluation of interactions between design factors. Due to this fact, more sophisticated design is required to model the response surface with higher order effects.

1.5.1.4 Box–Behnken Designs

Response surface methodology has been employed for optimization considering their advantages with regard to the requirement of constrained resource. The common efficient option involves the use of Box–Behnken designs (BBDs) which can be considered as an ideal alternative to full factorial designs or central composite designs. BBDs are rotatable second-order designs based on three-level incomplete factorial designs which avoids the corners of the cube, and fills in the combinations of low (-), center (0) and high (+) level ([Ferreira *et al.*, 2007a] and [Hanrahan and Lu, 2006]). As a consequence, all designed experiments lie on sphere around the centre and avoids extreme conditions (Esbensen *et al.*, 2004). For instance, Figure 1.6 illustrates a three-factor BBD with a central point which does not embed any factorial design.

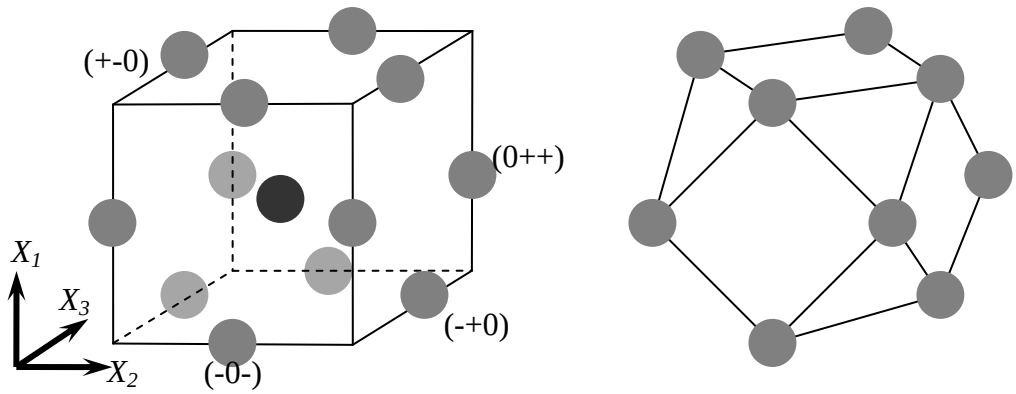

Figure 1.6 Geometrical illustration of Box-Behnken design for three factors (Esbensen *et al.*, 2004)

The number of experiments (N) required for the development of BBDs is defined as $N = 2K\ (K - 1) + C_0$, where K is number of factors and C_0 is the number of central point replicates ([Khajeh and Sanchooli, 2010] and [Ferreira *et al.*, 2007b]). BBDs not only allow understanding of how the response changes in a given direction but also permit single response optimization.

1.5.2 Pattern Recognition

It is generally agreed that pattern recognition is one of the first and most spectacular successes in chemometrics. It is the scientific tools dealing with objects characterization and classification by finding similarities and differences between samples based on measurement made.

Human perception can aid discrimination between samples with simple data matrices and interpretation that are made accordingly. In chemistry, this ability is important because much of chemistry involves recognition of patterns based on the data obtained. For example as shown in Figure 1.7, a chromatogram is graphed as a continuous plot rather than represented in tabular form, because interpretation of chromatogram can be easily made based on the presence of peaks. Similar graphical representation has also been widely adopted in other areas of chemistry such as molecular spectroscopy.

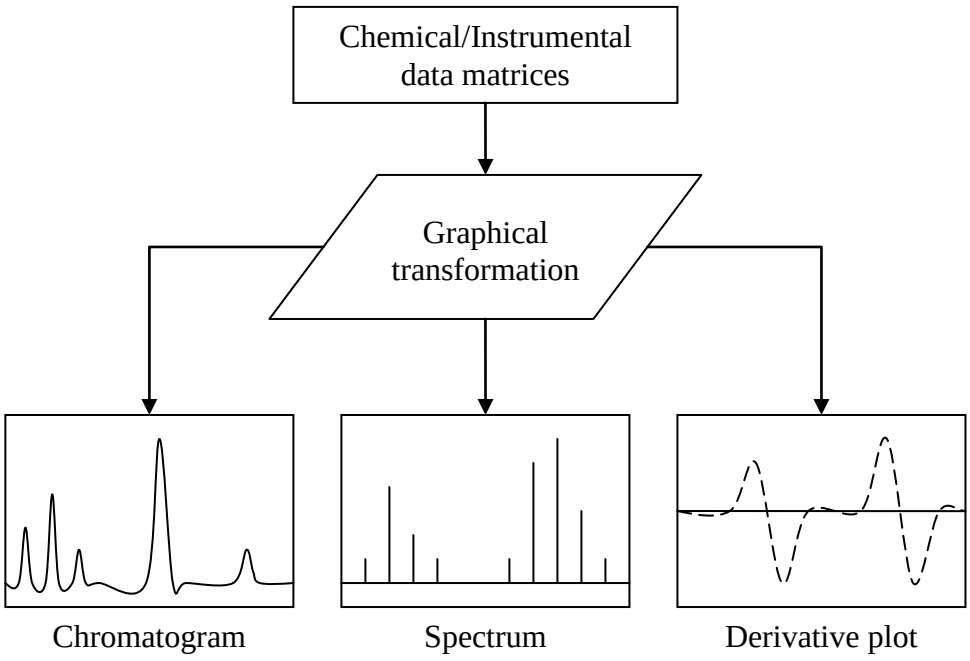

Figure 1.7 Schematic of graphical representation of data

However, this recognition skill is limited to matrices with small numbers of samples and/or factors. The existence of larger multivariate data matrices such as the various metal concentrations in different tissues of tilapia samples require the use of mathematical and statistical tools, in order to efficiently extract the maximum useful information in the shortest time. There are several choices of multivariate data analysis techniques available depending on the different analytical purposes. The main groups of methods consist of exploratory data analysis, discrimination and classification, regression and prediction.

1.5.2.1 Exploratory Data Analysis

Exploratory data analysis (EDA) is a statistical approach to characterize the data by useful summaries. It emphasizes primarily on graphical techniques for visually displaying the intrinsic data structures. In combination with human pattern-recognition capabilities, this graphical method provides analysts unparalleled power in exploring data to uncover its underlying structures.

EDA may encompass a variety of techniques for maximizing insight into a dataset; revealing latent structure, extracting significant factors, detecting anomalies or outliers, testing underlying assumptions, establishing parsimonious models and determination of optimal factors. The particular multivariate techniques employed in EDA consist mainly of principal component analysis (PCA) and factor analysis (FA).

1.5.2.2 Discrimination and Classification

Discrimination analysis is an unsupervised pattern recognition technique that differs from EDA to some extent. It is basically used to evaluate whether clustering exist in a dataset without adopting the class membership information throughout the calculation. The aim of unsupervised modeling is to sense similarities, where as EDA is usually employed as the preliminary stage priori to the method and there is no particular prejudice as to whether there are or how many clusters will be found (Brereton, 2009). In this regard, by examining the natural clustering tendencies of the samples, the understanding of the dataset is enhanced. In contrast to discrimination, classification is regarded as a supervised pattern recognition method that requires the training dataset with class membership information to be known in advance in order to develop models for prediction of class membership for future samples.

1.5.2.3 Multivariate Regression and Prediction

Multivariate regression and prediction is considerably different from the abovementioned pattern recognition techniques which are primarily qualitative and often exploratory. Regression involves developing a mathematical model that quantitatively relate sets of variables together which are already identified to have inter-relationships. Prediction is the process of applying the established model to estimate the values of underlying dependent variables based on a given set of measured independent or response variables. For example, the most common use of multivariate regression analysis has been in spectroscopic measurements that relate absorbance or reflectance within a certain range of wavelengths to the analyte concentrations of interest regardless the presence of potentially interfering components. Principal component regression (PCR) and partial least squares (PLS) are of the most commonly used multivariate algorithms advocated by many chemometricians. These techniques allow retaining of the multivariate nature of the original data by estimating a reduced number of factors from linear combinations of the subjected variables.

1.6 Objectives of Research

(a) To develop alternative method for simultaneous spectrophotometric determination of Cu^{2+}, Ni^{2+} and Zn^{2+} solution mixtures using multivariate calibrations.

(b) To study and to optimize the microwave-assisted digestion condition for the determination of trace metals in fish samples using experimental designs.

(c) To assess the presence of trace elements in freshwater aquaculture red tilapia and to evaluate their accumulation patterns using chemometric approaches.

(d) To analyze spatially the reasonable health risks due to the tilapia consumption using Monte Carlo simulation.

1.7 The Conceptual Framework

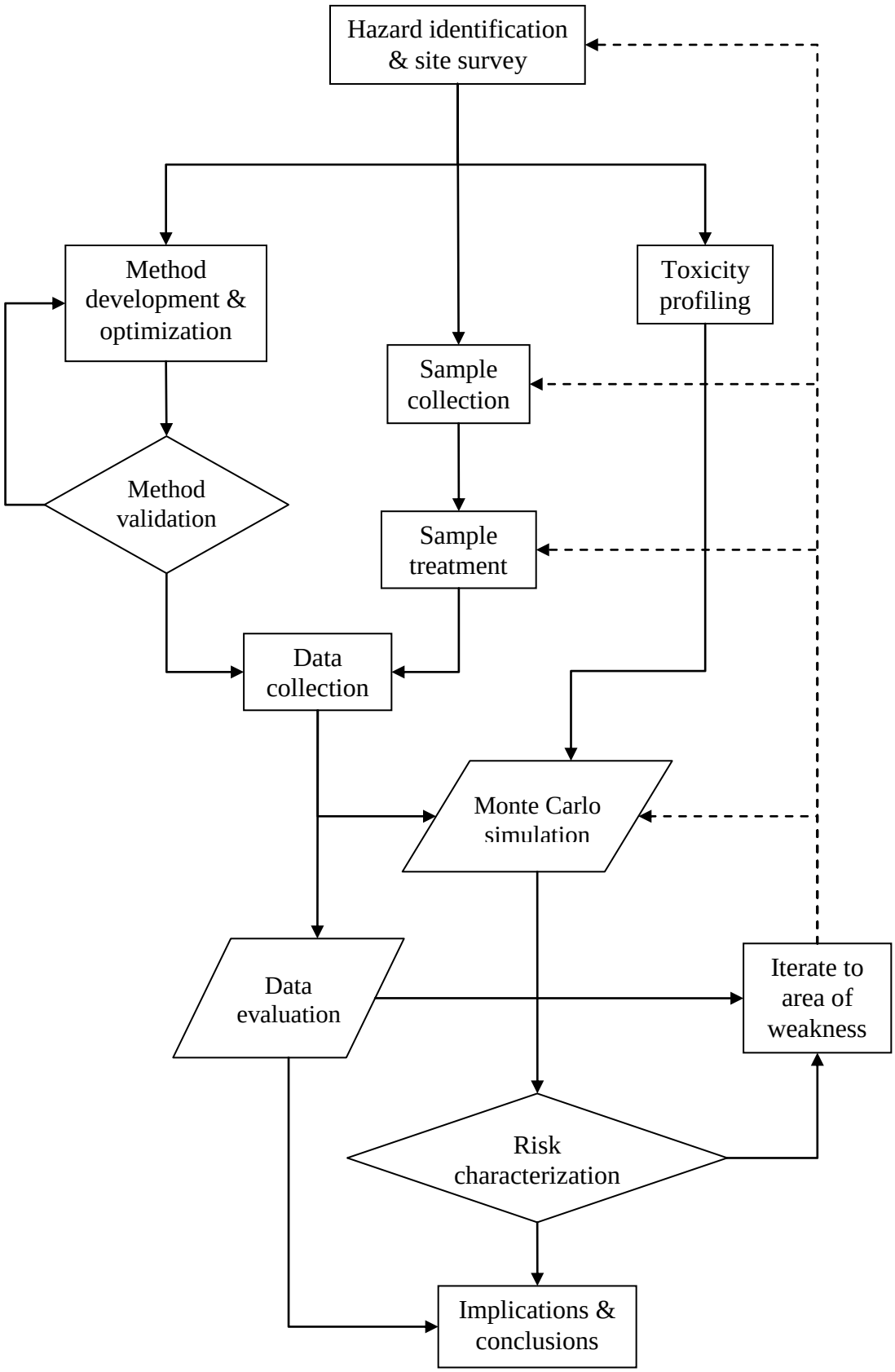

Figure 1.8 The conceptual framework

2 LITERATURE REVIEW

2.1 Profile Summaries for Hazardous Metals

Metals in the environment can generally be considered as naturally occurring constituents which are neither created nor destroyed by biological or chemical processes. However, their concentration levels may vary significantly across geographical regions due to geological processes and anthropogenic sources such as industrial and consumer wastes. Commercial processes such as mining, agriculture, manufacturing and the discarding of wastes in landfills are common sources (Samecka-Cymerman and Kempers, 2004). Even rainwater with its acidic pH, could cause part of the metal species to leach into the aquatic environment from the surrounding soil and rock ([Smuda et al., 2007] and [Matlock et al., 2003]). Some of these metals are dangerous to health or to the environment. Thus, the public, health professionals, scientist, regulators and also legislators have great interest in the metal concentrations in aquatic organisms especially that of commercially raised fishes.

Available information often indicate that fetuses and developing children are the most susceptible individuals, nevertheless, exposure to excessive metal concentration levels may also cause harm and even death to adults. Although documentation of human poisoning associated with consumption of metal contaminated fish is uncommon, there have been a number of catastrophic events such as the well known Minamata tragedy. Hence, quantitative assessments of these potential hazardous metals are undoubtedly essential for legislative protection of the health of fish consumers. Despite the fact that many metals may possibly cause hazardous impacts on humans, only cadmium, lead and mercury which have been proven hazardous in nature are included in the Commission Regulations of the European Union (EC 2001) for fish and fishery

products. United States Environmental Protection Agency (USEPA) has recommended that arsenic, cadmium, mercury and selenium as target analytes in screening studies since they have been identified as having the greatest potential toxicity resulting from ingestion of contaminated fish (USEPA, 2000a). Toxic effects of these metals are well recognized and have been described in numerous sources. Major sources used in this study are the Integrated Risk Information System (IRIS) database, Agency for Toxic Substances and Disease Registry (ATSDR) Toxicological Profiles, World Health Organization (WHO) Environmental Health Criteria monographs and some reviews.

2.1.1 Arsenic

Arsenic is a naturally occurring element that is usually found combined with other elements in a variety of mineral ores. It is mostly mobilized under natural conditions, for instance, weathering processes, volcanic emissions, geochemical reactions and also biological activities (Mohan and Pittman Jr., 2007). Although the ultimate source of arsenic is geological, anthropogenic activities such as mining and smelting, combustion of fossil fuels, industrial wastes and agriculture practices that involve application of arsenic additives in pest control, disease prevention, grow stimulation and etc. could well introduce additional impacts (Nachman *et al.*, 2005). Substantial amount of arsenic is usually released to the aquatic environments directly or via runoff and leaching pathway (Wang and Mulligan, 2006). According to the United States Food and Drug Administration (USFDA. 1993a), 90% of oral arsenic exposure route for human is through ingestion of fish and other seafood. Yet, the toxicity of arsenicals is highly dependent upon the nature of the arsenic containing compounds (ATSDR, 2007a).

Arsenic and many of its associated compounds are recognized potent poison, particularly the inorganic arsenic which has been assigned to Toxicity Class I by USEPA based on oral toxicity tests. Oral doses approximately 600 μg kg^{-1} day^{-1} or higher have fatal impact on human (USEPA, 2000b). Furthermore, available epidemiological studies have demonstrated that chronic exposure to inorganic arsenic even at low levels is strongly associated with a wide spectrum of adverse health consequences, primary cancers (bladder, kidney, liver, lung, skin) and other diseases that are related to cardiovascular, dermal, diabetic, gastrointestinal, genotoxic, hematological, hepatic, immunological, mutagenetic, neurological, renal, respiratory effects and so forth ([Chiou *et al.*, 2005], [Yang *et al.*, 2005], [Yoshida *et al.*, 2004], [Tseng *et al.*, 2003], [Mandal and Suzuki, 2002], [Smith *et al.*, 2002], [Milton *et al.*,

2001], [Biswas *et al.*, 2000] [Tseng *et al.*, 2000], [Tsai *et al.*, 1999], [Eguchi *et al.*, 1997], [Chen *et al.*, 1992] [Endo *et al.*, 1992], [Wu *et al.*, 1989] and [Armstrong *et al.*, 1984)]). Based on the IRIS (1988a) database, the oral cancer slope factor (*CSF*) of inorganic arsenic is 1.5×10^{-3} per μg kg^{-1} day^{-1} while the chronic reference dose (*RfD*) is 0.3 μg kg^{-1} day^{-1} based on a no observed adverse effects level (*NOAEL*) of 0.8 μg kg^{-1} day^{-1} with an uncertainty factor of 3.

Vast numbers of population particularly those in Asian countries are suffering from a variety of adverse health problems due to arsenic contamination from natural groundwater as well as industrial sources (Brammer and Ravenscroft, 2009). In this regard, USEPA (1975) and WHO (2001) have recommended a provisional guideline concentration of 10 μg l^{-1} arsenic in drinking water. A well known incident is arsenic contamination in natural groundwater on the southwestern coastal of Taiwan that leads to hyperpigmentation, keratosis, Blackfoot disease (BFD) and some cases of cancer (Tsai *et al.*, 1998). BFD is a severe peripheral vascular disease which ultimately leads to necrosis and gangrene and has not been observed in other parts of the world ([ATSDR, 2007a], [Tseng, 2005] and [Tseng, 2002]). According to Huang *et al.* (2003) study, the arsenic content of tilapias from aquaculture farms in BFD hyperendemic areas in southwestern Taiwan significantly increase with the arsenic levels in their culture sites. They reported that the percentage of inorganic arsenic in those tilapias (~7.4%) was higher compared to other seafood survey. Moreover, Wang *et al.* (2007) claimed that considerably high concentrations of arsenic were found bioaccumulated in aquaculture tilapias from those areas, where the concentration level was greater than that of marine fish, shellfish as well as other freshwater fishes. Therefore, it is suggested that based on all these, tilapia consumption might lead to potential health risks. Indeed, findings from Ling & Liao (2007), Jang *et al.* (2006) and Liao & Ling (2003) have indicated that

ingesting tilapia farmed in those regions poses potential cancer threats to Taiwan's population.

Similarly, numerous studies have documented that the groundwater and agricultural produce collected from the arsenic-affected blocks of Bangladesh contain significant levels of arsenic ([Azizur Rahman *et al.*, 2008], [Al Rmalli *et al.*, 2005] and [Das *et al.*, 2004]). In this regard, it is also reported that millions of inhabitants in these arsenic epidemic areas are at risk and part of them are suffering from arsenicosis indeed ([Chakraborti *et al.*, 2010], [Paul, 2004], [Mandal and Suzuki, 2002] and [Chowdhury *et al.*, 2001]). The original source of arsenicals in these regions has been suggested to be mainly derived from arsenic rich pyrite, which can be mobilized and redistributed under a series of redox reactions, ionic competitions and other undisclosed mechanisms ([Selim Reza *et al.*, 2010], [Zheng *et al.*, 2004] and [Nickson *et al.*, 2000]).

Besides these, a number of arsenic poisoning episodes due to industrial sources have also been documented globally. For instance, inhabitants nearby Toroku, Matsuo and Nakajo in Japan were diagnosed as suffering from chronic diseases associated with arsenical releases from factories in those areas (Mandal and Suzuki, 2002). All these incidents do not occur spontaneously where the sources can be traced back through time in many cases, thus, monitoring and assessment programmes are indispensable against arsenical risks.

2.1.2 Cadmium

Cadmium is very rare in nature and its compounds are often found in small quantities mixed in with the ores of other metals like zinc, lead, mercury and copper. Although geochemical sources of cadmium may be significant in some regions, the anthropic sources play a much greater part. Numerous field studies have revealed that there are varying degrees of cadmium contamination in aquatic systems due to direct or indirect inputs that are associated with industrial processes such as mining, smelting, refining, electroplating, manufacturing of paints, alloys, batteries, plastics as well as applications of pesticides and phosphate fertilizers in agricultural sectors ([Barton, 2010], [Cambier *et al.*, 2010] and [Hutton, 1983]). The great mobility of cadmium facilitates its dispersion in the biosphere. Consequently, it is not surprising that cadmium has been found to bioaccumulate in the tissues of fish and shellfish.

Cadmium is a hazardous substance with an extremely long biological half-life, which has been estimated at 10 to 30 years (USFDA, 1993b). Based on ATSDR (2008), it has been identified that long-term dietary intakes are the most worrying cadmium exposure pathway in humans with the exception of smoking (Lindén *et al.*, 2003). Due to intrahuman variability in cadmium sensitivity, USEPA has recommended an oral *RfD* of 1 $\mu g\ kg^{-1}\ day^{-1}$ with uncertainty factor of 10 based upon a *NOAEL* of 10 $\mu g^{-1}\ kg^{-1}\ day^{-1}$ derived from proteinuria studies in multiple humans (IRIS, 1987a).

The kidneys, liver, bones, respiratory and cardiovascular systems are the most obvious targeted sites in humans depending on the administration route of cadmium (WHO, 1992). Thus, relatively greater levels of cadmium are usually found bound to metallothionein in the respective organs. However, excessive cadmium exposure are associated with a wide variety of diseases such as anemia, anosmia, emphysema,

hypertension, kidney dysfunction, renal damage, osteoporosis and cancers ([Comelekoglu *et al.*, 2007], [Satarug *et al.*, 2002], [Uriu *et al.*, 2000], [Järup *et al.*, 1998], [WHO, 1992] and [Nakagawa *et al.*, 1990]). These include the well known itai-itai disease which impairs kidney function and progressively causes osteomalacia. This outbreak was documented and was caused by chronic cadmium poisoning due to improper handling of mining discharge in Toyama Prefecture and is regarded as one of the Four Big Pollution Diseases of Japan along with Minamata disease, Niigata Minamata disease and Yokkaichi Asthma (Almeida and Stearns, 1998).

In commercially raised fish, cadmium content is not only subjected to its availability in the environment but also to the fish feed compositions (Martins *et al.*, 2010). Depending on water chemistry effects, Wu *et al.* (2007) demonstrated that significant amount of cadmium could be accumulated in muscles (as well as gills, intestine, kidneys, liver) of aquacultured hybrid tilapias through water exposure compared to the controls. Similar findings had also been reported by Nogami *et al.* (2000) concerning dietary cadmium exposure in tilapias. They disclosed that noticeable amount of cadmium in muscles and viscera of control specimens were associated with cadmium content in pellets of commercial feed used. Based on these, cadmium should be included in all monitoring programs.

2.1.3 Lead

Pure lead element is extremely rare in nature. Its presence is incorporated with other elements as minerals scattered in deposits. Besides natural geochemical processes such as superficial soil erosion and atmospheric deposition, lead is widely dispersed as a contaminant derived from anthropic sources which include mining, smelting, plumbing, soldering, leaded gasoline, lead paints, lead-acid batteries, lead based semiconductors, polyvinyl chloride (PVC) plastic and pesticides (Al-Saleh *et al.*, 2009). As a result of accumulation and subsequent redistribution, lead is present in the tissues of fish that serve human consumption. According to a long-term exposure study conducted by Pizzol *et al.* (2010), it is confirmed that the critical route for non-occupational lead exposure is through ingestion which accounts for 99% of total lead intake.

Lead is insidious with negative health effects on individuals, particularly infants and young children. It has been shown to impair several organs and organ systems, including the haematopoietic, nervous, renal, cardiovascular, reproductive and immune systems which substantially lead to aminoaciduria, anemia, hypertension, miscarriage, neuropathy, neurocognitive and neurobehavioral disorders ([Counter et al., 2008], [Meyer et al., 2008], [Bellinger, 2005], [Xie and Yan, 2005], [Bellinger and Needleman, 2005] and [Liu, 1999]). Besides that, there have also been collective experimental results from animal studies suggesting an association between long-term lead ingestion and human carcinogenesis (WHO, 1995). As a result, the USEPA deemed it as "probable human carsinogen" (Group B2). However, existing epidemiological studies have not resulted in definitive evidence of a clear threshold in humans. On this basis, ATSDR and USEPA considered that it was inappropriate to develop minimum risk levels (MRLs) and *RfD* for lead ([ATSDR, 2007b] and [IRIS, 1988b]). Even so, a provisional tolerable weekly intake (PTWI) of 25 μg kg^{-1} $week^{-1}$ was recommended by

Joint FAO/WHO Expert Committee on Food Additives based on a model indicating daily intakes of lead between 3-4 μg kg^{-1} body weight by infants and children and is not associated with an increase in blood lead levels (FAO/WHO, 1999).

Bioaccumulation of lead in commercially valuable fish species for human consumption has been documented in several literatures ([Mendil *et al.*, 2010], [Storelli, 2008], [Celik and Oehlenschlager, 2007] and [Ureña *et al.*, 2007]). The corresponding lead concentrations might vary considerably with respect to both the species and geographical origins and in some cases even exceeded the permissible limit. Qiu *et al.* (2010) have suggested that potential human health risk may be associated with elevated levels of lead in farmed pompanos and snappers from South China. The major factors behind the accumulation may be related to feeds and/or sediments, as high concentrations of lead were also detected in those samples from the relevant sites. Indeed, experimental investigation on tilapia has indicated that dietary lead can be accumulated in various tissues including muscles (Dai *et al.*, 2010).

2.1.4 Mercury

Mercury is widely distributed in the environment in several forms primarily due to natural processes such as volcanic activities, forest fires, geologic deposits and erosions ([Yudovich and Ketris, 2005], [Gustin, 2003] and [Brunke *et al.*, 2001]). In addition to these, human activities also contribute noticeably to the dispersion of mercury into the biosphere. The major anthropogenic sources include mining and smelting, combustion processes related to power generation and waste incinerators, agricultural practice that utilizes pesticides/fungicides and industrial processes that involve the manufacture of metals, alkali, cement, batteries, papers and paints ([Park *et al.*, 2008], [Zhang and Wong, 2007], [Wong *et al.*, 2006], [Lee *et al.*, 2004], [Southworth *et al.*, 2004], [Wang *et al.*, 2004] and [Camargo, 2002]). These ultimately end up in landfills or incinerators. Much of the mercury eventually finds its way into aquatic food chains via a series of biogeochemical processes which progressively lead to bioaccumulation and biomagnification of methylmercury species in fish. Although the exact mechanisms remain largely unknown and may well vary among ecosystems, fish consumption is the general exposure pathway associated with mercury risk in humans (Berzas Nevado, 2010).

Methylmercury is the most important species of mercury in term of its toxicity and health effects from environmental exposures. This is more so as far as oral exposures through fish ingestion is concerned, since it is the predominant form of mercury in fish tissues (Chien, 2007). The central nervous system appears to be most sensitive to mercury toxicity in humans, although acute high-level exposures could also result in kidney failure, gastrointestinal damage, cardiovascular collapse and death with an estimated lethal dose of 10-60 mg kg^{-1} (ATSDR, 1999). Chronic exposures to relatively low concentration of mercury may give rise to a variety of health risks

especially in fetuses, children and pregnant women (Zahir *et al.*, 2005). Based on the limited data of neurologic changes in Iraqi children who had been prenatally exposed to methylmercury, an oral *RfD* of 0.1 μg^{-1} kg^{-1} day^{-1} with a composite uncertainty factor of 10 was derived by USEPA (IRIS, 1987b). On the other hand, due to limited evidence in experimental animals and inadequate data in epidemiological studies, USEPA has not worked out quantitative carcinogenicity for methylmercury.

Among the mercury poisoning episodes, Minamata disease is the first reported widespread outbreak associated with the ingestion of fish contaminated by methylmercury from industrial effluents discovered in Minamata City in Kumamoto Prefecture, in 1956 and Niigata City, Japan in 1965 (Harada, 1995). Minamata disease is a neurological syndrome characterized by a long list of symptoms including sensory disturbances, impairment of peripheral vision, paresthesia, incoordination of movements etc. (Ekino *et al.*, 2007). Epidemics of similar neurological disorders were reported in Iraq in 1956 and 1960 as a consequence of consuming flour from seed grain that had been treated with a mercury containing fungicide (WHO, 1990).

These incidents have raised enormous concerns, particularly the potential human health risk through fish consumption associated with mercury bioaccumulation and biomagnification. In a field study, Zhou & Wong (2000) have shown that mercury levels in aquacultured freshwater fish are primarily affected by their ambient concentrations and feeding behaviors. Based on biokinetic modeling results, Wang *et al.* (2010) further attested that the most significant pathway for mercury accumulation in farmed freshwater tilapia was through trophic transfer, where methylmercury was the predominant species under natural conditions. In this regard, consumption of predatory fish would definitely give rise to greater health risks.

2.1.5 Selenium

Selenium is widely, though unevenly distributed over the environment. Significant amounts of selenium are often found in soils and sediments which are easily leached into aquatic environment by natural processes such as run-off and weathering (Navarro-Alarcon and Cabrera-Vique, 2008). In addition to these, industrial and agricultural activities have also hastened the selenium dispersion ([Hamilton, 2004], [Lemly, 2004] and [Johns *et al.*, 1988]). Agricultural drain water, feed additives, fertilizers, pesticides, sewage sludge; fly ash from coal-fired power plants, oil refineries, and mining made selenium available to biota in aquatic environment ([Xie *et al.*, 2006], [Mars and Crowley, 2003], [Lemly, 2002] and [Peters *et al.*, 1999]). Its propensity to bioaccumulate within the base of food webs leads to potential toxicological impact and change in aquatic communities as well as humans ([Schmitt and Brumbaugh, 1990] and [Zhang *et al.*, 1990]). According to WHO (1986), fish is considered an important source of dietary selenium for the general population in most countries (Svensson *et al.*, 1992).

Selenium is an essential trace nutrient of fundamental importance to human health with a recommended dietary allowance of about 0.8 μg^{-1} kg^{-1} day^{-1} for adults (ATSDR, 2003). Selenium deficiency may cause hypothyroidism, ischaemic heart disease, Keshan disease and Kashin-Beck disease ([Choi *et al.*, 2009], [Hartikainen, 2005], [Ellis and Salt, 2003], [Johnson *et al.*, 2000] and [Suadicani *et al.*, 1992]). Despite that, exposure rate exceeding tolerable upper limit level of ~5.7 μg^{-1} kg^{-1} day^{-1} recommended by the Food and Nutrition Board (United States National Academy of Science) can also results in selenosis (USNAS, 2000). Acute selenosis is strongly associated with difficulty in walking, cyanosis of the mucous membranes, labored breathing and even death; while subacute cases include neurological dysfunction and respiratory distress (IRIS, 1991).

Prolonged exposure to moderate doses of selenium may well lead to anorexia, dermatitis, fatigue, gastroenteritis and hepatic degeneration ([ATSDR, 2003], [IRIS, 1991] and [WHO, 1986]). In some high-selenium areas of China, chronic selenosis have been reported associated with peripheral anesthesia and pain in the limbs; even exaggerated tendon reflexes, convulsions, paralysis/hemiplegia have been reported in extreme cases (Yang *et al.*, 1983). In this regard, a chronic toxicity of 5 μg^{-1} kg^{-1} day^{-1} with an uncertainty factor of 3 was also derived for selenium and selenium compounds by USEPA, based on a *NOAEL* of 15 μg^{-1} kg^{-1} day^{-1} level derived from a human epidemiological study (IRIS, 1991).

Similar to mercury, bioaccumulation and biomagnification of selenium in fish are predominated by dietary exposures, although other exposure pathways under elevated ambient concentrations may also exist (Lemly, 1997). Thus, utilization of the formulated or supplemental feeds in aquaculture industry which is intended to enhance the quantity and/or quality of fish considerably determine the benefit-risk balance related to its selenium content (Elia, 2011).

2.1.6 Other Metals

Other metals such as copper, iron, manganese and zinc are generally considered as essential nutrients for human health and life. Their nutritional importance in supporting biochemical processes have been extensively reviewed in numerous literatures and reports ([Dennehy and Tsourounis, 2010], [Cashman, 2006], [Raghunath *et al.*, 2006], [Benton, 2001] and [House, 1999]). On the other hand, the details concerning roles of cobalt, nickel and vanadium in biological systems remain largely unclear. Notwithstanding their health benefits, these metals could well pose hazardous effects if their exposures are excessive and thus they are regularly included in several reported works as well as in this study ([Qiu *et al.*, 2010], [Mendil *et al.*, 2010], [Allinson *et al.*, 2009], [Gladyshev *et al.*, 2009], [Ling *et al.*, 2009], [Chi *et al.*, 2007], [Cheung and Wong, 2006], [Lin *et al.*, 2005], [Allinson *et al.*, 2002] and [Han *et al.*, 1998]).

2.2 Analytical Options for Metal Analysis

In general, quantification of metals in an analytical solution can be accomplished via a wide variety of end-determination methods. Instrumentation techniques such as flame atomic absorption spectrometry (FAAS), inductively coupled plasma-mass spectrometry (ICP-MS) and alternative spectrophotometric methods can be considered to be of greatest practical importance for most metals.

2.2.1 Flame Atomic Absorption Spectrometry

Since the introduction of atomic absorption spectrometer (AAS), it remained one of the popular instruments for the determination of major or minor inorganic elements in agriculture, biology, environmental, food, medicine studies (Reilly, 2002). This is due to the fact that the instrument is relatively inexpensive and easy to handle even without a formal training in analytical chemistry. The general principle behind the operation of AAS is based on the fact that ground-state atoms absorb optical radiation at the same wavelength at which they emit (Kirchhoff and Bunsen, 1860). Thus, the concentration level can be confidently established from respective absorbance in accordance to Beer-Lambert Law.

Basically, this technique makes use of absorption of optical radiation by free atoms in the gaseous state for assessing the concentration of an element in a sample with the aid of standards. In order to promote ground-stage gaseous atoms for spectrometry analysis, it often requires an atomizer such as flames, electrothermal or plasma that operates at a high temperature. Sometimes it also involves cold-vapour or hydride generation depending on the objectives of the study and available resources. Of these, flame atomic absorption spectrometer (FAAS) is considered as the oldest and most commonly used of all the atomic spectrometry method. It is a relatively low

operating cost technique where principally an air/acetylene or a nitrous oxide /acetylene flame is applied to desolvate, vaporize and atomize the sample. Figure 2.1 represents the atomization processes in FAAS. Once the analyte is atomized, its concentration level can be derived from the attenuation of incident hollow cathode radiation that travels through the flame (Figure 2.2).

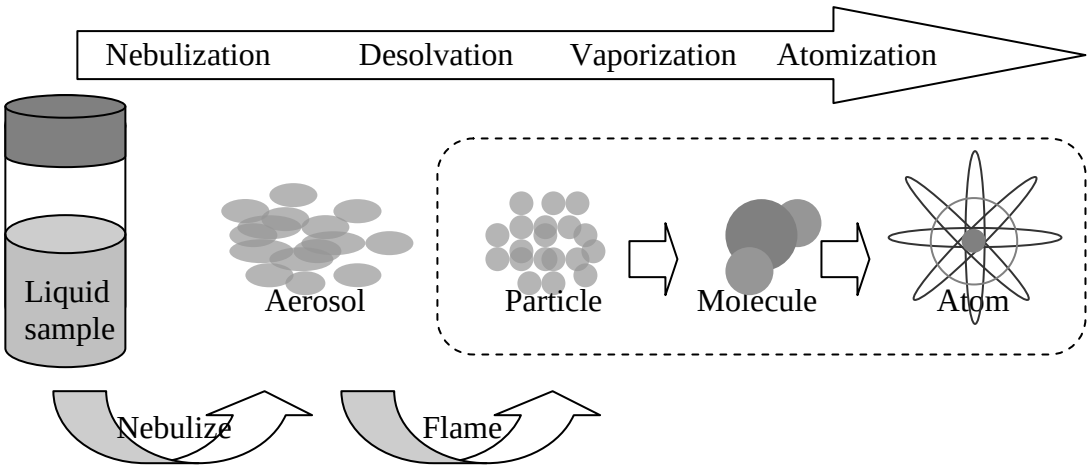

Figure 2.1 Schematic illustration of atomization processes in FAAS

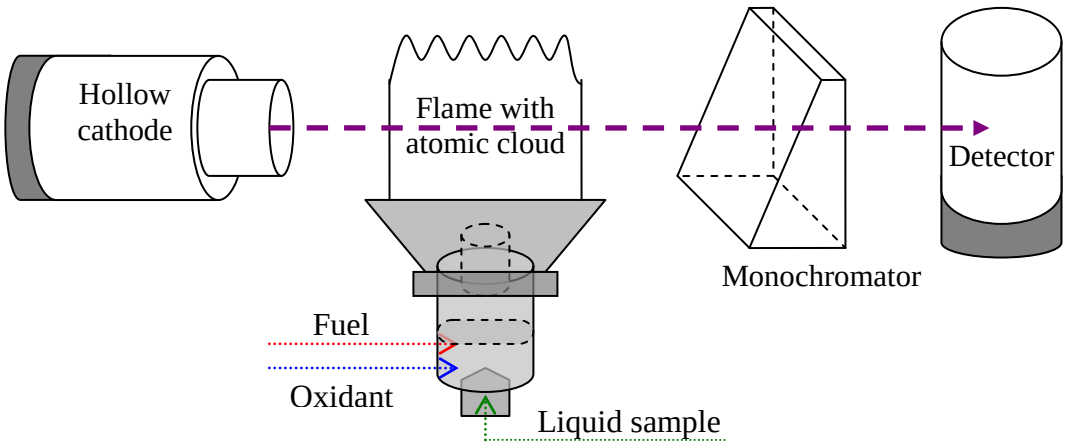

Figure 2.2 Schematic diagram of FAAS

However, the use of a flame limits the excitation temperature reached by a sample, consequently prohibits the atomization stage of refractory elements like B, Mo, V, Zr and etc. As a result, the sensitivity for these elements is not as good as other analytical techniques. On the other hand, high flame temperature can lead to undesired ionization of alkali and alkali earth elements in a sample matrix. This not only deteriorates the sensitivity of those easily ionizable elements, but also brings about unexpected increase in analytical signals of other targeted elements as a consequence of ionization suppression.

.

Despite these shortcomings, FAAS have been an adequate technique for most routine applications. Its application in assessing concentrations of certain elements in various environmental matrices has been extensively documented, particularly in fish species. Karadede & Ünlü (2000) used FAAS for quantifications of Cd, Co, Cu, Fe, Hg, Mn, Mo, Ni, Pb and Zn in environmental samples (include six fish species) from the Atatürk Dam Lake, Turkey. They reported that Cd, Co, Hg, Mo, and Pb are always below the instrument detection limits. These might be due to the moderate instrumental detection limits, flame atomization efficiency as well as the nature of those samples. Thus, in order to improve the overall method detection limits, major sample pretreatment such as separation or preconcentration steps are often required for determination of certain trace metals in a particular matrix priori to FAAS runs ([Divrikli *et al.*, 2007], [Venkatesh and Singh, 2005], [Gurnani *et al.*, 2003] and [Matoso *et al.*, 2003]). In this regard, Cesur (2003) applied solid-phase extraction method for the pre-concentration of Cd, Cu, Mn and Pb in water samples prior to FAAS determination. Citak *et al.* (2009) demonstrated the simultaneous coprecipitation technique using zirconium (IV) hydroxide prior to FAAS determination of Cd, Co, Cu, Fe, Ni and Pb in food samples. This technique has shown reasonable improvement of

overall detection limits, yet Cd, Co, Ni and Pb remain undetected in most samples which is possibly due to the nature of the samples and limitation of the FAAS technique.

Graphite furnace on the other hand, can enhance the detection limits by increasing the atom density and residence time of corresponding analytes during AAS operation. Atomization techniques such as cold-vapour for Hg analysis and hydride generation for quantification of As, Bi, Sb, Se, Te, Tl, Pb and other metals can also lead to better detection limits. These techniques take a longer run time, despite being more sensitive and selective. In addition to FAAS determination of Cu, Fe and Mn in environmental samples (sediment, water and fish) from the southern Atlantic coast of Spain, Usero *et al.* (2004) have also used graphite furnace atomic absorption spectrometer (GFAAS) for Cu, Cd, Cr, Ni, and Pb, cold-vapour and hydride generation techniques for Hg and As.

Several researchers from Turkey have also demonstrated the application of GFAAS as a conjugate to FAAS for the determination of those elements that are usually present in trace amounts in environmental samples. Dalman *et al.* (2006) have utilized FAAS to assess Cu and Zn levels in sediment and fish samples from the Southeastern Aegean Sea, while levels of Cd and Pb were evaluated by GFAAS. Likewise, Erdoğrul & Erbilir (2007) used FAAS to monitor concentrations of Fe and Mn in 108 individual fish samples from Sır Dam Lake, Kahramanmaraş, and utilized GFAAS in the analysis of Co, Ni and Pb. Recently, Mendil *et al.* (2010) also adopted a similar strategy to investigate seasonal metal content in commercially valuable fish species from Black Sea, where concentrations of Cu, Fe, Mn and Zn were evaluated using FAAS while determination of Cd, Co, Cr and Pb were carried out with GFAAS.

2.2.2 Inductively Coupled Plasma-Mass Spectrometry

ICP-MS is widely acknowledged as the premier technique for simultaneous trace elements analysis. It basically engages coupling together of an inductively coupled plasma (ICP) as a source to dissociate the sample into its constituent ions, with mass spectrometer (MS) as a method to quantify the resulting ions (Figure 2.3). Figure 2.4 illustrates a schematic of ICP-MS (Agilent, 2005a). The operation involves using high temperature argon plasma generated under a radio frequency and magnetic field in order to desolvate, decompose, vaporize and atomize the aerosol of nebulized sample and ionize the atoms. Consequently, the resulting positively charged sample ions are extracted through interface cones, and focused by a series of electrostatic lenses toward the mass analyzer in a compacted "ion beam" for further quantification based on their mass to charge ratio (m/z). ICP-MS is associated with wide elemental coverage, fast analysis times, dynamic analytical working range and very low detection limit. However, all these have to be compromised with higher capital and operation costs as well as skilled personnel compared to methods mentioned previously.

Notwithstanding the ICPMS advantages, there are some elements that remain poorly detected. This is mainly due to the direct and/or indirect interferences derived from the plasma gas, matrix components, or the solvent system used to prepare the sample solution (Nam *et al.*, 2008). As in other analytical techniques, both sensitivity and specificity can be improved by elimination of those spectral or non-spectral interferences.

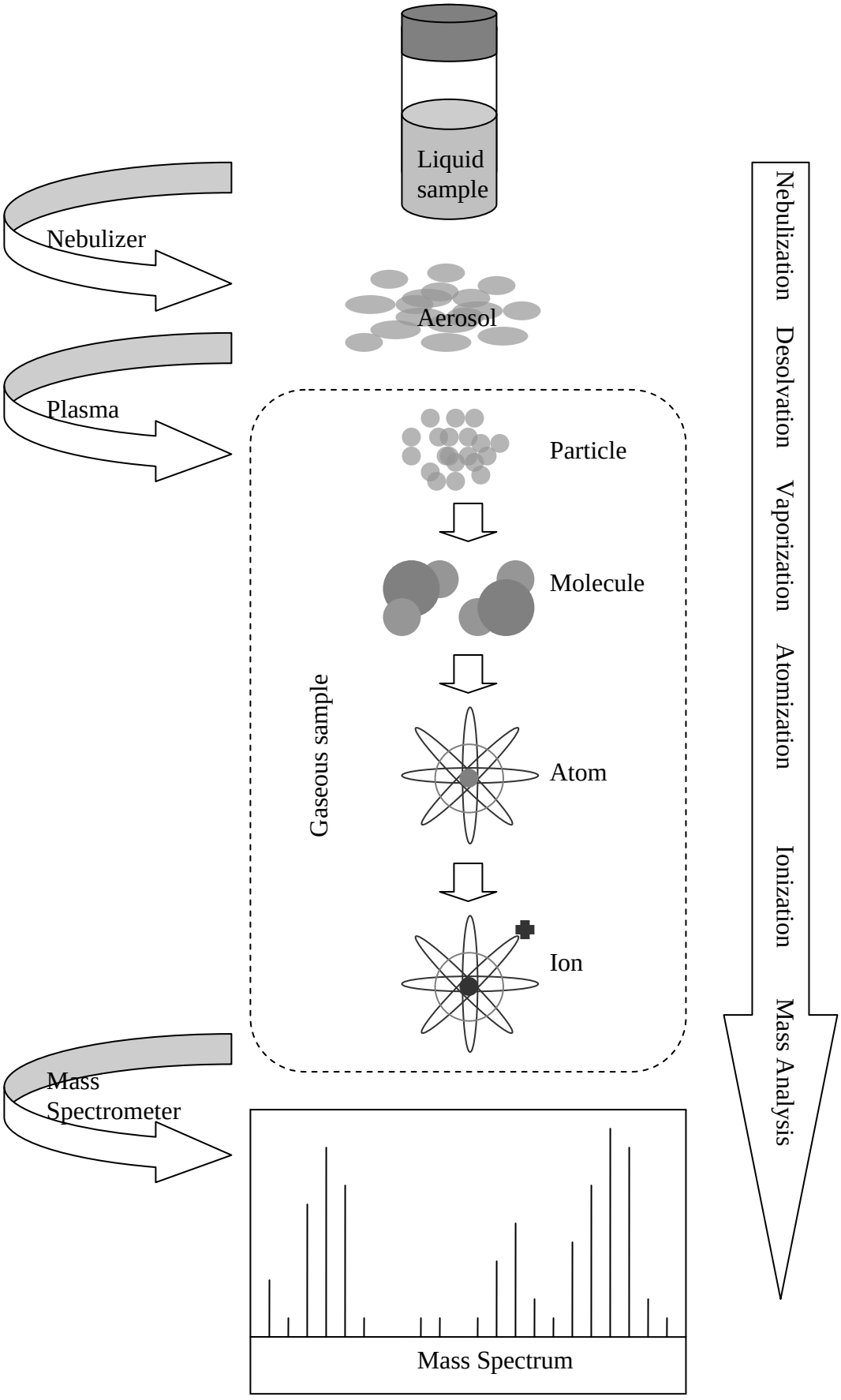

Figure 2.3 Schematic illustration of ionization process in ICP-MS (Agilent, 2005a)

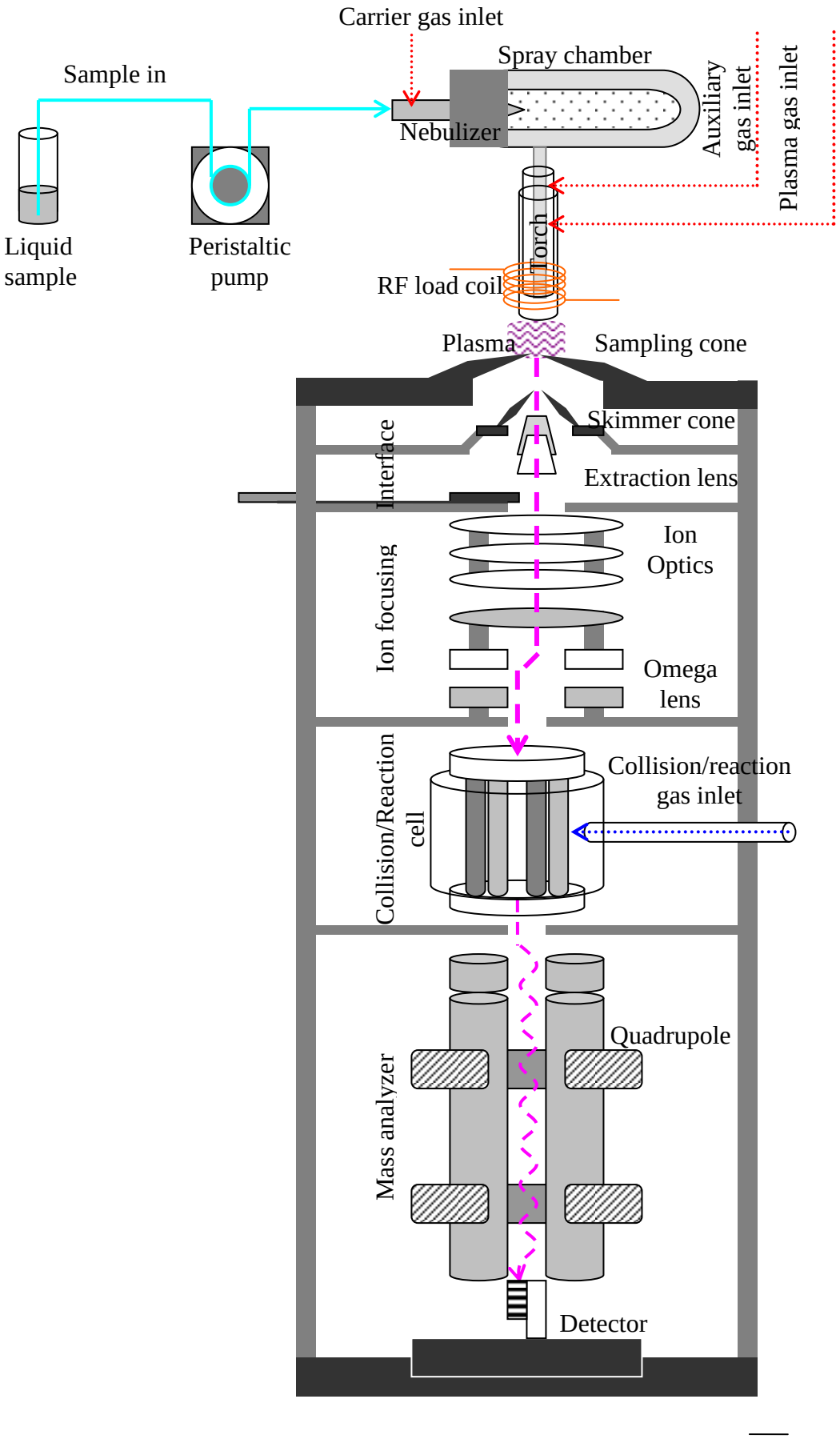

Figure 2.4 Schematic diagram of ICP-MS (Agilent, 2005a)

The most common circumstances for handling the predictable interference associated with non-analyte peaks involve utilizing alternative isotopes with lower natural abundances that does not suffer from any isobaric overlap and/or by elemental correction equations (USEPA, 1994). At the same time, proper isotope selection can also help to avoid doubly charged interferences resulting from secondary ionization. Yet, not all determinations are so straightforward, specifically, the quantification of ultratrace elements such as K, Ca, Fe etc. that suffer from major polyatomic plasma-based interferences due to plasma conditions.

The "cool" plasma approach is another very efficient way to overcome these problems. It adopts a lower plasma power to reduce the formation of argon-based interferences and also effectively remove the background signal due to easily ionized elements such as Na and Li. Unfortunately, operation under cool plasma conditions also bring in some difficulties for general analysis, most particularly poorer matrix tolerance due to less effective decomposition of molecular ions e.g. oxide species (Cornelis *et al.*, 2003). This can be overcome by using high resolution ICP-MS which allows polyatomic spectral interferences to be characterized using exact mass measurements. However, the cost of such instrument is very high compared to quadrupole instruments.

Under cost constraints, it is sometimes suggested that normal quadrupole ICP-MS technique equipped with collision/reaction cell (CRC) could be an alternative approach for the attenuation of these spectral interferences. This interesting approach has proved suitable for determination of multi-elements in complex matrices in one fell swoop, where the source and level of potential spectral interferences cannot easily be predicted (Fong *et al.*, 2009). In this technique, various gases can be efficiently employed in CRC prior to MS determination to reduce/eliminate those polyatomic ions

with larger atomic radii compared to analyte ions of similar mass by either chemical reaction, collisionally induced dissociation (CID) or kinetic energy discrimination (KED) ([Dufailly *et al.*, 2008], [Chen *et al.*, 2007], [Darrouzès *et al.*, 2007], [Tanner *et al.*, 2002] and [Tanner and Baranov, 1999]). In this regard, the chemistry and flow rate of the CRC gases are the significant parameters which affect both the background and analytical signals.

2.2.3 UV-Visible Spectrophotometric

Secondary UV-Visible spectrophotometric methods based on various chromogenic reagents offer far more economic ways for rapid determination of metal ions, compared to the abovementioned means (Eskandari *et al.*, 2006). This is the instrumental technique of choice in most laboratories, owing mainly to its simplicity that often demands very low cost equipment and cheap metallochromic indicators (Khoshayand *et al.*, 2008). In general, this technique makes use of absorption of light in UV or visible region by metal complexes under a specific condition to ascertain the concentration of corresponding metal ion in a sample solution in accordance to Beer-Lambert Law (Figure 2.5).

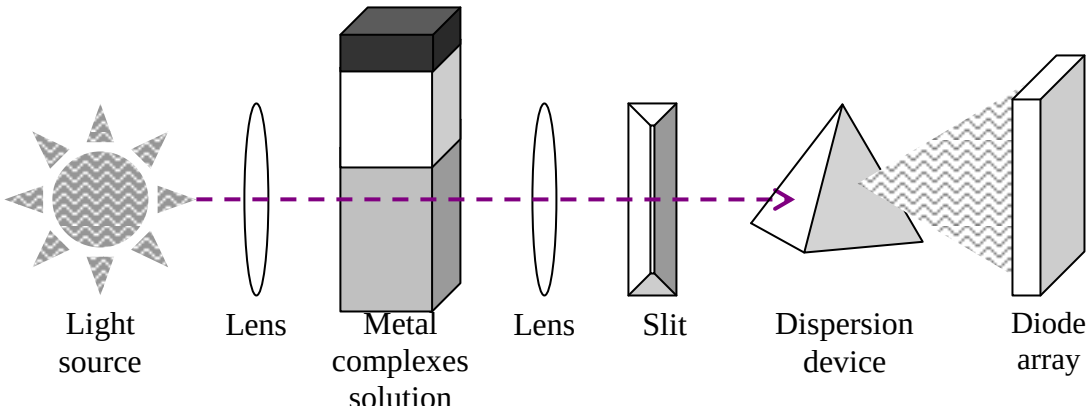

Figure 2.5 Schematic diagram of UV-Visible Spectrophotometer

However, the price to pay for performing spectrophotometric determination of metals under conventional approach is lack of specificity due to poorly resolved spectral lines in the case of constituent mixtures. To a certain extent, these may well hinder the calibration process, so a preliminary sample treatment is required, such as addition of suitable buffers and masking agents or extraction/separation step which definitely makes the operation laborious (Ghavami *et al.*, 2008). Yun & Choi (2000) have demonstrated the application of 1-Nitroso-2-naphthol as a chromogen for colorimetric

determination of Fe(III), Co(II), Cu(II) and Ni(II) in presence of Tween 80 under different pH conditions and masking agents. Zhang *et al.* (2005) used 2-(8-quinolylazo)-4,5-diphenylimidazol to chelate Cd(II), Co(II), Ni(II) and Zn(II) where subsequent to a reverse phase-high performance liquid chromatography (RP-HPLC) separation, UV-visible quantification of those metal chelates were carried out.

Alternatively, chemometric tools allow achieving of quantitative information from such systems without major pretreatment, where multivariate calibrations ease the interpretation of complicated spectra in real matrices (Abdollahi *et al*., 2003). In other words, employing chemometric methods enable compensation of interference, where multivariate calibration is performed by ignoring the concentration of all other components except the analyte of interest ([Niazi and Yazdanipour, 2008] and [Raimundo Jr. and Narayanaswamy, 2003]). For instance, partial least square (PLS), principal component regression (PCR) and artificial neural networks (ANNs) have been successfully applied for simultaneous determinations of metals in different matrices ([Moneeb, 2006], [Pettas and Karayannis, 2003] and [Ni *et al.*, 2002]). The details will be discussed in the following section.

2.3 Application of Chemometric Tools

Application of chemometric tools is widespread since the availability of personal computer and proliferation of commercial statistical and mathematical software. Notable expansions include the areas of agricultural, biological, environmental, food, forensic, medical, material and pharmaceutical sciences ([Madsen *et al.*, 2010], [Mas *et al.*, 2010], [Brown *et al.*, 2009] [Paul, 2009], [Brereton, 2007], [Escandar *et al.*, 2006], [Munck *et al.*, 1998] and [Berridge *et al.*, 1991]). The discipline of chemometrics originated in chemistry where many chemical problems typically involve the evaluation of chemical data generated by analytical instruments and study of quantitative structure-activity relationships (QSAR). According to Otto (2007) the actual definition of chemometrics is *"the chemical discipline that implements statistic and mathematic approaches to plan and identify optimal experimental processes and/or to evaluate chemical data for maximum information."*

2.3.1 Multivariate Calibrations in Spectrophotometric Metal Analysis

Since the development of photodiode array that is capable of rapid scanning of full spectra, multivariate regression and prediction has become indispensable tools for quantitative spectrophotometric analysis of complex mixtures. Over the years, chemometric tools such as principal component regression (PCR) and partial least squares (PLS) have been found to be effective for simultaneous determination of components in mixtures associated with high degree of spectral overlapping. The mathematical principle behind these algorithms have been well documented ([Zhang and Pan, 2011], [De Luca *et al.*, 2009], [Khoshayand *et al.*, 2008], [Ni *et al.*, 2005], [Brereton, 2003b] and [Ni, 1993]). The use of multivariate calibration techniques can avoid the process of pre-separation or extraction compared to conventional univariate calibrations.

2.3.1.1 Principal Component Regression

PCR is generally considered as a fundamental, yet very powerful multivariate calibration technique. Its basic concept is simply a multiple linear regression (MLR) that makes use of principal component (PC) scores resulting from principal component analysis (PCA), instead of the original independent variables. In spectrometry, PCR transformation is entirely based on the maximum spectral variations without taking any account of the the analyte concentrations. A detailed description of multivariate concentration determination using PCR from the viewpoint of an analytical chemist had been written by Keithley *et al.* (2009).

The applications of PCR in the simultaneous determination of multielemental aqueous solutions with chromogenic reagents by UV-Visible spectrophotometry have been reported by some researchers. For instance, PCR technique have been adopted by Alula *et al.* (2010) for simultaneous analysis of Cu(II) and Fe(II) by UV-Vis spectrophotometry using the chromogenic reagent 8-hydroxyquinoline at pH 4.0. Ghasemi & Niazi (2001) applied PCR for simultaneous determination of Co(II) and Ni(II) based on the absorbance spectra of 4-(2-pyridylazo) resorcinol complexed with metals at pH 8.2. Rodriguez *et al.* (1998) have also demonstrated the use of PCR for simultaneous spectrophotometric determination of Cu(II), Co(II), Fe(II), and Ni(II) with complexing agent 1,5-bis(di-2-pyridylmethylene) thiocarbonohydrazide at pH 4.0.

2.3.1.2 Partial Least Squares

Another approach, the partial least squares (PLS) have progressively become the *de facto* standard for multivariate regression and prediction (Keithley *et al.*, 2009). The term PLS have also been interpreted to signify projection to latent structures (Esbensen *et al.*, 2004). In spectrometry, PLS transformation includes both the errors associated with the analyte concentrations and the resulting spectra, whereas only the spectra errors are considered in PCR (Brereton, 2007). This slightly advantageous feature enables better estimation and is successful in some application, even if there are considerable errors in the prepared concentrations of calibration standard.

Based on this multivariate calibration technique, a number of spectrophotometric methods have also been proposed for simultaneous determination of metal ions in aqueous samples using various chromogens. For example, Zarei *et al.* (2006) have constructed PLS model for simultaneous spectrophotometric estimation of Co(II), Fe(II) and Ni(II) using complexing agent 1-(2-pyridylazo)-2-naphtol in micellar media. Gao & Ren (2005) have investigated PLS predictive ability for analyzing simultaneously Cd(II), Cu(II), Ni(II) and Zn(II) in the presence of both xylenol orange and cetyltrimethyl ammonium bromide at pH 9.22, as well as Cd(II), Co(II), Mn(II) and Zn(II) in the presence of both 2-(5-bromo-2-pyridylazo)-5-diethylaminephenol and cetyl pyridinium bromide at pH 8.0 (Gao and Ren, 1999). Ghasemi *et al.* (2004) have also applied PLS modeling to spectrophotometric simultaneous determination of Co(II), Cu(II), and Ni(II) using disodium-1-nitroso-2-naphtol-3,6-disulfonate at pH 7.5. Besides these, PLS have also been applied to the simultaneous determination of Co(II), Cu(II), Ni (II) and Zn (II) based on the formation of their complexes with zincon (Ghasemi *et al.*, 2003).

2.3.2 Experimental Designs in Microwave Assisted Sample Preparation

Microwave assisted sample preparation has certain merits over conventional techniques where the details concerning its application in analytical chemistry have been extensively discussed by Smith & Arsenault (1996). Since the introduction of microwave oven technology, a variety of microwave assisted digestion (MAD) methods have been developed in order to quantitatively prepare appropriate sample solutions for elemental analysis such as AAS, and ICPMS. From available literature, it is shown that the proposed MAD conditions and relevant reagents can be varied considerably, even if there is no significant difference between the sample matrices ([Ashoka *et al.* 2009], [Türkmen and Ciminli, 2007] and [Yang and Swami, 2007]). The variability opens up the way for further modification and improvement of MAD procedures based on available equipments.

There are several means to evaluate MAD performance. For instance, chemometric experimental designs as described in Chapter 1 allow extraction of desired information as efficient and as precise as possible. Box–Behnken design (BBD) have been applied by Khajeh & Sanchooli (2010) to optimize the irradiation power, time and temperature of microwave assisted extraction (MAE) procedure for FAAS determination of Fe and Zn in celery; Khajeh (2009) also used the same ideas in MAE optimization for Cu and Zn in wheat flour and corn bran matrices. Santelli *et al.* (2006) optimized irradiation power, time and hydrogen peroxide/nitric acid volumetric percentage in the focused-MAD of Fe, Mn and Zn in wheat flour using the Doehlert design.

All the studies mentioned are considered as single response optimizations, where a particular set of the best experimental conditions corresponds to each element. In other words, even though the elements were from exactly the same sample matrix, they require different sample preparation procedure because it is almost impossible to draw an optimum experimental condition for multiple elements, unless they have very strong correlation with one another. However, in order to assess the risk to human health from exposure to metal species, analytical laboratories are being challenged to develop techniques for a widening variety of elements. Thus, when considering more than one element, optimization becomes an issue of searching for a compromised experimental condition where performance is most satisfactory (Lewis *et al.*, 2005).

2.3.3 Pattern Recognition on Multielemental Dataset

The fluctuation of metal concentration levels across environmental samples can be due to natural variations in biology, climate, geology and/or other factors including anthropic factors. This means that the environmental dataset from elemental analysis not only reflects the metal profiles of those samples but also carries much information concerning environmental conditions. However, the relevant information cannot be easily retrieved by the naked eyes or sorted out by traditional univariate approaches due to the inherently multivariate nature of the original measurements. Thus, multivariate pattern recognition techniques such as PCA and/or factor analysis (FA) are the better options in order to gain useful insight from such data matrix.

PCA is the most basic but highly useful chemometric tool to manipulate multivariate measurements by decomposition of the original data matrix into a product of scores and loadings matrices, as well as noise (Figure 2.6). By this way, the variation in many variables can be summarized in operative reduced dimensions so as to uncover the latent structure in the data (Low *et al.*, 2009). De Andrade Passos *et al.* (2010) explored the mobility of trace metals in estuarine sediments using sequential extraction technique in conjunction with PCA. Davis *et al.* (2009) applied PCA to identify associations between metal distributions in urban and rural soils, and possible communities of sources. The metal accumulation between fish, river water and sediment samples from Catalonia was investigated by Peré-Trepat *et al.* (2007) using PCA. Although they were unable to deduce the sampling sites from their PCA results, they did identify the chemical similarities/dissimilarities among those studied metals.

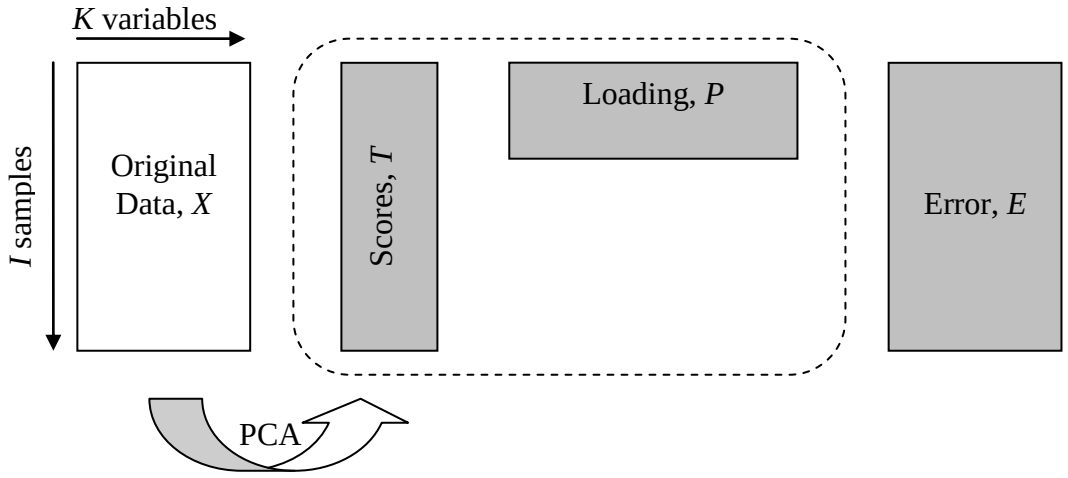

Figure 2.6 Conceptual illustration of PCA matrix transformation

3 SPECTROPHOTOMETRIC DETERMINATION OF METAL IONS USING MULTIVARIATE CALIBRATIONS

3.1 Introduction

In this chapter, a simple spectrophotometry method is proposed for the simultaneous determination of copper, nickel and zinc ions in water samples using 1-(2'-thiazolylazo)-2-naphthol (TAN). This chemometric approach was investigated and developed owing to the availability of digitized spectroscopic data, commercial statistical software and robust multivariate calibrations that allow rapid analyses of multi-component systems while avoiding preliminary treatments.

3.1.1 Background of Thiazolylazo Dye

In spectrophotometric operations, chromogenic reagents play an important role. Organic complexing agents such as 2-aminothiazole derivatives, commonly known as thiazolylazo dyes have attracted much attention not only due to the chromophoric azo groups (-N=N-) offering coloured azo-metal chelates but also because of their colour fastness and low price (Lemos *et al*., 2007). Besides application in spectrophotometry, the thiazolylazo dyes have also been successfully employed in direct titrations and liquid chromatography for analysis of many metal ions, especially for the transition metals ([Li *et al.*, 1995] and [Chromy and Sommer, 1967]). Furthermore, the limited solubility of these reagents and their metal complexes in aqueous solution allows their use in extraction and separation procedures which include solid phase, liquid-liquid and cloud point extraction ([Lemos *et al*., 2006], [Lee *et al.*, 2001] and [Visser *et al.*, 2000]).

The commercially available TAN is widely used for metal ions determination due its ability in forming azo-metal chelates with various cations depending on experimental conditions. For example, TAN mostly occur as water-soluble ions in both acidic (H_2R^+) and basic (R^-) solutions; whereas in neutral or slightly acidic/basic region, HR molecules that are soluble in organic solvents predominate (Figure 3.1). This situation can be observed from the reported pK_a (N^+H) of 1.68-2.14 and pK_a (OH) of 8.69-9.18 at 25 °C depending upon the composition of solvent mixtures and their ionic strengths (Niazi *et al.*, 2007). In this regard, Omar & Mohamed (2005) has demonstrated that the TAN complexation tendency with Cu^{2+}, Co^{2+}, Fe^{3+}, Mn^{2+}, Ni^{2+} and Zn^{2+} at 25°C are spontaneous, since their accompanying free energies of formation ($\Delta G°$) are found to be negative. In fact, there are a number of analytical applications that have been proposed concerning the analysis of transition metal ions using TAN under various experimental conditions ([Teixeira and Rocha, 2007], [Mehta *et al*., 2004], [Zaporozhets *et al.*, 1999] and [Watanabe and Matsunaga, 1976]). These techniques are basically considered as univariate approaches, where only a single metal ion can be determined under a particular experimental condition. Yet, the capability of TAN to form complexes with various cations show a great potential for application in simultaneous spectrophotometric assessment of the respective metal ions using multivariate calibration approaches.

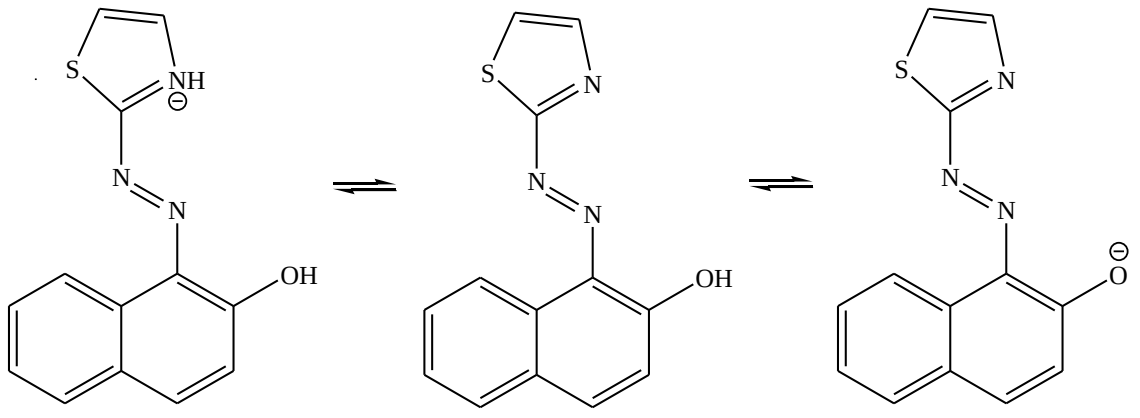

Figure 3.1 Schematic illustration of the equilibrium between the forms of TAN

3.1.2 Multivariate Calibrations

The conventional univariate calibrations that are practiced in the examples given above involved only a single absorbance at a feasible wavelength that corresponds to TAN-metal chelates absorption. Thus, models under such circumstances would be adequate if there are not any significant interference on the chosen wavelength. In fact, various factors may contribute to the measured absorbance at the studied wavelength, such as spectral overlaps resulting from non-targeted metal-azo complexes that form due to the versatility of TAN. As a consequence, the estimations are going to be biased if interfering species are not removed by physical or chemical separation before the system is subjected to spectrophotometric determination. Thus, it is suggested that multivariate calibrations using a wide distinctive range of spectrum can overcome the lack of selectivity in situations where univariate models failed. The multivariate approach can lead to a paradigm shift by considering non-traditional solution to such problems.

It is sensible to utilize a wider range of spectrum for spectrophotometric determinations rather than relying only on a single absorbance at a particular wavelength, since this can bring significant advantages (Bro, 2003). The general straightforward benefit of applying multiple redundant measurements over univariate approaches is improved precision in the estimation. Generally speaking, *n* repeating measurements will lead to reduction in the standard deviation of the mean by a factor of $\sqrt{n}$, which is commonly called signal averaging (Beebe *et al.*, 1998). Furthermore, inverse calibration approaches such as principal component regression (PCR) and partial least squares (PLS) allow condensation of the original spectral matrix (includes the concentrations matrix in PLS) into a product of manageable matrices, one contains the information of calibration samples (scores matrix), another about the spectra

(loadings matrix) and also an error matrix that is related to experimental/instrumental noise. In this regard, predictions can be made using a reduced number of factors to limit the possible errors. Besides this, one of the most pronounced reasons for using multivariate calibrations is that they allow simultaneous study of multiple metal chelates which is almost impossible with univariate analyses. This directly shortened the amount of time required for method development.

3.2 Materials and Methods

3.2.1 Instrumentation

Absorbance spectra corresponding to wavelengths from 200.0 nm to 800.0 nm were acquired using a Cary 50 UV-Visible spectrophotometer from Varian (Autralia) at 10.0 mm path length quartz cuvette from Hellma (Germany), with a scan rate of 4800nm/min. All the resulting spectra were digitized in 1.0 nm intervals by Cary WinUV, Ver. 3.00 software and exported as SPC file format for subsequent quantitative data evaluations using the CAMO® Unscrambler® V. 9.7. And a pH meter (Eutech CyberScan pH 1100, USA) was used for pH measurements.

3.2.2 Reagents and Standard Materials

All chemicals used in this work were at least of analytical grade. Ultra pure water (UPW) with resistivity more than 18MΩ cm was obtained from ELGA® *PURELAB® UHQ II* (UK).

3.2.2.1 Ammonium Acetate Stock Solution

1.00 mol dm^{-3} of ammonium acetate stock solution was prepared using *Trace*SELECT® ≥99.9999% (metals basis) quality salt from Fluka (Netherlands). It is a very cheap and widely available chemical that gives clear and colourless solutions suitable for use in spectrophotometry for maintaining the pH of sample solutions (pH 6.7).

3.2.2.2 TAN Stock Solution

Stock solution of chromogenic reagent consisting ~ 0.70 g L^{-1} TAN was prepared by dissolving the required amount of 1-(2-thiazolylazo)-2-naphthol puriss p.a. from Fluka (Japan) with LiChrosolv® grade methanol from Merck (Germany).

3.2.2.3 Triton X-100 Stock Solution

Surfactant stock solution, 10.0% (v/v) Triton X-100 ($C_{14}H_{22}O(C_2H_4O)_n$) was prepared by appropriate dilution of SigmaUltra Triton® X-100 from Sigma-Aldrich (USA). Its molecular structure is given in Figure 3.2. Nonionic surfactant Triton® X-100 not only facilitates the solubility and stability of both TAN and TAN-metal complexes in the final solution, but also eases the cleaning process. In addition, it was also found that the addition of Triton X-100 can enhance the absorbance of TAN-metal solution (Mehta *et al*., 2004).

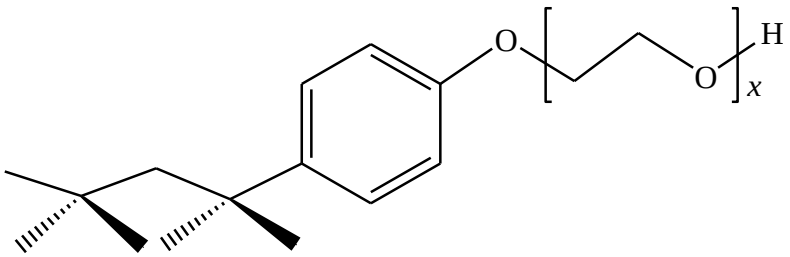

Figure 3.2 Molecular structure for Triton-X 100 where x = 9-10

3.2.2.4 Calibration and Validation Standard Solutions

All calibration and validation standard solutions or synthetic mixtures were prepared by pipetting 1.000 mL of ammonium acetate stock solution, 1.000 mL of 10.0% Triton X-100 and 1.000 mL of TAN stock solution to 25.00 mL volumetric flasks containing appropriate aliquots of the CertiPUR® metal ion standard solutions from Merck (Germany). Under such condition, the complexing agent is always in excess in order to handle the possible presence of unexpected competitive species. For the test set, aliquots of metal standard were substituted by 20.00 mL of tap water and spiked with known amounts of the desired metals.

3.2.3 Cleaning

All the plasticware or glassware involved in this study were cleaned by overnight soaking in dilute 10% nitric acid (w/v) and then soaked overnight in UPW water prior to use.

3.2.4 Calibration and Validation Set Design

In spectrophotometry, multivariate calibration involves modeling a regression relationship to connect between the spectral data and the concentration data, so the model can be applied for future prediction. Figure 3.3 illustrates conceptually the calibration and prediction steps in spectrophotometry by regression. In order to construct a reliable multivariate model with adequate analytical performance, the calibration samples must be representative. This implies that the calibration set has to cover the potential sources of variation as much as possible, particularly the deviation in the concentrations of the targeted analytes. Thus, a 7-level full factorial design was employed with the intent to figure out all possible combinations concerning Cu^{2+}, Ni^{2+} and Zn^{2+} mixtures, where concentration of each metal was varied between 0.050 ppm and 0.600 ppm so as to ensure a satisfactory distribution in the calibration range.

Compromise between the reasonable number of calibration samples and predictive quality is necessary, although a large number of calibration samples usually lead to reduction of prediction error (Lorber and Kowalski, 1988). Hence, a subset consisting of 84 mixtures out of a total of 343 combinations was randomly selected for calibration so as to mimic the designed distribution (Workman JR *et al.*, 1996). These were analyzed in triplicates to ensure model precision. As a result, a data matrix composed of 252 samples was obtained, where the first 152 samples were considered as the calibration set for model estimation and the rest were treated as validation set for

confidence assessment. In order to maximize statistically the information content in the calibration set, sample blanks and individual standards containing solely Cu^{2+} or Ni^{2+} or Zn^{2+} ions, from 0.050 ppm to 0.600 ppm were included in the calibration matrix as well. These lead to a total of 228 calibration samples and 100 test samples.

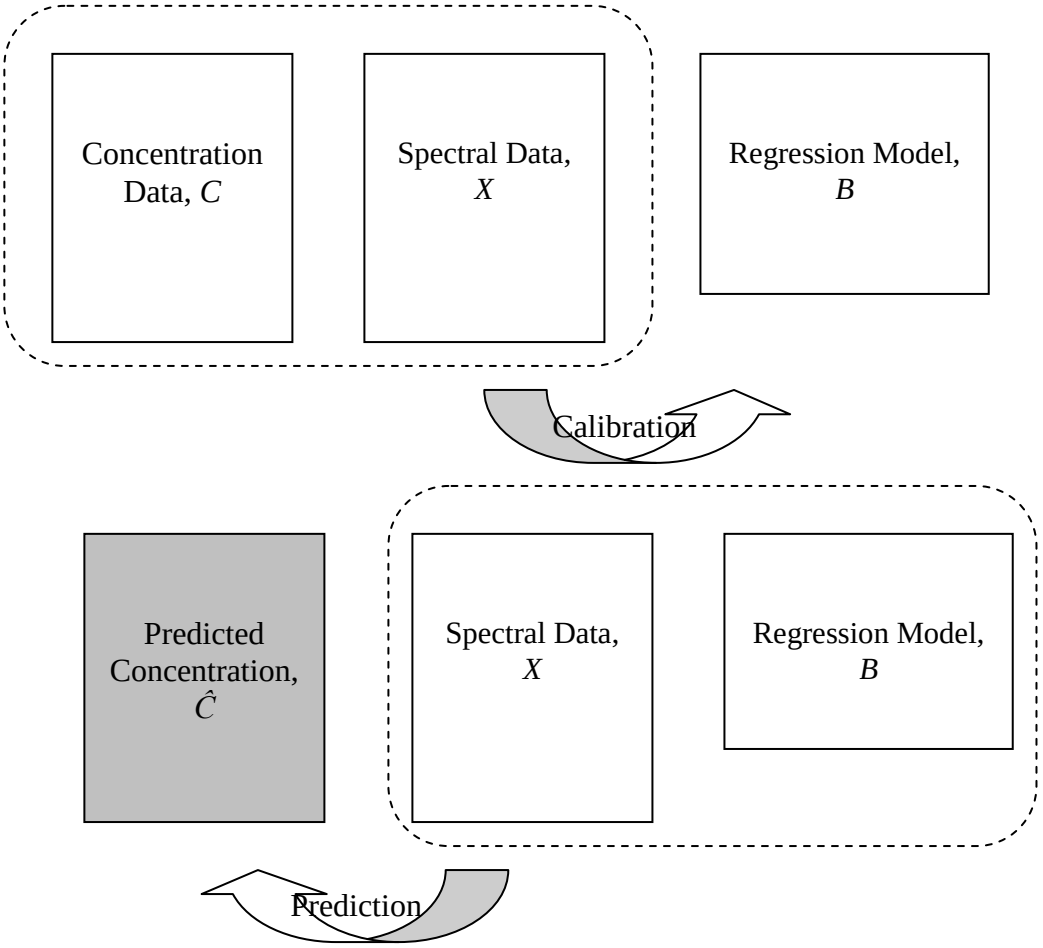

Figure 3.3 Conceptual illustration of multivariate calibration and prediction

3.3 Results and Discussion

TAN reacted with Cu^{2+}, Ni^{2+} and Zn^{2+} instantaneously at room temperature to form coloured complexes (from brown to red) in the presence of Triton X-100, and their possible chemical structures are as proposed in Figure 3.4 (Omar and Mohamed, 2005).

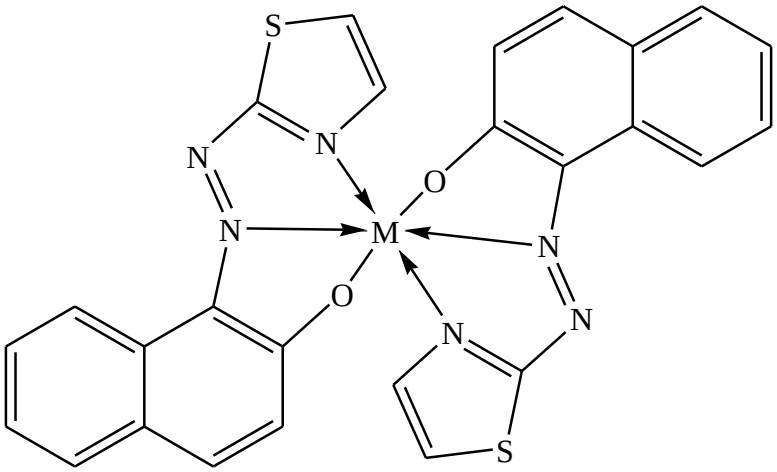

Figure 3.4 Proposed structure of TAN-metal complexes

It is observed in Figure 3.5 that the zero order UV-visible absorption spectra over 300-750 nm of those individual metal ion solutions for Cu^{2+}, Ni^{2+} and Zn^{2+} are almost similar, where they peaked around 491 nm mostly due to the excess chromogenic reagent TAN (Visser *et al*., 2000). However, it could still be identified that there are some noteworthy minute deviations in the absorption spectra between the yellow and red regions owing to the unique characteristic of particular TAN-metal species. These observations are consistent with the findings reported by Omar & Mohamed (2005). Consequently, the wavelength range from 550 to 700 nm with 1 nm intervals is highlighted as they can provide the greatest amount of information about the TAN-metal complexes (Figure 3.5). In spite of the distinctive region, the spectrum of each component seems to overlap each other. Therefore, their concentration levels in a mixture solution cannot be determined directly using traditional calibration procedure

without prior treatment. Due to this reason, multivariate calibration that fully utilizes the highlighted part of the absorption spectra was adopted for simultaneous estimation of the concentration of each metal ion in the mixture solution without much laborious operation.

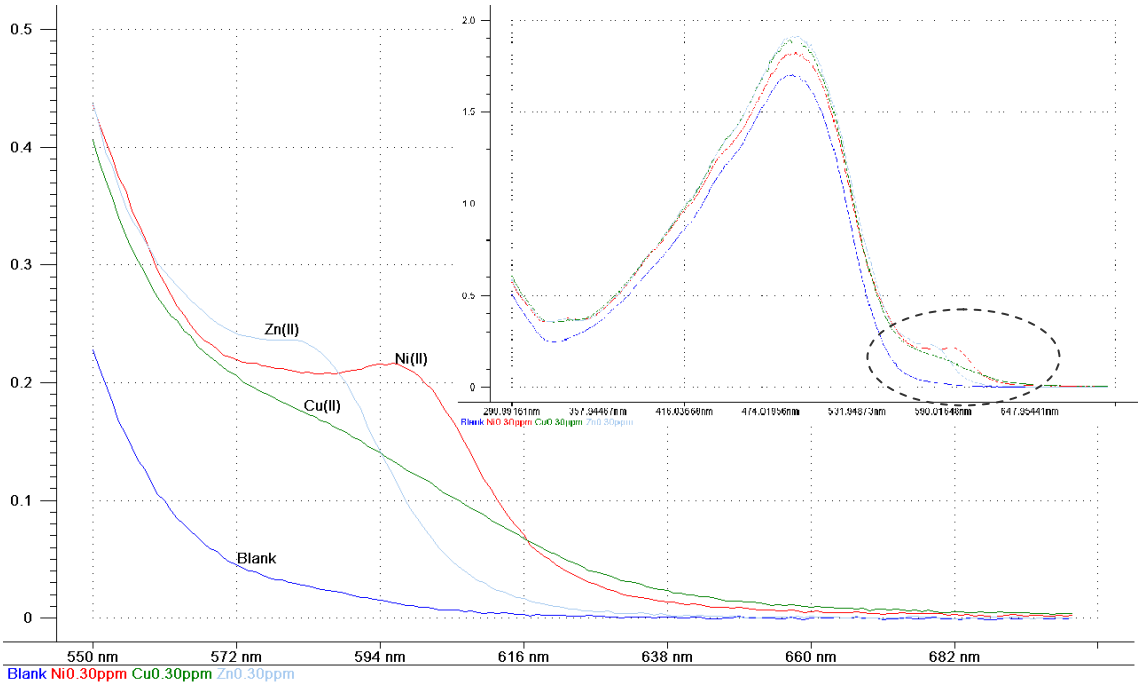

Figure 3.5 Zero order spectra of blank, 0.30 ppm of Cu^{2+}, Ni^{2+} and Zn^{2+} with excess TAN at pH 6.7 in 0.4 % Triton X-100

3.3.1 PLS and PCR

PLS and PCR are two well-known inverse multivariate linear calibration methods particularly in the field of spectrometry. Both have been demonstrated as useful techniques to quantitatively analyze spectra with increased matrix complexity (Qu *et al.*, 2008). For this reason, PLS and PCR were performed on the calibration set (228×151) to develop models for estimating Cu^{2+}, Ni^{2+} and Zn^{2+} in water. As a result, two optimized models were established and consequently validated with a test set (100×151).

The selection of optimal number of factors/PCs used to construct PLS or PCR model represents a decisive step in improving the predictive power of the methods (Samadi-Maybodi and Darzi, 2008). For example, the fit can be improved as the number of factors/PCs in the model increases. However, overfitting is going to be another matter of concern as including too many factors/PCs will also include 'noise', since 'noise' may be fitted as well (Kalivasa, 2005).

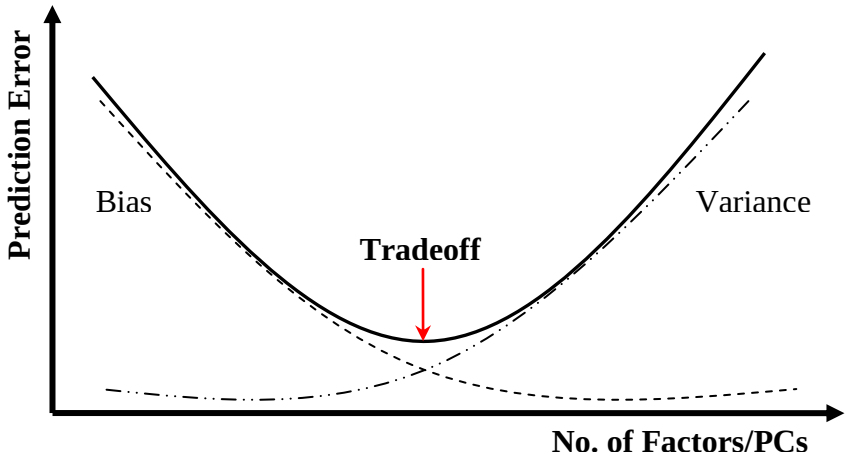

Figure 3.6 Conceptual illustration of bias/variance tradeoff in predictive modeling

Figure 3.6 displays the conceptual illustration of the bias/variance dilemma in predictive modeling. Thus, the criteria adopted for the selection of appropriate number of factor or principal components (PCs) involves selecting the model including the smallest number of factors/PCs which results in an insignificant difference between the corresponding root mean square error of calibration (*RMSEC*) and root mean square error of prediction (RMSEP). The *RMSEC* and *RMSEP* can be referred to the average modeling and predictive errors (Hadad *et al.*, 2008). The ratio *RMSEC* or R*MSEP* is given by the following equation:

$$RMSEC \text{ or } RMSEP = \sqrt{\frac{\sum_{i=1}^{n}(\hat{c}_i - c_i)^2}{n}} \qquad \text{(Equation 3.1)}$$

where $\hat{c}_i$ and c_i are the estimated concentration and the reference concentration of the *i*th sample and *n* is referred to the number of sample in the calibration/prediction set.

Figure 3.7 to Figure 3.10 show the variation of *RMSEC*/*RMSEP* as a function of the number of factors/PCs in PLS and PCR respectively. In this case, considering only the first three factors/PCs in both the PLS and PCR calibration models were found to be optimum for whichever compound. For Zn^{2+} in particular, both PLS and PCR models suffered from overfitting errors if the number of adopted PC/factor is more than three. This is sensible in spectrophotometry, since it is usually expected to get as many significant factors/PCs as the targeted compounds in the mixture, especially in the case of non-highly overlapping system when standards are available during the calibration step (Şxahin *et al.*, 2007). Moreover, Table 3.1 clearly shows that only by using the first three factors/components the regression models can describe more than 99% of the calibration.

Table 3.1 Total explained calibration variance using first three factors/PCs

	PLS				**PCR**		
Factor	**Cu^{2+}**	**Ni^{2+}**	**Zn^{2+}**	**PC**	**Cu^{2+}**	**Ni^{2+}**	**Zn^{2+}**
1	43.35	57.52	44.98	1	43.33	57.52	45.00
2	45.33	80.79	97.29	2	45.32	80.80	97.29
3	99.40	99.85	99.73	3	99.38	99.84	99.73

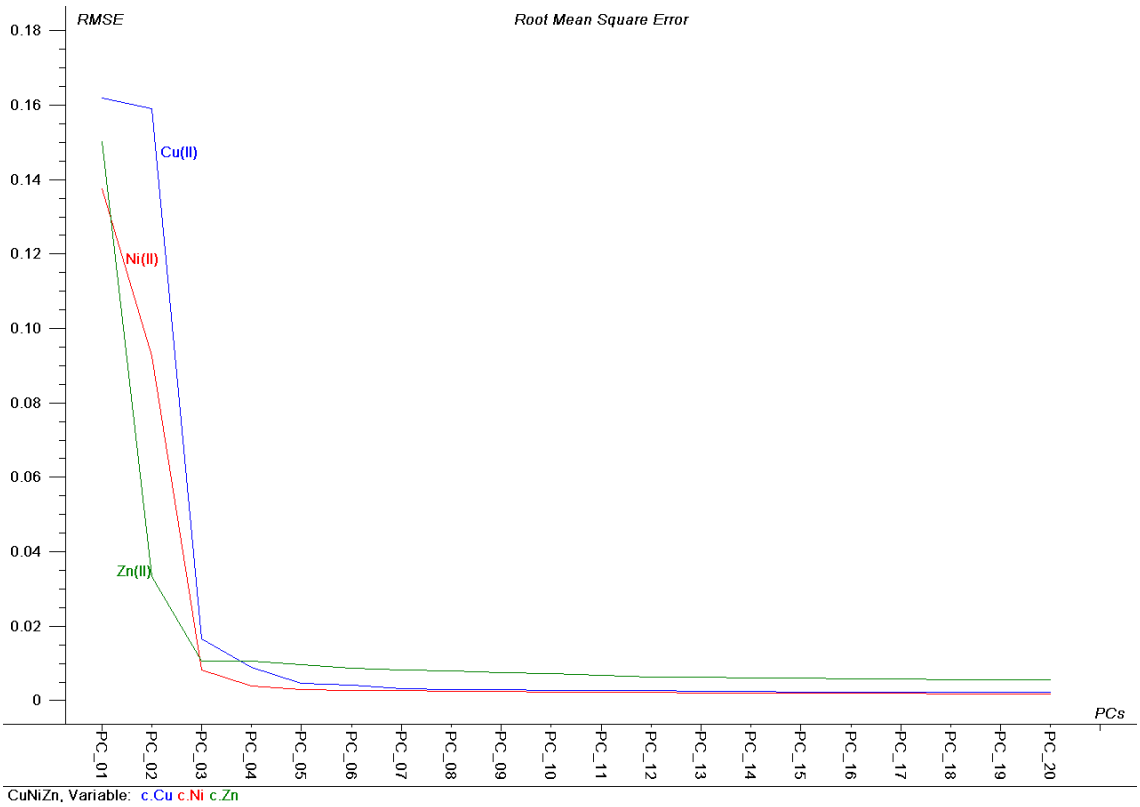

Figure 3.7 Plot of RMSEC vs. number of factors for PLS model

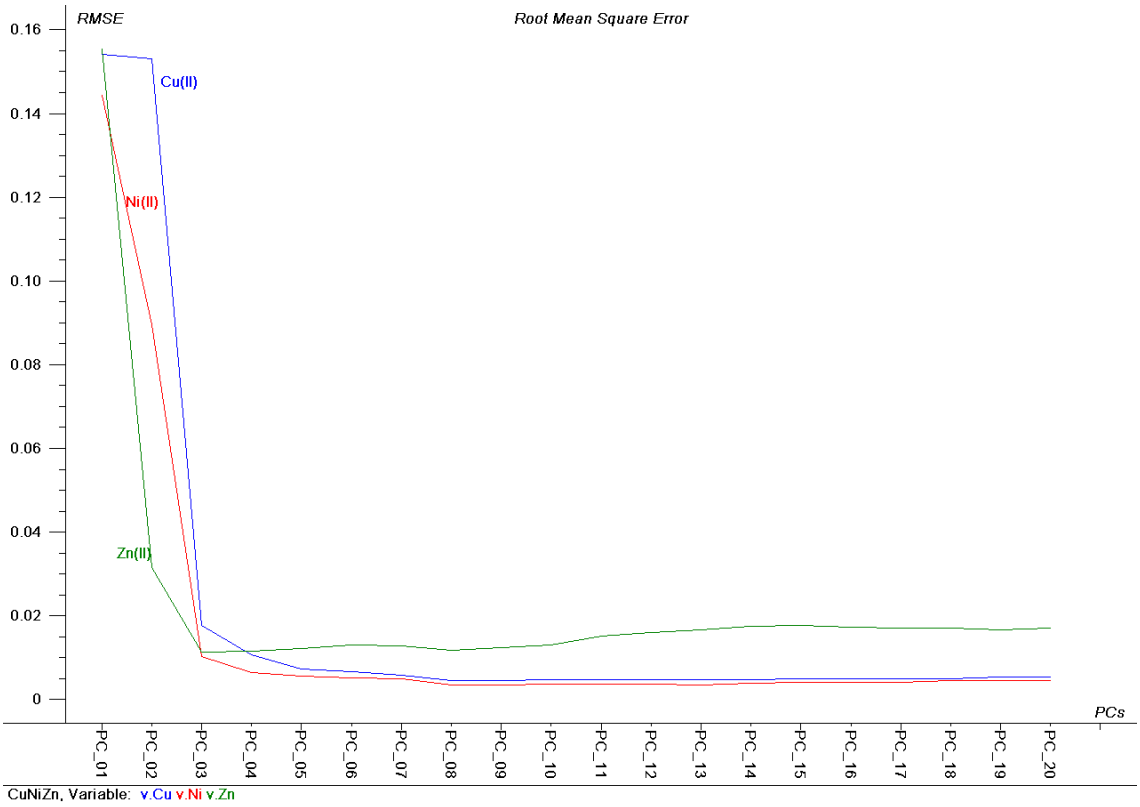

Figure 3.8 Plot of RMSEP vs. number of factors for PLS model

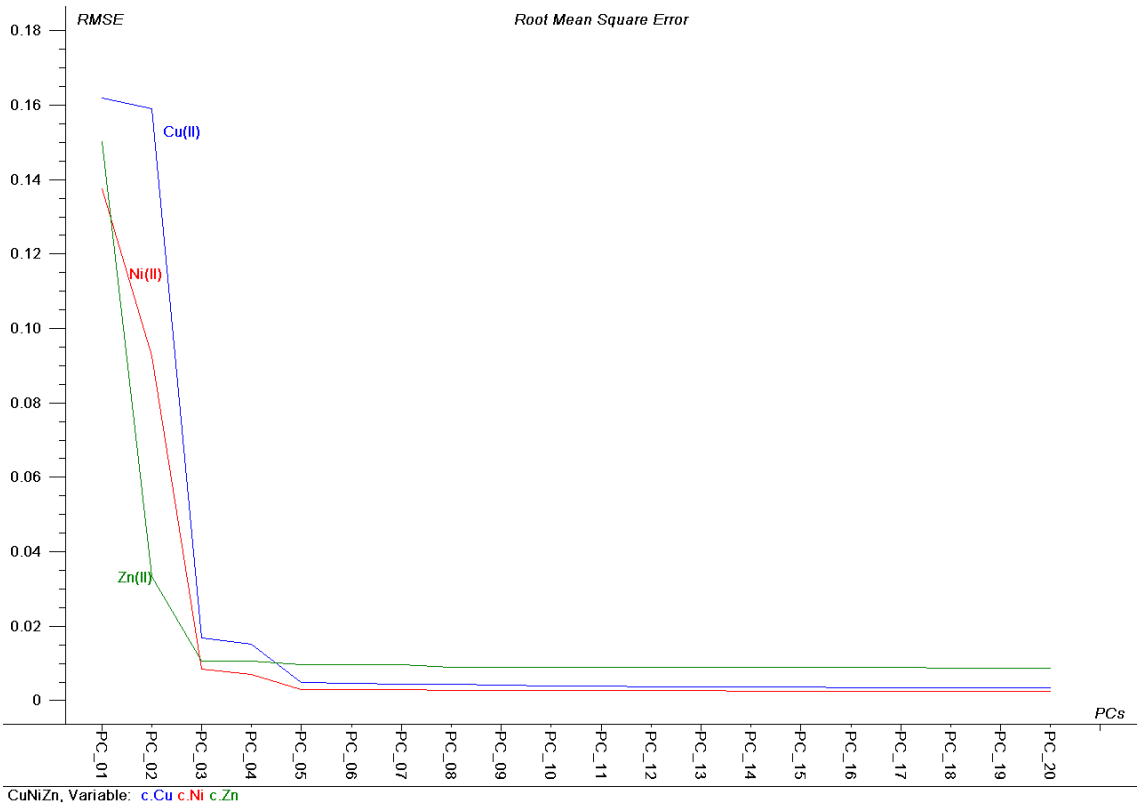

Figure 3.9 Plot of RMSEC vs. number of PCs for PCR model

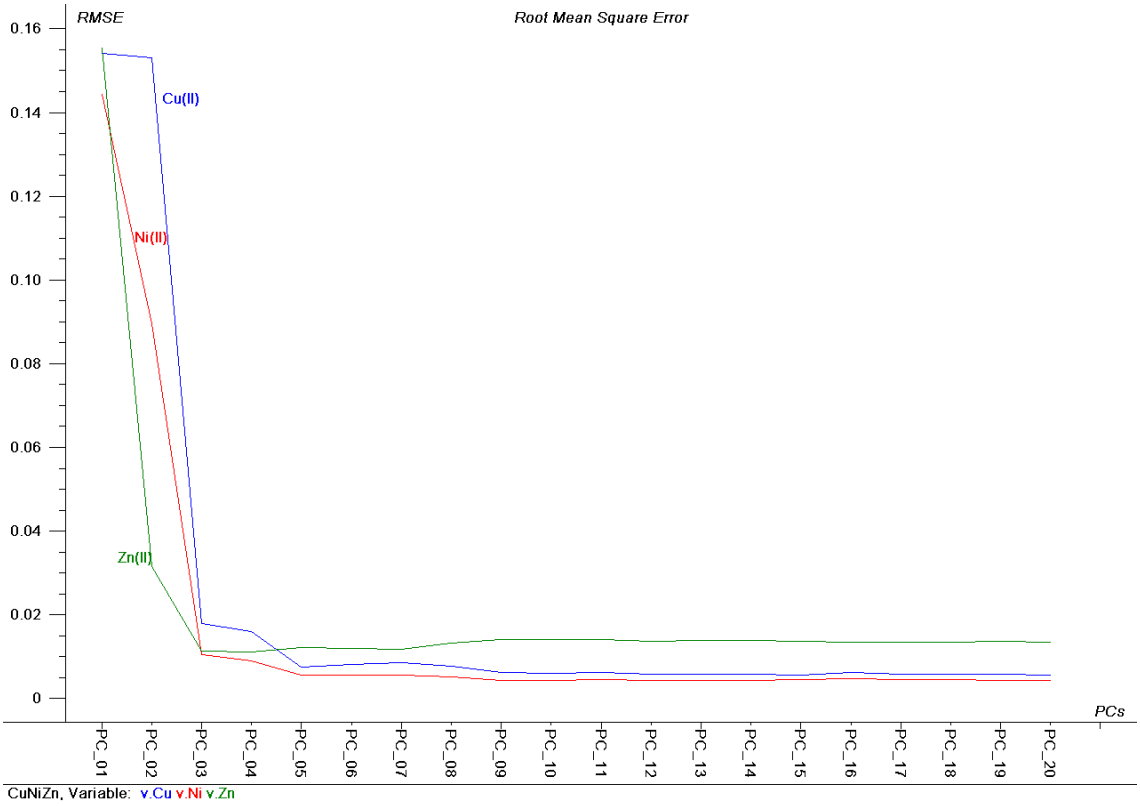

Figure 3.10 Plot of RMSEP vs. number of PCs for PCR model

The performance of the regression models constructed using the first three factors/PCs was statistically evaluated by the bias that express the average residuals, the standard errors of calibration/standard errors of performance (*SEC*/*SEP*) which describe the precision of results, *RMSEC*/*RMSEP* that is used for direct estimation of the modelling and prediction errors and the correlation between predicted and experimental values (*R*). These descriptive statistics can be expressed by the following equations (Esbensen *et al.*, 2004):

$$Bias = \frac{\sum_{i=1}^{n}(\hat{c}_i - c_i)}{n} \qquad \text{(Equation 3.2)}$$

$$SEC \ or \ SEP = \sqrt{\frac{\sum_{i=1}^{n}(\hat{c}_i - c_i - Bias)^2}{n}} \qquad \text{(Equation 3.2)}$$

where $\hat{c}_i$ and c_i are the estimated concentration and the reference concentration of *i*th sample and *n* is the number of sample in calibration/prediction set.

The relevant parameters are summarised in Table 3.2 and Table 3.3. According to Jha *et al.*, (2005), a good model should have a low value of *SEC*/*SEP* and RMSEC/RMSEP, a high value of *R*, and a small difference between *SEC* and *SEP*. Large difference indicates that either too many latent factors/PCs are used or 'noise' is modelled (Lammertyn *et al.*, 1998). The resulting R^2 values are near to 1, which demonstrated that the predicted concentrations are very close to the actual concentrations for each compound in all cases. All these clearly reveal that the calibration data are well modeled using PLS and PCR, and the developed models can be fitted pretty well to the validation set that is not present in the calibration.

Table 3.2 Calibration validation results for both PLS and PCR models

Calibration	Cu^{2+}		Ni^{2+}		Zn^{2+}	
	PLS-2	**PCR**	**PLS-2**	**PCR**	**PLS-2**	**PCR**
No. of Sample	228	228	228	228	228	228
Slope	0.9940	0.9938	0.9984	0.9984	0.9973	0.9973
Offset	0.0013	0.0014	0.0003	0.0004	0.0006	0.0006
Correlation, *R*	0.9970	0.9969	0.9992	0.9992	0.9986	0.9986
R^2	0.9940	0.9938	0.9985	0.9984	0.9973	0.9973
RMSEC	0.0166	0.0169	0.0082	0.0084	0.0106	0.0106
SEC	0.0166	0.0170	0.0082	0.0084	0.0106	0.0106
Bias	-2.206×10^{-8}	-2.160×10^{-8}	5.964×10^{-9}	5.212×10^{-9}	6.536×10^{-11}	-1.536×10^{-9}
No. of Factors/PCs	3	3	3	3	3	3
Explained Variance	99.404%	99.382%	99.848%	99.841%	99.727%	99.726%

Table 3.3 Validation results for both PLS and PCR models

Validation	Cu^{2+}		Ni^{2+}		Zn^{2+}	
	PLS-2	**PCR**	**PLS-2**	**PCR**	**PLS-2**	**PCR**
No. of Sample	100	100	100	100	100	100
Slope	1.0021	1.0018	0.9984	0.9880	0.9914	0.9913
Offset	0.0147	0.0150	-0.0048	-0.0047	0.0072	0.0071
Correlation	0.9986	0.9986	0.9996	0.9996	0.9986	0.9986
R^2	0.9910	0.9908	0.9975	0.9975	0.9976	0.9976
RMSEP	0.0177	0.0180	0.0103	0.0104	0.0113	0.0113
SEP	0.0088	0.0090	0.0056	0.0057	0.0105	0.0105
Bias	0.0154	0.0156	-0.0086	-0.0087	0.0042	0.0042
No. of Factors/PCs	3	3	3	3	3	3
Explained Variance	99.672%	99.076%	99.904%	99.746%	99.747%	99.761%

Besides that, both modelling and prediction quality using only 3 factors/PCs by PLS or PCR are quite similar to each other. These are clearly observed in their loadings (Figure 3.11) and regression coefficients (Figure 3.12), where PLS and PCR outcomes are almost fully overlaid on each other. Based on these, it can be suggested that there should be no significant predictive difference between PLS and PCR models for future samples.

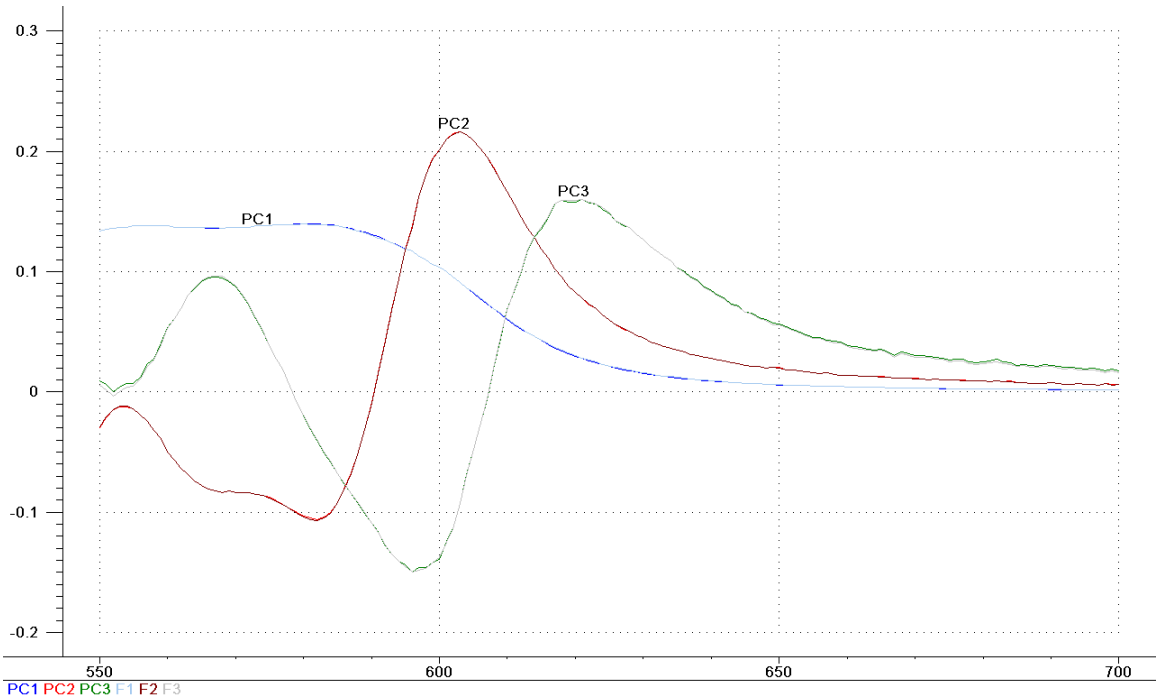

Figure 3.11 First three loadings for both PLS and PCR models

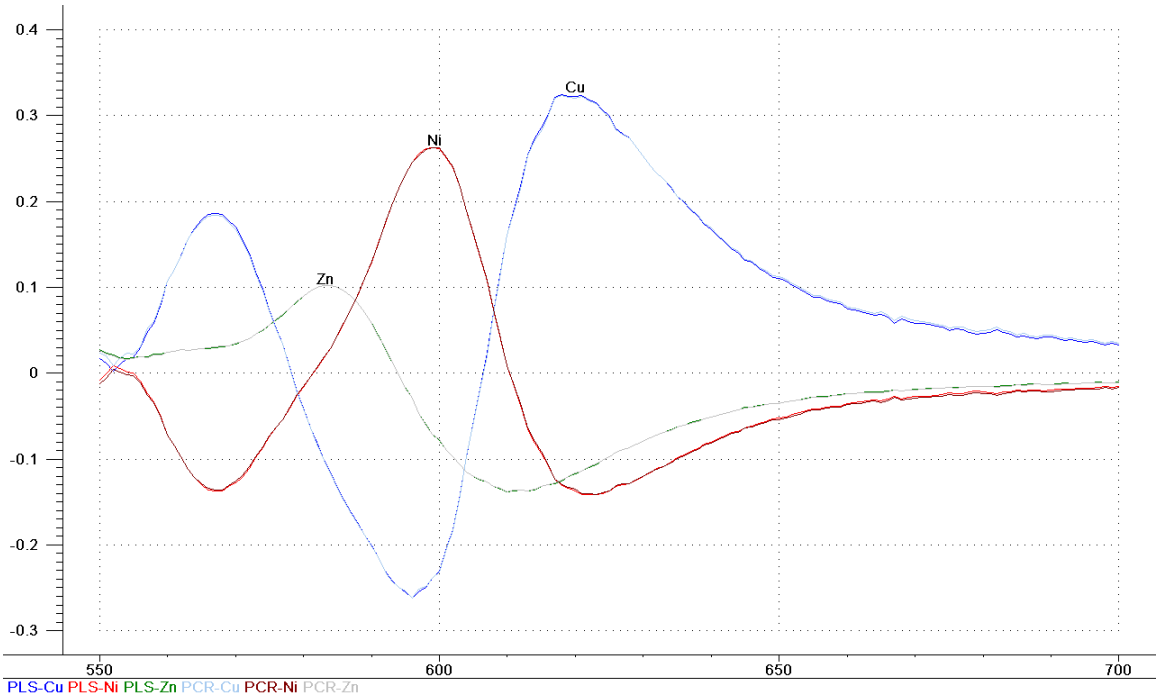

Figure 3.12 Both PLS and PCR raw regression coefficients for each component using three factors/PCs

Some general findings can also be deduced from the loadings plot (Figure 3.11). The first factor/PC loading that plateaus around 550-583 nm corresponds to the excess TAN reagent. The second factor/PC loading that peaked at 599 nm is plausibly due to the distinctive absorption pattern of the TAN-Ni complex at that wavelength (Figure 3.5). The third factor/PC is dominated by the variation in the concentration matrix.

Similar conclusions can also be deduced from the regression coefficients plot (Figure 3.12). Since theoretically these regression vectors are not supposed to contribute any interfering absorbance, they should reflect the net absorption pattern of each pure TAN-metal complex. For example if three-factor/PC models are considered, Zn regression coefficients that peak around 584 nm can be related to the shoulder peak of TAN-Zn complex in Figure 3.5, while Ni^{2+} regression models display the characteristic TAN-Ni peak at 599nm. Cu regression models utilized the dissimilarity found between TAN-Cu complex absorbance spectra and others for the estimation of Cu^{2+} ion concentration levels. All above observations support the sufficiency of three factors/PCs in describing the multivariate models.

3.3.2 Analytical Figures of Merit

Estimation of analytical figures of merit (FOM) is important and necessary in order to characterize the quality of the established analytical methodology for comparison or verification. According to the International Union of Pure and Applied Chemistry (IUPAC), the FOM of the so called sensitivity (*SEN*) is defined as the derivative of the calibration function in univariate analytical chemistry approaches (Inczédy et *al.*, 1998). In other words, *SEN* is the calibration slope in classical models (pseudo-univariate), and for an inverse model it is sensible that *SEN* to be the inverse of the slope (Olivieri *et al.*, 2004). Thus, the multivariate *SEN* that expresses the changes in UV-visible absorbance

spectrum as a function of the particular analyte concentration in this study has to be proportional to the norm of the final regression vector by inverse calibrations (PLS and PCR); since the norm of the regression vector is proportional to the norm of the net absorbance of target analyte ([Sanz *et al.*, 2003] and [Lorber, 1986]). Hence, *SEN* in an inverse model is expressed as ([Petrucelli *et al*., 2007] and [Collado *et al.*, 2000]):

$$SEN = \frac{1}{\|b_k\|} \qquad \text{(Equation 3.4)}$$

where || || stands for the Euclidian norm of vector and b_k is the vector of final regression coefficients appropriate for the *k*th wavelength, which can be attained from any multivariate regression model.

On the other hand, analytical sensitivity (γ) appears to be a more useful FOM than *SEN* for method comparison purposes. It can be defined as the ratio between *SEN* and instrumental noise in direct analogy to univariate calibration, as the given quotient (Espinosa-Mansilla *et al*., 2004):

$$\gamma = \frac{SEN}{\|\varepsilon\|} \qquad \text{(Equation 3.5)}$$

where ε is a measure of the instrumental noise and it can be taken as an approximation to standard deviation of several blanks ([Ostra *et al*., 2008], [Marsili, Sobrero and Goicoechea, 2003] and [Iñón *et al*., 2003]). The reciprocal of γ (γ^{-1}) can be interpreted as the minimum discernible concentration of a particular metal ion by the respective methods (Samadi-Maybodi and Darzi, 2008). It allows one to compare analytical

methods regardless of the specific technique, equipment, and scale employed (Gil García *et al.*, 2008).

Different approaches exist for estimating the limit of detection (*LOD*) and limit of quantification (*LOQ*) in multivariate calibration. The simplest is the one that is derived by comparison with the univariate approach. It is approximately three times the instrumental noise divided by the sensitivity of the analyte of interest for *LOD* and 10 times for *LOQ*. They have been proposed according to the following expressions ([Samadi-Maybodi and Darzi, 2008], [Brás *et al.*, 2005], [Goicoechea and Olivieri, 1999] and [Boquk and Rius, 1996]):

$$LOD = \frac{3\|\varepsilon\|}{SEN} \qquad \text{(Equation 3.6)}$$

$$LOQ = \frac{10\|\varepsilon\|}{SEN} \qquad \text{(Equation 3.7)}$$

The estimated FOM for PLS and PCR models concerning simultaneous spectrophotometric determination of Cu^{2+}, Ni^{2+} and Zn^{2+} in water sample are shown in Table 3.4. No significant difference in analytical performance was observed between PLS and PCR models, since the trends in their first three loadings are very similar (Figure 3.11). From Table 3.4, it can be observed that the γ^{-1} values are in ppb region for the three compounds, and this suggests that they are good methods for multivariate determination (Samadi-Maybodi and Darzi, 2008). The *LOD* of Zn^{2+} is observed to be relatively higher than others since its associated 'noise' is greater. This suggests the lack of tolerability of Zn models in presence of unexpected interferences, where distortion of the net absorbance is due to a higher spectral overlap (Boquk and Rius, 1996).

Table 3.4 Analytical figures of merit for PLS and PCR models

FOM	Cu^{2+}		Ni^{2+}		Zn^{2+}	
	PLS	**PCR**	**PLS**	**PCR**	**PLS**	**PCR**
$\| b_k \|$ / ppm / AU	1.9469	1.9470	1.2367	1.2319	0.7983	0.7979
$\| \varepsilon \|$ / AU	0.0009	0.0010	0.0009	0.0009	0.0078	0.0078
SEN / AU ppm^{-1}	0.5136	0.5136	0.8119	0.8118	1.2527	1.2533
γ^{-1} / ppm	0.002	0.002	0.001	0.001	0.006	0.006
LOD / ppm	0.005	0.006	0.003	0.003	0.02	0.02
LOQ / ppm	0.02	0.02	0.01	0.01	0.06	0.06

3.3.3 Application on Spiked Samples

It is sometimes argued that the real predictive value of any calibration models cannot be judged solely by using synthetic mixtures, it has to be tested on real world samples (Rodriguez-Nogales, 2006). For this reason, tap water samples spiked with known amount of metals were analyzed in order to evaluate the precision, accuracy and recovery of the proposed analytical procedures. The results for intraday and interday validations of ternary spiked mixtures are shown in Table 3.5 and Table 3.6 respectively.

As can be seen, the predictive ability of both models for all the analytes in a real matrix is always in good agreement. Yet, the interday prediction by PLS models seem to have slightly more precision compared to PCR models. This is probably due to the spectral transformation algorithm in PLS that is weighted to the concentration. Thus, PLS model can perform better than PCR in the presence of variations that are not related to analyte concentration, such as random linear baselines (Huang *et al.*, 2009).

Table 3.5 Intraday validation of Cu^{2+}, Ni^{2+} and Zn^{2+} in spiked tap water

Intraday		**PLS**			**PCR**		
Ion Species	**Spiked / ppm**	**Found / ppm**	***RSD* / %**	**Recovery / %**	**Found / ppm**	***RSD* / %**	**Recovery / %**
Cu^{2+}	0.000	n.d.	-	-	n.d.	-	-
	0.100	0.103 ± 0.002	3	103 ± 2	0.103 ± 0.002	3	103 ± 2
	0.300	0.309 ± 0.002	1	103 ± 1	0.310 ± 0.002	1	103 ± 1
	0.500	0.526 ± 0.003	1	105 ± 1	0.526 ± 0.003	1	105 ± 1
Ni^{2+}	0.000	N.D.	-	-	N.D.	-	-
	0.100	0.106 ± 0.001	2	106 ± 1	0.106 ± 0.001	2	106 ± 2
	0.300	0.307 ± 0.001	1	102 ± 1	0.307 ± 0.001	1	102 ± 1
	0.500	0.509 ± 0.001	1	102 ± 1	0.509 ± 0.002	1	102 ± 1
Zn^{2+}	0.000	0.149 ± 0.006	3	-	0.149 ± 0.006	3	-
	0.100	0.259 ± 0.006	2	110 ± 2	0.259 ± 0.006	2	110 ± 2
	0.300	0.452 ± 0.006	2	102 ± 2	0.452 ± 0.006	2	102 ± 2
	0.500	0.633 ± 0.006	1	97 ± 1	0.633 ± 0.006	1	97 ± 1

n.d.: not detected

Table 3.6 Interday validation of Cu^{2+}, Ni^{2+} and Zn^{2+} in spiked tap water

Interday		**PLS**			**PCR**		
Ion Species	**Spiked / ppm**	**Found / ppm**	***RSD* / %**	**Recovery / %**	**Found / ppm**	***RSD* / %**	**Recovery / %**
Cu^{2+}	0.000	n.d.	-	-	n.d.	-	-
	0.100	0.107 ± 0.006	9	107 ± 3	0.112 ± 0.006	10	112 ± 6
	0.300	0.306 ± 0.004	2	102 ± 1	0.308 ± 0.006	3	103 ± 2
	0.500	0.517 ± 0.004	1	103 ± 1	0.519 ± 0.005	2	104 ± 1
Ni^{2+}	0.000	n.d.	-	-	n.d.	-	-
	0.100	0.102 ± 0.003	6	102 ± 6	0.098 ± 0.004	8	98 ± 4
	0.300	0.303 ± 0.003	2	101 ± 2	0.300 ± 0.004	3	100 ± 1
	0.500	0.503 ± 0.003	1	100 ± 1	0.500 ± 0.003	1	100 ± 1
Zn^{2+}	0.000	0.145 ± 0.006	4	-	0.137 ± 0.009	12	-
	0.100	0.251 ± 0.006	3	106 ± 4	0.24 ± 0.01	8	104 ± 3
	0.300	0.451 ± 0.006	1	102 ± 2	0.446 ± 0.007	3	103 ± 2
	0.500	0.633 ± 0.006	2	97 ± 2	0.627 ± 0.008	2	98 ± 2

n.d.: not detected

3.3.4 Influence of pH

Once a satisfactory model has been developed, it would be good if it can remain "robust" to small variations in the experimental conditions. The effect of pH on the absorption spectra of TAN-metal complexes in Triton X-100 solutions was studied over the pH range of 3-12 adjusted by diluted HNO_3 and NaOH solutions. It was observed that the resulting absorbances within the study region were increased by increasing pH from 3.3 to 5.9 and remained constant between 5.9 and 7.1 (where the prediction inaccuracy was less than 2%). The absorbance kept increasing as pH went up, but inaccuracy became higher (more than 5%) and the spectra lost their characteristics after pH 8.4.

3.3.5 Influence of Ammonium Acetate

Ammonium acetate is a relatively cheap chemical, which is colourless, used for controlling final solution at around pH 6.7. The effect of ammonium acetate concentration was studied in this work. As expected, there is no significant ($P \geq 0.05$) deviation in the predicted values when applying 0.25 mL to 5.00 mL of 1.00 mol dm^{-3} of ammonium acetate. This indirectly demonstrates the tolerability of those models on ammonium and acetate ions.

3.3.6 Influence of Surfactants

When the concentration of surfactant exceeds the critical micelle concentration (CMC), micelles are formed homogeneously in aqueous solution. The non-polar core of micellar system provides high solubilization capacity for TAN and its complexes. This allows development of spectrophotometry procedures with enhanced absorbance of TAN-metal complexes, thereby avoiding the extraction steps ([Rojas and Ojeda, 2009], [Ghavami *et al.*, 2008], [Mehta *et al.*, 2004] and [Lee and Choi, 2001]) Furthermore, it also acts as

nonionic detergent that eases the cleaning process. In this work, the function of Triton X-100 as a non-ionic surfactant in the colour reactions was studied and the optimum working range of the surfactant have been investigated. The results showed that 0.1-0.2 % of Triton X-100 (v/v) were insufficient to fully dissolve both the excess TAN and its complexes which lead to significant predictive error; although the concentration applied was greater than the CMC of Triton X-100 (0.22-0.24 mM). Where the concentration of Triton X-100 was increased from 0.4 to 2.0 %, no significant difference was observed in those spectra as well as the predicted values. Hence, the suggested Triton X-100 concentration is ~0.4 % so as to maintain the optimum predictive performance with adequate amount of surfactant.

Besides that, the effect of Triton X-100 was also studied by substituting it with other solvents such as 50%-methanol and polysorbate-20 (commercially known as Tween-20). Fluctuating and comparatively low absorbance spectra were obtained in the 50%-methanolic solution probably due to the volatility of methanol and the solubility of TAN and its complexes. Conversely, the spectra acquired using comparable amounts of Tween-20 and Triton X-100 are very similar, indeed the predicted values on test samples fall between an acceptable range (deviations of less than 5%). Thus, it is believed that colourless nonionic micellar solutions are indispensable solvents in spectrophotometry when dealing with organic chromogens.

3.3.7 Influence of Foreign Ions

The influence of some possible foreign species was also investigated by analyzing a standard mixture solution containing 0.300 ppm of each Cu^{2+}, Ni^{2+}, Zn^{2+}, and to which increasing amounts of interfering species were added. The tolerated limit of a foreign species was set as the inaccuracy caused is not greater than 5%. The tolerable ratios of

various foreign ions are depicted in Table 3.7. The experimental results show that Hg^{2+}, Pb^{2+} and Fe^{3+} caused cationic interferences as a result of formation of coloured complexes with TAN which absorb within the studied wavelengths ([Rodriguez-Nogales, 2006] and [Omar and Mohamed, 2005]). If Zn^{2+} is to be simultaneous determined, As^{5+}, Cd^{2+}, Cr^{3+} ions must be absent because they produce interferences even at concentration levels similar to the analyte concentration.

Table 3.7 Tolerance ratios for foreign ions in the determination of 0.30 ppm of Cu^{2+}, Ni^{2+} and Zn^{2+} mixture

Tolerated ratio	**Cu**	**Ni**	**Zn**
>100	Cd^{2+}, Mg^{2+} ,Mn^{2+}	Al^{3+}, As^{5+}, Ca^{2+}, Cd^{2+}, Cr^{3+}, Mg^{2+}, Mn^{2+} ,Se^{4+}	
> 20	Al^{3+}, As^{5+}, Ca^{2+}, Cr^{3+}, Se^{4+}	Fe^{3+}	Mg^{2+}
> 1	Fe^{3+}, Hg^{2+}, Pb^{2+}	Hg^{2+}, Pb^{2+}	Al^{3+}, Ca^{2+}, Fe^{3+}, Hg^{2+}, Pb^{2+}, Mn^{2+}, Se^{4+}

3.3.8 Stability of Samples

The stability of TAN-metal complexes was investigated by comparing the absorption spectrum and the estimated concentrations of the solutions at different times of interval. The samples containing ternary mixture of Cu^{2+}, Ni^{2+} and Zn^{2+} complexes with concentration levels of 0.100 ppm, 0.300ppm and 0.500 ppm prepared by the method discussed above were found to be stable for at least a week at 10 °C.

4 PRELIMINARY EVALUATION OF REAGENT EFFECT ON FISH METAL RECOVERIES BY MAD-FAAS

4.1 Introduction

The alternative spectrophotometry method proposed in the previous chapter is suitable for analysis of particular metals in water/aqueous samples with similar matrices within the study range. However, it is often the case that the sample is not easily dissolved such as in fish tissues which are one of the main targets in this study. In such situations, other analytical procedures are required for proper handling of such samples. In this chapter, the preliminary evaluation of the significant effects of adding other reagents prior to nitric acid microwave digestion and atomic absorption spectrometric (AAS) analysis were demonstrated using fractional factorial design. In this design, a subset of a full factorial design is selected in a systematic way that still renders the possibility of estimating the desired main effects and some interactions from a limited number of experiments.

4.1.1 Background of Sample Preparation

Due to simplicity and budget constraints, quantification of metals in fish sample matrices is most often accomplished via AAS as documented elsewhere ([Custódio *et al.*, 2011], [Tuzen, 2009] and [Manutsewee *et al.*, 2007]) This method generally requires destruction of the solid sample matrix to produce an appropriate solution of the analyte before the instrumental analysis. Thus, the sample preparation technique and its effective combination with AAS determination are going to have crucial impacts on the analytical outcomes ([Khajeh and Ghanbari, 2011], [Demirel *et al.*, 2008] and [Sim *et al.*, 2006]). For example, the adopted sample dissolution protocols have to assure

adequate decomposition of the fish tissues matrix with no significant losses or contamination of metals throughout the process, and the resulting sample solutions are appropriate for the AAS sample introduction system.

Basically, dry ashing and wet ashing are two main streams of the reported sample preparation options that are geared towards AAS analysis ([Hseu, 2004] and [Ybañez *et al.*, 1992]). Proper ashing is decisive to the overall analytical performance. Dry ashing usually refers to incineration of samples at high temperature with muffle furnace which requires no added reagents and less attention once ignition begins (Nielsen, 2010). However, the length of time under such circumstance is longer and likely to cause analyte losses due to volatilization as well as undesired interactions with the crucibles. On the other hand, these probably would not be critical in wet ashing that utilizes various chemical reagents and heating devices, particularly when they are carried out in closed systems. The benefit of closed systems is that significantly higher operating temperatures can be reached compared to open systems which have working temperatures that are limited by the boiling point of the reagent used. The considerable increase in temperature boosts the reaction kinetics dramatically, consequently allowing faster quantitative recovery.

4.1.2 Closed-Vessel Microwave Assisted Digestion

Microwave sample preparation techniques have become increasingly popular and have widespread use in analytical laboratories all over the world. In elemental analysis, this technique has been commonly used as a wet digestion procedure for the rapid dissolution of analytical samples prior to instrumental analysis. A typical closed-vessel microwave assisted digestion (MAD) is usually carried out in pressurized vessels under

the heating of microwave radiation in a controlled oven, utilizing various oxidizing reagents or reagent mixtures (Figure 4.1).

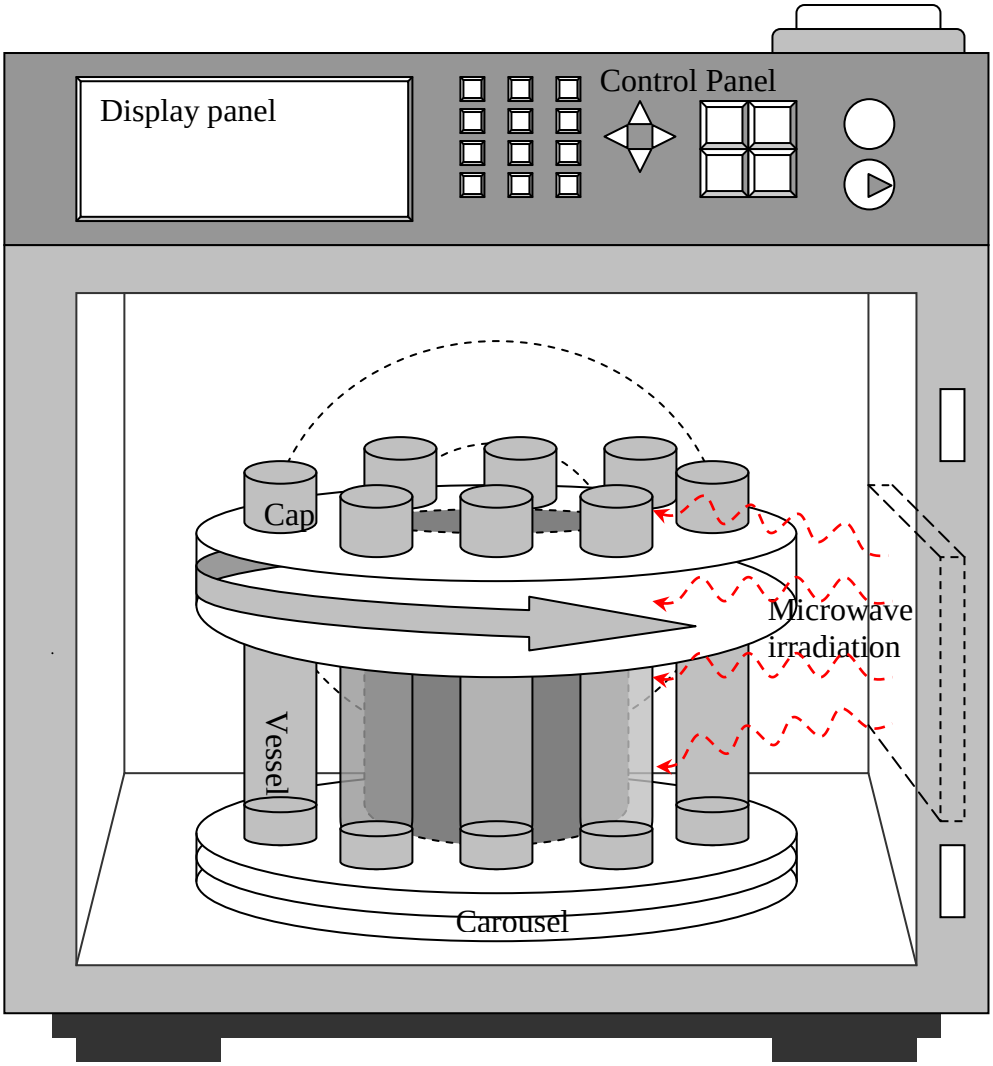

Figure 4.1 Schematic diagram of a typical microwave accelerated reaction system

Although the MAD approach is not a universal sample preparation technique, it has been the method of choice for fish metal analysis that offers certain advantages over conventional protocols. This technique could be considered as reasonably economical and a rapid solution for fish sample preparation in the long run because it requires smaller amounts of reagents compared to other conventional wet digestion procedures. Similar to other closed-system sample dissolutions, the high pressure created raises the boiling point of the reagents used and results in an increase of their oxidation potential

and substantially increases the dissolution rate of tissue matrix. Besides this, with MAD, it is also possible to avoid hazard due to the use of perchloric acid which is potentially explosive when it comes into contact with easily oxidized materials (Smith and Arsenault, 1996). Furthermore, precision and accuracy under pressurized MAD circumstance are generally reported to be as good as or better than those attained via conventional procedures.

Notwithstanding the advantage over conventional procedures, many different recommendations of reagent combination aside from nitric acid can be found in the literature for the preparation of aquatic samples by MAD ([Hamilton *et al*., 2007], [Mendil and Uluözlü, 2007], [Manutsewee *et al.*, 2007], [Retief *et al.*, 2006] and [Scancar *et al.*, 2004]). These reagents may limit or increase the complexity of analysis depending upon the analytical task. Therefore, a number of factors should be considered in order to carry out MAD for desired analytes in a targeted matrix with a particular detection method.

There are several means that can be applied for studying the main effects of addition of other reagents to nitric acid prior to MAD. The most common approach to investigate their effects on overall analytical performance is by varying only one operating parameter at a time while holding the others fixed. This approach is rather time-consuming and not economical compared to chemometric design of experiment (DoE) methods, and the results obtained under such manner could be very misleading because factors involved are rarely independent [(Stalikas *et al.*, 2009) and (Jalbani *et al.*, 2006)]. In this regard, DoE can make possible the understanding of circumstances that are not explainable in a traditional manner, for example, the interaction between factors that influence analytical responses (Cerutti *et al.*, 2004).

4.2 Materials and Methods

4.2.1 Instrumentation

4.2.1.1 Flame Atomic Absorption Spectrometer

A GBC 933AA flame atomic absorption spectrometer (FAAS) equipped with a D_2 lamp as background correction was used for the metal analysis. Cu, Fe and Zn hollow cathode lamps were run under operational conditions suggested by the manufacturer. These conditions are shown in Table 4.1. All measurements were performed using an air-acetylene flame with optimized flow rates.

Table 4.1 AAS instrumental parameters

Elements	**Wavelength /nm**	**Slit width /nm**	**Lamp current /mA**	**Calibration Range / mg L^{-1}**	**R^2**
Cu	324.7	0.5	3.0	0.00-0.50	0.999
Fe	248.3	0.2	8.0	0.00-9.00	0.999
Zn	213.9	0.5	3.0	0.00-1.50	0.994
Hg	254.7	0.5	4.0	0.000-0.010	0.999

4.2.1.2 Cold Vapour Atomic Absorption Spectrometer

FAAS method is not sensitive enough for fish mercury analysis, so NIC RA-3 cold-vapour atomic absorption spectrometer (CVAAS) was used. The main idea is Hg can exist as monatomic vapour at ambient temperatures, so spectrometric measurements can be made on the concentrated atomic cloud released from the reduced sample solution in the presence of $SnCl_2$ as reductant and HCl as reaction medium. The respective cold-vapour generation can be expressed by following equations:

$$SnCl_{2\,(p)} + 2HCl_{\,(aq)} \rightarrow SnCl_4^{2-}{}_{(aq)} + 2H^+{}_{(aq)} \qquad \text{(Equation 4.1)}$$

$$SnCl_4^{2-}{}_{(aq)} + 2Cl^-{}_{(aq)} + Hg^{2+}{}_{(aq)} \leftrightarrow SnCl_6^{2-}{}_{(aq)} + Hg^0{}_{(aq)} \qquad \text{(Equation 4.2)}$$

$Hg^0_{(aq)} \leftrightarrow Hg^0_{(g)}$ (Equation 4.3)

Since Hg^0 is separated as gaseous product from their matrix under this technique, the sensitivity is generally enhanced as some matrix interferences are eliminated. Figure 4.2 shows a simple representation of CVAAS flow system for Hg determination, where headspace of the sampler was purged before the atomic aqueous Hg are drawn into the gaseous phase by a continuously flow of carrier gas into the absorption cell for spectrometric acquisition.

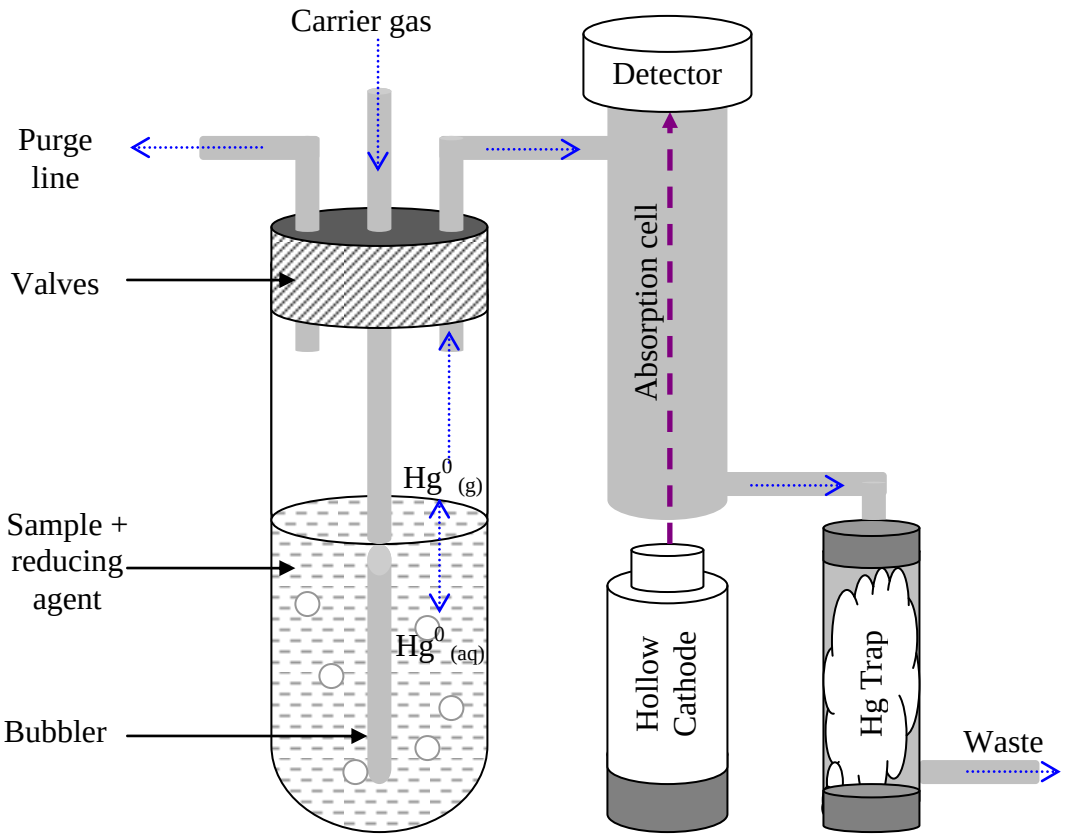

Figure 4.2 Schematic diagram of CVAAS measurement by reducing vapourization

4.2.1.3 Microwave Accelerated Reaction System

The microwave digestions were carried out in a CEM MarXpress Microwave Accelerated Reaction System (USA). In this study, 0.50 g of samples were accurately weighed directly into each precleaned 55 mL self-regulating pressure control PFA® polymer digestion vessels equipped with TFM® vent plug and PFA® Teflon® liners.

Simultaneous digestion of sample triplicates and sample blank were performed in the closed-vessel MAD according to the reagent combinations as designed in Table 4.2 and Table 4.3. The microwave power applied was 800 W and the temperature was programmed as a ramp to 200 °C in 15.0 minutes, held for 15.0 minutes and cooled down in 20 minutes as suggested by the manufacturer.

Table 4.2 Factors and levels used in factorial design

Variable	**Symbol**	**Low Level (-)**	**Central (0)**	**High Level (+)**
Volume of HNO_3	A	4.00 mL	7.00 mL	10.00 mL
Volume of H_2O_2	B	0.00 mL	1.00 mL	2.00 mL
Volume of HCl	C	0.00 mL	1.00 mL	2.00 mL
Volume of H_2O	D	0.00 mL	2.50 mL	5.00 mL

Table 4.3 Design matrix and the results of the two-level fractional factorial design

No.	**HNO_3 (A)**	**H_2O_2 (B)**	**HCl (C)**	**H_2O (D)**	**Recovery %**			
					Cu	**Fe**	**Hg**	**Zn**
1	-	-	-	-	102 ± 5	88 ± 7	69 ± 11	94 ± 7
2	+	-	-	+	96 ± 12	77 ± 10	81 ± 13	88 ± 11
3	-	+	-	+	90 ± 1	81 ± 4	51 ± 10	92 ± 8
4	+	+	-	-	88 ± 4	79 ± 8	76 ± 7	87 ± 3
5	-	-	+	+	93 ± 9	90 ± 4	51 ± 5	90 ± 5
6	+	-	+	-	98 ± 13	78 ± 12	65 ± 5	90 ± 4
7	-	+	+	-	98 ± 4	97 ± 8	48 ± 5	103 ± 1
8	+	+	+	+	119 ± 4	87 ± 10	56 ± 9	110 ± 6
9	0	0	0	0	107 ± 3	86 ± 4	65 ± 2	106 ± 4

4.2.2 Reagents and Standard Materials

All chemicals used in this work were at least of analytical grade. Ultra pure water (UPW) was obtained from ELGA® *PURELAB® UHQ II* system (resistance > 18MΩ cm). 65% nitric acid, 30% hydrochloric acid and 30% hydrogen peroxide solutions were of Suprapur® quality from Merck (Germany). Cu, Fe, Hg and Zn calibration solutions were prepared by appropriate dilution of 1000 mg L^{-1} CertiPUR® standard solutions from Merck (Germany) with 0.5 mol L^{-1} HNO_3 solution. Reducing reagent consisting of 10% of $SnCl_2$ in 10% HCl was prepared by dissolving an appropriate amount of $SnCl_2 \cdot 2\ H_2O$ of pro analysis grade (< 0.000001% Hg) from Merck (Germany).

The verification was carried out using fish protein certified reference material for trace metals (DORM-3) from National Research Council Canada (NRCC). This reference material consists of sprayed dried fish protein homogenate that has been sieved to pass a 297 μm screen, blended and stored in amber bottled.

4.2.3 Experimental Design

The experimental planning was conducted using a two-level fractional factorial design. This design consists of a series of experiments under various conditions, where the minimum number of experiment runs (*N*) can be estimated by the following expression:

$$N = 2^{K-f} \qquad \text{(Equation 4.4)}$$

where K is the number of variables, and f indicates the degree of fractionality.

The chosen variables were the volume of nitric acid (65%), hydrogen peroxide (30%), hydrochloric acid (30%) and UPW. Maximum and minimum levels of each

factor (Table 4.2) were established mostly according to the data based on the USEPA Method 3052 guideline for microwave assisted acid digestion of siliceous and organically based matrices (USEPA 1996). For instance, addition of hydrogen peroxide (30%) in catalytic amounts (0.1 to 2 mL) may aid in the complete oxidation of the organic sample constituents whilst the addition of 2 mL hydrochloric acid could be appropriate for stabilization of iron in solution and the addition of 5 mL UPW may improve the solubility of metals and prevent temperature spikes due to exothermic reaction.

The experiments were statistically designed and processed using The CAMO® Unscrambler® V. 9.7 and Microsoft® Excel® 2003. Table 4.3 shows the experimental design matrix using Cu, Fe Hg and Zn recoveries (after taking into account the sample blanks) as analytical response. All the experiments were carried out in random order and in triplicates, using 0.50 ± 0.01 g of DORM-3 to uphold the method detection limit via AAS. By making replicates, not only the precision of the results can be improved but this also allows estimation of the associated variability due to experimental measurements (Figure 4.3).

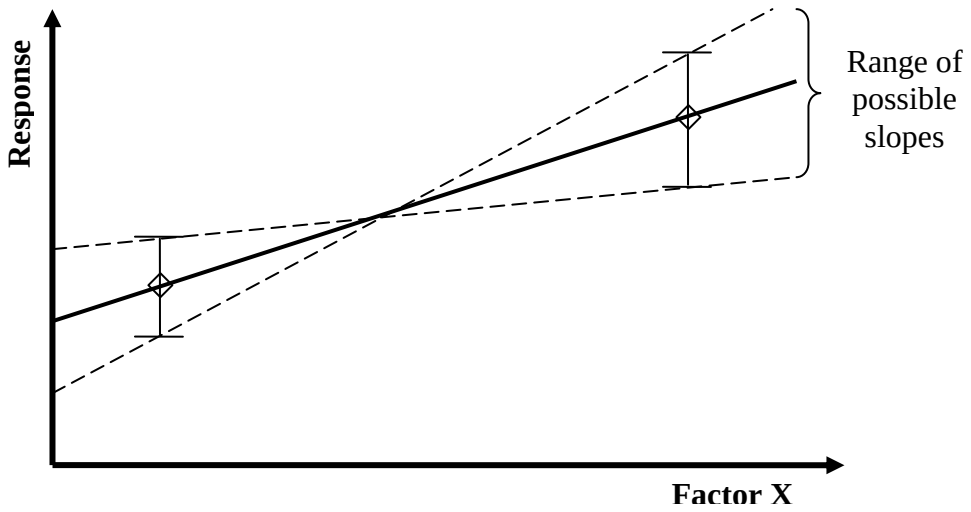

Figure 4.3 Reproducibility and variability check with replicates

4.3 Results and Discussion

The analytical recoveries obtained for DORM-3 in each of the factional factorial designed MAD method are shown in Table 4.3. At first glance, it could be discerned that Hg suffered from low recovery in most cases compared to the other metals without taking into consideration the reagent mixture applied.

The basic principles for determination of total Hg adequately via CVAAS are that the MAD process not only has to permit quantitative liberation of the Hg species from the sample matrix, but also oxidizes them to Hg^{2+}. These ensure that the total Hg in a sample can be subsequently transformed to elemental Hg^{0} when subjected to wet reduction in CVAAS measurements. Based on these, satisfactory recovery of Hg should have been achieved under the combination of strong acids, oxidants and high temperature microwave exposures that will lead to total dissolution. Yet, such vigorous MAD conditions could well lead to loss of volatile Hg species due to self-regulating pressure release mechanism of the digestion vessels (Figure 4.4). Furthermore, it has also been proposed that the Hg adsorption and diffusion through the container walls as well as volatilization during storage, even during the vessel cooling period are the causes of the considerable losses ([Torress *et al.*, 2009] and [Parker and Bloom, 2005]). Those losses are extremely significant when dealing with trace amount of metals, Hg in particular. Thus, the MAD procedures discussed in this chapter are not appropriate for the quantification of trace amount of Hg via CVAAS under reducing vapourization. Hence, the focus was extended towards the evaluation and optimization of MAD performance via two-stage experimental design in the next chapter.

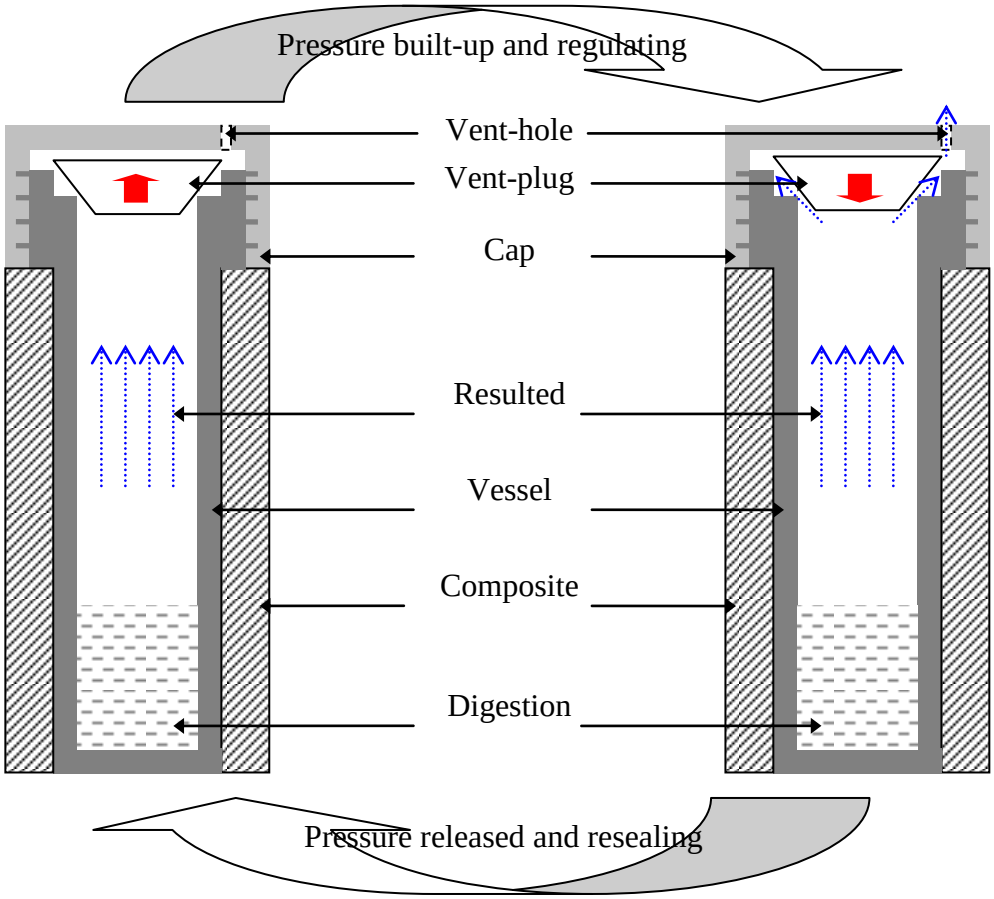

Figure 4.4 Self-regulating pressure release mechanism

On the other hand, it could be noticed from Table 4.3 that the first experiment which involved solely 4.00 mL of 65% HNO_3 is sufficient for satisfactory Cu and Zn recoveries from DORM-3. Similar findings have also been demonstrated by other researchers concerning the usage of HNO_3 exclusively in fish matrices ([Khajeh, 2009] and [Pérez Cid. *et al.*, 2001]). However, when dealing with other elements such as Fe, its recovery could probably be enhanced by introducing small amounts of other reagents. The addition of other reagents with nitric acid prior to digestion may permit more complete oxidation of organic sample matter and address specific decomposition, elemental stability and solubility problems (USEPA, 1996).

4.3.1 Analysis of Effects

Full factorial design requires many more experiment runs, yet it is not necessary to perform all combinations to study the associated main effects. Thus fractional factorial design will definitely be a more economical alternative in the initial stage of this study (Momen *et al.* 2007). This is due to the fact that the number of experiment runs can be reduced to half, at least, compared to the full factorial design method if the degree of fractionality *f* is equal to 1 as in this study.

In our case, the main effect of a given reagent can be regarded as its effect on the metal recovery, while volumes of all other reagents are held at their mean designed value. For example, the main effect of HNO_3 on Cu recovery via MAD can be estimated from following equation:

Main effect of HNO_3 = Mean Cu recovery at 10.00 mL HNO_3 – Mean Cu Recovery at 4.00 mL HNO_3 (Equation 4.5)

An interaction reflects changes in the effect of a given reagent, when the volume of another reagent is shifted from its designed mean value to its maximum level. For instance, the influence of HNO_3 on Cu recovery during MAD may well depend on the volume of H_2O_2 added, so the possible interaction between them can be written as following:

Interaction = ½ (Effect of HNO_3 on Cu at 2.00 mL of H_2O_2 - Effect of HNO_3 on Cu without H_2O_2) (Equation 4.5)

However, the price to pay for performing fewer experiments is the problem of confounding, which means that some effects cannot be studied independently of each other. In table 4.4, AB=CD means that the interaction between HNO_3 and H_2O_2 were mixed up with the interaction between HCl and H_2O. Nevertheless, the main effects confounded with three-variable interactions (such as A=BCD) or more are negligible and can be disregarded since those interactions are very unlikely to be significant ([Esbensen *et al.*, 2004] and [Barrentine, 1999]).

4.3.1.1 Main Effect of HNO_3

Table 4.4 shows the outcomes of estimated effects on metal recoveries. The significance of the effect of each factor is reflected by its associated *p*-value that is judged by the *F*-ratio. In detail, the *F*-ratio is given by the ratio between the explained variance and residual variance which expresses the associated effect of the factor as compared to random noise. Based on the results, as the volume of HNO_3 is increased from 4.00 to 10.00 mL, there is a general rise of 4% in the recovery of Cu, but a decrease in Fe recovery (about 9% in average), and no significant main effect is observed on Zn recovery. Therefore we believe that using 10 mL 70% HNO_3 as suggested by the CEM MarXpress Microwave manufacturer for the MAD of 0.5 g animal tissue is adequate for the determination of Cu and Zn, but not for Fe.

Table 4.4 Estimates of effect on metal recovery based on fractional factorial design

Variable	**Cu**			**Fe**			**Hg**			**Zn**		
R^2	0.926			0.863			0.938			0.931		
Curvature	$p=4.929\times10^{-3}$			$p=0.373$			$p=6.865\times10^{-2}$			$p=5.705\times10^{-3}$		
	Effect	***F*-ratio**	***p*-value**	**Effect**	***F*-ratio**	***p*-value**	**Effect**	**F-ratio**	***p*-value**	**Effect**	***F*-ratio**	***p*-value**
HNO_3 (A=BCD)	4.34	106.00	0.009	-9.13	198.17	0.005	12.68	1.96×10^3	0.001	-1.11	3.59	0.199
H_2O_2 (B=ACD)	2.18	26.78	0.035	2.82	18.83	0.049	-6.85	573.38	0.002	7.31	154.73	0.006
HCl (C=ABD)	7.53	319.61	0.003	6.99	116.23	0.009	-16.1	3.18×10^3	0.001	8.32	200.36	0.005
H_2O (D=ABC)	3.51	69.24	0.014	-2.00	9.46	0.091	-3.19	123.85	0.008	1.46	6.130	0.132
AB=CD	4.26	102.15	0.010	3.06	22.22	0.042	-0.31	1.14	0.397	1.85	9.930	0.088
AC=BD	8.94	451.32	0.002	-2.24	11.92	0.075	-1.67	33.97	0.028	4.69	63.57	0.015
AD=BC	11.1	693.53	0.001	5.24	65.36	0.015	1.01	12.54	0.071	9.21	245.76	0.004

Note: A: HNO_3
B: H_2O_2
C: HCl
D: H_2O

PRELIMINARY EVALUATION OF REAGENT EFFECT

4.3.1.2 Main Effects of Addition of Other Reagents

From the results, additions of 2.00 mL of HCl and/or H_2O_2 to HNO_3 have resulted in a significant increase of the recoveries of Fe, Cu and Zn during MAD (*p*-values < 0.05 for both HCl and H_2O_2). These effects are consistent with those reported by Bermejo-Barrera *et al.* (2000). It is quite clear that adding H_2O_2 to HNO_3 could aid in the completeness of fish muscle digestion (especially organic based Zn), because H_2O_2 not only increases the oxidation power of HNO_3 during digestion, it also increases the pressure in the closed vessel which enhances the attack on organic materials present in the sample (Krachler *et al.* 2002). However, as proposed by Sapkota *et al.* (2005), mixtures of HNO_3 and H_2O_2 alone cannot dissolve all the digested materials that are present in the sample completely, leading to relatively lower recoveries as shown in Experiment No. 3 and No. 4 (Table 4.3). Addition of HCl does aid stabilization of Fe ions due to the solubility of the iron oxide and iron itself in dilute HCl solution (USEPA 2007). Whereas, addition of H_2O shows no significant effect on Fe and Zn recoveries, but is likely to be significant on Cu recovery (Effect = 3.506, *p*-value < 0.05).

4.3.2 Models Check

As illustrated in Figure 4.5, by including center samples in the designed matrix where all factors take their mid-levels, it is possible to diagnose the possibility of a curvature (Figure 4.5). Based on the results tabulated in Table 4.4, there seems to be a strong non-linear relationship between the designed factors and the recovery in both models for Cu and Zn (*p*-value for curvature test < 0.05). Therefore, these models are unable to describe the true shape of the response surface adequately due to considerable lack of fit. In such cases, higher order interactions such as quadratic and/or cubic terms could be of concern.

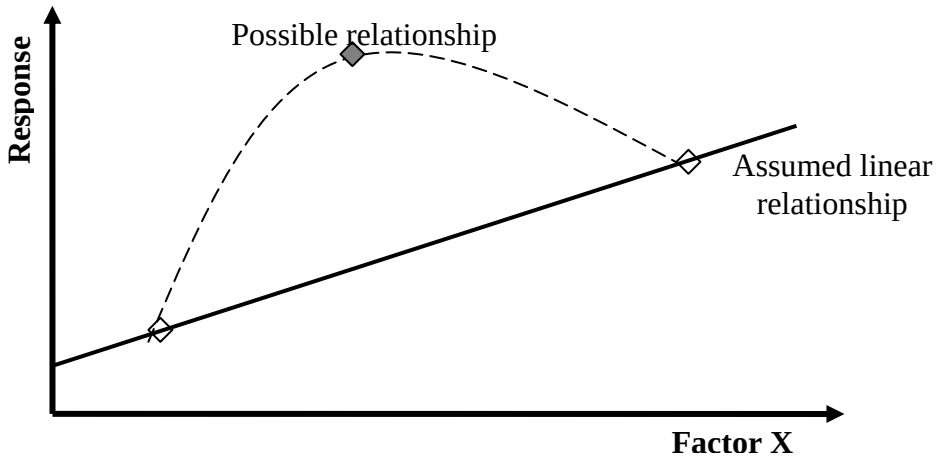

Figure 4.5 Curvature test with center sample

On the other hand, there is insufficient prove to reject the hypothesis on possible curvature in Fe model that established from 4 main factors and 3 second order interactions. In Table 4.5, the results from analysis of variance (ANOVA) show that HNO_3, H_2O_2, HCl and the interactions are significant factors that contribute to Fe recovery during MAD (p-value < 0.005). The average Fe recovery within the designed regions is around 85% which equals the B-coefficient of the intercept (β_0) in the ANOVA. Figure 4.6 illustrates a series of estimated response surfaces and contours associated with those significant factors. It is observed that higher Fe recovery can be achieved by introducing H_2O_2 and HCl while limiting the volume of HNO_3 under the aforementioned experimental condition.

Table 4.5 Analysis of variance of Fe linear model

Fe	*SS*	*DF*	*MS*	*F*-ratio	*p*	β_k	*Std Err*
Model	1.12×10^3	7	159.484	16.299	0.0000		
Error	185.916	19	9.785				
Adjusted	1.30×10^3	26	50.089				
Intercept	1.85×10^4	1	1.85×10^4	1.89×10^3	0.0000	84.838	1.951
HNO3 (A=BCD)	500.319	1	500.319	51.131	0.0000	-1.522	0.213
H2O2 (B=ACD)	47.529	1	47.529	4.857	0.0401	1.407	0.639
HCl (C=ABD)	293.449	1	293.449	29.99	0.0000	3.497	0.639
H2O (D=ABC)	23.894	1	23.894	2.442	0.1346	-0.399	0.255
AB=CD	56.097	1	56.097	5.733	0.0271	1.411	0.589
AC=BD	30.088	1	30.088	3.075	0.0956	-1.034	0.589
AD=BC	165.014	1	165.014	16.864	0.0006	2.42	0.589
Model Check							
Main	865.191	4	216.298				
Interaction	251.198	3	83.733	8.557	0.0008		
Lack of Fit	3.277	1	3.277	0.323	0.5769		
Pure Error	182.639	18	10.147				
Total Error	185.916	19	9.785				

R = 0.926; $\mathbf{R}^2$ = 0.857

SS = sum of squares; *DF* = degrees of freedom; *MS* = mean squares; *p* = *p*-value; β_k = Regression coefficients; *Std Err* = Standard Error.

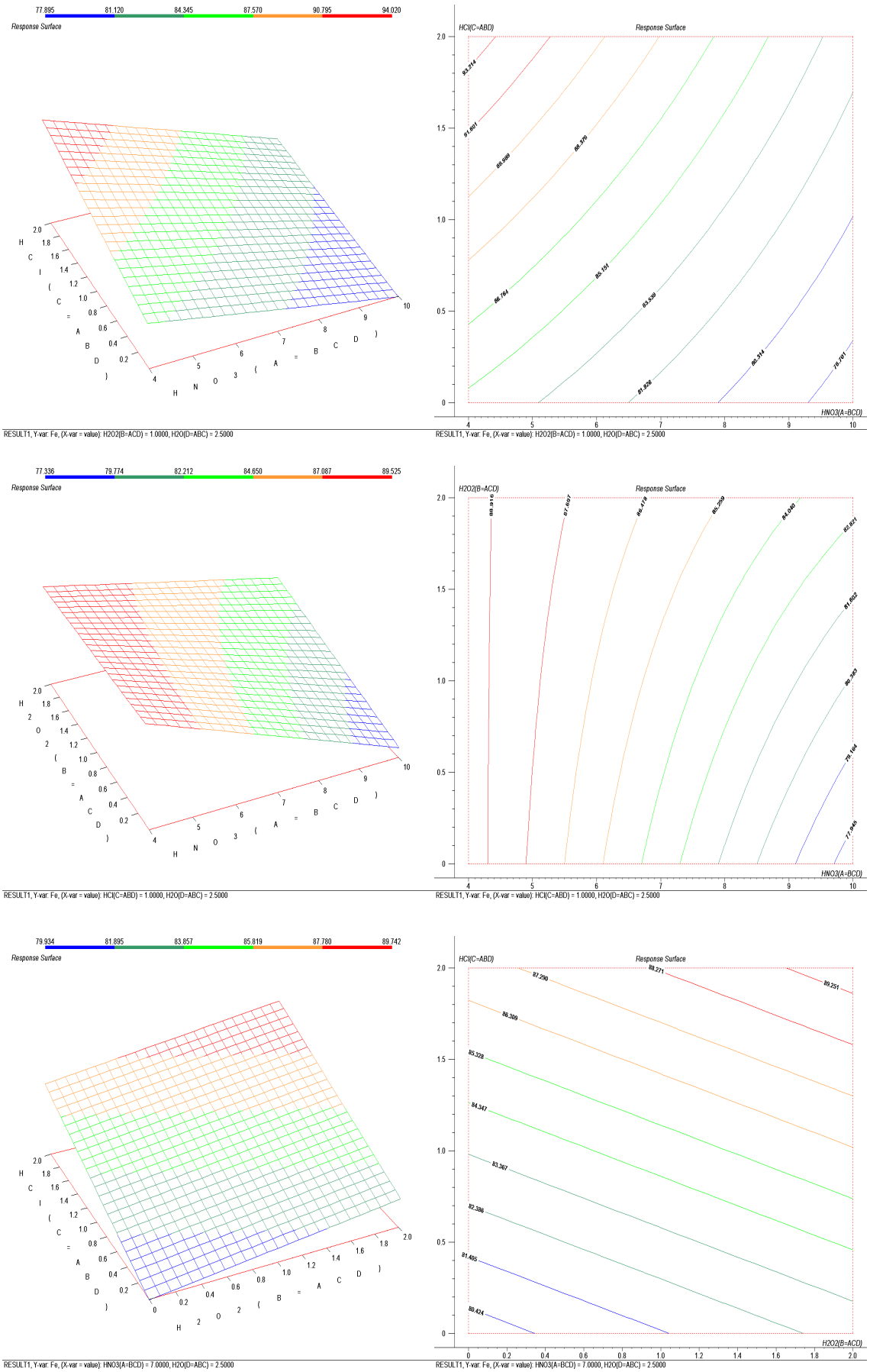

Figure 4.6 Estimated response surface and contour plots

5 OPTIMIZATION OF MAD CONDITION FOR TRACE METAL ANALYSIS BY ICP-MS

5.1 Introduction

Notwithstanding the advantages of closed vessel microwave assisted digestion (MAD) in making dissolution much more vigorous and rapid, it does have potential safety hazards. Thus, precaution is required particularly when dealing with reactive samples involving highly exothermic reactions during the decomposition process. As a safety precaution, the digestion vessels are usually equipped with some sort of pressure regulation mechanisms such as that shown in the discussion section of the previous chapter. However, these kinds of pressure regulating systems do give rise to the possibility of analyte loss through vapour release, if the MAD conditions such as heating rates, microwave power, reagent mixtures etc. are not compatible. Hence, MAD conditions that may have considerable influence on the overall recovery are of concern.

This chapter describes the optimization of single stage temperature-controlled MAD performance for multi-element determination in fish tissue with quantitative recoveries and time efficiency using a two-stage experimental design. In the screening stage, Plackett-Burman design (PBD) was performed to evaluate the suspected influential factors on MAD recoveries, for instance, digestion time, ramp, temperature, power limit, and the addition of hydrogen peroxide and/or hydrochloric acid to nitric acid. In the optimization stage, Box–Behnken design (BBD) is employed to attain the best microwave performance condition via response surface methodology.

5.1.1 Microwave Settings and Conditions

Many different recommendations of microwave oven settings and conditions can be obtained from the literature depending upon the analytical challenges and the microwave systems ([Costa *et al.*, 2009], [Uluozlu *et al.*, 2007], [Yang and Swami, 2007], [Bugallo *et al.*, 2007], [Pérez *et al.*, 2001] & [Zhou *et al.*, 1998]). The use of nitric acid alone for the treatment of fish tissues was found to result in low recovery in certain aspects, thus various combinations of digestion reagents with multiple digestion stages are frequently proposed. Sometimes cooling steps are also included between the heating cycles which enhances considerably the total turnaround time of the sample preparation process. On the other hand, single stage MAD methods are well recognized universally. Their respective temperature/pressure programmes are transferable regardless of the instrument model of the microwave system with high reproducibility. Therefore, single stage temperature/pressure programmes are often found in standard MAD protocols such as USEPA methods ([USEPA 1994a], [USEPA 1996] and [USEPA 2007]).

As far as reagents are concerned, aside from nitric acid, reagents such as hydrochloric acid and hydrogen peroxide are also employed depending on the sample to be digested, the targeted analytes and the detection techniques. EPA method 3052 recommended a generalized multi-element MAD prior to analysis protocol using a combination of 9.0 mL of concentrated nitric acid with appropriate amount of hydrochloric acid and/or hydrogen peroxide and/or water which considerably exceed the need for fish tissue matrix (USEPA 1996). On the other hand, using diluted acids in a closed and high-pressure vessel at temperatures above the boiling point of these acids is a simple alternative and its use is growing. Diluted solutions can absorb microwave energy more intensely owing to their water content. This feature reduces reagent

consumption, contamination, and preparation time but may well cause limitation to the detection technique or increase the complexity of analysis (Soylak *et al.* 2007). It is thus imperative that the factors that may affect the overall efficiency of MAD processes such as oxidizing reagents, microwave radiation applied power, temperature, ramp and digestion time should be investigated for desired targets in line with the quantification technique applied.

5.1.2 Evaluation of MAD Performance

There are several means evaluating of the overall MAD conditions which lead to quantitative recovery. As claimed by many chemometricians, the multivariate experimental designs which allow the simultaneous study of several variables are faster to implement and more cost effective than traditional univariate approaches ([Stalikas *et al.*, 2009], [Ferreira *et al.*, 2007a], [Soylak *et al.*, 2007], [Jalbani *et al.*, 2006] and [Cerutti *et al.*, 2004]).

5.1.2.1 Two-Stage Experimental Design

The well known two-level PBDs can be considered as the simplest and cheapest statistical designs to estimate the main effect of each input factor in the early experimental sequence. These designs allow simultaneous screening of K number of designed factors with no more than $K + 4$ experiments ([Guyot, 2004] and [Plackett and Burman, 1946]). However, PBDs do not allow the study of the interactions between factors, so a following stage of a more sophisticated design is required to precisely model the response surface with higher order interactions based on those significant inputs retained by PBDs.

The common efficient option in response surface methodology (RSM) is Box–Behnken designs (BBDs) which can be regarded as an ideal alternative to full factorial designs or central composite designs (CCDs). These designs allow the understanding of how the overall recovery of a targeted analyte changes in a given direction, thus permitting its optimization. To construct a BBD, the minimum number of experiments (*N*) that are generally required can be expressed by following equation:

$$N = 2K(K-1) + C_0 \qquad \text{(Equation 5.1)}$$

where *K* is number of parameters and C_0 is the number of central points ([Ferreira *et al.*, 2007b] and [Hanrahan & Lu, 2006]).

5.1.2.2 Optimization of Multiple Elements

It is nearly impossible to achieve a particular MAD condition that is optimized for multiple elements in a specified matrix and vise versa, unless there are extremely strong correlations between them. Therefore, in order to perform simultaneous determination of multiple-elements in a given matrix, optimization of MAD becomes an issue of searching for a compromised experimental condition where the resulting recoveries are most satisfactory (Lewis *et al.*, 2005).

5.2 Materials and Methods

5.2.1 Instrumentation

5.2.1.1 ICP-MS

The ICP-MS system used was an Agilent 7500ce from Agilent Technology which is equipped with an octopole reaction system (ORS). The sample introduction system consists of a glass concentric nebulizer and a temperature-controlled spray chamber. The sample solutions were pumped by a peristaltic pump from tubes arranged on an ASX 500 autosampler. Sampler and skimmer cones are made of nickel. Tuning the ICP–MS parameters is indispensable to address sensitivity and matrix tolerability for efficient experiments. The ICP-MS operating conditions were optimized daily with the help of a tuning solution from Agilent Technologies (USA) consisting of 1 μg L^{-1} each of Li, Co, Y, Ce, and Tl in 2% HNO_3 which was spiked with 0.5% HCl in order to cover the entire mass region of interest including the chloride interferences.

5.2.2.2 Microwave Assisted Digestion

The MAD process was performed using the same microwave system as stated in the previous chapter. However the amount of each subjected sample was reduced to approximately 0.25 g which corresponds to 50% of the sample size in the aforementioned MAD study. The digestion experiments were carried out in random order under a temperature-controlled mode in accordance with the designed MAD conditions. In a particular digestion circle, there were always triplicates of a sample together with the sample blank. After digestion, the sample was cooled before being transferred to a 50.00 mL polypropylene volumetric flask and the volume was made up to the mark with ultra pure water (UPW). Diluted sample solutions were filtered through 0.45 μm PTFE membrane into polyethylene vials and stored below 8 °C for analysis by ICP-MS within 5 days using external calibration approach.

5.2.2 Reagent and Standard Materials

5.2.2.1 Acids and Reagents

UPW with resistivity more than 18MΩ cm was obtained from ELGA® *PURELAB® UHQ II* (UK) system and was employed to prepare all standard and sample solutions. 65% nitric acid, 30% hydrochloric acid and 30% hydrogen peroxide solutions were of Suprapur® quality from Merck (Germany).

5.2.2.2 Calibration Standards

ICP multi-element stock standard solution consists of 1000 mg L^{-1} Fe and 10.0 mg L^{-1} each of Ag, As, Cd, Cr, Cu, Mn, Ni, Pb, Se, Zn in 5% HNO_3 obtained from Agilent Technologies (USA). 10.0 mg L^{-1} Hg mono-element stock standard solution was also obtained from Agilent Technologies (USA), while 1000 mg L^{-1} Sn ICP standard solution was from Merck (Germany). Fresh calibration standards were prepared by appropriate dilution of the stock standard solution in respective acid solution in order to mimic the sample matrix.

5.2.2.3 Internal Standards

^{6}Li, Sc, Ge, Rh, In, Tb, Lu and Bi from Agilent Technologies (USA) were added on line as internal standards (ISTD) for the elimination of matrix effects and instrumental drift correction. Basically, these isotopes had been identified as not being present in the sample solution at the detectable levels. Besides that, the general criteria adopted for the selection of an ISTD during ICP-MS measurement is based on the proximity in the mass of targeted isotope, so that the physical and chemical properties of chosen ISTD could be as close to the analyte as possible (Tangen and Lund, 1999).

5.2.2.4 Gaseous

The purity of argon, helium and hydrogen supplies were higher than 99.999%.

5.2.2.5 Certified Reference Materials

Similarly, the certified fish protein homogenate DORM-3 from National Research Council Canada (NRCC) was adopted as the standard reference material for PBD and the BBD throughout the study. The other CRMs involved were DOLT-4 (NRCC) which consists of vacuum stripped dogfish livers with particle size ≤ 610 μm and ERM-CE278 from Institute for Reference Materials and Measurements (Belgium) made up of freeze dried mussel tissues homogenate that is screened at 125 μm.

5.2.3 Experimental

5.2.3.1 Cleaning

For the analysis of trace level of analytes, it is necessary to keep the blank value as low as possible. In order to avoid cross-contamination between different assignments, it is necessary to soak all the plasticware overnight in 10% (v/v) HNO_3 (Sun and Ko, 2004). For vessel cleaning, microwave digestion was carried out by ramping to 180 °C in 10 minutes and held for 10 minutes using 10 mL 65% HNO_3 as suggested by the manufacturer during method development or blank digestion utilizing the developed MAD condition. The digestion vessels were then soaked or rinsed thoroughly with UPW and dried prior to use.

5.2.3.2 Experimental Design

PBDs are reduced experimental plans for preliminary screening. It was employed to screen the main effects of the following parameters that were initially selected to define the single stage microwave digestion conditions. They are: total irradiation time (*A*), ramp time (*B*), digestion temperature (*C*), microwave power limit (*D*) and the addition of H_2O_2 (*E*) and/or HCl (*F*) to HNO_3. Maximum and minimum levels of each parameter (Table 5.1) were established based on available literature information ([Türkmen *et al.*, 2009], [Tüzen, 2009], [USEPA 2007], [Saavedra *et al.*, 2004] [Zhou *et al.*, 1998], [Smith and Arsenault, 1996] and [USEPA 1996]).

Table 5.1 Parameters and levels used in multivariate design

Parameter	**Symbol**	**Low Level (-)**	**Central (0)**	**High Level (+)**
Radiation time / min.	*A*	15.00	22.50	30.00
Ramp / min.	*B*	5.00	10.00	15.00
Temperature / °C	*C*	160	180	200
Power / W	*D*	800 (50%)	-	1600 (50%)
H_2O_2 / mL	*E*	0.000	-	2.000
HCl / mL	*F*	0.000	-	0.500

Consequently, the most significant microwave setting parameters were evaluated further under BBDs in order to identify the high-recovery trends. All the experiments were carried out in triplicates in random order using DORM-3 so as to increase the degree of freedom and for obtaining a better statistical evaluation. Further verification was accomplished with DOLT-4 and ERM-CE278 to investigate the reliability of the developed methods. The experimental data were processed using The CAMO® Unscrambler® V. 9.7 and Microsoft® Excel® 2003.

5.3 Results and Discussion

5.3.1 ICP-MS Tuning

The performance of ICP-MS depends greatly on the efficiency of the ionization process in plasma corresponding to several factors such as plasma temperature, sample residence time, density and water vapour content of the sample aerosol; as well as the capability to diminish polyatomic interference ions from entering the quadrupole mass analyzer. Proper adjustment of parameters summarized in Table 5.2 can be beneficial in improving the efficiency of ICP-MS for trace metal analysis.

Table 5.2 ICP-MS operating conditions

Tuning parameter	
Plasma RF power:	1500 W
Reflected power:	< 15 W
Plasma gas flow:	15 L min^{-1}
Auxiliary gas flow:	1.0 L min^{-1}
Sampling depth:	7.0 – 9.0 mm
Carrier gas flow:	0.8 – 1.0 L min^{-1}
Makeup gas flow:	0.1 – 0.3 L min^{-1}
Peristaltic pump:	0.1 rps
Collision gas type:	None / He / H_2
Collision gas flow:	0 – 5.0 L min^{-1}
Spray chamber temperature:	2 °C
Sampler & skimmer cones:	Ni

ICP-MS analysis using normal/no-gas mode (the ORS is turned off) with correction equations is analogous to the standard ICP-MS approach that is well-recognized by USEPA (1998). Proper isotope selection allows retaining of adequate sensitivity against those low-mass and high-mass isotopes which are considerably free from major spectral interferences compared to those isotopes in medium-mass region (Table 5.3). It makes intuitive sense that the greater the sensitivity of an ICP-MS system, the lower is the detection limit (*DL*); so the typical ion count for $^{7}Li^{+}$ (representing low-mass elements) and $^{205}Tl^{+}$ (representing high-mass elements) were tuned using 1 μg L^{-1} of abovementioned tuning solution to > 10000 s^{-1} and > 20000 s^{-1} under this analytical mode.

Aside from instrumental sensitivity, there could be other factors that affect the *DL* for a given isotope in a given sample such as background "noise" and potential interferences, since the *DL*s for ICP-MS are most often quoted as (Elliott *et al.*, 2007):

$$DL = \frac{3\sigma_{blank}}{sensitivity} \qquad \text{(Equation 5.2)}$$

where the standard deviation of the blank (σ_{blank}) is expressed in counts per second (cps), and the sensitivity is expressed in cps per unit concentration (μg L^{-1}). For these reasons, the instrument "noise" was monitored at m/z = 220 (where no ions are expected) and kept at < 20 s^{-1}.

The ratios of $^{140}Ce^{2+}/^{140}Ce^{+}$ and $^{156}CeO^{+}/^{140}Ce^{+}$ which have been widely adopted to examine the processing ability of the plasma associated with potential spectral interferences due to the formation of doubly charged ions and oxide ions were maintained as < 3 % and < 1 % (Mc. Curdy and Potter, 2001). All these can be done by simple adjustment of plasma and torch conditions.

Table 5.3 Summary of analyte masses, analytical conditions and method detection limits for studied elements

Analyte	Isotope	ISTD	ORS	Potential Interferences	Integration time / s	MDLs / μg kg^{-1}
V	51	^{45}Sc	He	$^{35}Cl^{16}O^{+}$, $^{37}Cl^{14}N^{+}$	1.5	1
Cr	52	^{45}Sc	He	$^{40}Ar^{12}C^{+}$, $^{35}Cl^{16}O^{1}H^{+}$, $^{36}Ar^{16}O^{+}$,$^{37}Cl^{14}N^{1}H^{+}$	1.5	2
Mn	55	^{45}Sc	He	$^{40}Ar^{16}N^{1}H^{+}$, $^{38}Ar,^{17}O^{+}$	0.3	7
Fe	56	^{45}Sc	H_2	$^{40}Ar^{16}O^{+}$, $^{40}Ca^{16}O^{+}$	0.3	30
Co	59	^{72}Ge	He	$^{23}Na^{35}Cl^{1}H^{+}$, $^{43}Ca^{16}O^{+}$	0.3	1
Ni	60	^{72}Ge	He	$^{44}Ca^{16}O^{+}$, $^{23}Na^{37}Cl^{+}$, $^{43}Ca^{16}O^{1}H+$	0.3	30
Cu	63	^{72}Ge	He	$^{40}Ar^{23}Na^{+}$, $^{12}C^{16}O^{35}Cl^{+}$, $^{12}C^{14}N^{37}Cl^{+}$	1.5	9
Zn	66	^{72}Ge	He	$^{48}Ca^{18}O^{+}$	0.3	49
As	75	^{72}Ge	He	$^{40}Ar^{35}Cl^{+}$, $^{40}Ca^{35}Cl^{+}$	1.5	11
Se	78	^{72}Ge	H_2	$^{40}Ar^{38}Ar^{+}$	1.5	1
Ag	107	^{103}Rh	Normal		0.3	10
Cd	111	^{103}Rh	Normal		0.3	1
Sn	120	^{103}Rh	He		0.3	16
Hg	202	^{209}Bi	Normal		3.0	7
Pb	*	^{209}Bi	Normal		0.3	6

* Pb = ^{206}Pb + ^{207}Pb + ^{208}Pb

Although the conditions that lead to the $^{156}CeO^{+}/^{140}Ce^{+}$ minimum may not exactly assure the maximum sensitivity for targeted elements, it corresponds to the most robust running set for environmental analysis (Nelms, 2005). For instance, the plasma radio frequency (RF) forward power was set to 1500 W with reflected power < 15 W, plasma gas flow of 15 L min^{-1} and auxiliary gas flow of 1.0 L min^{-1} in order to sustain high-temperature argon plasma discharge that enhances the degree of decomposition of refractory species and the sensitivity for elements with high first ionization potential such as As, Se, Cd and Hg. However, the analytical sensitivity for low-mass isotopes may be lost significantly if RF power is too high (Agilent 2005b). Similarly, lengthening the sampling depth may aid in breaking down many of the interfering polyatomic species such as metal oxides by extending sample residence time in plasma, but leads to sensitivity loss as well. On the other hand, sample nebulization efficiency and its uptake rate are subject to carrier gas flow, makeup gas flow and peristaltic pump speed. Basically, a high sample introducing rate increases the analytical sensitivity, but also promotes formation of oxides and doubly charged ions due to the associated cooling effect on the plasma.

The temperature of spray chamber was precisely maintained at 2 °C in order to condense off those larger aerosol droplets from the nebulized stream particularly the water vapour (Figure 5.1). This also prevents possible signal drift resulting from discrepancy in room temperature. This will limit the solvent loading significantly and consequently retains the plasma temperature/energy which assists decomposition, ionization as well as diminishing the associated oxide interferences (Agilent 2005a).

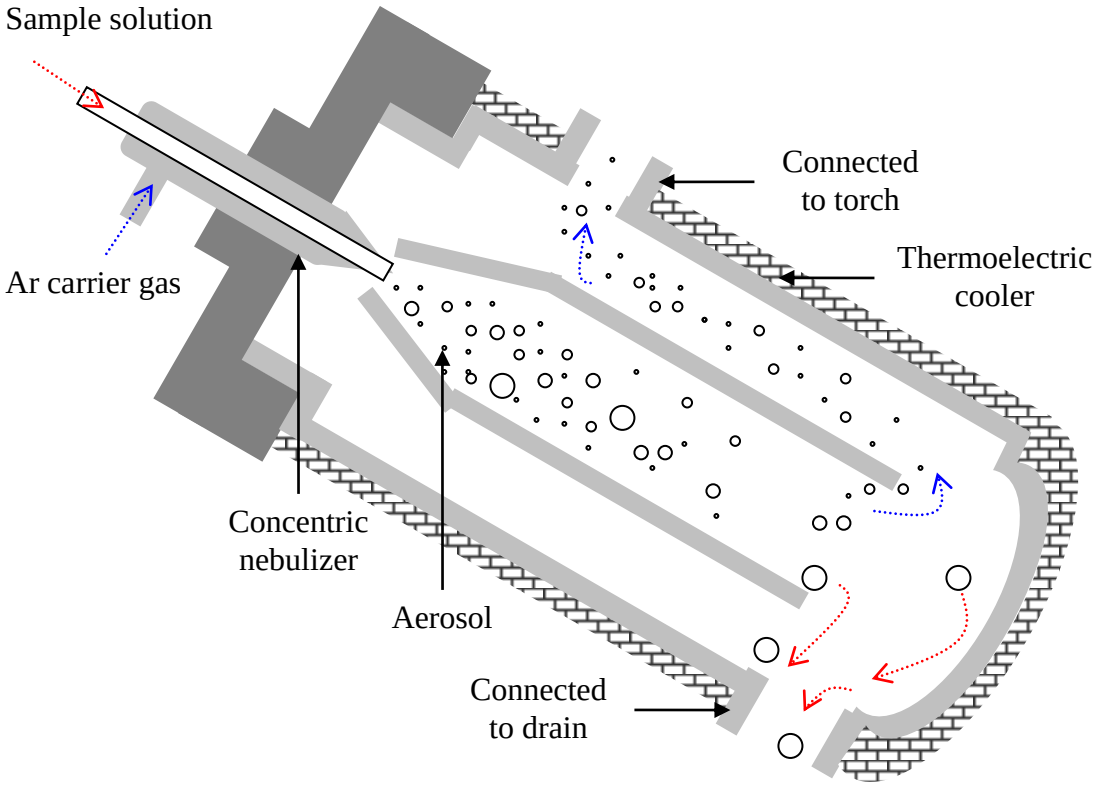

Figure 5.1 Schematic of a temperature-controlled spray chamber

ORS was activated during the quantification of isotopes with masses of interest in medium-mass region of the spectrum which predominantly suffer from polyatomic interference ions derived from the plasma gas and the matrix of sample solution listed in Table 5.3. Basically, the higher helium/hydrogen gas flow in the ORS, the greater their collisions and/or reactions probabilities with interference ions and thus enhances the removal of interfering spectra. However, the collision/reaction stream leads to dilution and results in significant loss of the targeted ion counts. Therefore, under helium/collision mode, the helium flow was tuned between 3.0 – 5.0 L min^{-1} until typical ion counts of at least 5000 s^{-1} for both $^{59}Co^{+}$ and $^{89}Y^{+}$ (both representing medium mass isotopes) were obtained; $^{78}Ar_2^{+}$ and $^{75}ArCl^{+}$ ion counts and $^{51}ClO^{+}/^{59}Co^{+}$ ratio were below 30 s^{-1}, 30 s^{-1} and 3% respectively. Likewise, typical ion counts for both $^{80}Ar_2^{+}$ and $^{78}Ar_2^{+}$ dimers were also maintained below 50 s^{-1} and 20 s^{-1} by adjustment of the hydrogen flow during hydrogen/reaction mode.

5.3.2 Sample size in MAD

From the safety aspect, if more amount of sample is subjected to MAD, the resulting pressure will be higher and will result in a more exothermal reaction. Notwithstanding this, it has been reported that dramatic increases in pressure have resulted in no virtual increase in temperature during the decomposition of carbohydrates, proteins and fats which can result in pressure/temperature-control failure and posing an explosion hazard (Smith and Arsenault, 1996). The decomposition of protein compounds in particular tends to liberate gas and develops higher pressure at a higher temperature compared to carbohydrates (Mester and Sturgeon, 2003). Thus for fish muscles which are composed primarily of proteins and fats, the mass of the analytical portion must be carefully selected in order to reduce the risks associated with the use of pressurized microwave digesters.

From literature reports, sample weights around 0.5-0.8 g are frequently used to ensure wider representativeness in the sub-sample and to attain sufficient analytical signal ([Cui *et al.*, 2010], [Lalonde *et al.*, 2010] and [Roa *et al.*, 2010]). In our case, sample weights were limited to 0.25 g (a minimum sub-sample suggested by NRCC to ensure certified values for DORM-3), despite increasing analytical uncertainties. Obviously, by reducing the sample size, the entire digestion process requires lesser amount of acids/oxidizing reagents. Consequently, the digested solutions would not be subjected to high dilution rates during ICP-MS analysis so the method detection limits (MDLs) could be retained.

5.3.3 2-level Plackett-Burman design

There is no point in loading the digestion vessel with 9 mL of HNO_3 as recommended by USEPA (1996) since the sample size is only about 0.25 g. The volume of HNO_3 was therefore fixed at 2.5 mL (approximately 10 times the sample amount) throughout the study and other input parameters were varied according to the designed conditions as displayed in Table 5.1 and Table 5.4. The final volume was brought to 10.0 mL with UPW in order to allow intense absorption of microwave energy, and also to prevent temperature spikes due to exothermic reactions. Furthermore, sample digestion should be achieved with the lowest possible acid mixture concentration, lowest temperature and shortest digestion time in order to prevent alterations of the inner surface of the digestion vessels as well as to minimize potential hazards ([Erdoğan *et al.*, 2006], [Rio Segade *et al.*, 2003] and [Silvestre *et al.*, 2000]).

Initially, a 2-level PBD was applied to screen the main effects of the 6 potential parameters noted above that probably contribute to the MAD recovery of targeted metals because a full factorial design will require at least 2^6 number of experiment runs and is not practical. However, the drawback for performing fewer experiments is the problem of confounding that had been mentioned in the previous chapter. Nevertheless, higher order interactions confounded with the main effects in this PBD are negligible ([Esbensen *et al.*, 2004] and [Barrentine, 1999]). Table 5.4 shows the Plackett-Burman matrix and metal recoveries (after taking into account the reagent blanks) that had undergone each designed condition. High recoveries were obtained for a certain array, which seem to indicate that the optimum is likely to be somewhere inside the investigated region.

Table 5.4 Design matrix and the results of the two-level Plackett-Burman design

No.	*A*	*B*	*C*	*D*	*E*	*F*	*Clarity*	*Color*	Metal Recovery /%							
									Cr	**Fe**	**Cu**	**Zn**	**Cd**	**As**	**Hg**	**Pb**
1	-	+	-	+	+	+	1	1	73 ± 3	102 ± 9	104 ± 7	93 ± 1	100 ± 1	121 ± 4	103 ± 5	66 ± 5
2	+	-	+	+	+	-	0	0	101 ± 9	100 ± 12	102 ± 1	115 ± 1	102 ± 3	117 ± 3	89 ± 1	92 ± 11
3	-	+	+	+	-	-	0	1	88 ± 9	100 ± 2	107 ± 5	101 ± 3	106 ± 3	134 ± 9	107 ± 3	80 ± 15
4	+	+	+	-	-	+	0	1	94 ± 5	102 ± 1	104 ± 3	95 ± 2	98 ± 3	118 ± 3	103 ± 1	123 ± 9
5	+	+	-	-	+	-	0	1	84 ± 7	96 ± 7	108 ± 5	114 ± 10	107 ± 2	124 ± 2	103 ± 6	60 ± 8
6	+	-	-	+	-	+	0	1	108 ± 9	101 ± 1	105 ± 4	96 ± 2	104 ± 2	124 ± 2	107 ± 15	120 ± 15
7	-	-	+	-	+	+	0	0	87 ± 9	95 ± 11	103 ± 2	95 ± 4	102 ± 1	116 ± 4	109 ± 5	103 ± 2
8	-	-	-	-	-	-	1	1	87 ± 11	94 ± 1	110 ± 1	103 ± 1	111 ± 1	134 ± 6	97 ± 10	57 ± 15

Clarity: 1 = thin residue coat; 0 = clear

Color: 1 = pale yellow; 0 = colorless

5.3.3.1 Evaluation of Digestion Completeness

The completeness of decomposition could be judged by the clarity of the resulting solution. From Table 5.4, it is noted that a yellowish residue thin coat was present at the bottom of the PFA vessel which reflects the incompleteness of the digestion process in experiment no. 1 and no. 8 with a relatively lower recovery for Cr and Pb. Based on the results from the high order interaction effect (HOIE) tests, these thin coats could be significantly eliminated by subjecting the sample to longer irradiation period and/or higher temperature. However, total decomposition of the sample does not always guarantee quantitative recoveries, because there is a possibility of analyte loss through vapour release during the pressure build-up inside the vessel as noticed in the previous chapter. As an example, losses of Cr and Ni have been reported by Reis *et al.* (2008), although the digestion was complete. On the other hand, shortening of ramp time and/or increase of microwave temperature and/or addition of H_2O_2 could significantly eliminate the yellowish color of the digested solution. This is due to the increase in total oxidation potential under the condition described above, which will enhance reoxidization of NOx into NO_3^- and thus suppressing the formation of yellow nitrogen oxide. Again, both observations do not reflect the actual MAD performance unless quantification is carried out.

5.3.3.2 Main Effects of Microwave Setting

It is not necessary to address the main effects of all studied parameters on each element individually because the aim of this study is to work out a compromised MAD condition for simultaneous multi-element determination via ICP-MS. Figure 5.2 shows a combined Pareto chart which allows identification of potentially important parameters affecting MAD metal recovery at a glance. Some of these parameters offer positive effects and others give negative influences. In fact, recovery of a particular metal is highly depends on the chemical behavior of that metal substance before and after digestion. In general, for a 95% confidence interval (which considering only the magnitude of effects), parameters which main effects exceed the range ± 7.5 are considered statistically significant.

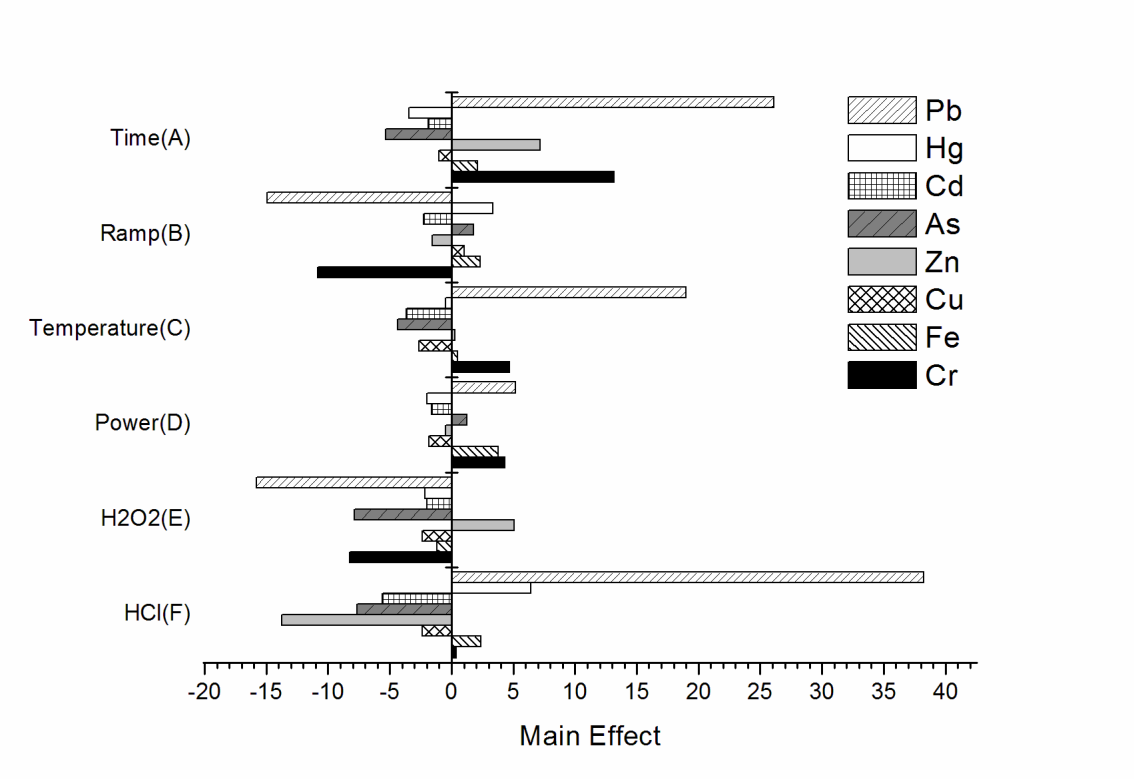

Figure 5.2 Combined Pareto chart

Among the parameters shown in Figure 5.2, radiation time (*A*) is one of the most influential parameters on the recoveries of Cr, Zn, and Pb. Lengthening the total radiation time from 15 mins. to 30 mins. ensures sufficient reaction time for total sample decomposition. However, the longer the radiation time, the higher is the possibility of losing volatile analytes due to pressure regulation. In general, as organic matrices are decomposed, significant increases in internal vessel pressure are observed due to the formation of CO_2 and NO_2 as well as volatile chlorine, as in our case (Smith and Arsenault, 1996). Thus, a proper temperature ramp is required in order to control the situation where the bulk of gaseous by-products are evolved from most of the digestion process over the critical temperature range (Mester and Sturgeon, 2003).

It is observed from Figure 5.2 that increasing the ramp time (*B*) from 5 mins. to 15 mins. could reduce the recoveries of Cr, Cd and Pb significantly. This is due to the fact that although high ramp time setting can avoid vigorous reaction, it shortens the microwave energy exposure rate held at maximum operating temperature. Consequently, this results in insufficient reaction time at higher temperature. Obviously, these suggest that there are significant interactions between ramp time and total radiation time and/or operating temperature.

Temperature (*C*) is undoubtedly the ultimate determinant of digestion quality. At a temperature range of approximately 140°C, carbohydrates are the first constituent to decompose (Mester and Sturgeon, 2003). Proteins decompose at about 150 °C, followed by lipids at around 160 °C (Smith and Arsenault, 1996). By increasing the digestion temperature there is an increase in pressure, therefore resulting in the risk of analyte lost as well as safety hazard issues. This is the reason why both time and temperature share the same effect directions for all the elements studied (Figure 5.2).

On the other hand, microwave power limit (*D*) has the least important effect on the overall recovery of metals due to the fact that microwave power is controlled on the basis of feedback readings by the temperature monitoring system. More powerful setting shows numerical enhancement of Cr, Fe and Pb recoveries but its effects are not statistically significant compared to others. Thus microwave power limit was maintained at 50% of 1600 W for optimization study so that there is room for expanding the number of vessel per digestion cycle if needed.

5.3.3.2 Main Effects of Reagent Addition

MAD is mostly carried out with the aid of oxidizing acids, primarily, nitric acid with other reagents. The selection of specific reagents or reagent mixture depends on the nature of the sample and solubility of the resulting salts. Results obtained show that there are limitations in applying HNO_3 alone, especially for Cr, where incomplete digestion and moderate solubility of Cr lead to relatively low recovery. The addition of H_2O_2 (E) with HNO_3 prior to digestion permits more complete oxidation, however, generation of high pressure could well result in loss of volatile compounds via pressure regulation. Figure 5.2 indicates that the addition of 2.00 mL of H_2O_2 enhances recovery of Zn only but manifests negative effects on the recovery of other elements. For this reason, H_2O_2 was not used in the next stage of this study.

Figure 5.2 also shows that addition of 0.50 mL of HCl (*F*) is the most significant parameter that enhances Pb recovery. HNO_3/HCl mixture under elevated temperature produces NOCl which dissociates into corrosive Cl_2 thus aiding attack on the sample. Furthermore, it is appropriate for the stabilization of Fe in solution (USEPA 1996). However, the introduction of HCl in sample preparation process can lead to major difficulty in trace metal analysis with a standard quadrupole ICP-MS equipment

because Cl^- ions retained in the final sample solution matrix induces Cl-combined polyatomic interferences. As a result, more spectroscopic interferences arise in the determination of, ^{51}V, ^{52}Cr, ^{59}Co, ^{60}Ni, ^{63}Cu and ^{75}As due to the formation of $^{51}ClO^+$, $^{51}ClN^+$, $^{52}ClOH^+$, $^{52}ClNH^+$, $^{59}NaClH^+$, $^{60}NaCl^+$, $^{63}COCl^+$, $^{63}CNCl^+$, $^{75}ArCl^+$ and $^{75}CaCl^+$ etc. Nevertheless, the ICP-MS in this study is equipped with ORS, which assists in minimizing the effect of polyatomic ions by chemical reaction, collisionally induced dissociation and/or kinetic energy discrimination ([Dufailly *et al.*, 2008], [Chen *et al.*, 2007], [Darrouzès *et al.*, 2007], [Tanner *et al.*, 2002] and [Tanner and Baranov, 1999]). Thus, it is of importance to choose the appropriate quantification technique in evaluating the performance of a digestion process. Considering all the above observations, the digestion procedure established by experiment no. 6 could be regarded as an acceptable condition. However for this experiment, a 30 minutes total irradiation time is required. Therefore, RSM was applied in order to seek for a compromised region that is more efficient temporally by adjusting only the microwave setting.

5.3.4 Box Behnken Design

Basically, PBDs do not allow interaction between variables. However, the interaction between parameters could be important, so three of the most significant microwave setting parameters (radiation time, ramp and temperature) were chosen for evaluation under BBD. Other parameters were kept constant as assigned in experiment no. 6 and those were the microwave power limit (50% of 1600W), volume of H_2O_2 (0 mL) and volume of HCl (0.5 mL). The results obtained indicate that the quadratic models suffered significant lack of fit, so additional cubic interactions were considered for the response surfaces modeling. The polynomial equations below explain the relationship of the three variables which are radiation time (*A*), ramp time (*B*), temperature (*C*) and recovery. β_k are the regression coefficients.

$$\text{Recovery} = \beta_0 + \beta_1 A + \beta_2 B + \beta_3 C + \beta_{1,2} AB + \beta_{1,3} AC \qquad \text{(Equation 5.1)}$$
$$+ \beta_{2,3} BC + \beta_{1,1} A^2 + \beta_{2,2} B^2 + \beta_{3,3} C^2$$
$$+ \beta_{1,2,2} AB^2 + \beta_{1,1,2} A^2 B + \beta_{1,1,3} A^2 C$$

This helped to improve the overall R^2. A series of response surfaces and contours fittings ($R^2 > 0.8$) corresponding to MAD recoveries are displayed in Figure 5.3 – Figure 5.9. By evaluation of these plots, the optimum MAD region for each element can be summarized (Table 5.5).

Table 5.5 Estimated optimum microwave setting and working condition for multi-element analysis

Parameter	**Radiation Time (*A*) / min**	**Ramp (*B*) / min.**	**Temperature (*C*) / °C**	**R^2**
Cr	30.0	5.0 -6.7	185 - 188	0.826
Fe	30.0	15.0	180 - 182	0.897
Cu	24.4	10.4 - 10.5	180	0.901
Zn	24.4	10.5 - 10.8	180	0.904
As	23.1	10.4	180	0.945
Hg	30.0	10.0	178 -180	0.840
Pb	30.0	10.0	180-183	0.854
Working	25.0	10.5	185	

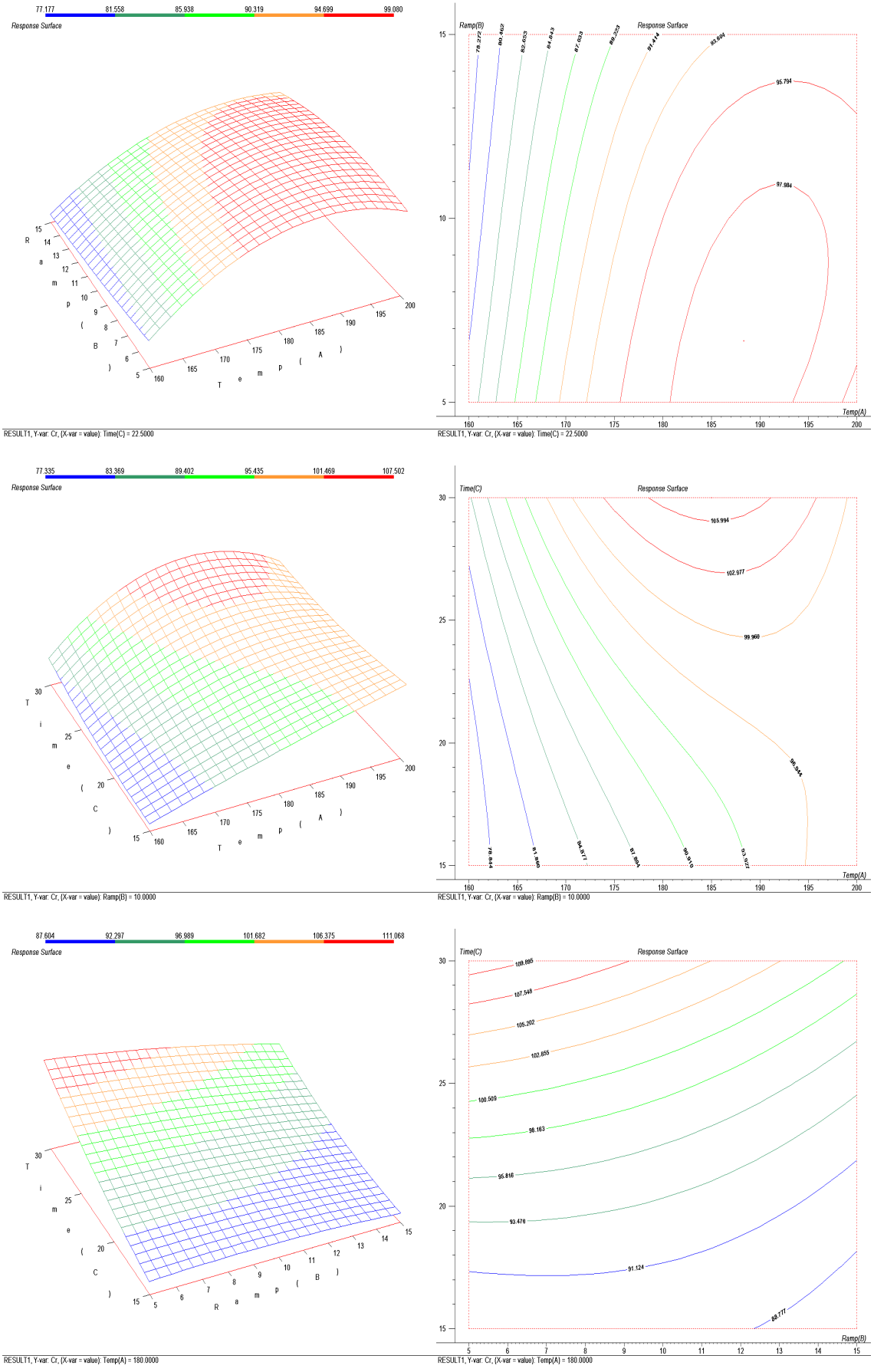

Figure 5.3 Estimated response surface and contour plots for Cr

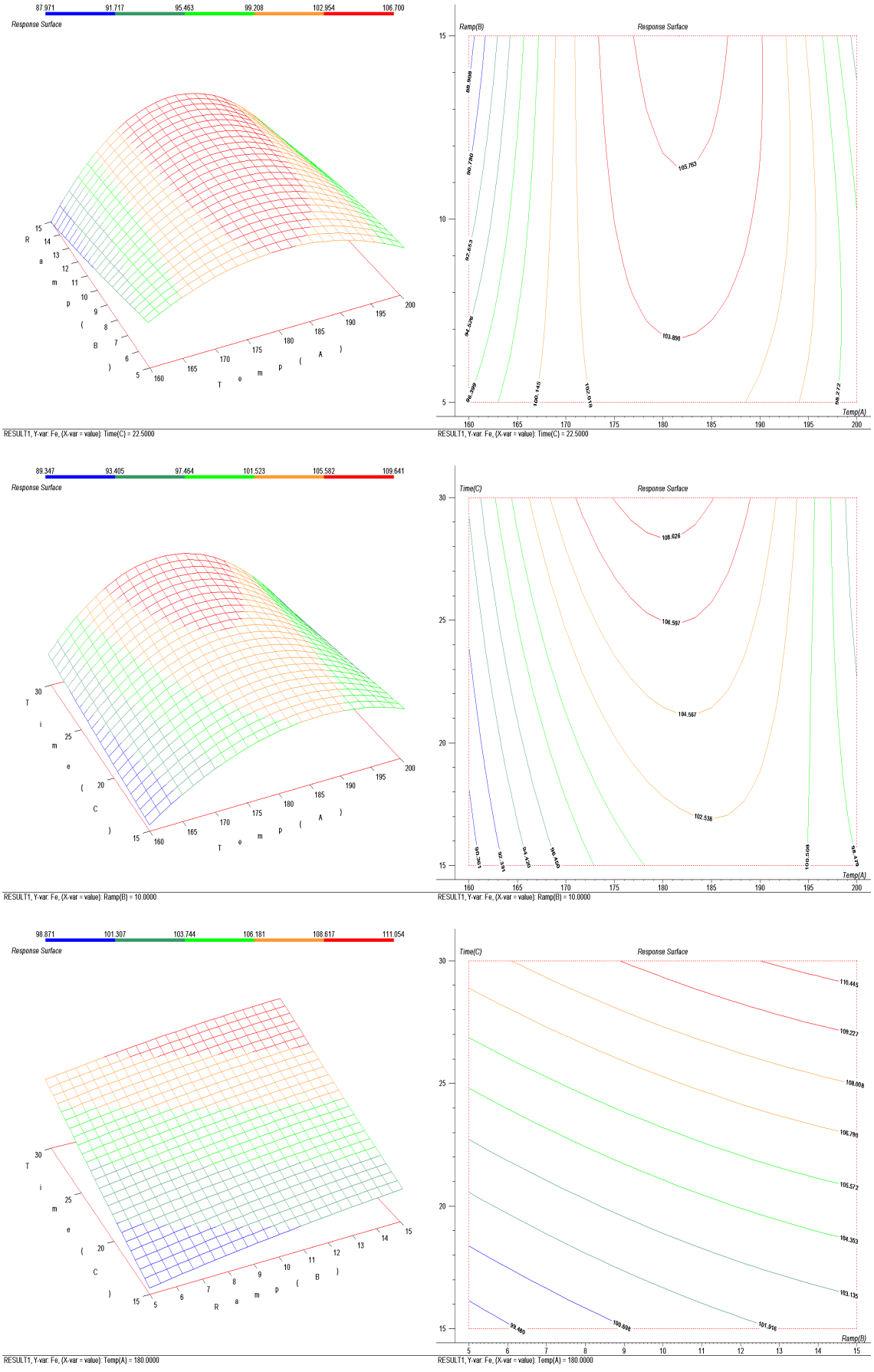

Figure 5.4 Estimated response surface and contour plots for Fe

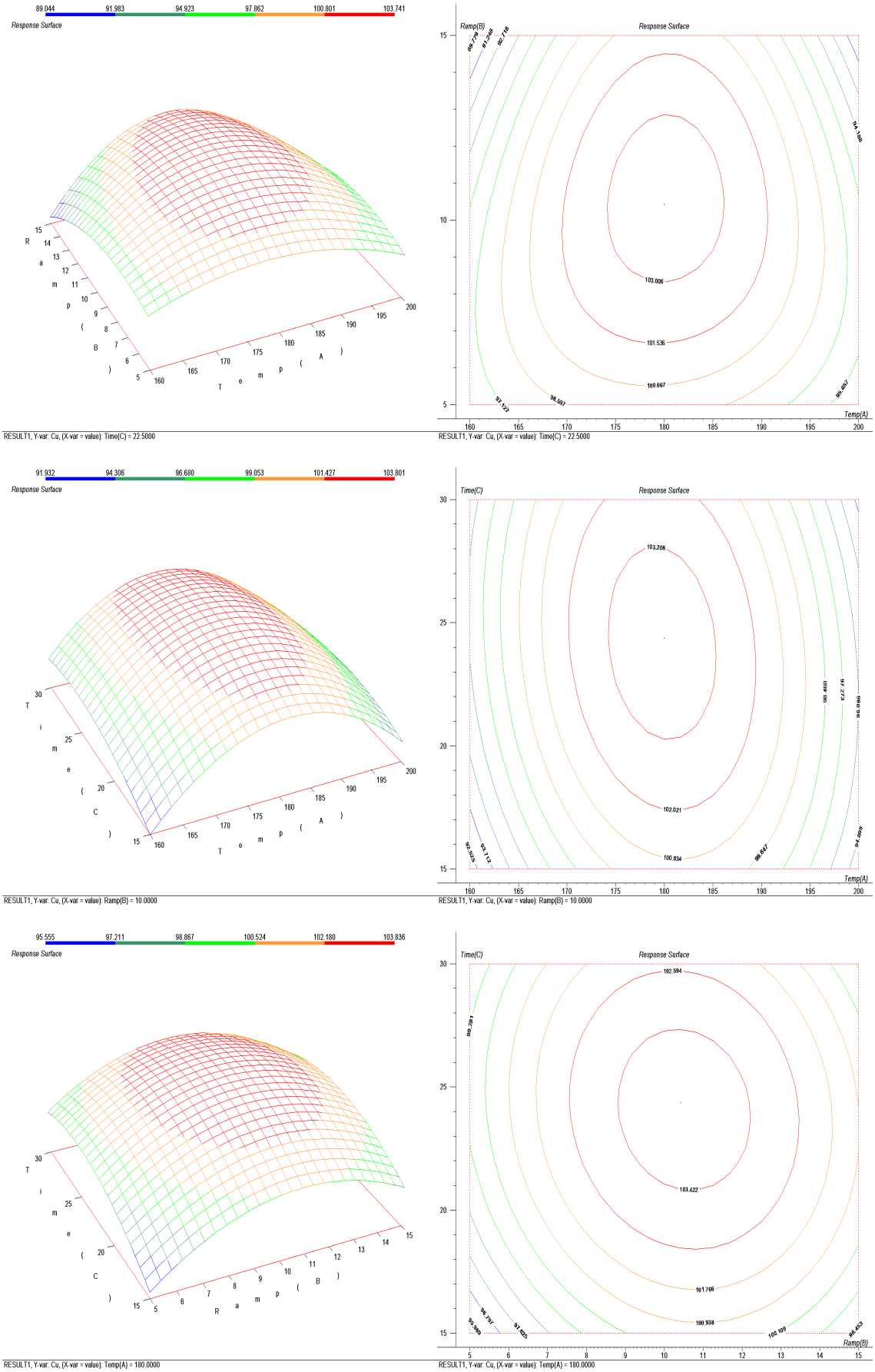

Figure 5.5 Estimated response surface and contour plots for Cu

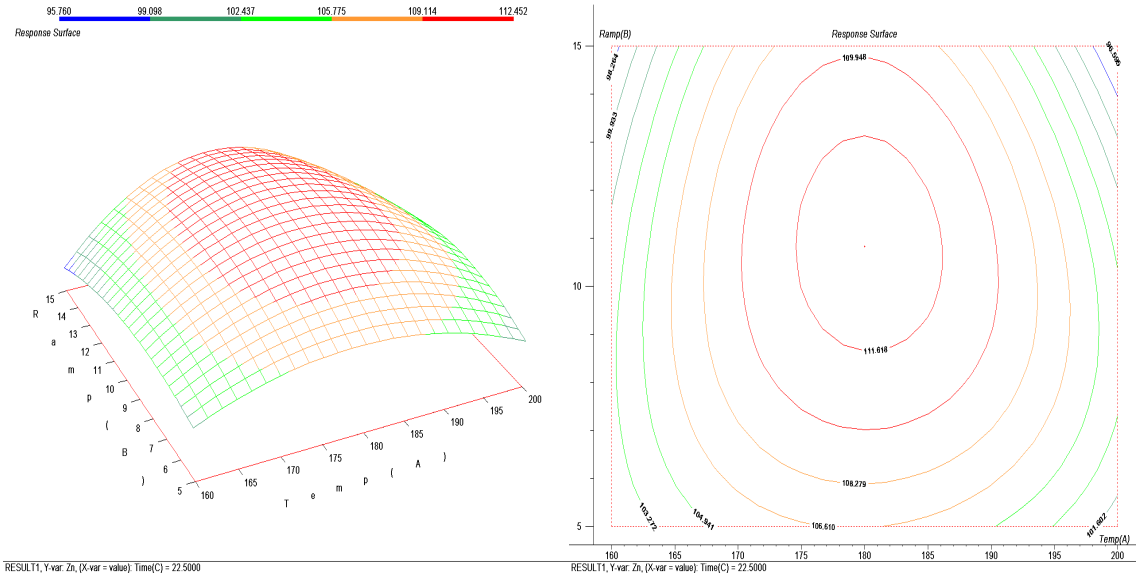

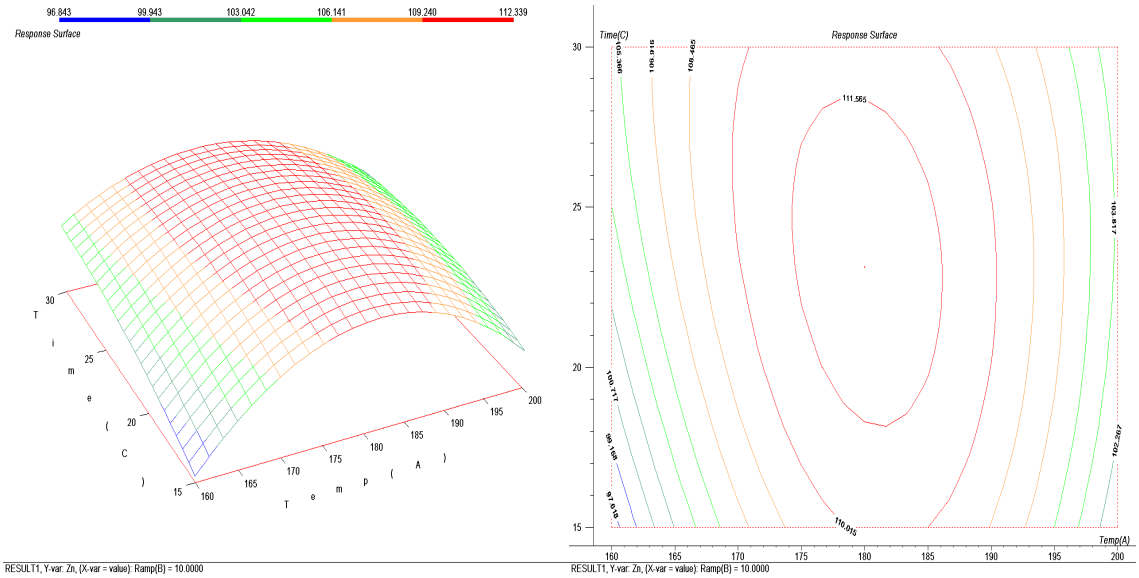

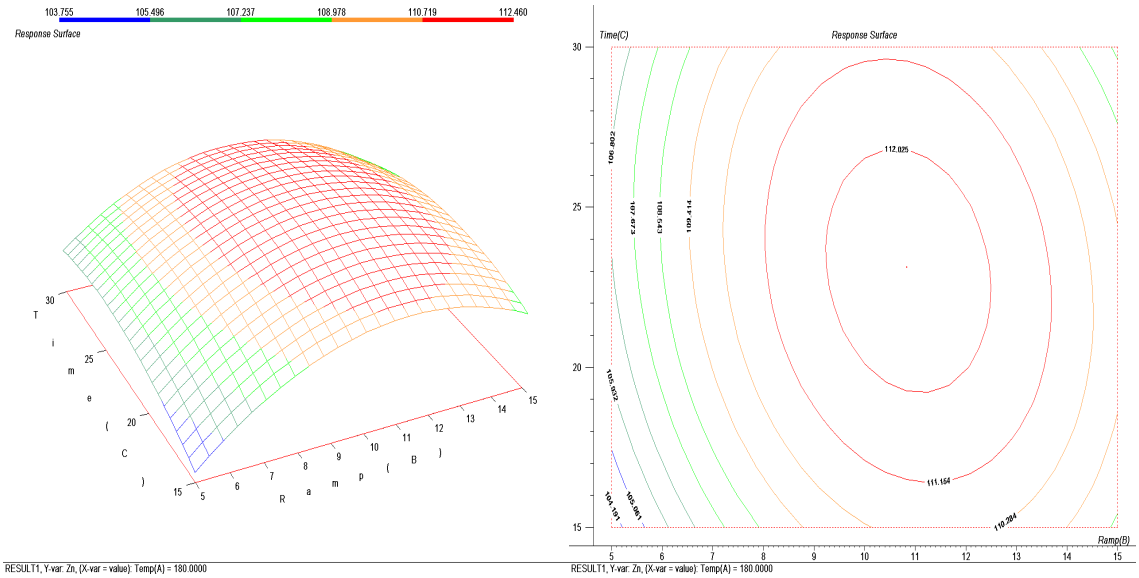

Figure 5.6 Estimated response surface and contour plots for Zn

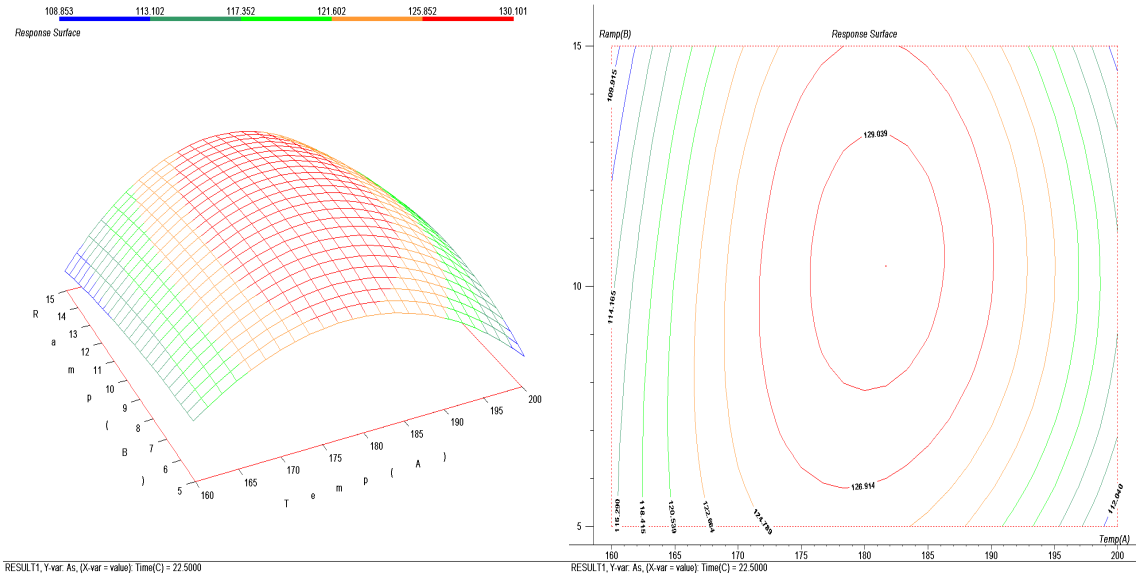

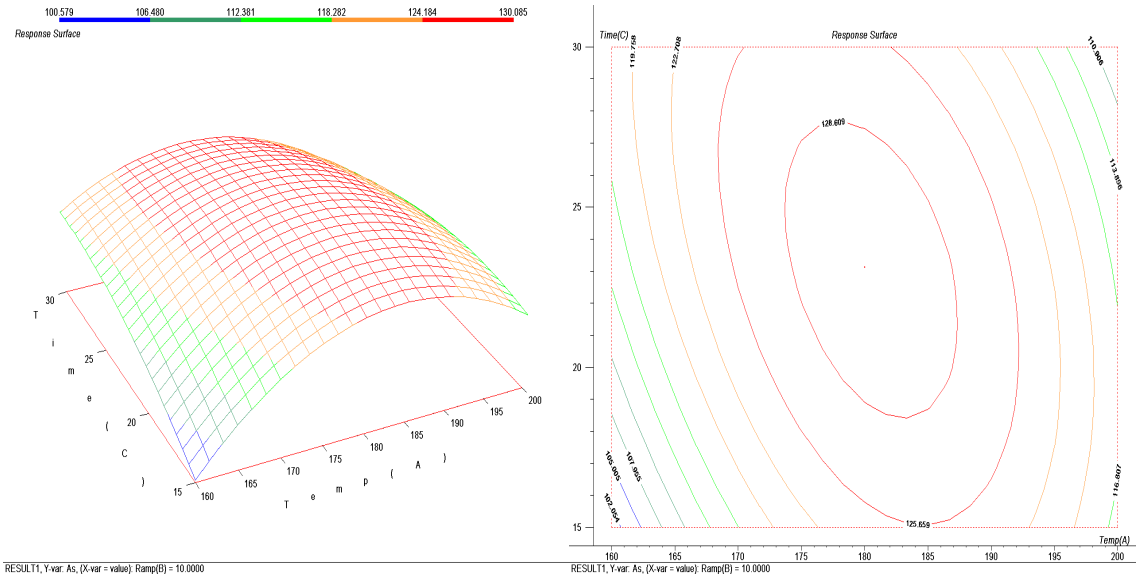

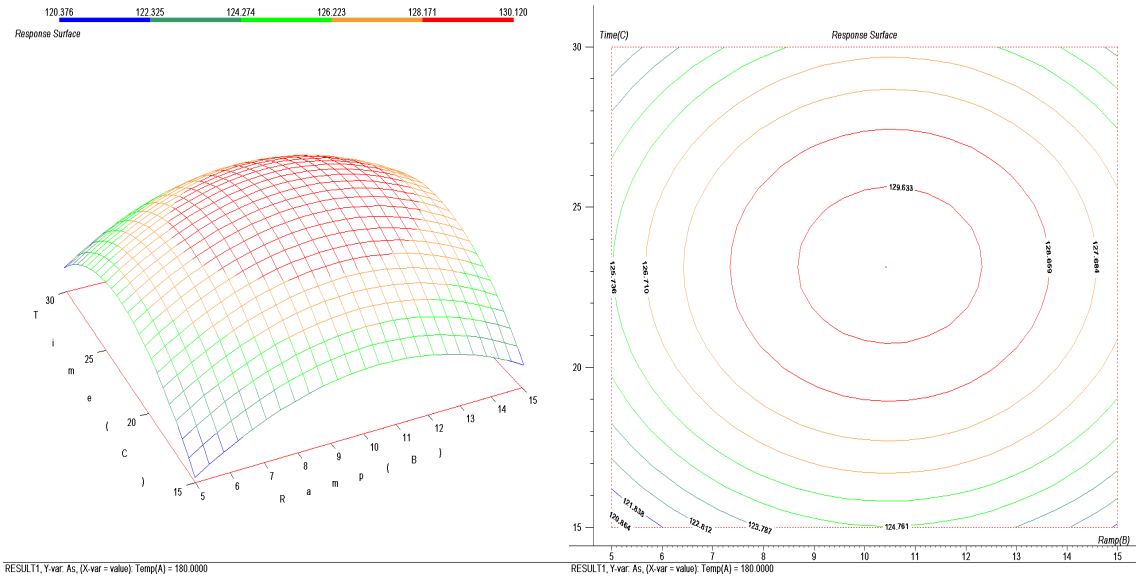

Figure 5.7 Estimated response surface and contour plots for As

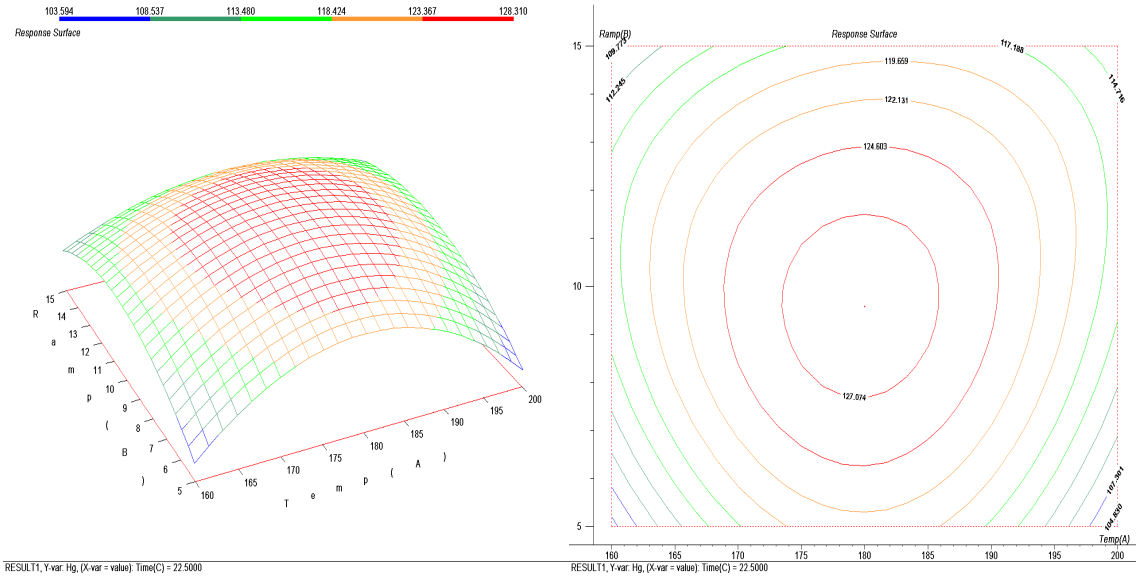

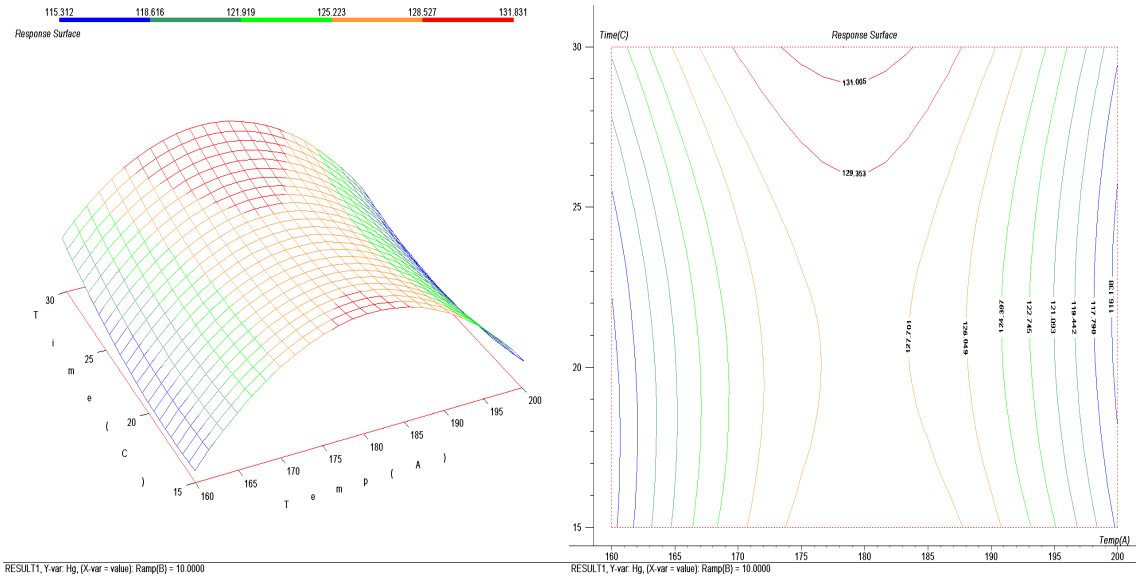

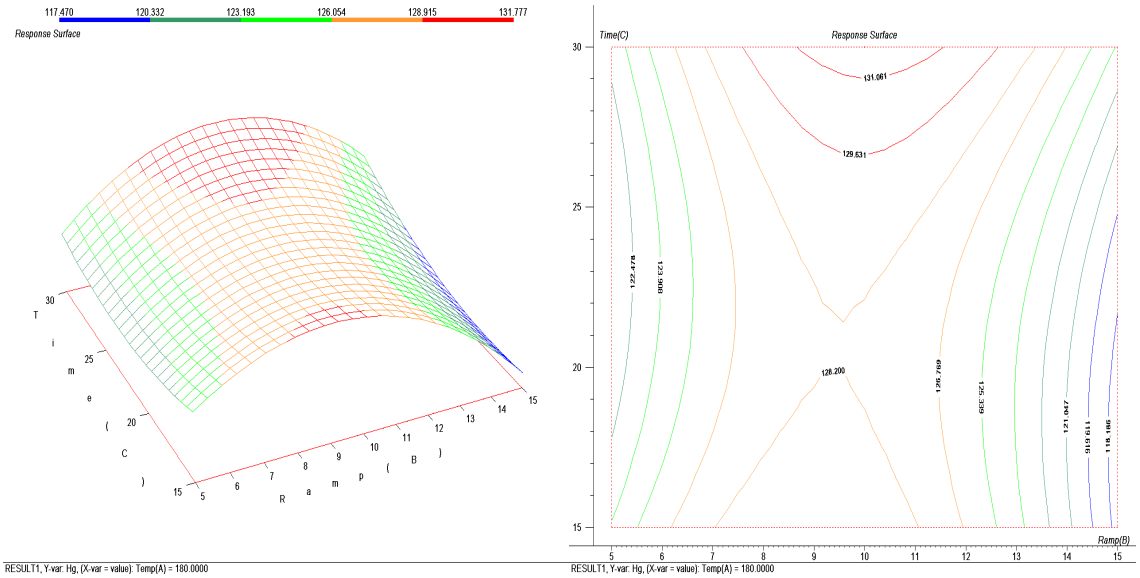

Figure 5.8 Estimated response surface and contour plots for Hg

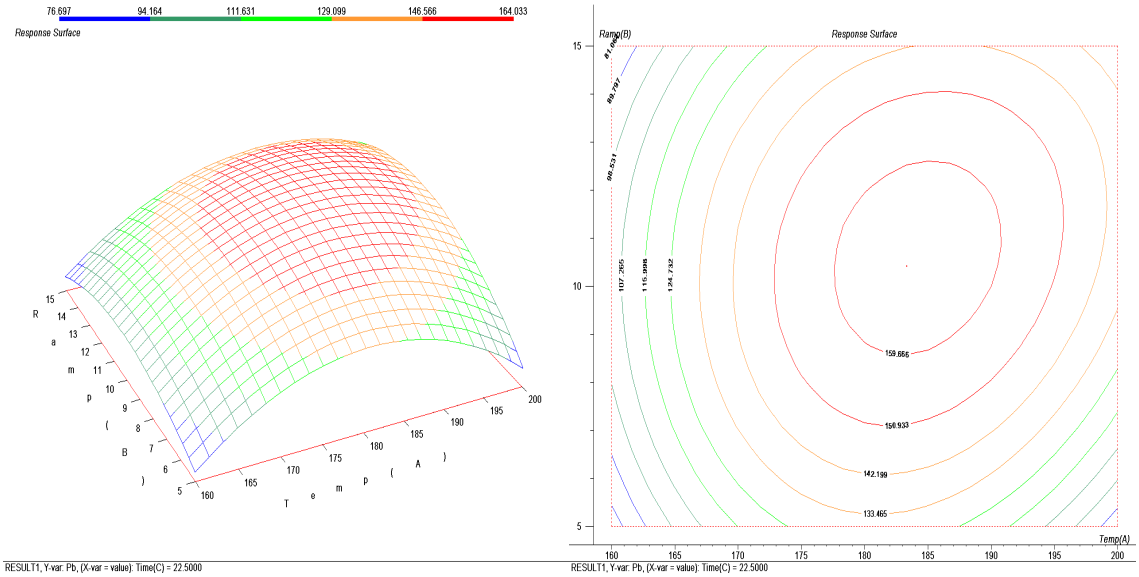

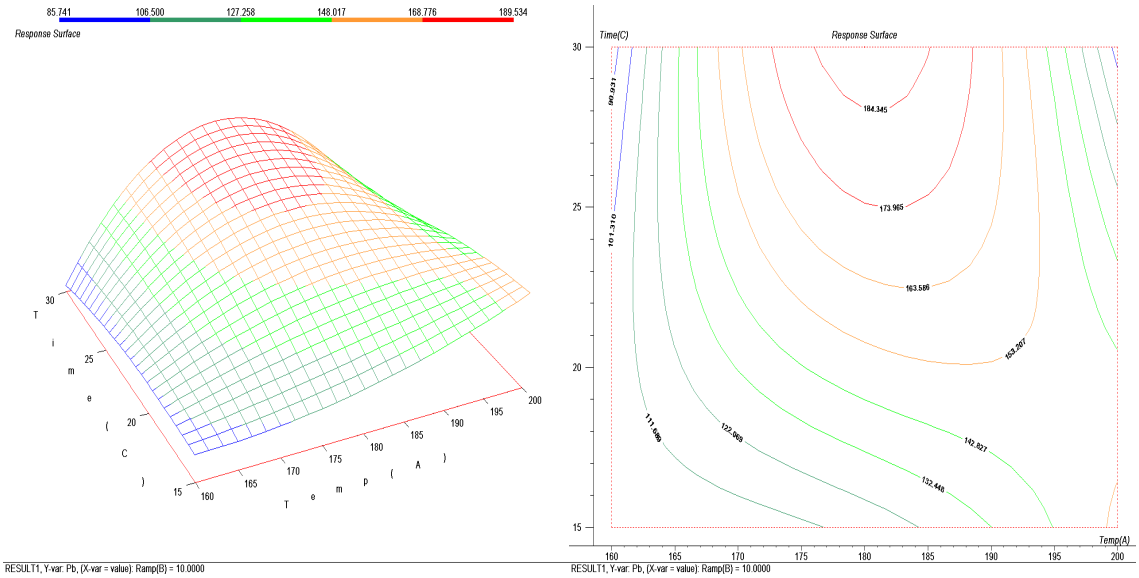

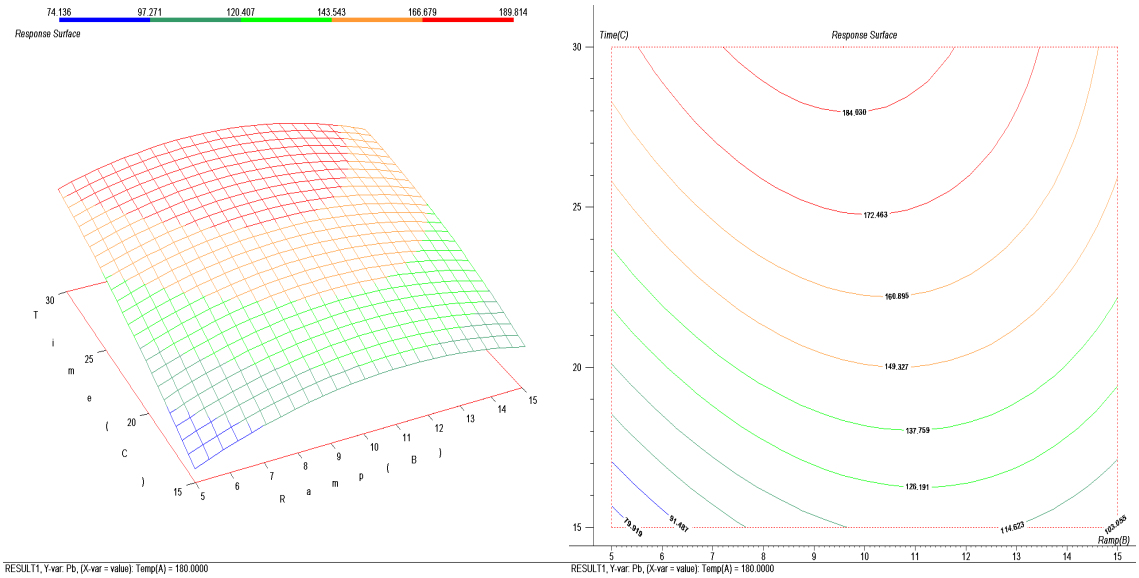

Figure 5.9 Estimated response surface and contour plots for Pb

In order to establish a single condition for sample digestion which allows simultaneous determination of the studied analytes, working values of radiation time, ramp and temperature were fixed at 25 min., 10.5 min. and 185 °C respectively. This is the compromised condition where quantitative recovery of all elements could be achieved in a shorter time. The accuracy and repeatability of the proposed procedure was confirmed with DOLT-4, ERM-CE278 and DORM-3 (Table 5.6). It is noticed that recoveries for both Cr and Fe are relatively lower because the working ramp and irradiation time varied considerably compared to the estimated optimum condition. Most of the other concentrations obtained matched the certified values at 95% level of confidence with relative standard deviation (*RSD*) less than 5%. However, it could also be noticed that recoveries of Hg were always higher than 100%. This can be attributed to Hg adsorption on the transfer tubing, spray chamber and nebulizer which causes the memory effects that obstructs the determination of Hg. In addition, the overall repeatability for Ni was slightly higher than 5%, which is probably due to the adulterations from sampling cone and skimmer cone.

Due to the lack of availability of literature reports based on MAD of DORM-3 and DOLT-4, it is reasonable to compare the present results with other appropriate CRM such as DORM-2 and DOLT-3. The comparison is given in Table 5.7. From this table, it seems that the present single stage MAD method is favorable over other previously reported microwave procedures in various aspects such as heating cycle, acids/oxidizing reagents consumption, time efficiency, element tolerability or recoveries.

Table 5.6 Analysis of certified reference materials

	DORM-3				DOLT-4				ERM-CE-278			
	Certified / mg kg^{-1}	**Found / mg kg^{-1}**	**Recovery / %**	***RSD* /%**	**Certified / mg kg^{-1}**	**Found / mg kg^{-1}**	**Recovery /%**	***RSD* /%**	**Certified / mg kg^{-1}**	**Found / mg kg^{-1}**	**Recovery /%**	***RSD* /%**
V	-	1.47 ± 0.03	-	0.8	0.6$^{\#}$	0.57 ± 0.04	96	3.0	-	0.45 ± 0.02	-	2.1
Cr	1.9 ± 0.2	1.7 ± 0.1	90	2.2	1.4$^{\#}$	1.0 ± 0.4	71	1.5	0.78 ± 0.06	0.70 ± 0.02	90	1.4
Mn	4.6$^{\#}$	3.0 ± 0.4	65	5.5	-	9.8 ± 0.2	-	0.9	7.7 ±0.2	7.7 ± 0.6	100	3.1
Fe	347 ± 20	316 ± 8*	91	1.1	(18.3 ± 0.8) × 10^{2}	(16.8 ± 0.6) × 10^{2*}	92	1.3	-	125 ± 1	-	0.5
Co	-	0.27 ± 0.01	-	1.6	0.25$^{\#}$	0.25 ± 0.01	100	2.0	-	0.376 ± 0.005	-	0.6
Ni	1.3 ± 0.2	1.37 ± 0.03	105	1.0	1.0 ± 0.1	1.0 ± 0.3	100	9.8	-	1.1 ± 0.2	-	7.3
Cu	15.5 ± 0.6	16.3 ± 0.8	105	2.0	31 ± 1	34.2 ± 0.6*	110	0.7	9.5 ± 0.1	10 ± 1	104	5.0
Zn	53 ± 3	54 ± 2	102	1.6	116 ± 6	130 ± 6*	112	1.9	83 ± 2	85 ± 7	102	3.3

Mean ± 95% confidence intervals

Note: $^{\#}$: Reference value; –: not certified; *: significance different ($p < 0.05$)

Table 5.6 (continue)

	DORM-3				DOLT-4				ERM-CE-278			
	Certified / mg kg^{-1}	**Found / mg kg^{-1}**	**Recovery / %**	***RSD* /%**	**Certified / mg kg^{-1}**	**Found / mg kg^{-1}**	**Recovery /%**	***RSD* /%**	**Certified / mg kg^{-1}**	**Found / mg kg^{-1}**	**Recovery /%**	***RSD* /%**
As	6.9 ± 0.3	7.3 ± 0.2	106	1.2	9.7 ± 0.6	9.4 ± 0.3	97	1.1	6.1 ± 0.1	6.5 ± 0.1*	106	0.8
Se	3.3$^{\#}$	4.0 ± 0.4	121	3.8	8 ± 1	10 ± 1	115	4.7	1.8 ± 0.1	1.93 ± 0.06	105	1.2
Ag	0.04$^{\#}$	0.020 ± 0.003	50	5.8	0.93 ± 0.07	0.989 ± 0.008	106	0.3	-	0.19 ± 0.01	-	2.4
Cd	0.29 ± 0.02	0.31 ± 0.01	107	1.7	24.3 ± 0.8	24.6 ± 0.2	101	0.3	0.348 ± 0.007	0.36 ± 0.02	103	2.8
Sn	0.07 ± 0.01	0.070 ± 0.005	100	3.1	0.17$^{\#}$	0.19 ± 0.02	112	4.1	-	0.12 ± 0.01	-	3.5
Hg	0.38 ± 0.06	0.44 ± 0.02	116	1.8	2.6 ± 0.2	3.01 ± 0.05*	116	0.7	0.196 ± 0.009	0.22 ± 0.2*	112	3.7
Pb	0.40 ± 0.05	0.44 ± 0.02	110	1.5	0.16 ± 0.04	0.20 ± 0.01	125	1.5	2.00 ± 0.04	2.1 ± 0.1	105	2.1

Mean ± 95% confidence intervals

Note: $^{\#}$: Reference value; –: not certified; *: significance different ($p < 0.05$)

Table 5.7 Comparison of MAD recoveries with literature reports

CRM	Reagents	No. of Cycles	Instrument	Percentage Recovery / %													Reference
				Cr	Mn	Fe	Ni	Cu	Zn	As	Se	Ag	Cd	Sn	Hg	Pb	
DORM-3	2.5 mL HNO_3 + 0.5 mL HCl +7 mL H_2O	1, 25 min.	ICP-MS	90	#	91	105	105	102	106	#	#	107	100	116	110	This study
DORM-3	3 mL HNO_3 + 2 mL H_2O_2 + 3 ml H_2O	3, 45 min.	ICP-MS	85	#	95	99	86	84	57	#	#	107	-	-	-	Ashoka *et al.*, 2009
DORM-3	3 mL HNO_3 + 2 mL H_2O_2 + 3 ml H_2O	5, 50 min.	ICP-MS	66	#	93	84	95	87	99	#	#	107	-	-	-	Ashoka *et al.*, 2009
DORM-2	15 mL HNO_3 + 2 mL H_2O_2	3, 22 min.	ICP-OES + DMA	109	89	95	80	89	93	89	-	-	116	-	95	92	Ikem & Egilla, 2009
DORM-2	7 mL HNO_3	3, 19 min.	ICP-MS + ICP-AES	-	-	-	-	78	93	96	-	-	96	-	-	94	Vicente-Martorel *et al.*, 2009

Note: #: Not certified; –: not reported

Table 5.7 (continue)

CRM	Reagents	No. of Cycles	Instrument	Percentage Recovery / %													Reference
				Cr	Mn	Fe	Ni	Cu	Zn	As	Se	Ag	Cd	Sn	Hg	Pb	
DORM-2	2 mL HNO_3 + 0.3 mL HF + 2 mL H_2O_2	2, 1 hr. 55 min.	ICP-MS + CVAAS	98	106	112	84	84	85	83	99	77	118	-	101	175	Yang & Swami, 2007
DOLT-4	2.5 mL HNO_3 + 0.5 mL HCl +7.mL H_2O	1, 25 min.	ICP-MS	#	#	92	100	110	112	97	115	106	101	#	116	125	This study
DOLT-3	3 mL HNO_3 + 2 mL H_2O_2 + 3 ml H_2O	3, 45 min.	ICP-MS	#	#	103	113	105	97	49	5	105	102	#	-	156	Ashoka *et al.*, 2009
DOLT-3	3 mL HNO_3 + 2mL H_2O_2 + 3ml H_2O	5, 50 min.	ICP-MS	#	#	102	82	105	100	95	98	110	104	#	-	105	Ashoka *et al.*, 2009
DOLT-3	4 mL HNO_3 + 2 mL H_2O_2	3, 19 min.	ICP-MS + ICP-AES	#	#	-	-	85	96	108	-	-	95	#	-	72	Vicente-Martorel *et al.*, 2009

Note: #: Not certified; –: not reported

Table 5.7 (continue)

CRM	Reagents	No. of Cycles	Instrument	Percentage Recovery / %													Reference
				Cr	Mn	Fe	Ni	Cu	Zn	As	Se	Ag	Cd	Sn	Hg	Pb	
ERM-CE278	2.5 mL HNO_3 + 0.5 mL HCl + 7 mL H_2O	1, 25 min.	ICP-MS	90	100	#	#	104	102	106	105	#	103	#	112	105	This study
ERM-CE278	5 mL HNO_3 + 2 mL H_2O_2	5, 45 min	ICP-MS	101	103	#	#	101	99	99	98	#	98	#	95	99	Cubadda *et al.*, 2006
ERM-CE278	5 mL HNO_3	3, 30 min.	ICP-AES + HR-ICP-MS	95	88	#	#	126	n.d	89	-	#	106	#	102	-	Caimi *et al.*, 2004
ERM-CE278	6 mL HNO_3	1, 20 min.	FAAS + CVAAS + ETAAS	100	-	#	#	108	101	97	-	#	95	#	99	104	Saavedra *et al.*, 2004

Note: #: Not certified; –: not reported

6 EVALUATION OF TRACE METALS IN AQUACULTURE RED TILAPIA AND PRELIMINARY HEALTH RISK ASSESSMENT

6.1 Introduction

Metals are widespread in the environment due to both natural and anthropogenic activities. Their associated health effects vary greatly depending on the metal species. Some species are biologically essential, whereas others could be potentially hazardous. Under particular conditions, these metals can be bioconcentrated and/or biomagnified in fish tissues gradually to hazardous levels and subsequently transferred to humans at the highest trophic level of food chain ([Mendil *et al.*, 2010], [Qiu *et al.*, 2010], [Heier *et al.*, 2009], [Ling and Liao, 2007] and [Harada, 1995]). The toxic metal species pose chronic effects even at low concentrations resulting from multiple exposures over a significant period of time, and biologically essential species could well produce deleterious effects if their intake is excessive (Celik and Oehlenschlager, 2007). These undesired health risks from metals ingestion have brought about public awareness because of the the increasing reliance on aquaculture fish supply as an important source of protein.

The concentration of these metals in aquacultured fish species is highly dependent on the metal concentration levels of the feed and the habitat of the fish (Uysal *et al.*, 2009). As the product of the equilibrium between their concentrations in fish and its rate of ingestion and excretion, the concentration of each metal species vary from organ to organ; some bind primarily to lipids and others to proteins (Al-Kahtani, 2009). In this regard, it is suggested that metal content could provide characteristic information for classification. The pattern of metal distribution is usually evaluated

using univariate procedures, but multivariate pattern recognition techniques such as principal component analysis (PCA) can provide further interpretation. PCA is used to transform the original data matrix into a product of two matrices, one which contains information about samples (scores matrix) and the other about metal concentrations (loading matrix). This helps to improve the interpretability of the results where the latent structures in the data could be made much clearer for easier perception (Low, *et al.*, 2009).

This chapter covers the evaluation of trace metals in commercially raised red tilapia (*Oreochromis spp*) sampled from low-tech earthen ponds at Kg. Geylang (KG), ex-mining pools at Glami Lemi (GL), and the more expensive concrete tanks at Pertang (PT) located in Jelebu, Malaysia (Figure 6.1). These production environments raise a number of potential food safety and quality issues associated with their produce on the basis of potentially varying metal input levels ([Liu *et al.*, 2010], [Liao *et al.*, 2008] & [Sapkota *et al.*, 2008]). The corresponding metal accumulation patterns relating organs and elements, as well as production sites and elements were evaluated with PCA. The goal of PCA is to find similarities and differences between tilapia samples based on the data obtained from inductively coupled plasma-mass spectrometry (ICP-MS) measurements. Based on PCA, classification can be established and the key discriminants that distinguish different samples can be indentified. At the same time, the potential health risks associated with trace metals via consumption of the edible potions of these tilapias are seek to be analyzed spatially.

6.1.2 Background of Sampling Site

Jelebu is a suburban district with blossoming semi-agricultural industry located in the northern part of Negeri Sembilan, Malaysia. Most of the areas in Jelebu are hilly and rugged terrains because of the central mountain range running through the state. The agricultural activities in this area are dominated by plantation of cash crops such as rubber and oil palm. Pineapple, sugarcane, durian and livestock productions are implemented in a commercial scale as well. In olden days, there were also booming tin-mines operating in this area. These days, however, part of those abandoned mining pits have been converted to aquaculture fishponds. In view of all these activities, agriculture runoffs, effluents and mine tailings/residuals could be potential sources of pollution in the aquaculture produce.

Figure 6.1 The map of sampling sites showing Glami Lemi (A), Pertang (B) and Kg. Geylang (C) at the Jelebu area

6.2 Materials and Methods

6.2.1 Reagent and Standard Materials

All chemicals and standards involved in this work are exactly as those stated in the previous chapters, unless otherwise specified.

6.2.2 Cleaning and Decontamination

For analytical efficiency and to reduce possible decontamination activities, all apparatus and sampling equipment were cleaned by overnight soaking in dilute 10% nitric acid (w/v) and then soaked overnight in ultrapure water (UPW).

6.2.3 Sample Collection and Preparation

6.2.3.1 Field Sampling

Sampling of Fish

Red tilapia samples were collected from 3 different aquaculture ponds located in Jelebu, Malaysia. The sampling sites were ex-tin mining pools in GL (N 03° 00.54’ E 102° 01.65’), concrete tanks in PT (N 02° 55.99’ E 102° 13.26’) and earthen ponds in KG (N 02° 54.42’ E 102° 03.45’) as illustrated in Figure 6.1. Specimens collected during the sampling period were individually wrapped in extra heavy duty aluminum foil and placed into a waterproof plastic bag, then sealed and labeled. Packaged samples were cooled with blue ice packets in an insulated box immediately before being transferred to the processing laboratory on the same day. They were stored under a ≤ -20 °C freezer until dissection can be performed.

Sampling of Water

Surface water was collected from aquaculture ponds using direct method priori to sediment and tilapia samples at the same site. The sampling bottles were rinsed twice with water sample before collection. The closed-sampler was submersed; the bottle was opened to fill-in the sample and then recapped in sub-surface (USEPA 1999). The bottles were wrapped entirely with aluminum foil and well labeled before being transferred to the processing laboratory.

Sampling of Sediments

Surface sediment samples were grabbed from the bottom of the ex-mining pool and earthen pond using a dredger. The samples were placed into individual foil wrapped sampling jar, labeled and returned to the laboratory where they were stored under ~4 °C.

6.2.2.2 Sample Preprocessing

Preprocessing Fish Samples

Maximum length and weight of partially thawed samples were recorded prior to dissection. Consequently, each dissected sample was grinded down using an analytical mill (IKA, Germany) as to improve sample homogeneity. They were then dried with freeze-drier (CHRiST, Germany) while moisture content of each sample was determined according to its weight loss. Those dried samples were further homogenized and kept in amber jars under desiccator before the microwave assisted digestion (MAD) procedure.

Preprocessing of Sediment Samples

All foreign matters (stones, detritus and roots) were removed from the sample and the remaining sediment was freeze dried, homogenized, and then passed through a 50-mesh sieve. The samples were kept in amber jars under desiccator for further analysis.

6.2.2.3 Microwave Assisted Digestion

Digestion of Fish Sample

In order to ensure quantitative recovery, information on microwave assisted digestion (MAD) condition was adopted from the optimization study discussed in previous chapter. About 0.250 g of dried sample were digested with 2.50 mL 65% HNO_3, 0.50 mL 30% HCl and 7.00 mL ultra pure water (UPW) in a self-regulating pressure control PFA® vessel under MarXpress Microwave Accelerated Reaction System (CEM Corporation, USA). The temperature was ramped to 185 °C in 10.5 minutes and held for 14.5 minutes. After digestion, the sample was cooled before being transferred to a 50.00 mL polypropylene volumetric flask and the volume was made up to the mark with UPW.

Digestion of Aqueous Sample

9.00 mL of water sample and 1.00 mL of 65% HNO_3 were pipetted into a precleaned vessel for MAD. The ratio between acid and sample adopted here is aligned with 5 mL HNO_3 to 45 mL aqueous sample proposed in USEPA Method 3015. The temperature were brought to 160 °C in 10 minutes and gradually risen to 170 °C during the second 10 minutes (USEPA 1994b). Cooled down sample solution was transferred quantitatively to a 25.00 ml volumetric flask and made up to the mark with UPW.

Extraction of Sediment Sample

Approximately 0.500 ± 0.005 g of dry, finely powdered sediment sample was accurately weighed into a precleaned digestion vessel. 3.00 mL of 65% HNO_3, 2.00 mL of 30% H_2O_2 and 5.00 mL of UPW were added (Roychowdhury *et al.*, 2002). The vessel was closed and tightened before being loaded into the microwave oven. The temperature was risen to 175 °C in 5.5 minutes and remained for 4.5 minutes (USEPA 2007). After cooling for 20 minutes, the vessels were opened carefully. Each digested solution was transferred quantitatively to a 50.00 ml volumetric flask and made up to the mark with UPW.

Handling of Resulting Solutions

All the diluted sample solutions were filtered though 0.45 μm PTFE membrane and kept in plastic vials below 8 °C and were analyzed within 5 days using ICP-MS. Replicates and corresponding blanks were also prepared in accordance to those respective manners.

6.2.3 Validation of Microwave Sample Preparation Method

The analytical performance of the abovementioned microwave assisted digestion/extraction (MAD/MAE) procedures via ICP-MS analysis were checked with appropriate certified reference materials (CRMs) such as DORM-3 dogfish muscle, DOLT-4 dogfish liver, SLRS-4 riverine water from the National Research Council Canada (NRCC), ERM-CE278 mussel tissues and BCR-146R powdered sewage sludge from Institute for Reference Materials and Measurements (Belgium), and NIST-1464a estuarine sediment from National Institute of Standards and Technology (USA). The results are shown in Table 5.6, Table 6.1 and Table 6.2.

Table 6.1 Analysis of riverine water certified reference material

	SLRS-4			
	Certified / mg L^{-1}	**Found / mg L^{-1}**	**Recovery / %**	***RSD* /%**
V	0.3 ± 0.1	0.368 ± 0.005	115	3.8
Mn	3 ± 1	3.47 ± 0.04	103	3.0
Fe	103 ± 37	115 ± 2	112	4.2
Co	0.03 ± 0.01	0.055 ± 0.001	168	0.5
Cu	3 ± 1	2.88 ± 0.04	96	3.7
As	0.7 ± 0.2	0.694 ± 0.009	99	3.3

Mean ± 95% confidence intervals

6.2.4 ICP-MS Analysis

V, Mn, Fe, Co, Cu, Zn, As, Se, Cd, Hg and Pb concentrations were analyzed by Agilent 7500ce ICP-MS system with an octopole reaction system (ORS) using external calibration approach with internal standards as described in Chapter 5.

Table 6.2 Analysis of sludge and sediments certified reference materials

	BCR-146R				NIST 1646a			
	Certified / mg kg^{-1}	**Found / mg kg^{-1}**	**Recovery / %**	***RSD* /%**	**Certified / mg kg^{-1}**	**Found / mg kg^{-1}**	**Recovery /%**	***RSD* /%**
V	-	-	-	-	44.8 ± 0.8	24.7 ± 0.1	55	0.9
Mn	298 ± 9	301 ± 2	101	1.9	235 ± 3	120 ± 1	51	1.9
Co	6.5 ± 0.3	5.94 ± 0.05	91	2.1	5$^{\#}$	3.79 ± 0.01	76	0.9
Cu	831 ± 16	775 ± 6	93	2.0	10.0 ± 0.3	9.35 ± 0.04	93	1.0
Zn	3043 ± 58	2947 ± 24	97	2.1	49 ± 2	46.3 ± 0.2	95	1.0
As	-	-	-	-	6.2 ± 0.2	6.1 ± 0.1	98	5.8
Cd	18.5 ± 0.4	18.1 ± 0.6	98	9.2	0.148 ± 0.007	0.156 ± 0.003	105	4.8
Pb	583 ± 17	520 ± 17	89	8.6	12 ± 1	7.8 ± 0.2	67	5.9

Mean ± 95% confidence intervals

Note: $^{\#}$: Reference value; –: not certified

6.3 Results and Discussion

6.3.1 Morphometric Data

Effort had been made to sample red tilapias of harvestable size from the aquaculture production sites wherever possible so as to provide sufficient statistical power for the estimation of the variability of trace metal levels in commercial sized tilapias commonly consumed locally (USEPA 2000a). Their respective morphometric data are summarized in Table 6.3.

Table 6.3 Biometric parameters for tilapia from different sampling site

	GL / Ex-mining Pool	**PT / Concrete Tank**	**KG / Earthen Pond**
Location	N 03° 00.541’ E 102° 01.650’	N 02° 55.994’ E 102° 13.263’	N 02° 54.427’ E 102° 03.450’
Fish length (*l*) / cm	29 ± 1	28 ± 1	25 ± 1*
Weight (*m*) / kg	0.52 ± 0.06	0.54 ± 0.03	0.33 ± 0.04*
Condition factor (*CF*)	2.2 ± 0.1	2.5 ± 0.3*	2.3 ± 0.2
Hepatosomatic Index (*HSI*)	1.3 ± 0.5	1.5 ± 0.4	1.5 ± 0.4

Mean ± 95% confidence intervals, n = 20

* Significant difference ($p < 0.05$) between groups

The condition factors (*CF*s) have been widely used to compare growth conditions of fish which include the degree of maturity and nourishment (Williams, 2000). *CF*s can be estimated by the following equation:

$$CF = \frac{100{,}000m}{l^3} \qquad \text{(Equation 6.1)}$$

where *m* is the weight of tilapia in grams, and *l* is length of the fish in millimeters. Hepatosomatic index (*HSI*) is defined as the ratio of liver weight to body weight that provides an indication of the status of energy reserve in a fish. The fact that both factors are indicative of the overall fish health, this makes them good candidates to be considered in this study (Ureña *et al.*, 2007). Despite the fact that samples farmed in earthen ponds were smaller compared to other sites, there was no significant difference among the HSIs ($P > 0.05$). The only exception are the samples collected from concrete tank which showed higher CF than others.

Notwithstanding the size variation, there were rarely statistically significant correlation between the metal concentrations measured and the size/age of the individual fish. This is probably because freshwater fishes are known to regulate constant internal metal concentrations ([Henry *et al.*, 2004], [Allinson *et al.*, 2002] and [Amundsen *et al.*, 1997]). In fact, metal concentrations in a tissue depend on the specific metabolism of metal species in the tissue considered as well as the availability of the metal species in surrounding environment. Generally, metal uptake in fish is via water and diet exposures which are then transferred to other target organs. Consequently metal concentrations are mostly measured in gills, liver or muscles. The latter is of the most concern to humans because it is the main tissue consumed as food. Gills are regarded as important because it is where metals undergo direct intake from the water. Liver plays a crucial role in storage, redistribution, detoxification or transformation and also an active site of pathological effects induced by toxic metals (Evans *et al.*, 1993).

Table 6.4 Metal concentrations in freeze dried Tilapia tissues

	Ex-Tin Mining Pool (GL)			Concrete Tank (PT)			Earthen Pond (KG)		
	Muscles	**Liver**	**Gills**	**Muscles**	**Liver**	**Gills**	**Muscles**	**Liver**	**Gills**
V	0.017 ± 0.003	0.6 ± 0.1	0.46 ± 0.09	0.009 ± 0.001	0.05 ± 0.01	0.051 ± 0.009	0.028 ± 0.007	1.0 ± 0.2	0.7 ± 0.2
Mn	1.1 ± 0.1	11 ± 2	26 ± 5	0.83 ± 0.07	3.9 ± 0.6	7 ± 2	0.76 ± 0.07	4.4 ± 0.2	4.6 ± 0.5
Fe	22 ± 4	(2.7 ± 0.5) × 10^3	(3.1 ± 0.5) × 10^2	17 ± 1	(2.6 ± 0.6) × 10^2	(1.6 ± 0.1) × 10^2	22 ± 2	(1.2 ± 0.2) × 10^3	(3.1 ± 0.5) × 10^2
Co	0.06 ± 0.01	1.7 ± 0.3	0.62 ± 0.07	0.010 ± 0.001	0.23 ± 0.07	0.22 ± 0.02	0.020 ± 0.003	0.29 ± 0.06	0.11 ± 0.02
Cu	1.2 ± 0.1	(0.7 ± 0.1) × 10^3	1.9 ± 0.1	0.82 ± 0.05	(3.7 ± 0.6) × 10^2	1.7 ± 0.1	0.72 ± 0.05	(3.9 ± 0.2) × 10^2	1.6 ± 0.2
Zn	17.5 ± 0.8	85 ± 6	64 ± 3	14.9 ± 0.6	71 ± 6	65 ± 4	15.8 ± 0.9	72 ± 3	70 ± 3

Mean ± 95% confidence intervals, n = 20

All reported values are referred to dry base in mg kg^{-1}

Table 6.4 (continue)

	Ex-Tin Mining Pool (GL)			Concrete Tank (PT)			Earthen Pond (KG)		
	Muscles	**Liver**	**Gills**	**Muscles**	**Liver**	**Gills**	**Muscles**	**Liver**	**Gills**
As	4.7 ± 0.4	2.6 ± 0.4	1.66 ± 0.09	3.5 ± 0.4	0.48 ± 0.04	0.50 ± 0.05	1.9 ± 0.2	0.76 ± 0.08	0.9 ± 0.2
Se	1.5 ± 0.1	6.7 ± 0.7	1.63 ± 0.07	1.05 ± 0.05	2.7 ± 0.4	1.07 ± 0.09	1.36 ± 0.06	2.3 ± 0.1	1.06 ± 0.09
Cd	0.22 ± 0.07	0.52 ± 0.08	0.2 ± 0.1	0.07 ± 0.02	0.39 ± 0.05	0.083 ± 0.008	0.09 ± 0.03	0.25 ± 0.06	0.08 ± 0.01
Hg	0.035 ± 0.002	0.13 ± 0.09	0.005 ± 0.001	0.026 ± 0.002	0.040 ± 0.005	0.025 ± 0.005	0.023 ± 0.002	0.048 ± 0.004	0.014 ± 0.002
Pb	0.048 ± 0.007	0.20 ± 0.02	0.42 ± 0.07	0.040 ± 0.007	0.11 ± 0.01	1.3 ± 0.5	0.09 ± 0.02	0.61 ± 0.02	1.7 ± 0.5

Mean ± 95% confidence intervals, n = 20

All reported values are referred to dry base in mg kg^{-1}

6.3.2 Distribution of Metals in Red Tilapia

Table 6.4 indicates levels of ten metals expressed in mg kg^{-1} dry tissues in the muscles, liver and gills of red tilapias from three different aquaculture sites. All metal concentrations showed significant differences between organs on dry weight basis ($p < 0.001$).

6.3.2.1 Metal Concentrations in the Liver

As in other studies, it is observed that metal concentrations are generally higher in liver compared to the gill and muscle tissues regardless of the sample origin. Higher accumulation ratios of metals in the liver are due to the greater binding tendency of the metals with oxygen carboxylate, amino groups, nitrogen and/or sulphur of the mercapto group in the metallothionein protein which have been reported at high concentrations in the liver (Al-Yousuf *et al.*, 2000).

6.3.2.2 Metal Concentrations in the Gills

The results have demonstrated that gill tissues contained higher concentrations of both Mn and Pb compared to other tissues except samples collected from KG, where there was no statistical difference between Mn content in liver and gills. This could be due to the availability of Mn in the surrounding medium, where only 0.015 ± 0.007 mg L^{-1} of total Mn was detected in the ambient water for KG compared to 0.11 ± 0.06 mg L^{-1} for GL and 0.05 ± 0.02 mg L^{-1} for Pertang. This suggests that Mn and Pb uptake mode is mainly via water, not diet. These observations are consistent with the findings of Kebede & Wondimu (2004) and Karataş & Kalay (2002) that showed higher concentration of Mn and Pb in the gill tissues compared to the liver and muscles of *Tilapia zillithan* and *Oreochromis niloticus*. The considerable amount of Mn and Pb observed in the gill tissues are due to the binding capacity of the mucous layer that

covers the organs and their close contact with the surrounding environment (Palaniappan *et al.*, 2008). Consequently, the accumulation of Mn and Pb in red tilapia is expected to be directly correlated with the concentration of metals in ambient water which makes origin tracking feasible.

6.3.2.3 Metal Concentrations in the Muscles

Compared to the other tissues, the muscles show lower concentrations of metals, however, in this study, it was found that concentration of As is highest in muscle tissues (Table 6.4). This phenomena have been previously observed by Has-Schön *et al.* (2006) in carps, tenches, svals, mullets and eels of River Neretva (Croatia). Due to the fact that the level of As in gills are considerably lower than that of the muscle tissue, it is suggested that As in muscles could be predominantly accumulated via diet (Pedlar and Klaverkamp, 2002). All these emphasize that metals have different affinity toward different organs.

Since the information about trace element concentrations in the muscles of aquaculture tilapias is important to human consumption, the metal element concentrations are summarized in Table 6.5 as mean ± 95% confidence interval in wet weight basis for comparison purposes. Table 6.5 disclosed that the general trends of bioaccumulation of metals in the muscles look similar regardless of the production sites to a certain extent. Ag (< 0.002 mg kg^{-1}) and Sn (< 0.004 mg kg^{-1}) were not detected in all cases, even in the samples from ex-tin mining pools. The accumulation orders were found to be: Fe > Zn > As > Se > Mn ≈ Cu > Cd. This accumulation pattern might be related to the equilibrium and/or physiological regulation processes with respect to *Oreochromis spp* itself ([Cheung *et al.*, 2006], [Henry *et al.*, 2004] and [Allinson *et al.*, 2002]).

Table 6.5 Total metal concentrations in tilapia muscle and permissible limits

Nation	Sites	V	Mn	Fe	Co	Cu	Zn	As	Se	Ag	Cd	Sn	Hg	Pb	Sources
Malaysia	*GL*	0.0039 ± 0.0008	0.26 ± 0.03	5 ± 1	0.014 ± 0.003	0.27 ± 0.03	4.0 ± 0.2	1.07 ± 0.07	0.35 ± 0.03	n.d.	0.05 ± 0.02	n.d.	0.0081 ± 0.0005	0.011 ± 0.002	This study
	PT	0.0022 ± 0.0003	0.21 ± 0.01	4.4 ± 0.3	0.0025 ± 0.0003	0.21 ± 0.01	3.8 ± 0.2	0.91 ± 0.01	0.27 ± 0.02	n.d.	0.019 ± 0.004	n.d.	0.0067 ± 0.0005	0.010 ± 0.002	
	KG	0.006 ± 0.001	0.17 ± 0.01	4.7 ± 0.3	0.0044 ± 0.0007	0.16 ± 0.01	3.5 ± 0.2	0.41 ± 0.03	0.296 ± 0.009	n.d.	0.020 ± 0.006	n.d.	0.0049 ± 0.0005	0.020 ± 0.004	
	Bandar	-	0.11 ± 0.01	2.88 ± 0.09	-	0.31 ± 0.04	1.92 ± 0.06	-	-	-	0.015 ± 0.002	-	-	0.42 ± 0.09	Mokhtar *et al.* *2009*
	Jugra	-	0.20 ± 0.04	5.1 ± 0.2	-	0.32 ± 0.02	2.36 ± 0.07	-	-	-	0.006 ± 0.002	-	-	0.40 ± 0.02	

All reported values (mean ± 95% confidence intervals / mg kg^{-1}) refer to wet base for comparison purpose.

-: not reported; n.d.: not detected

Table 6.5 (continue)

Nation	Sites	V	Mn	Fe	Co	Cu	Zn	As	Se	Ag	Cd	Sn	Hg	Pb	Sources
Taiwan	*Chu-Pei*	-	0.3 ± 0.2	-	-	0.3 ± 0.1	12 ± 8	0.1 ± 0.1	0.17 ± 0.06	-	-	-	-	0.04 ± 0.06	Ling *et al.*, 2009
	Long-Jing	-	0.5 ± 0.5	-	-	0.9 ± 0.9	12 ± 9	0.29 ± 0.03	0.5 ± 0.2	-	-	-	-	0.5 ± 0.2	
	Sheng-Keng	-	1 ± 2	-	-	0.4 ± 0.2	13 ± 13	0.2 ± 0.1	0.3 ± 0.1	-	-	-	-	0.1 ± 0.1	
	Pentung	0.015 ± 0.002	0.5 ± 0.1	-	-	1.3 ± 0.4	10.8 ± 0.9	0.32 ± 0.06	0.42 ± 0.02	-	0.011 ± 0.004	-	-	0.18 ± 0.05	Lin *et al.*, 2005
India	*Cochin*	-	n.d.	-	0.12 ± 0.01	1.12 ± 0.04	4.56 ± 0.02	4.14 ± 0.01	n.d.	-	n.d.	-	n.d.	0.2 ± 0.01	Sivaperumal *et al.*, 2007

All reported values (mean ± 95% confidence intervals / mg kg^{-1}) refer to wet base for comparison purpose.

-: not reported; n.d.: not detected

Table 6.5 (continue)

	V	Mn	Fe	Co	Cu	Zn	As	Se	Ag	Cd	Sn	Hg	Pb	Sources
Malaysian Food Act 1983 and Food Regulations 1985	-	-	-	-	30	100	1	-	-	1	40	0.05	2	Food Act and Regulations 1995
Commission Regulation (EC)	-	-	-	-	-	-	-	-	-	0.05	-	0.5	0.2	EC 2000
USEPA Risk-Based Concentrations	6.8	190	950	0.41	54	410	0.41[a]	6.8	6.8	1.4	810	0.14[b]	-	USEPA 2010

All reported values (mean ± 95% confidence intervals / mg kg^{-1}) refer to wet base for comparison purpose.

-: not reported;

[a]Inorganic As

[b]MeHg

On the other hand, deviation in V, Co, Hg and Pb accumulation patterns are suspected to provide the key indications of different sources of elements that are attributed to individual production farm under particular environmental conditions. Therefore, there would be a certain amount of discrepancy in the associated health risks between production sites.

For a better illustration of metal distribution pattern in the muscles of tilapias from different production sites, the metal pollution index (*MPI*) was employed (Usero *et al.*, 1996):

$$MPI = (CW_{k=1} \times CW_{k=2} \times ... \times CW_k)^{\frac{1}{K}} \qquad \text{(Equation 6.2)}$$

where CW_k is the content for the *k*th metal in the sample on wet basis. Figure 6.2 displays probabilistic distributions of MPIs disregarding any possible correlations among the metal concentrations.

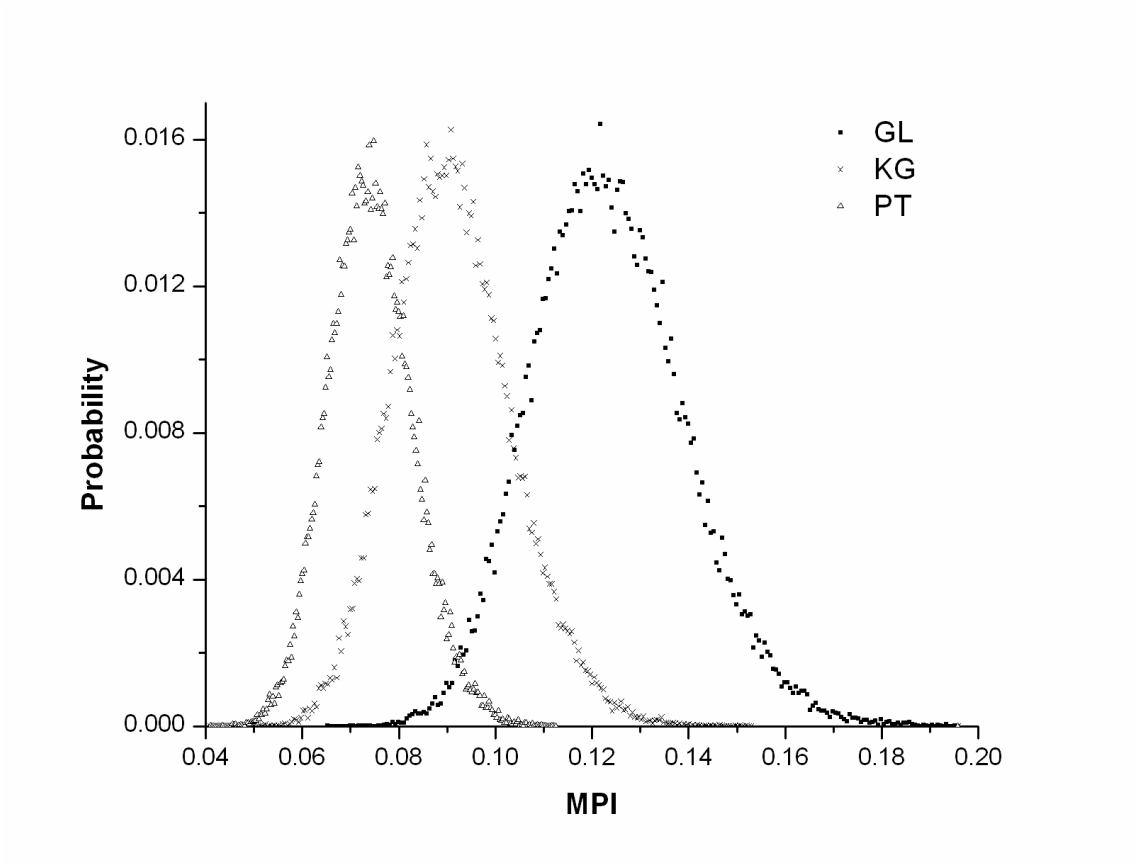

Figure 6.2 Probabilistic metal distributions in tilapias from GL, PT and KG

It is clearly demonstrated that the mean total metal accumulation levels for GL > KG > PT. Once again, the pronounced variation in the bioaccumulation profiles could be attributed to the bioavailability and chemistry characteristics of metals in each particular site. Thus, it is suggested that there might be a relatively higher risk associated with the consumption of red tilapia harvested from ex-tin mining pond compared to others.

A comparison with established limits and other literature reports is also given in Table 6.5. At present, there are no recommended maximum limits for V, Mn, Fe, Co and Se in Malaysia. As for the rest of the investigated metals, their concentration levels in the muscle tissues were found to be well below the maximum levels granted in the Malaysian Food Act 1983 and Food Regulations 1985 (Food Act and Regulations 1995). The only exception is the mean total As content in samples collected from GL which is just numerically above the Malaysian legal allowance margin. Although As level in fishes is not considered under Commission Regulations (EC 2001), this brings about potential toxicological risks in the consumption of tilapia cultivated in ex-tin mining pond. Despite the fact that the maximum permissible concentration based on total As is widely adopted in many countries, great diversity of As species found in tilapia differ significantly in their toxicity according to its oxidation state and/or organic substituents, from the innocuous arsenobetaine (Figure 6.3) to the toxic inorganic arsenic species As(III) and As(V) (Shiomi, 1994). Thence, the USEPA advocates inorganic As uptake for the assessment of human health risk, instead of total As exposure (USEPA 2000b). In fact, arsenobetaines are the predominant compound found in tilapia, whereas inorganic As represents only a minimal portion that accounts for less than 10% of total As in most cases ([Soeroes *et al.*, 2005], [Wang *et al.*, 2005], [Huang *et al.*, 2003] and [Li *et al.*, 2003]). For this reason, in order to accurately evaluate the risk profile, individual arsenic species must be considered. With the abovementioned idea in mind, it

is expected that the mean inorganic As level would be below the risk-based concentration (0.41 mg kg^{-1}) listed by the USEPA (2010).

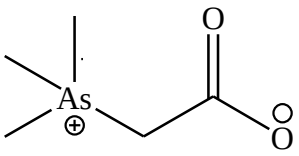

Figure 6.3 Molecular structure of arsenobetaine

Besides As content, Table 6.5 revealed that metal concentrations in tilapia from current study are significantly lower than most reported values ([Ling *et al.*, 2009], [Mokhtar *et al.*, 2009], [Sivaperumal *et al.*, 2007] and [Lin *et al.*, 2005]). Concentration levels of Mn, Cu, Fe and Pb are below or in the lower range compared to samples from Fisheries Research Institute at Chu-Pei, Taiwan which had been deemed as a reference site that is considered to be free from anthropogenic emissions (Ling *et al.*, 2009). Concentration levels of Cd are observed to be relatively higher than others particularly for those samples from GL, where the mean Cd composition is similar to the maximum level specified by Commission Regulations (EC 2001). Considerably higher As and Cd levels could be subjected to natural variation due to geographical origin and/or the utilization of formulated feeds where the mean concentrations observed in commercially available feeding pellets are 0.8 - 1.4 mg As kg^{-1} and 0.06 - 0.19 mg Cd kg^{-1} compared to 4 - 10 μg As kg^{-1} and 0.03 – 0.31 μg Cd kg^{-1} in water. Although it is generally agreed that metals released form a sediment phase and may partially influence the bioavailability of metal to farmed tilapia, it is likely that the uptake via metal-enriched feed contributed more significantly to the bioaccumulations in commercial size tilapias, since the relative gill ventilation capacities decline with size while the relative feeding rates are about the same ([Wang *et al.*, 2007] and [Van der Oost *et al.*, 2003]).

Therefore, there is a need on the part of regulatory authorities to monitor possible human-driven As transition in commercially farmed tilapia.

6.3.3 Principal Component Analysis

6.3.3.1 Metal Distribution Pattern among Tissues

For better graphical representation, principal component analysis (PCA) was conducted to get an overview of the multivariate distribution pattern of metals in the studied tissues. Prior to PCA, logarithm transformation was implemented to remove skewness and kurtosis which helps to balance the data distribution (Türkmen *et al.*, 2009). Then PCA is used to transform the original data matrix which composes of 180 samples and 11 metal variables (20 samples of each organ from each sampling site) into a product of two matrices, once which contains information about metal concentrations (loadings matrix) and the other about samples (scores matrix). This helps to improve the interpretability of results where the true multivariate structures in the data could be made much clearer for easier perception (Low *et al.*, 2009).

K noncollinear variables yield *K* principal components (PCs), but this achieves no simplification. Each PC is associated with an eigenvalue (λ), PC1 has the largest eigenvalue, λ_1 and carries the largest variance of the original data and subsequent PCs carry variance in a decreasing order. The results obtained are summarized in Table 6.6. When the first few PCs account for most of the variation, it can be concentrated on them and disregard the remaining PCs. This allows matrices to be transformed into conceptual images with many variables and the latent structures can be revealed in a relative small number of dimensions.

Table 6.6 Percent explained variance for PCA

PC, j	Eigenvalues, λ_j	Percent variance / %	Cumulative Percent / %
1	7.293	66.30	66.30
2	2.268	20.63	86.93
3	0.511	4.64	91.57
4	0.370	3.36	94.93
5	0.216	1.97	96.90
6	0.167	1.51	98.41
7	0.059	0.53	98.94
8	0.052	0.48	99.42
9	0.041	0.37	99.79
10	0.015	0.14	99.93
11	0.007	0.07	100.00

The Kaiser Criterion (1960) and Cattell (1966) scree test are the most often used guidelines for determining the number of PCs to be extracted. Based on Kaiser Criterion (1960), any PCs that explained less than a single unit of the observed variable's variation are dropped. In order words, only those with an eigenvalue greater than 1 are retained and interpreted. Cattell's (1966) recommendation is to retain only those PCs above the point of inflection on a scree plot of eigenvalues against PCs number (Figure 6.4). Nevertheless, both outcomes suggest that only the first two PCs contained significant information. Together, they accounted for about 87% of the variability associated with metal concentrations in all tissues as indicated in Figure 6.5. Hence, the following results and discussion are focused on PC1 and PC2.

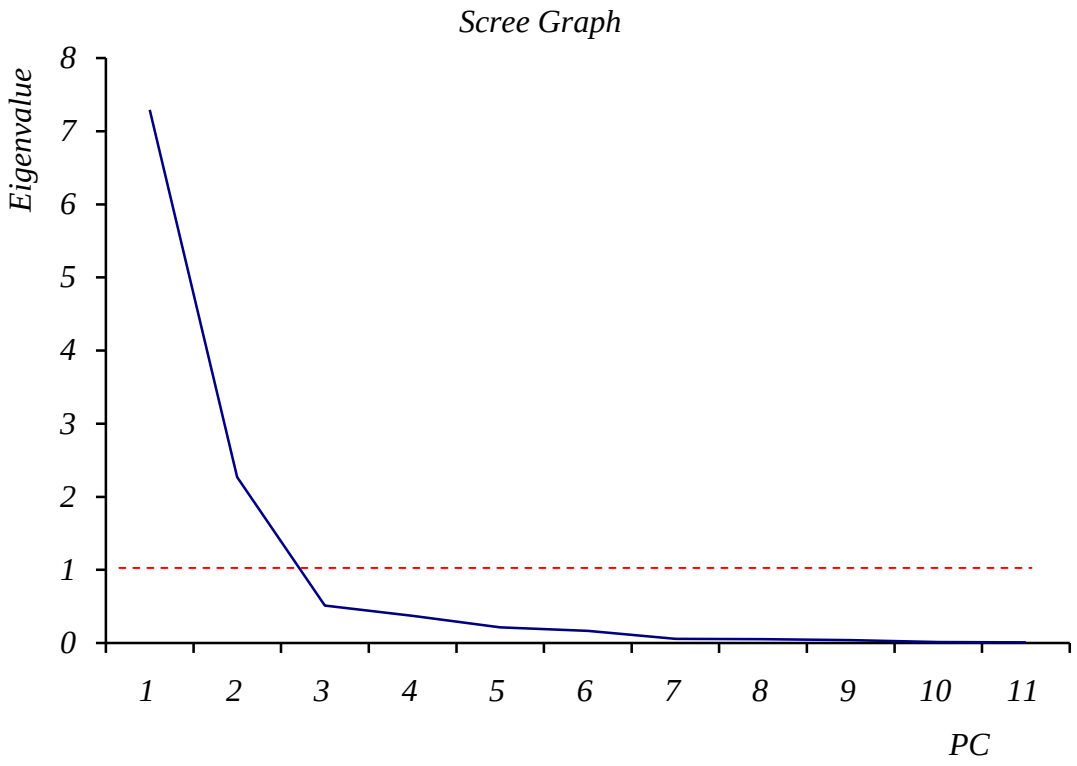

Figure 6.4 Scree graph for PCA with 11 metal variables

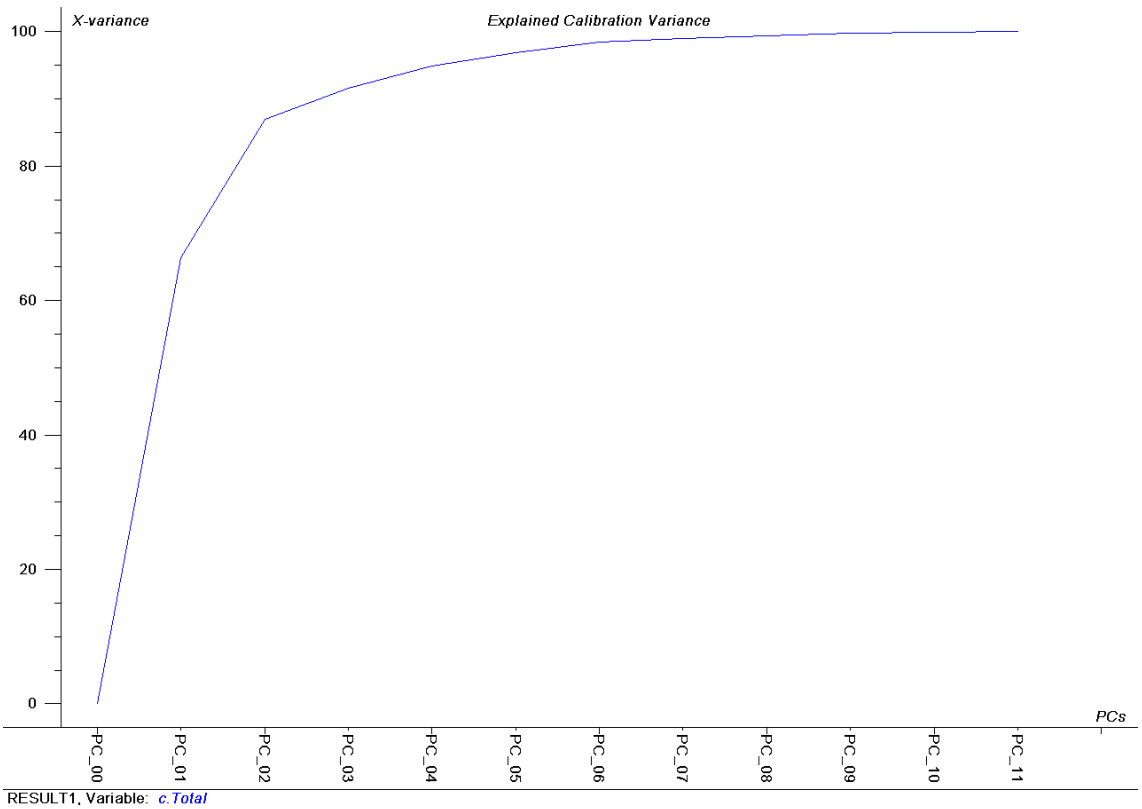

Figure 6.5 Plot of total explained variance vs. number of PCs for PCA

The results of a PCA are usually discussed in terms of PC scores and loadings since they complement each other. The former tells about the samples' variation, while the latter describes how the original measurement variables are related to each new PC axes. The loadings corresponding to the first two PCs are displayed in Table 6.7.

Table 6.7 The first two unrotated loadings

No.	Variable, k	Loading on PC1, $a_{k,1}$	Loading on PC2, $a_{k,2}$
1	V	0.357	-0.390
2	Mn	0.212	-0.297
3	Fe	0.427	-0.156
4	Co	0.351	-0.198
5	Cu	0.656	0.572
6	Zn	0.162	-0.120
7	As	-0.088	0.082
8	Se	0.117	0.110
9	Cd	0.148	0.187
10	Hg	0.059	0.266
11	Pb	0.138	-0.479

Geometrically the loadings are defined as cosines of the angle between the original axis and the corresponding PC axis (Eriksson *et al.*, 2006). Thus, as the loading approaches 1 or –1, it indicates that the variable axis is parallel with the corresponding PC axis, meaning that this variable contributes much variation to that PC. Conversely, if the loading is close to 0, they are considered perpendicular to each other, so the variable does not donate much to the variance explained by the corresponding PC. In our case,

most of the variables donate to the variance described by both retained PCs, so the interpretation could not be that easy.

Complementarily, correlation loadings plot (Figure 6.6) is used to depict the correlations between the variables and the PCs that may assist in interpreting the latent data structure. In Figure 6.6, the outer ellipse donates 100% explained variance while the inner ellipse shares 50% of explained variance. Those variables that fall between both ellipses and close to each other will have a high positive correlation, whereas those in diagonally opposed quadrants will have a tendency to be negatively correlated (Esbensen *et al.*, 2004). From Figure 6.6, there could be at least three distinct metal classes based on their position on the quadrants, but none of them are observed to be highly correlated negatively.

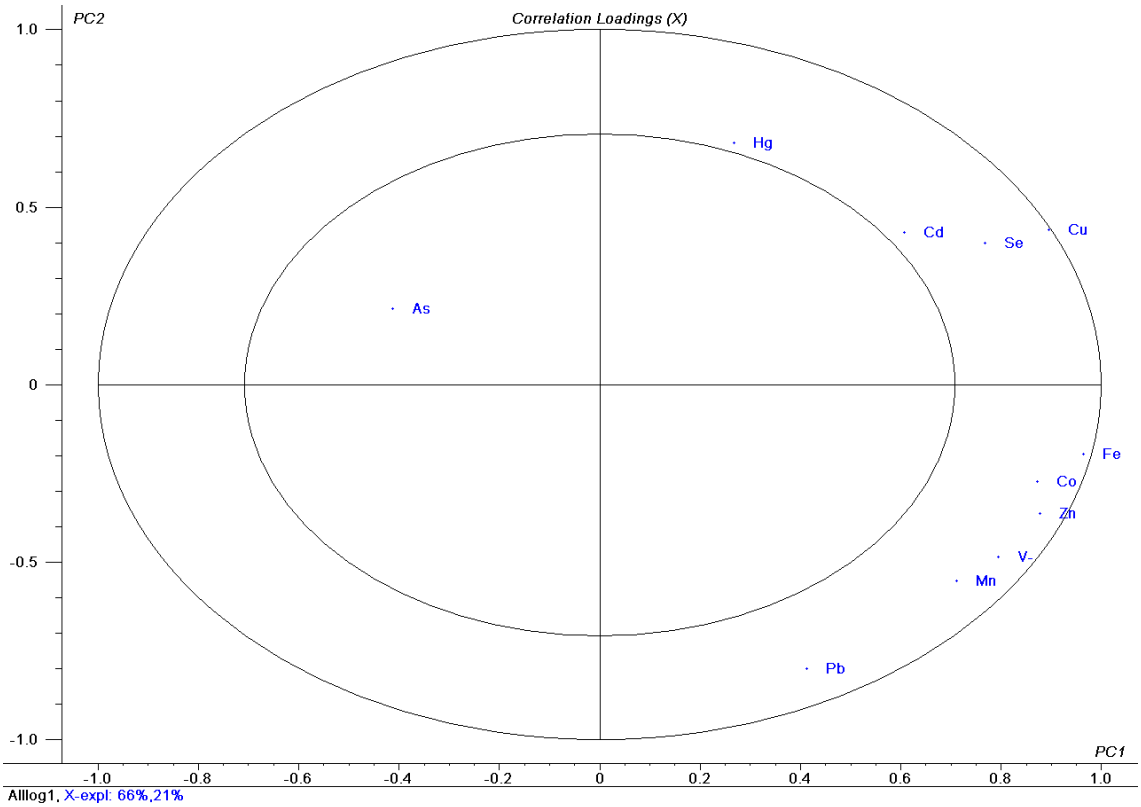

Figure 6.6 Correlation loadings plot for first two PC

On the other hand, the scores are the coordinates of the sample in the new coordinate space resulting from a projection onto the axes defined by those retained PCs. In this way, the relevant variation in the data can be represented by a smaller number of dimensions. In our case, the information for 11 metal variables of the *i*th sample, $Z_{i,1}$, $Z_{i,2}$, $Z_{i,3}$, …, $Z_{i,11}$ can be re-expressed in terms of the retained PCs. In general, the score on *j*th PC for *i*th sample is the linear combination of the variables having the variance, λ_j:

$$t_{i,j} = \sum_{k=1}^{11} (a_{k,j} Z_{i,k}) \qquad \text{(Equation 6.3)}$$

where the $a_{k,j}$ in above equation represents the loading of the *k*th element on the *j*th PC, given the constraint $\sum_{k=1}^{11} (a_{k,j}^2) = 1$.

Transforming and plotting these scores on PC space can be helpful in expressing samples variations visually, where the homogeneity, groupings, outliers and trends can be revealed. Figure 6.7 illustrates a plane spanned by the first two PCs that yielded three distinct clusters within a 95% confidence ellipse based on Hotelling's T^2 statistic. None of the PC scores lie outside the Hotelling's T^2 ellipse, indicating that no potential outlier was detected. In other words, none of the samples behave extremely differently. From the figure, cluster I is made up of muscle tissues, cluster II composed of liver tissues and cluster III consisted of gill tissues. The results point out that the metal content in red tilapias is highly influenced by the targeted organ rather than the production sites.

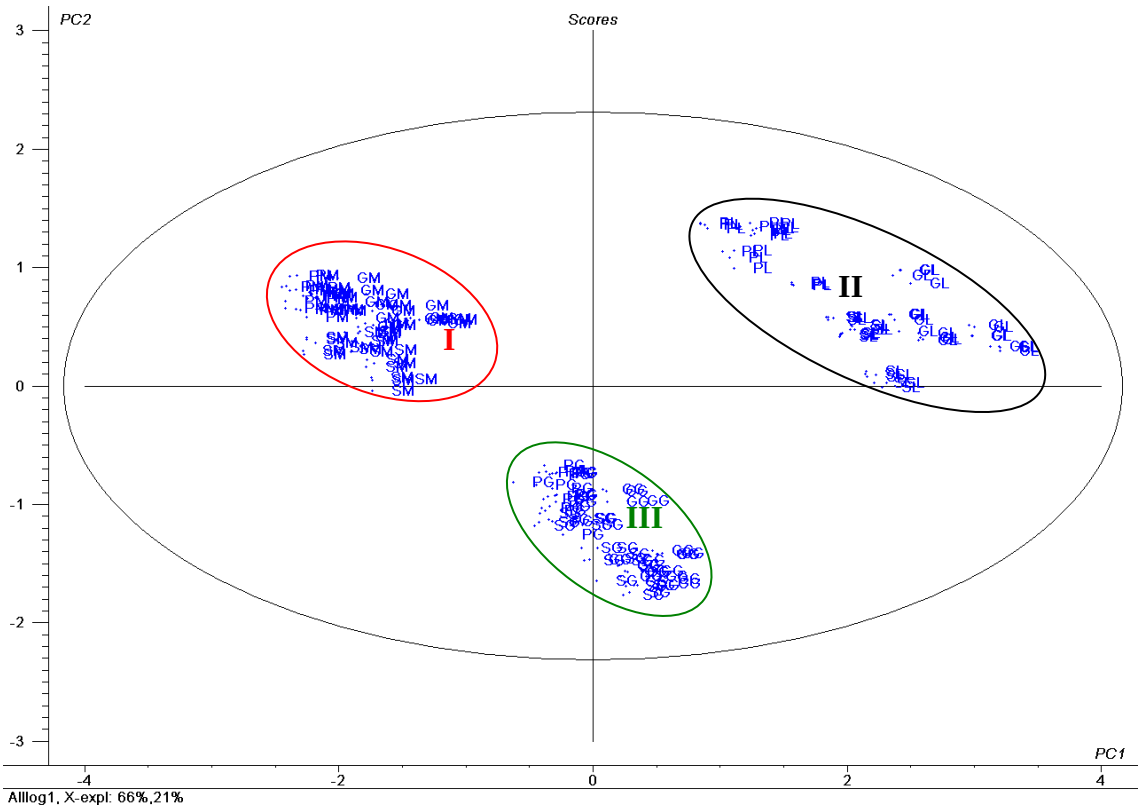

Figures 6.7 Scores plot of PC1 against PC2. First letters G, P and S donate the different sampling sites (Glami Lemi, Pertang, and Kampung Geylang repectively); second letters M, L, and G refer to different organ (muscles, liver and gills)

In addition to the loadings and scores plots, the scores-loadings bi-plot from PCA covers lots more information. It maps both the loadings and the scores projected onto the first two PCs in parallel which enables simultaneous interpretation of possible sample clusters and their corresponding variable relationships. From Figure 6.8, it is noticed that muscle samples are compactly grouped at the upper-left region that is primarily loaded by arsenic. This observation reinforces the fact that most metals studied except arsenic exhibit lowest concentrations in the muscles. Accumulation of arsenic, specifically in muscle tissues bring about potential toxicological risks in their consumption which requires further investigation.

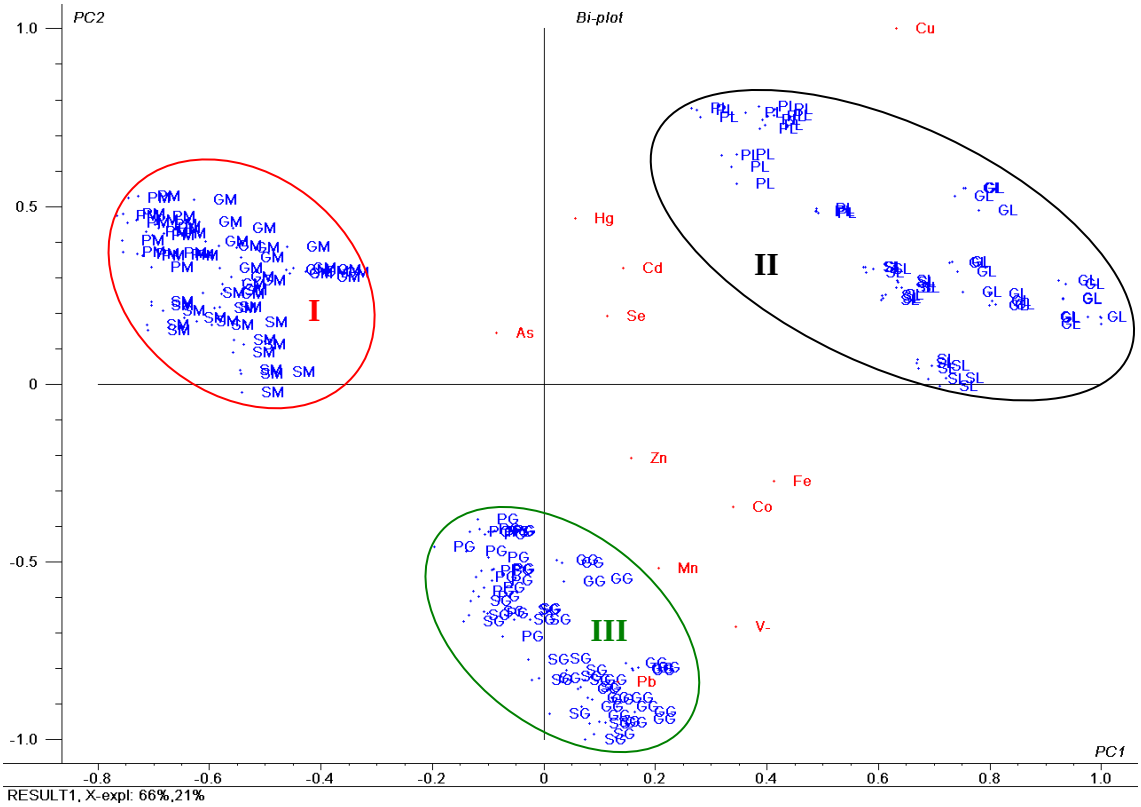

Figure 6.8 PCA bi-plot for all samples. First letters G, P and S donate the different sampling sites (Glami Lemi, Pertang, and Kampung Geylang repectively); second letters M, L, and G refer to different organ (muscles, liver and gills)

From Figure 6.8, it is also noted that almost all metals (except As) are mapped on the positive region of PC1. In other words, samples at the right-hand side of the scores plot contain higher total metal concentrations compared to those at the left-hand side. In general, the results indicate that total metal accumulation in liver > gills > muscles, which is in good agreement with the literatures. At the upper-right region of the bi-plot, it is observed that the more dispersed cluster II are made up of liver samples with a higher accumulation ratio of metals, particularly in Cu. High variation in Cu, Cd and Se levels makes liver samples stand out more than the others. These findings confirm the trends of the results in Table 6.4 where the average concentrations of the

major elements follow the sequence: Fe > Cu > Zn in liver, and Fe > Zn > Cu in other tissues. Fe is commonly found in compounds such as hemoglobin or myoglobin as well as ferritin and hemosiderin in fish liver (Sures *et al.*, 1999). Due to the physiological role of liver in blood synthesis, Fe concentrations in this organ are considerably higher than others (Wagner and Boman, 2003). Furthermore, it has been reported that about 95% of the whole body Cu accumulation are transferred into the liver of a fish in the form of tetrahedral metallothionein and metalloenzymes complex species. Zn on the other hand, can form stable five or six-membered ring chelates via zinc metalloenzymes and Zn^{2+}-protonated enzymes ([Al-Yousuf *et al.*, 2000]; [Laurén and McDonald, 1987] and [Stagg and Shuttleworth, 1982]). As far as non-essential metals are concerned, Cd shows distinct affinity to the liver. Wu *et al.* (2007) suggest that Cd is transferred via the circulatory system or the enterohepatic circulation to liver where xenobiotic detoxification takes place. This involves the removal of oxidative damage induced by Cd via selenium-dependent glutathione peroxidase at the selenocysteine site (Zirong and Shijun, 2007).

Figure 6.8 also suggests that gill samples in cluster III can be discriminated from the others with high and negative scores on PC2. Pb concentration exhibits the most negative loading on PC2 followed by V, Mn, Co, Fe and Zn, leading to the clustering of the gill samples beneath the PC1 axis. This agrees with the observation of high Pb and Mn accumulation ratio in the gills compared to other tissues as discussed previously. These results suggest that As, Cu and Pb could be regarded as the key discriminants that distinguish between the samples of tissues in aquacultured red tilapias.

Not infrequently, the unrotated loadings do not always provide an easy interpretation of each individual variable. To overcome this, new factors that fit the data

equally well but have simpler structure than the initial PCs can be obtained by appropriate rotation (Abdi, 2003). With orthogonal varimax rotation proposed by Kaiser (1958), Figure 6.9 shows a biplot where each variable tend to load strongly (either positively or negatively) on only one rotated PC, and near zero on another. In other words, each original variable is associated with either one of the rotated PCs and thus simplifies the interpretation of distinct variables and the cause of their variation. From these rotated loadings, the first dimension (rotated PC1) isolates As and opposes V, Mn, Fe, Co, Zn and Pb. On the other hand, the rotated PC2 relates strongly to Cu, Se, Cd and Hg. The interpretation is quite similar to the original PCA where As, Cu and Pb are found to be most distinctive variables.

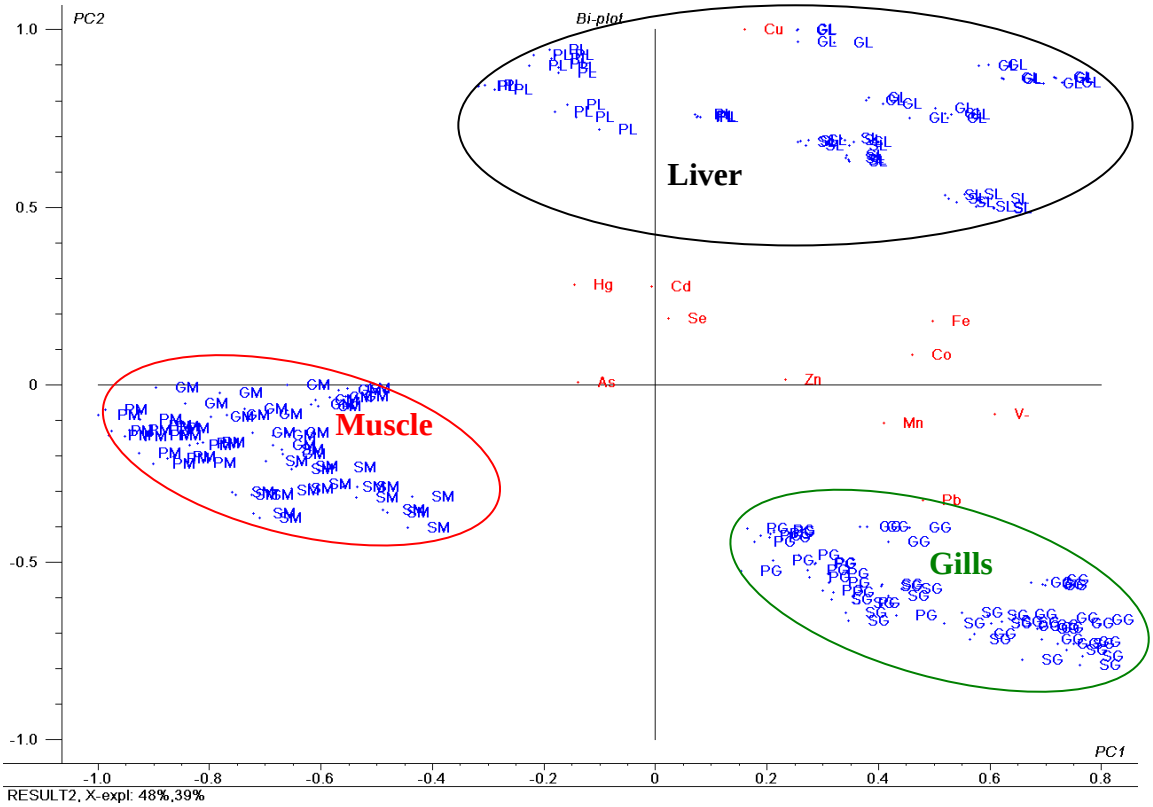

Figure 6.9 Varimax-rotated PCA bi-plot for all samples. First letters G, P and S donate the different sampling sites (Glami Lemi, Pertang, and Kampung Geylang repectively); second letters M, L, and G refer to different organ (muscles, liver and gills)

6.3.3.2 Metal Distribution Pattern among Sampling Sites

Metal compositions have been widely used to assign geographical origins of various matrices such as wine, honey, coffee, tea and potatoes ([Paneque *et al.*, 2010], [Fernández-Torres *et al.*, 2005], [Anderson and Smith, 2002], [Fernández-Cáceres *et al.*, 2001] and [Anderson *et al.*, 1999]). In the case of aquaculture products, trace elements have primarily been investigated for safety purposes but very little work has been done to explore the correlation between metal content and aquacultural origin. Examining the two-dimensional scores plot in Figure 6.7, relative dispersion of liver samples within cluster II suggests that variation in liver metals could provide sufficient information to develop a classification for the red tilapias based on the production environment. The bi-plot of PC2 vs. PC1 (Figure 6.10) explaining nearly 85% of the total variance indicates a natural separation of liver samples from three aquaculture sites. In particular, the samples from earthen pond have high and positive scores on PC2, where V and Pb content are responsible for the discrimination of these samples from the others. These two metals have significant positive loading on the second component. On the contrary, the other samples collected from the ex-tin mining pool and concrete tank exhibit negative scores on PC2. Nevertheless, the former samples are differentiated from the latter samples on PC1 that is positively loaded by all studied metals. This result indicates that samples collected from the concrete tank contain lower concentration of all metals, whereas samples from ex-tin mining pool shows a preferential association with higher metal content, with Co being the key parameter that differentiates them from the others. Once again, the varimax-rotated PCA bi-plot (Figure 6.11) shows similar outcomes. These observations suggest that V, Pb and Co are the most important variables that relate liver samples and production sites.

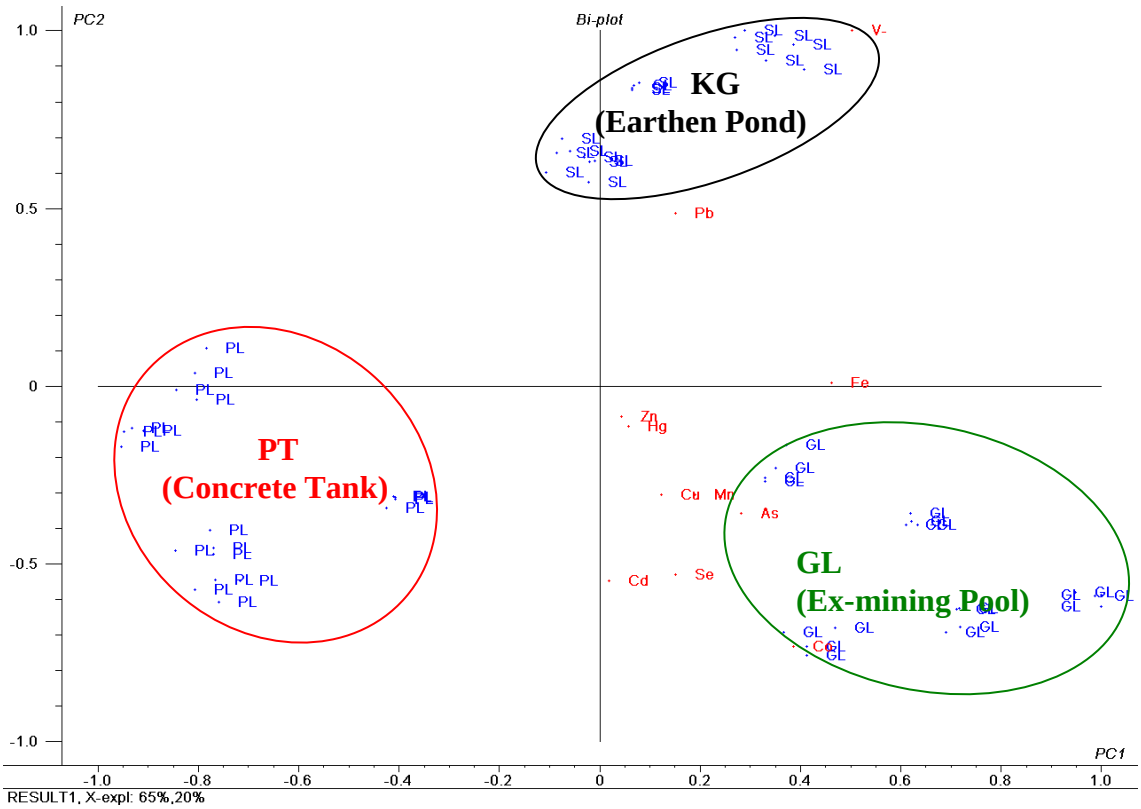

Figure 6.10 Unrotated PCA bi-plot for liver samples.

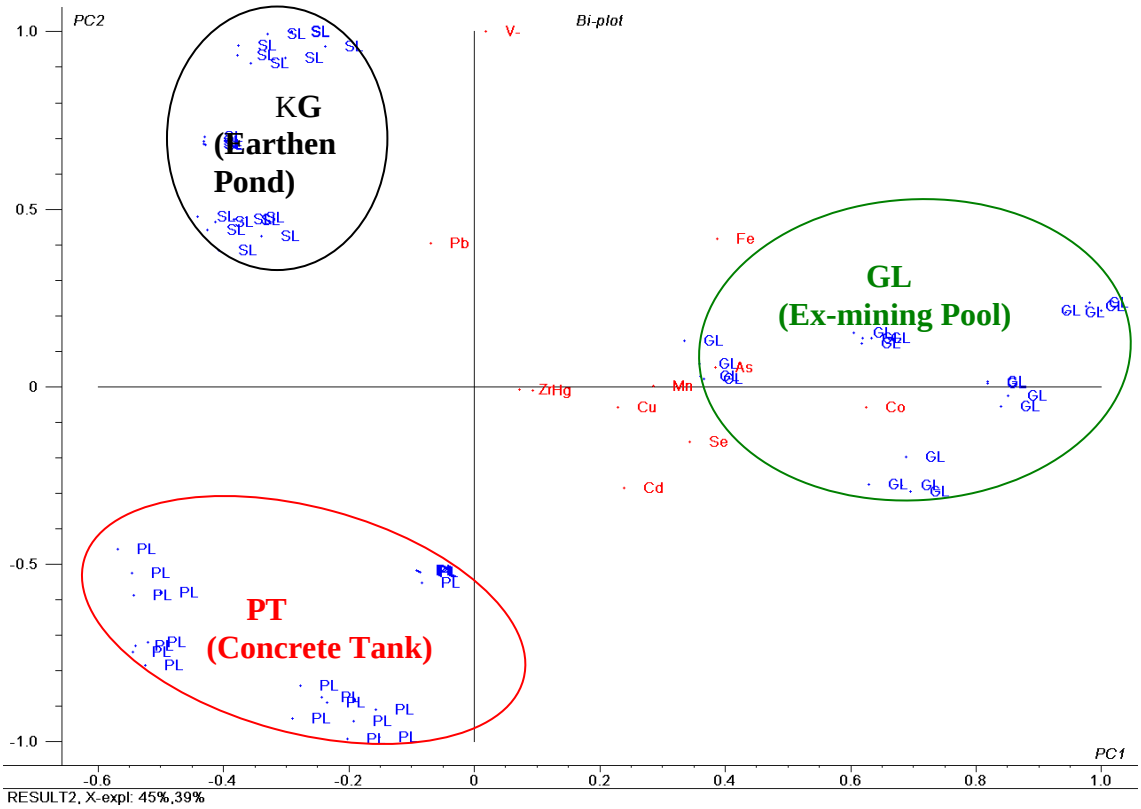

Figure 6.11 Varimax-rotated PCA bi-plot for liver samples

Notwithstanding this conclusion, it can be argued that metal levels in gills rather than liver are noteworthy for production site investigation due to direct exposure of gills to ambient water. The PCA bi-plot of the gill samples on the first two PCs dimensions that accounted for 76% of the total explained variance are presented in Figure 6.12 (unrotated) and Figure 6.13 (varimax-rotated). Three distinct clusters corresponding to different sampling sites can be observed. Gill samples from earthen pond also observed to be associated with higher concentrations of V and Pb as they are separated from others along the PC2 axis in Figure 6.12. The variables that mainly affect the separation between the rest of the samples are Co and Mn which exist in higher concentration in gill samples collected from ex-tin mining pool. Likewise, Figure 6.13 indicates that gill samples from earthen pond can be discriminated against those collected from ex-tin mining pool through PC1 (strongly correlated with Mn, Co positively and Pb negatively) and those collected from concrete tank via PC2 (strongly associated with V). Verily, the affinity of Mn and Pb to gills can make them good makers for distinguishing between production sites.

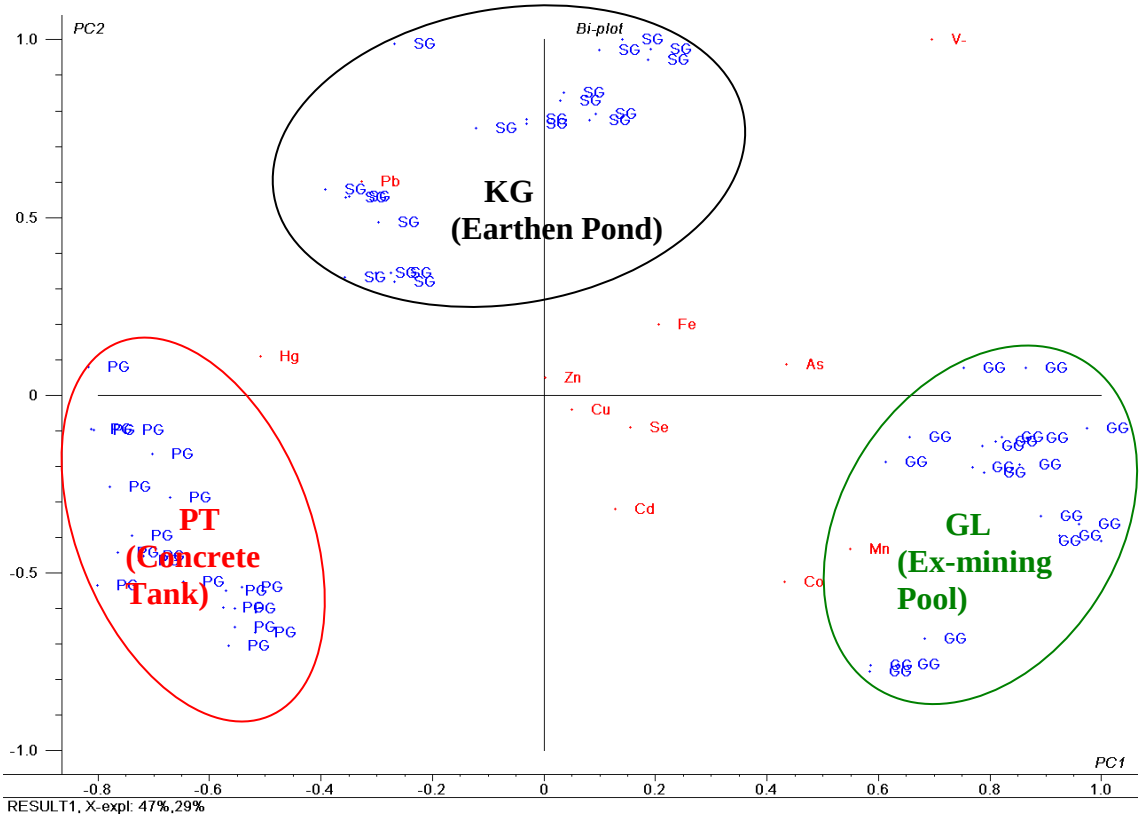

Figure 6.12 Unrotated PCA bi-plot for gill samples

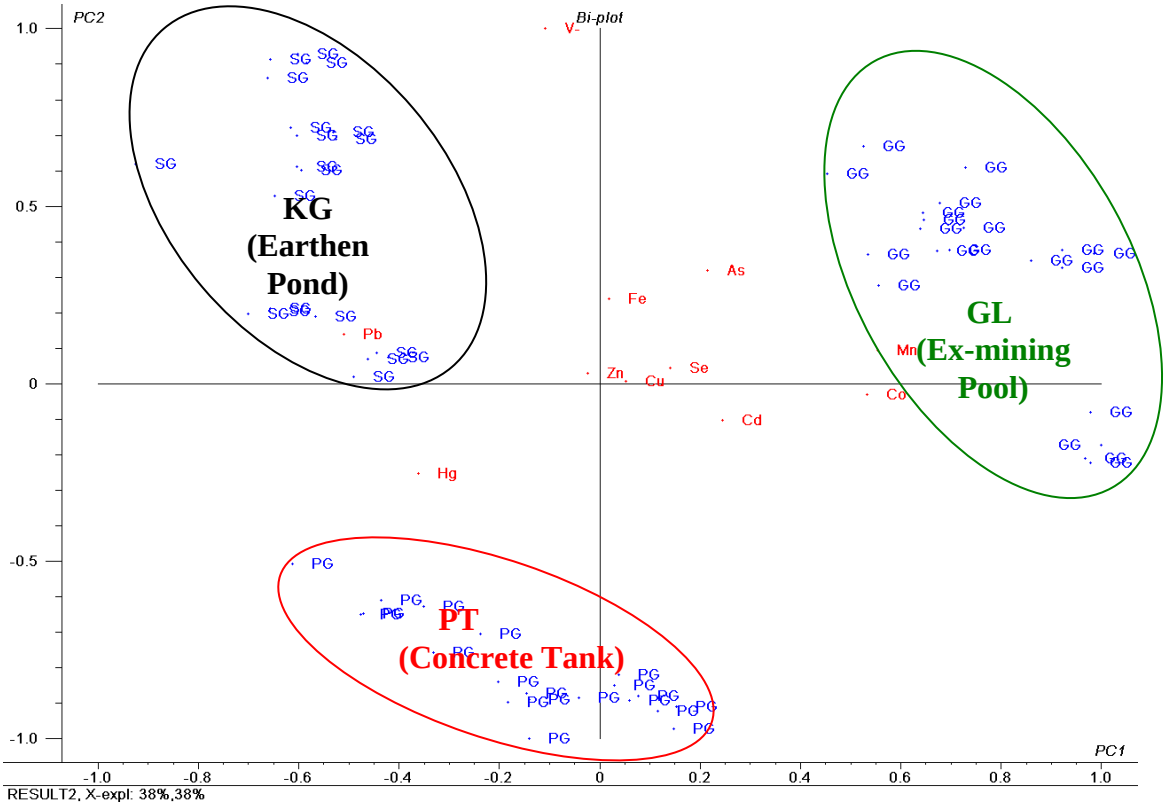

Figure 6.13 Varimax-rotated PCA bi-plot for gill samples

For muscle samples, the PCA bi-plot with 77% of the total explained variance (Figure 6.14 and Figure 6.15) also demonstrates similar clustering tendencies related to production sites. According to the outcomes of PCA, samples harvested from earthen pond are highly associated with V and Pb, while the remaining metal species are found to correspond to those from ex-tin mining pool, whereas samples from the concrete tank exhibit lower concentration for most metals. In view of the findings that muscle tissues corresponding to GL are associated with higher levels of trace metals (particularly Mn, Co, Cu, As, Cd and Hg), once again it is implied that health risk associated with consumption of red tilapia harvested from ex-tin mining pond might be considerably higher compared to other aquaculture production sites.

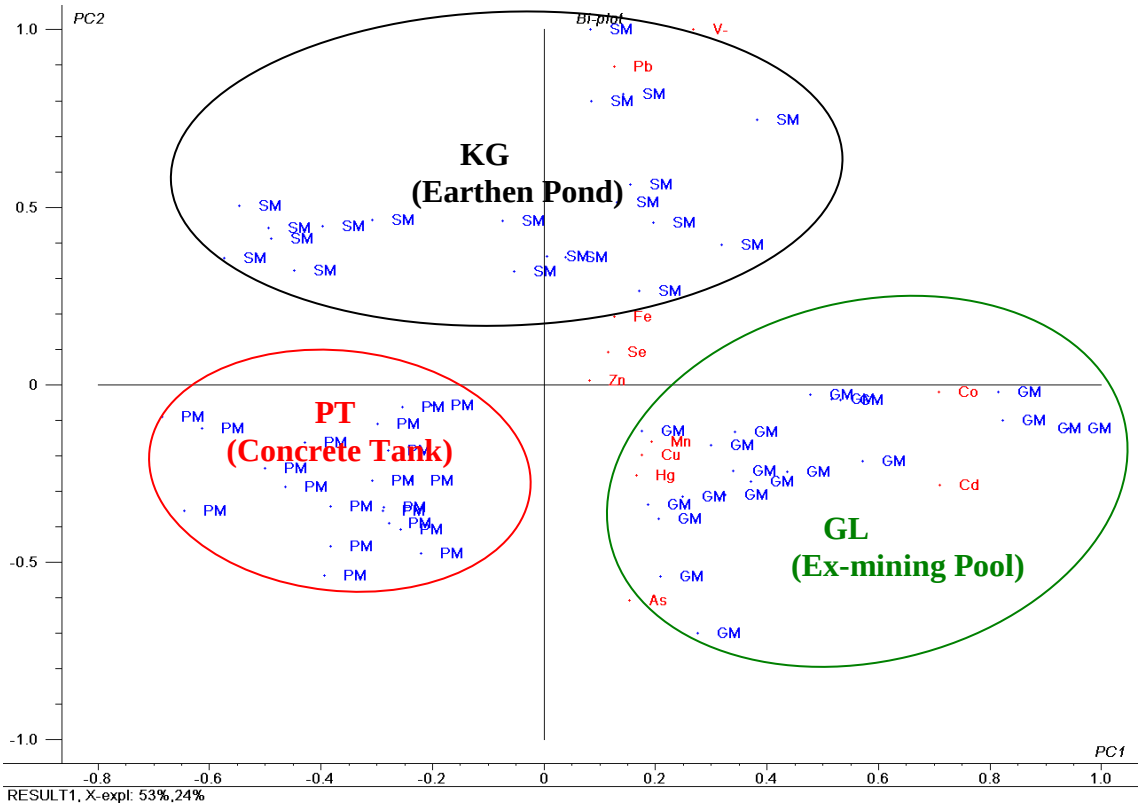

Figure 6.14 Unrotated PCA bi-plot for muscle samples

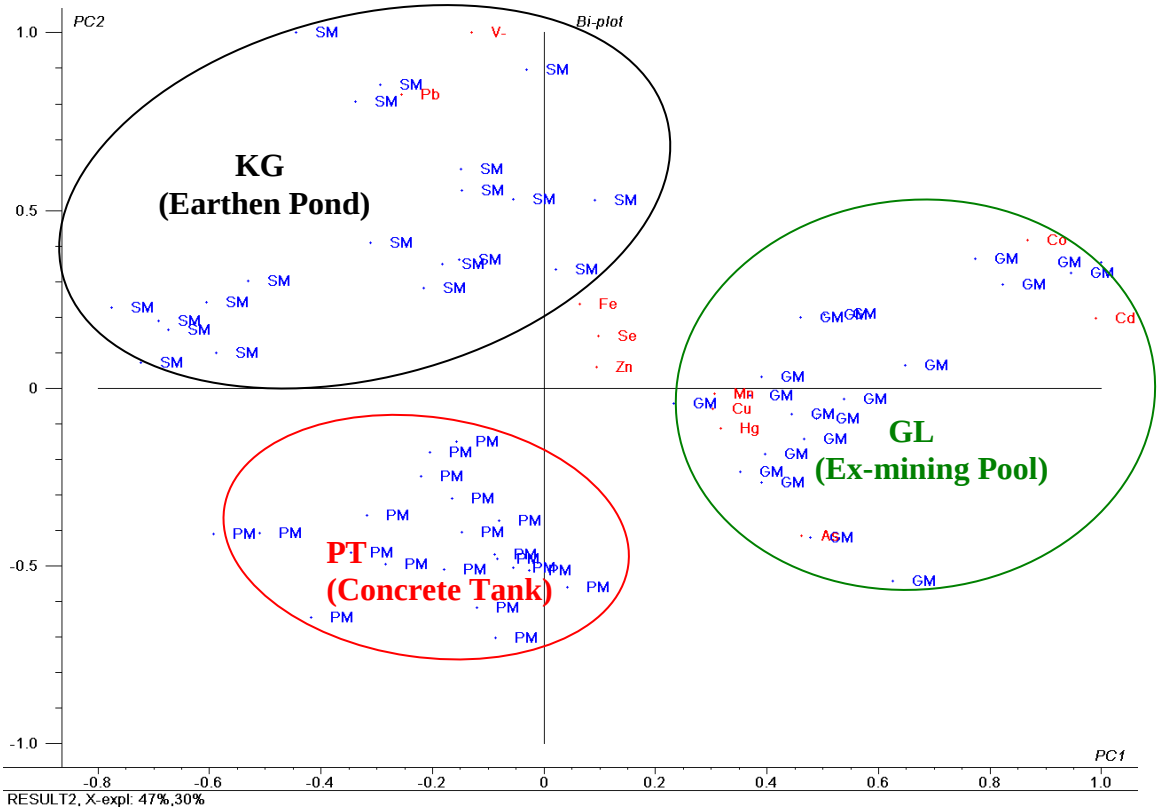

Figure 6.15 Varimax-rotated PCA bi-plot for muscle samples

6.3.4 Preliminary Human Health Risks Assessment

Several studies have linked tilapia ingestion to nutritional benefits but their metal composition can counteract the positive effects (Castro-González and Méndez-Armenta, 2008). In view that tilapia consumption involves intake of a mixture of metal compounds, thus the potential risks depend on the exposure and toxicity of each metal. In other words, metal distribution patterns discussed above do not reflect the actual risk profile quantitatively.

6.3.4.1 Non-carcinogenic Risk Assessment

Hazard Quotient (*HQ*) and/or Hazard Index (*HI*) set by United States Environmental Protection Agency (USEPA) are commonly used to assess the potential non-carcinogenic health risk associated with a variety of metal exposures via fish ingestion (USEPA 2000b). Both of them are often estimated according to experimental data and modeling assumptions.

In the assessment of human health risks due to ingestion of metals, it is essential to consider both the metal intake and dose that lead to adverse effects in humans. In general, metals exposure through red tilapia ingestion is a function of the concentration of the metals in the muscle, the gastrointestinal absorption of metals and the amount ingested. The equation for estimating daily ingestion exposure of *k*th metal can be expressed as follows (Asante-Duah, 1998):

$$E_k = \frac{CW_k \times FIR \times GI_k \times EF \times ED}{BW \times AT} \qquad \text{(Equation 6.4)}$$

where CW_k is the concentration of *k*th metal in fresh muscle tissue (μg kg^{-1}); *FIR* is the mean daily ingestion rate (kg day^{-1}); GI_k is the gastrointestinal absorption factor for *k*th metal; *EF* is the exposure frequency (days $years^{-1}$); *ED* is exposure duration (years); *BW* is the body weight (kg); and *AT* is averaging time (days).

Equation 6.4 can be rewritten using the aforementioned parameters and the experimental results.

$$E_k = \frac{[CD_k \times \chi_k \times (1-w)] \times FIR \times GI_k \times EF \times ED}{BW \times AT} \qquad \text{(Equation 6.5)}$$

where CD_k is the concentration of kth metal in dried muscle (μg kg^{-1}); χ_k is assumed to be 1 for all studied metals as well as Hg because more than 90% of total Hg in muscle tissue is in the form of MeHg (Chien *et al.*, 2007); except for As where χ_{As} is the ratio of inorganic As content to total As content in tilapia; w is the water content of tilapia and the term (1 - w) converts the dry weight content to wet weight; GI_k was conservatively assumed to be 1 where the ingested dose is equal to the absorbed dose and cooking procedures has no effect on the metals (Health Canada 2004); EF, ED and AT were not considered in the preliminary non-carcinogen risk assessment (Health Canada 2004).

Owing to sparse observed data, this work considered CD_k, χ_{As}, w and BW in a probabilistic manner by employing Monte Carlo (MC) simulation. Before the MC simulation is carried out, CD_k and w from experimental results were fitted with appropriate distributions and their goodness of fit were evaluated with Kolmogorov-Smirnov (K-S) and Anderson-Darling (A-D) tests using EasyFit Professional, Version 5.4. The results from both tests showed that CD_k are log-normally distributed while w followed a normal distribution. Log-normal approximation has been widely employed for concentration data which tended to be skewed to the right where fitting into normal distribution may be questionable ([Jang *et al.*, 2009], [Low *et al.*, 2009], [Ling and Liao, 2007], [Jang *et al.*, 2006] and [Singh *et al.*, 2001]). The statistical distribution of χ_{As} was based on log-normal distribution as suggested by Jang *et al.* (2009 and 2006). This had been derived from analytical data reported by Huang *et al.* (2003). The distribution of BW was derived from the Malaysian adult body mass index survey outcome reported by Azmi *et al.* (2009). In the absence of a better statistical information, FIR was assumed to be in accordance to Malaysian's annual per-capita freshwater fish consumption as recorded in FAOSTAT (2007). Table 6.8 and Table 6.9 listed the

approximated statistical distributions and the sources of aforementioned parameters. In MC simulation method, these independent distributions of exposure variables were regarded as input parameters to estimate the probability functions for the daily exposure doses using Equation 6.5. Briefly, the simulation was performed at 50 thousand iterations with each parameter sampled independently from its respective distribution using Microsoft Excel.

Table 6.8 Parameters and their distributions for risk estimation

Parameters	**Distributions/Values**	**Estimation method**	**Data Sources**
CD_k	Please refer Table 6.9	MC simulation	This study
χ_{As}	ln N (0.05, 2.71)	MC simulation	Jang *et al.* 2009, 2006 and Huang *et al.* 2003
w	N (0.77, 0.02)	MC simulation	This study
FIR	0.00952 kg day^{-1}	Constant	FAOSTAT 2007
EF	365 days year^{-1}	Constant	This study
ED	30 years	Constant	This study
BW	N (62.7, 18.7)	MC simulation	Azmi *et al.* 2009
AT	26645 days	Constant	WHO 2008

The data follow the specified distribution based on K-S and A-D statistics with $P > 0.05$. ln N (μ_g, σ_g) denotes a log-normal distribution with a geometric mean of μ_g and a geometric standard deviation of σ_g while N (μ_a, σ_a) denotes a normal distribution with an arithmetic mean of μ_a and an arithmetic standard deviation of σ_a.

Table 6.9 Log-normal distribution of trace metals in dried tilapia muscles from different production sites

	GL	PT	KG
V	ln N (0.02, 1.50)	ln N (0.01, 1.26)	ln N (0.03, 1.48)
Mn	ln N (1.11, 1.23)	ln N (0.81, 1.21)	ln N (0.75, 1.21)
Fe	ln N (21.2, 1.4)	ln N (17.2, 1.2)	ln N (21.4, 1.2)
Co	ln N (0.06, 1.42)	ln N (0.01, 1.23)	ln N (0.02, 1.38)
Cu	ln N (1.13, 1.24)	ln N (0.82, 1.12)	ln N (0.71, 1.18)
Zn	ln N (17.4, 1.1)	ln N (14.8, 1.1)	ln N (15.7, 1.1)
As	ln N (4.63, 1.18)	ln N (3.43, 1.27)	ln N (1.85, 1.19)
Se	ln N (1.51, 1.17)	ln N (1.04, 1.11)	ln N (1.35, 1.10)
Cd	ln N (0.18, 1.75)	ln N (0.06, 1.76)	ln N (0.07, 2.17)
Hg	ln N (0.04, 1.14)	ln N (0.03, 1.14)	ln N (0.02, 1.28)
Pb	ln N (0.05, 1.40)	ln N (0.04, 1.50)	ln N (0.08, 1.57)

The data follow the log-normal distribution based on K-S and A-D statistics with $p > 0.05$. All reported values of ln N (μ_g, σ_g) refer to the geometric mean and geometric standard deviation on dry basis.

The potential non-carcinogenic health risks associated with metal exposures are expressed by the *HQ* and/or *HI*. The HQ_k concerning tilapia intake is defined by the ratio of the estimated ingestion exposure level of the *k*th metal to its oral reference dose (RfD_k) and can be represented as follows (USEPA 2000b):

$$HQ_k = \frac{E_k}{RfD_k} \qquad \text{(Equation 6.6)}$$

Considering the fact that tilapia consumption involves exposures to a mixture of metal compounds, there is the need to evaluate the cumulative health risks. Despite potential uncertainties, the common approach in the assessment of aggregate non-carcinogenic risks posed by more than one metal is by summing the *HQ* of each metal (assuming additive effects) and expressing the summation as *HI* (Wcisło *et al.*, 2002):

$$HI = \sum_{k=1}^{n} HQ_k \qquad \text{(Equation 6.7)}$$

However, due to the lack of information on plausible correlations among CD_k, and ignoring these correlations can bias the MC estimations, USEPA Region III insisted on the inclusion of the exposure variables only in MC simulation whereas *RfD*s are treated as single numbers (Smith, 1994) Therefore, in order to evaluate the aggregate health risk associated with trace metals from red tilapia, the *HQ*s and *HI*s were calculated arithmetically by applying Equation 6.6 and Equation 6.7 on the simulated E_k so that the variability in risks are entirely contributed by the exposure assumptions. The *RfD*s used to estimate *HQ*s and *HI*s are also listed in Table 6.10. Since *RfD* of Pb was not covered by USEPA (2010), it was derived from provisional tolerable weekly intake levels of 25 μg kg^{-1} $week^{-1}$ (3.57 μg kg^{-1} day^{-1}) established by the Joint FAO/WHO Expert Committee on Food Additives (1999). Each *RfD* provides an estimate of continuous daily exposure of a particular metal over an extended period that is likely to be without an appreciable risk of adverse effects in humans. Traditionally, if any of the estimated HQ_k is more than 0.2 or the *HI* value exceeds 1, it is likely that non-carcinogenic effects may occur, with a probability which tends to increase as the value of *HQ* or *HI* increases and vice versa ([Castilhos *et al.*, 2006] and [Wang *et al.*, 2005]).

Table 6.10 Probabilistic estimation of reasonable maximum exposures and non-carcinogenic risks associated with the consumption of red tilapias

		GL				PT				KG			
	RfD_k / μg kg^{-1} day^{-1}	E_k / μg kg^{-1} day^{-1}		HQ_k		E_k / μg kg^{-1} day^{-1}		HQ_k		E_k / μg kg^{-1} day^{-1}		HQ_k	
		Percentile		Percentile		Percentile		Percentile		Percentile		Percentile	
		95th	99th	95th	99th	95th	99th	95th	99th	95th	99th	95th	99th
V	5	0.0014	0.0024	0.0003	0.0005	0.0007	0.0011	0.00013	0.00021	0.0024	0.0039	0.0005	0.0008
Mn	140	0.08	0.014	0.0006	0.0010	0.06	0.10	0.0004	0.0007	0.06	0.09	0.0004	0.0007
Fe	700	1.8	3.0	0.003	0.004	1.3	2.1	0.0018	0.0030	1.6	2.6	0.002	0.004
Co	0.3	0.005	0.008	0.016	0.027	0.0007	0.0012	0.002	0.004	0.0016	0.0027	0.005	0.009
Cu	40	0.09	0.14	0.002	0.004	0.06	0.10	0.0015	0.0024	0.05	0.09	0.0013	0.0022
Zn	300	1.2	2.1	0.004	0.007	1.1	1.8	0.004	0.006	1.1	1.9	0.004	0.006

Table 6.10 (continue)

		GL				PT				KG			
	RfD_k / μg kg^{-1} day^{-1}	E_k / μg kg^{-1} day^{-1}		HQ_k		E_k / μg kg^{-1} day^{-1}		HQ_k		E_k / μg kg^{-1} day^{-1}		HQ_k	
		Percentile		Percentile		Percentile		Percentile		Percentile		Percentile	
		95th	99th	95th	99th	95th	99th	95th	99th	95th	99th	95th	99th
[a]As	0.3	0.051	0.110	0.17	0.37	0.039	0.085	0.13	0.28	0.021	0.043	0.07	0.14
Se	5	0.11	0.18	0.02	0.04	0.08	0.12	0.015	0.024	0.10	0.16	0.02	0.03
Cd	1	0.021	0.35	0.021	0.035	0.007	0.013	0.007	0.013	0.011	0.021	0.011	0.021
[b]Hg	0.1	0.003	0.004	0.03	0.04	0.0019	0.0032	0.019	0.032	0.0017	0.0028	0.017	0.028
Pb	3.67	0.004	0.006	0.0011	0.0018	0.003	0.006	0.0010	0.0016	0.008	0.014	0.0023	0.0038
HI				0.27	0.52			0.18	0.37			0.13	0.25

[a]Inorganic As

[b]assuming total detected Hg is equal to MeHg

The reasonable maximum exposures (RME) estimated between the 95th and the 99th percentile of simulated distributions are displayed in Table 6.10. In general, they were determined from cumulative density functions which correspond to the probability density functions. Based on exposures at the 95th percentile, it is observed that all *HQ* of individual elements are less than 0.2 and *HI*s are below 1 regardless of the origin of the samples. This implies that the consumption of tilapia over a lifetime from the abovementioned production sites are unlikely to cause deleterious effects for Malaysians. Nevertheless, if other exposure routes are considered, cumulative potential health risks may exist. Thus, if the investigated production sites are compared, it is fair to conclude that potential non-carcinogenic risk associated with intake of red tilapias from GL > PT > KG. In addition, Table 6.10 also shows that there is discrepancy of *HQ* among different metals. A noteworthy observation is that HQ_{As} from As exposure can be observed to display the highest value and donates more than 50% of the respective *HI*. Based on this, it is suggested that limiting the As content in the feeding pellets would definitely be the most effective manner in an attempt to ameliorate the As hazards associated with consumption of commercially raised tilapias due to the factors explained in the earlier section of this chapter. It is also noticed that the exposures of Fe and Zn were the highest, yet, the risk corresponding to their exposures contributed not more than 3% of the estimated *HI*. This may be related to their high tolerability. In addition, exposures of V, Mn, and Cu via ingestion of tilapias could be deemed as non-significant, since each of them contributes less than 1% of the *HI*. These could well be the reasons why the concentration levels of V, Mn, Fe, Cu and Zn in fishes are unlikely to be of regulatory concern ([EC 2001] and [Food Act and Regulations 1995]).

6.3.4.2 Potential Arsenic Carcinogenic Risk

The United States Food and Drug Administration (1993a) pointed out that fish and other seafood ingestion account for about 90% of total As exposure route in human where dietary intake of inorganic As is strongly associated with wide spectrum carcinogenesis. Since As has been identified to be the key contaminant that highly influence the aggregate non-carcinogenic risk, it is deemed worthwhile to consider the long-term arsenic-induced cancer risk in this work. The carcinogenic risks (*CR*s) that indicate the incremental probability of an individual developing cancer over a lifetime as a consequence of oral exposure to inorganic As can be estimated by the following relationship which assumes that there are multiple stages for cancer (USEPA 2000b):

$$CR_{As} = E_{As} \times SF_{As} \qquad \text{(Equation 6.8)}$$

where E_{As} is the daily ingestion exposure of inorganic As (μg kg^{-1} day^{-1}) and SF_{As} is the slope factor for inorganic As which corresponds to 0.0015 per (μg kg^{-1} day^{-1}). By assuming that *FIR* is 0.00952 kg day^{-1} (FAOSTAT, 2007); GI_{As} is 1; the total exposure duration is defined as the *EF* of 365 days $year^{-1}$ for *ED* of 30 years; *AT* for lifetime exposure is approximated to the Malaysian life expectancy of 26645 days (WHO 2008); and substituting the aforementioned parameters in Equation 6.5 and Equation 6.8, probability functions of E_{As} and CR_{As} are derived. The 5th, 25^{th}, 50^{th}, 75^{th}, 95^{th} and 99^{th} percentiles are displayed in Table 6.11 which provides a complete description on the likelihoods of various risk levels. It is observed that all the estimated risks are within the generally acceptable risk range (10^{-4} to 10^{-7}). However in this case, CR_{As} of 10^{-5} is regarded as the benchmark level that allocates a reasonable margin of protectiveness because there are other sources of inorganic As exposure (USEPA 2000b). Indeed, about 28%, 20% and 8% of CR_{As} with respect to GL, PT and KG are found to be greater

that 1×10^{-5} which indicate that cancer risks potentially exist. In addition, there are significant variations in tilapia ingestion rate among different communities, thus, to conserve 95% of CR_{As} to be equal or lower than 10^{-5}, it is generally advisable to regulate tilapia intake within the simulated risk-based consumption limit (Table 6.11). This helps to assure the balance between benefit and risk of the tilapia consumption ([Burlingame and Pineiro, 2007] and [Castilhos *et al.*, 2006]).

Table 6.11 Probabilistic estimation of As exposures and cancer risks associated with consumption of red tilapia

Percentile	GL		PT		KG	
	E_{As} / μg kg^{-1} day^{-1}	CR_{As}	E_{As} / μg kg^{-1} day^{-1}	CR_{As}	E_{As} / μg kg^{-1} day^{-1}	CR_{As}
5th	6.04×10^{-7}	9.05×10^{-7}	4.43×10^{-7}	6.65×10^{-7}	2.44×10^{-7}	3.66×10^{-7}
25th	1.71×10^{-6}	2.57×10^{-6}	1.25×10^{-6}	1.88×10^{-6}	6.77×10^{-7}	1.02×10^{-6}
50th	3.52×10^{-6}	5.28×10^{-6}	2.62×10^{-6}	3.93×10^{-6}	1.39×10^{-6}	2.09×10^{-6}
75th	7.27×10^{-6}	1.09×10^{-5}	5.45×10^{-6}	8.18×10^{-6}	2.87×10^{-6}	4.30×10^{-6}
95th	2.10×10^{-5}	3.15×10^{-5}	1.60×10^{-5}	2.41×10^{-5}	8.43×10^{-6}	1.26×10^{-5}
99th	4.51×10^{-5}	6.76×10^{-5}	3.50×10^{-5}	5.26×10^{-5}	1.77×10^{-5}	2.66×10^{-5}
RBCL /kg day^{-1}	3.02×10^{-3}		3.94×10^{-3}		7.50×10^{-3}	

RBCL – Risk-based consumption limit refers to benchmark level of 10^{-5} at 95th percentile

7 CONCLUSION

In this work, a microwave assisted digestion-inductively coupled plasma-mass spectrometry (MAD-ICP-MS) procedure have been developed under two-stage experimental design for the multi-element analysis in fish tissues. This method exhibit wider element tolerability with quantitative recoveries which requires less sample, acids/oxidizing reagents and heating cycle compared to other studies in literature and was successfully employed to determine the trace levels in various tissues of red tilapias sampled from aquacultural sites in Jelebu.

As demonstrated in this work, principal component analysis (PCA) provides a simple way to visualize the clustering tendency among different tissues of red tilapia, and helps to identify which metals contribute most to the variation. It can be observed that there are some general trends in metal content of particular organs and the distribution pattern with respect to their production sites. It is suggested that Cu, As and Pb are the best describers in characterizing the studied organs, where liver tissues are associated with high Cu, gills with high Pb and muscles with high As. These results also show the potential for distinguishing between the aquaculture sites of red tilapia samples under the experimental condition of this work, where V, Co and Pb are observed to be the key discriminants for sample origins.

In assessing the safety of human intake of red tilapia, the concentration levels of V, Mn, Fe, Co, Cu, Zn, As, Se, Cd, Ag, Sn, Hg and Pb in the muscle tissues are found to be below the prescribed limits except for As and Cd contents in samples from the ex-tin mining ponds. Results from preliminary risk assessments suggest that non-carcinogenic risks posed by trace metals via consumption of red tilapias from the

investigated sites were well within the tolerable regions. Among the studied metals, As was identified as the key contaminant which is probably brought about by the utilization of metal-enriched feeding pallets. The carcinogenic risk of As is of concern due to the 95^{th} percentile risk levels which are found to exceed 1×10^{-5} for a Malaysian. Thus, it is generally advisable to regulate the consumption rate of red tilapia so as to improve balance between the substantial benefit and risk. In general, health risks associated with ingestion of red tilapia can be ranked as ex-mining pond > concrete tank > earthen pond, although the estimated Metal Pollution Index (MPI) is in the order of ex-mining pond > earthen pond > concrete tank. This reflects that MPI is inconsistent in revealing the hazardous situation of metal pollution because it does not take into account the potential health consequences associated with each targeted metal species.

Additionally, the application of spectrophotometric method for simultaneous determination of Cu^{2+}, Ni^{2+} and Zn^{2+} ions in water samples using 1-(2-thiazolylazo)-2-naphthol (TAN) in the presence of triton x-100 was also studied by multivariate calibrations. These techniques can be regarded as simple, rapid and inexpensive and do not require tedious sample pretreatment. The analytical results by regression models with only three factors/PCs revealed that there is no substantial difference in the predictive ability between the partial least squares (PLS) and principal component regression (PCR) models on the zero order spectral data. Good tolerance between the predicted values and the validation samples have also been clearly demonstrated under current experimental conditions, although there could be some limitations due to the presence of undesirable interference species.

8 REFERENCES

1. Abdi, H. (2003). Factor Rotations in Factor Analyses. In: Lewis-Beck M., Bryman, A., Futing T. Eds. *Encyclopedia of Social Sciences Research Methods*. Thousand Oaks (CA): Sage.
2. Abdollahi, H., Zolgharnein J., Azimi, G.H. and Jafarifar, D. (2003). *Talanta* **59(6)**, 1141.
3. Agilent (2005a). *Inductively Coupled Plasma-Mass Spectrometry: A Primer.* USA: Agilent Technologies, Inc.
4. Agilent (2005b). *Agilent 7500 ICP-MS ChemStation (G1834B) Operator's Manual*. Japan: Agilent Technologies, Inc.
5. Al Rmalli, S.W., Haris, P.I., Harrington, C.F. and Ayub, M. (2005). *Sci. Total Environ.* **337(1-3)**, 23.
6. Al-Kahtani, M.A. (2009). *Am. J. Appl. Sci.* **6(12)**, 2024.
7. Allinson, G., Nishikawa, M., De Silva, S.S., Laurenson, L.J.B. and De Silva, K. (2002). *Ecotoxicol. Environ. Safe.* **51**, 197.
8. Allinson, G., Salzman, S.A., Turoczy, N., Nishikawa, M., Amarasinghe, U.S., Nirbadha, K.G.S. and De Silva, S.S. (2009). *Bull. Environ. Contam. Toxicol.* **82**, 389.
9. Almeida, P. and Stearns, L. (1998). *Soc. Probl.* **45(1)**, 37.
10. Al-Saleh, I., Al-Enazi, S. and Shinwari, N. (2009). *Regul. Toxicol. Pharmacol.* **54(2)**, 105.
11. Alula, M.T., Mohamed, A.M.I. and Bekhit, A.A. (2010). *Thai J. Pharm. Sci.* **34**, 93.
12. Al-Yousuf, M.H., El-Shahawi, M.S. and Al-Ghais, S.M. (2000). *Sci. Total Environ.* **256**, 87.

13. Amundsen, P-A., Staldvik, F.J., Lukin, A.A., Kashulin, N.A., Popova, O.A., and Reshetnikov, Y.S. (1997). *Sci. Total Environ.* **201**, 211.

14. Anderson, K.A. and Smith, B.W. (2002). *J. Agric. Food Chem.* **50**, 268.

15. Anderson, K.A., Magnuson,B.A., Tschirgi, M.L. and Smith, B. (1999). *J. Agric. Food Chem.* **47**, 1568.

16. Armstrong, C.W., Stroube, R.B., Rubio, T. and Backett, W.S. (1884). *Arch. Environ. Health* **39**, 276.

17. Asante-Duah, K. (1998). *Risk Assessment in Environmental Management*. Chichester: John Wiley & Sons.

18. Ashoka, S., Peake, B.M., Bremner, G., Hageman, K.J. and Reid, M.R. (2009). *Anal. Chim. Acta* **653(2)**, 191.

19. ATSDR (1999). *Toxicological Profile for Mercury*, USDHHS, Public Health Service, Atlanta, GA

20. ATSDR (2003). *Toxicological Profile for Selenium*, USDHHS, Public Health Service, Atlanta, GA.

21. ATSDR (2007a). *Toxicological Profile for Arsenic*, USDHHS, Public Health Service, Atlanta, GA.

22. ATSDR (2007b). *Toxicological Profile for Lead*, USDHHS, Public Health Service, Atlanta, GA.

23. ATSDR (2008). *Toxicological Profile for Cadmium*, USDHHS, Public Health Service, Atlanta, GA.

24. Azizur Rahman, M., Hasegawa, H., Mahfuzur Rahman, M., Mazid Miah, M.A. and Tasmin, A. (2008). *Ecotoxicol. Environ. Safe.* **69(2)**, 317.

25. Azmi, M.Y., Junidah, R., Siti Mariam, A., Safiah, M.Y., Fatimah, S., Norimah, A.K., Poh, B.K., Kandiah, M., Zalilah, M.S., Wan Abdul Manan, W.M., Siti Haslinda, M.D., and Tahir, A. (2009). *Mal. J. Nutr.* **15(2)**, 97.

26. Balcerzak, M. (2002). *Anal. Sci.* **18**, 737.

27. Barrentine, L.B. (1999). *An introduction to design of experiments: a simplified approach* edited by K. Zielske and A. Koudstaal. Milwaukee: ASQ Press.

28. Barton, H.J. (2010). *Biol. Trace Elem. Res.* DOI: 10.1007/s12011-010-8896-6.

29. Beebe, K.R., Pell, R.J. and Seasholtz, M.B. (1998). *Chemometrics: A Practical Guide.* New York: John Wiley & Sons.

30. Bellinger, D.C. (2005). *Birth Defects Res. A* **73**, 409.

31. Bellinger, D.C. and Needleman, H.L. (2003*). New Engl. J. Med.* **349**, 500.

32. Benton, D. (2001). *Neurosci. Biobehav. Rev.* **25(4)**, 297.

33. Bermejo-Barrera, P., Moreda-Pĩneiro, A., Mũniz-Naveiro, O., Gõmez-Ferńandez, A.M.J. and Bermejo-Barrera, A. (2000). *Spectrochim. Acta B* **55**, 1351.

34. Berridge, J.C., Jones, P. and Roberts-McIntosh, A.S. (1991). *J. Pharm. Biomed. Anal.* **9(8)**, 597.

35. Berzas Nevado, J.J., R.C. Rodríguez Martín-Doimeadios, Guzmán Bernardo, F.J., Jiménez Moreno, M., Herculano, A.M., do Nascimento, J.L.M. and Crespo-López, M.E. (2010). *Environ. Int.* **36(6)**, 593.

36. Biswas, U., Sarkar, S., Bhowmik, M.K., Samanta, A.K. and Biswas, S. (2000). *Small Ruminant Res.* **38(3)**, 229.

37. Boquk, R. and Rius, F.X. (1996). *Chemometr. Intell. Lab. Syst.* **32**, 11.

38. Brammer, H. and Ravenscroft, P. (2009). *Environ. Int*. **35(3)**, 647.

39. Brereton, R.G. (2003a). *Features: Chemometrics*. The Alchemist, The ChemWeb Magazine. Chichester: John Wiley & Sons.

40. Brereton, R.G. (2003b). *Chemometrics: Data Analysis for the Laboratory and Chemical Plant.*

41. Brereton, R.G. (2007). *Applied Chemometrics for Scientists.* Chichester: John Wiley & Sons.

42. Brereton, R.G. (2009). *Chemometrics for Pattern Recognition*. Chichester: John Wiley & Sons.

43. Bro, R. (2003). *Anal. Chim. Acta* **500**, 185.

44. Brown, S.D., Tauler, R., and Walczak, B. (2009). *Comprehensive Chemometrics*. Amsterdam: Elsevier.

45. Brunke, E.G., Labuschagne, C. and Slemr, F. (2001). *Geophys. Res. Lett.* **28**, 1483.

46. Bugallo, R.A., Segade, S.R. and Gómez, E.F. (2007). *Talanta* **72(1)**, 60.

47. Caimi, S., Senofonte, O., Kramer, G.N., Robouch, P. and Caroli, S. (2004). *Int. J. Environ. Anal. Chem.* **8 (6-7)**, 551.

48. Burlingame, B. and Pineiro, M. (2007). *J. Food Comp. Anal.* **20(3-4)**, 139.

49. Camargo, J.A. (2002). *Chemosphere* **48**, 51.

50. Cambier, S., Gonzalez, P., Durrieu, G. and Bourdineaud, J-P. (2010). *Ecotoxicol. Environ. Safe.* **73(3)**, 312.

51. Cashman, K.D. (2006). *Int Dairy J.* **16(11)**, 1389.

52. Castilhos, Z.C., Rodrigues-Filho, S., Rodrigues, A.P.C., Villas-Bôas, R.C., Siegel, S., Veiga, M.M. and Beinhoff, C. (2006). *Sci. Total Environ.* **368(1)**, 320.

53. Castro-González, M.I. and Méndez-Armenta, M. (2008). *Environ. Toxicol. Pharmacol.* **26(3)**, 263.

54. Cattell, R.B. (1966). *Multivar. Behav. Res.* **1**, 245.

55. Celik, U. and Oehlenschlager, J. (2007). *Food Control 18*, 258.

56. Cerutti, S., Salonia, J.A., Ferreira, S.L.C., Olsina, R.A. and Martinez, L.D. (2004). *Talanta* **63(4)**, 1077.

57. Cesur, H. (2003). *Turk. J. Chem.* **27**, 307.

58. Chakraborti, D., Rahman, M.M., Das, B., Murrill, M., Dey, S., Mukherjee, S.C., Dhar, R.K., Biswas, B.K., Chowdhury, U.K., Roy, S., Sorif, S., Selim, M., Rahman, M. and Quamruzzaman, Q. (2010). *Water Res.* **44(19)**, 5789.

59. Chen, C.J., Chen, C.W., Wu, M.M. and Kuo, T.L. (1992). *Br. J. Cancer* **66**, 888.

60. Chen, Z.L., Khan, N.I., Owens, G. and Naidu R. (2007). *Microchem. J.* **87**, 87.

61. Cheung, K.C. and Wong, M.H. (2006). *Environ. Geochem. Health* **28**, 27.

62. Chi, Q.Q., Zhu G.W. and Langdon, A. (2007). *J. Environ. Sci.* **19**, 1500.

63. Chien, L.C., Yeh, C.Y., Jiang, C.B., Hsu, C.S and Han, B.C. (2007). *Chemosphere* **67**, 29.

64. Chiou, J.M., Wang, S.L., Chen, C.J., Deng, C.R., Lin, W. and Tai, T.Y. (2005). *Int. J. Epidemiol.* **34**, 936.

65. Choi, Y.J., Kim, Y.J., Lee, H.S., Kim, C.I. Hwang, I.K., Park, H.K. and Oh, C.H. (2009). *J. Food Comp. Anal.* **22(2)**, 117.

66. Chowdhury, U.K., Rahman, M.M., Mandal, B.K., Paul, K., Lodh, D., Biswas, B.K., Basu, G.K., Chanda, C.R., Saha, K.C., Mukherjee, S.C., Roy, S., Das, R., Kaies, I., Barua, A.K., Palit, S.K., Quamruzzaman, Q. and Chakraborti, D. (2001) *Environ. Sci.* **8**, 393.

67. Chromy, V. and Sommer, L. (1967). *Talanta* **14**, 393.

68. Citak, D., Tuzen, M. and Soylak, M. (2009). *Food Chem. Toxicol.* **47(9)**, 2302.

69. Comelekoglu, U., Yalin, S., Bagis, S., Ogenler, O., Sahin, N.O., Yildiz, A., Coskun, B., Hatungil, R. and Turac, A. (2007). *Ecotoxicol. Environ. Safe.* **66(2)**, 267.

70. Cornelis, R., Caruso, J., Heumann, K.G. and Crews, H. (2003). *Handbook of Elemental Speciation: Techniques and Methodology*. Chichester: John Wiley and Sons.

71. Costa, L.M., Santos, D.C.M.B., Hatje, V., Nóbrega, J.A. and Korn, M.G.A. (2009). *J. Food Compos. Anal.* **22(3)**, 238.

72. Counter, S.A., Buchanan, L.H. and Ortega, F. (2008). *Clin. Biochem.* **41**, 41.

73. Cubadda, F., Raggi, A. and Coni, E. (2006). *Anal. Bioanal. Chem.* **384**, 887.

74. Cui, X.L, Wang, Y.J. and She, X.L. (2010). *J. Ocean Univ. China* **9(3)**, 235.

75. Custódio, P.J., Pessanha, S., Pereira, C., Carvalho, M.L. and Nunes, M.L. (2011). *Food Chem.* **124(1)**, 367.

76. Dai, W., Du, H.H., Fu, L.L., Liu, H.T. and Xu, Z.R. (2010). *Appl. Clay Sci.* **47(3-4)**, 193.

77. Dalman, Ö., Demirak, A. and Balcı, A. (2006). *Food Chem.* **95(1)**, 157.

78. Darrouzès, J., Bueno, M., Lespès, G., Holeman, M. and Potin-Gautier, M. (2007). *Talanta* **71**, 2080.

79. Das, H.K., Mitra, A.K., Sengupta, P.K., Hossain, A., Islam, F. and Rabbani G.H. (2004). *Environ. Int.* **30(3)**, 383.

80. Davis, H.T., Aelion, C.M., McDermott, S. and Lawson, A.B. (2009). *Environ. Poll.* **157(8-9)**, 2378.

81. De Andrade Passos, E., Alves, J.C., dos Santos, I.S., Alves, J.d.P.H., Garcia, C.A.B. and Costa, A.C.S. (2010). *Microchim. J.* **96(1)**, 50.

82. De Luca, M., Oliverio, F., Ioele, G. and Ragno, G. (2009). *Chemometr. Intell. Lab. Syst.* **96(1)**, 14.

83. Demirel, S., Tuzen, M., Saracoglu, S. and Soylak, M. (2008). J. Hazard. Mater. 152(3), 1020.

84. Dennehy, C. and Tsourounis, C. (2010). *Maturitas* **66(4)**, 370.

85. Divrikli, U., Kartal, A.A., Soylak, M, and Elci, L. (2007). *J. Hazard. Mater.* **145(3)**, 459.

86. DOF (2008). *Annual Fisheries Statistics 2008*, Department of Fisheries, Putrajaya, Malaysia.

87. Dufailly, V., Noël, L. and Guérin, T. (2008). *Anal. Chim. Acta* **611**, 134.

88. EC (2001). *Commission Regulation No 466/2001*, OJEC L77/1, European Commission.

89. Eguchi, N., Kuroda, K., Okamoto, A. and Horiguchi, S. (1997). *Arch. Environ. Contam. Toxicol.* **32**, 141.

90. Ekino, S., Susa, M., Ninomiya, T., Imamura, K. and Kitamura, T. (2007). *J. Neurol. Sci.* **262(1-2)**, 131.

91. Elia, A.C., Prearo, M., Pacini, N., Dörr, A.J.M. and Abete, M.C. (2011). *Ecotoxicol. Environ. Safe.* **74(2)**, 166.

92. Elliott, S., Sturman, B., Anderson, S., Brouwers, E. and Beijnen, J. (2007). ICP-MS: When Sensitivity Does Matter. In: *Spectroscopy Solution for Material Analysis, Special Issues, April 2007.* Iselin: Advanstar Communications Inc.

93. Ellis, D.R. and Salt, D.E. (2003). *Curr. Opin. Plant Biol.* **6**, 273.

94. Endo, G., Kuroda, K., Okamoto, A. and Horiguchi, S. (1992). *Bull. Environ. Contam. Toxicol.* **48**, 131.

95. Erdoğan, S., Erdemoğlu, S.B. and Kaya, S. (2006). *J. Sci. Food Agric.* **86**, 226.

96. Erdoğrul, Ö. and Erbilir, F. (2007). *Environ. Monit. Assess.* **130**, 373.

97. Eriksson, L., Johansson, E., Kettaneh-Wold, N., Trygg, J., Wikström, C. and Wold, S. (2006). Multi- and Megavariate Data Analysis. Umeå: Umetrics AB.

98. Esbensen, K.H. Guyot, D, Westad, F. and Houmøller, L.P. (2004). *Multivariate Data Analysis - in Practice 5ed.* Oslo: Camo Process AS.

99. Escandar, G.M., Damiani, P.C., Goicoechea, H.C., and Olivieri, A.C. (2006). *Microchem. J.* **82(1)**, 29.

100. Eskandari, H., Saghseloo, A.G. and Chamjangali, M.A. (2006). *Turk. J. Chem.* **30**, 49.

101. Evans, D.W., Dodoo, D.K., and Hanson, P.J. (1993). *Mar. Pollut. Bull***. 26**, 329.

102. FAOSTAT (2007). Food and Agriculture Organization of the United Nations, Available from: http://faostat.fao.org/

103. FAO/WHO (1999). *53rd Report of the Joint FAO/WHO Expert Committee on Food Additives*, Rome.

104. Fernández-Cáceres, P.L., Martín, M.J., Pablos, F. and González, A.G. (2001). *J. Agric. Food Chem.* **49(10)**, 4775.

105. Fernández-Torres, R., Pérez-Bernal, J.L., Bello-López, M.A., Callejón-Mochón, M., Jiménez-Sánchez, J.C. and Guiraúm-Pérez, A. (2005). *Talanta* **65(3)**, 686.

106. Ferreira, S.L.C., Korn, M.d.G.A., Ferreira, H.S., da Silva, E.G.P., Araújo, R.G.O., Souza, A.S., Macedo, S.M., Lima, D.d.C., de Jesus, R.M., Amorim, F.A.C. and Bosque-Sendra, J.M. (2007a). *Appl. Spectrosc. Rev.* **42(5)**, 475.

107. Ferreira, S.L.C., Bruns, R.E., Ferreira, H.S., Matos, G.D., David, G.D., Brandão, G.C., da Silva, E.G.P., Portugal, L.A., dos Reis, P.S., Souza, A.S. and dos Santos, W.N.L. (2007b). *Anal. Chim. Acta* **597**, 179.

108. Food Act and Regulations (1995). *Food Act 1983 and Food Regulations 1985, MDC*. Ministry of Health, Malaysia.

109. Gao, L. and Ren, (1999). *Chemometr. Intell. Lab. Syst.* **45(1-2)**, 87.

110. Gao, L. and Ren, S.X. (2005). *Spectrochim. Acta A* **61(13-14)**, 3013.

111. Ghasemi, J. and Niazi, A. (2001). *Microchem. J.* **68(1)**, 1.

112. Ghasemi, J., Ahmadi, Sh. and Torkestani, K. (2003). *Anal. Chim. Acta* **487(2)**, 181.

113. Ghasemi, J., Shahabadi, N. and Seraji, H.R. (2004). *Anal. Chim. Acta* **510(1)**, 121.

114. Ghavami, R., Najafi, A. and Hemmateenejad, B. (2008). *Spectrochim. Acta A* **70(4)**, 824.

115. Gladyshev, M.I., Sushchik, N.N., Anishchenko, O.V., Makhutova, O.N., Kalachova, G.S. and Gribovskaya, I.V. (2009). *Food Chem.* **115(2)**, 545.

116. Gurnani, V., Singh, A.K. and Venkataramani, B. (2003). *Anal. Chim. Acta* **485(2)**, 221.

117. Gustin, M.S. (2003). *Sci. Total Environ.* **304(1-3)**, 153.

118. Hadad, G.M., El-Gindy, A. and Mahmoud, W.M.M. (2008). *Spectrochim. Acta A* **70(3)**, 655.

119. Hamilton, M.A., Rode, P.W., Merchant, M.E. and Sneddon, J. (2007). *Microchem. J.* **88(1)**, 52.

120. Hamilton, S.J. (2004). *Sci. Total Environ.* **326(1-3)**, 1.

121. Han, B.C., Jeng, W.L., Chen, R.Y., Fang, G.T., Hung, T.C. and Tseng, R.J. (1998). *Arch. Environ. Contam. Toxicol.* **35**, 711.

122. Hanrahan, G. and Lu, K. (2006). *Crit. Rev. Anal. Chem.* **36**, 141.

123. Harada, M. (1995). *Crit. Rev. Toxicol.* **25**, 1.

124. Hartikainen, H. (2005). *J. Trace Elem. Med. Biol.* **18(4)**, 309.

125. Has-Schön, E., Bogut, I. and Strelec, I, (2006). *Arch. Environ. Contam. Toxicol.* **50**, 545.

126. Health Canada (2004). *Federal contaminated site risk assessment in Canada, Part 1: Guidance on human health preliminary quantitative risk assessment (PQRA)*, Health Canada, Ottawa.

127. Heier, L.S., Lien, I.B., Strømseng, A.E., Ljønes, M., Rosseland, B.O., Tollefsen K.E. and Salbu, B. (2009). *Sci Total Environ* **407(13)**, 4047.

128. Henry, F., Amara, R., Courcot, L., Lacouture, D. and Bertho, M-L. (2004). *Environ. Int.* **30(5)**, 675.

129. House, W.A. (1999). *Field Crop Res.* **60(1-2)**, 115.

130. Hseu, Z.Y. (2004). *Bioresour. Technol.* **95(1)**, 53.

131. Huang X.G, Zhang, H.S., Li, Y.X., and Li, M.F. (2009). *J. Chil. Chem. Soc*. **54(3)**, 204.

132. Huang, Y.K., Lin, K.H., Chen, H.W., Chang, C.C., Liu, C.W., Yang, M.H. and Hsueh, Y.M. (2003). *Food Chem. Toxicol.* **41**, 1491.

133. Hutton, M. (1983). *Ecotoxicol. Environ. Safe.* **7**, 9.

134. Ikem, A. and Egilla, J. (2009). *Food Chem.* **110**, 301.

135. Inczédy, J., Lengyel, T., Ure, A.M., Gelencsér, A. and Hulanicki, A. (1998). IUPAC, Compendium of Analytical Nomenclature, 3rd ed., Oxford: Blackwell Scientific Publications.

136. IRIS (1987a). *Cadmium*, USEPA, Cincinnati, Ohio.

137. IRIS (1987b). *Methylmercury (MeHg)*, USEPA, Cincinnati, Ohio.

138. IRIS (1988a). *Arsenic, inorganic*, USEPA, Cincinnati, Ohio.

139. IRIS (1988b). *Lead and Compounds (Inorganic)*, USEPA, Cincinnati, Ohio.

140. IRIS (1991). *Selenium and Compounds*, USEPA, Cincinnati, Ohio.

141. Jalbani, M., Kazi, G.T., Arain, M.B., Jamali, M.K., Afridi, I.H., Sarfraz, R.A. (2006). *Talanta* **70(2)**, 307.

142. Jang, C.S., Lin, K.H., Liu, C.W. and Lin M.C. (2009). *Stoch. Environ. Res. Risk Assess.* **23(5)**, 603.

143. Jang, C.S., Liu, C.W., Lin, K.H., Huang, F.M. and Wang, S.W. (2006). *Environ. Sci. Technol.* **40**, 1707.

144. Järup, L., Berglund, M., Elinder, C.G., Nordberg, G. and Vahter, M. (1998). *Scand. J. Work Environ. Health* **24**, 1.

145. Jha, S.N., Chopra, S. and Kingsly, A.R.P. (2005). *Biosyst. Eng.* **91(2)**, 157.

146. Johns, C., Luoma, S.N. and Elrod, V. (1988). *Estuar. Coast. Shelf Sci.* **27**, 381.

147. Johnson, C.C., Ge, X., Green, K.A. and Liu, X. (2000). *Appl. Geochem.* **15**, 385.

148. Josupeit, H. (2008). *Tilapia market report – December 2008*, FISHINFOnetwork, Globefish.

149. Kaiser, H.F. (1958). *Psychometrika* **23**, 187.

150. Kaiser, H.F. (1960). *Educ. Psychol. Meas.* **20**, 141.

151. Kalivasa, K.H. (2005). *Anal. Lett.* **38(14)**, 2259.

152. Karadede, H. and Ünlü. E. (2000). *Chemosphere* **41**, 1371.

153. Karataş, S. and Kalay, M. (2002). *Turk. J. Vet. Anim. Sci.* **26**, 471.

154. Kebede, A. and Wondimu, T. (2004) *Bull. Chem. Soc. Ethiop.* **18(2)**, 119.

155. Keithley, R.B., Wightman, R.M. and Heien, M.L. (2009). *TrAC, Trends Anal. Chem.* **28(9)**, 1127.

156. Khajeh, M. (2009). *J. Food Comp. Anal.* **22**, 343.

157. Khajeh, M. and Ghanbari, M. (2011). *Food Anal. Methods* **4**, 431.

158. Khajeh, M. and Sanchooli, E. (2010). *Food Anal. Methods* **3**, 75.

159. Khoshayand, M.R., Abdollahi, H., Shariatpanahi, M., Saadatfard, A. and Mohammadi, A. (2008). *Spectrochim. Acta A* **70(3)**, 791.

160. Kirchhoff, G. and Bunsen, R. (1860). *Annalen der Physik und der Chemie* **110**, 161.

161. Krachler, M., Mohl, C., Emons, H. and Shotyk, W. (2002). *Spectrochim. Acta B* **57**, 1277.

162. Lalonde, B.A., Ernst, W. and Comeau, F. (2010). *Arch. Environ. Contam. Toxicol.* DOI: 10.1007/s00244-010-9632-0.

163. Lammertyn J., Nicolai, B., Ooms, K., De Smedt V. and De Baerdemaeker. J. *Trans. ASAE* **41**, 1089.

164. Laurén, D.J. and McDonald, D.G. (1987). *Can. J. Fish. Aquat. Sci.* **44**, 105.

165. Lee, S.J., Seo, Y.C., Jurng, J.S., Hong, J.H., Park, J.W., Hyun, J.E. and Lee, T.G. (2004). *Sci. Total Environ.* **325(1-3)**, 155.

166. Lee, S.K. and Choi, H.S. (2001). *Bull. Korean Chem. Soc.* **22(5)**, 463.

167. Lee, W., Lee, S.E., Lee, C.H., Kim, Y.S. and Lee, Y.I. (2001). *Microchem. J.* **70**, 195.

168. Lemly, A.D. (1997). *Biomed. Environ. Sci.* **10**, 415.

169. Lemly, A.D. (2002). *Selenium assessment in aquatic ecosystem - a guide for hazard evaluation and water quality criteria.* NewYork: Springer-Verlag.

170. Lemly, A.D. (2004). *Ecotoxicol. Environ. Safe.* **59(1)**, 44.

171. Lemos, V.A., Santos, E.S., Santos, M.S., and Yamaki, R.T. (2007) *Microchim. Acta* **158**, 189.

172. Lemos,V.A., Santos, J.S. and Baliza, P.X. (2006). *J. Braz. Chem. Soc.* **17(1)**, 30.

173. Lewis, G.A., Mathieu, D. and Phan R.T.L. (2005). *Pharmaceutical Experimental Design.* New York: Taylor & Francis.

174. Li, L.Y., Gui, M.D. and Zhao, Y.Q. (1995). *Talanta* **42(1)**, 89.

175. Li, W.H., Wei, C., Zhang, C., Hulle, M.V., Cornelis, R. and Zhang, X.R. (2003). *Food Chem. Toxicol.* **41**, 1103.

176. Liao, C.M. and Ling, M.P. (2003). *Arch. Environ. Contam. Toxicol.* **45**, 264.

177. Liao, C.M., Shena, H.H., Lina, T.L., Chen, S.C., Chen, C.L., Hsu, L.I. and Chen, C.J. (2008). *Ecotox. Environ. Safe.* **70**, 27.

178. Lin, T.S., Lin, C.S. and Chang, C.L. (2005). *Bull. Environ. Contam. Toxicol.* **74**, 308.

179. Lindén, A., Olsson, I-M., Bensryd, I., Lundh, T., Skerfving, S., and Oskarsson, A. (2003). *Ecotoxicol. Environ. Safe.* **55(2)**, 213.

180. Ling, M.P. and Liao, C.M. (2007). *Environ. Int.* **33**, 98.

181. Ling, M.P., Hsu, H.T., Shie, R.H., Wu, C.C. and Hong, Y.S. (2009). *Bul. Environ. Contam. Toxicol.* **83**,558.

182. Liu, C.P., Luo, C.L., Gao, Y., Li, F.B., Lin, L.W., Wu, C.A. and Li, X.D. (2010). *Environ. Pollut.* **158(3)**, 820.

183. Liu, Y.Y. (1999). *Occup. Health* **19,** 8.

184. Lorber, A. (1986). *Anal. Chem.* **58**, 1167.

185. Lorber, A. and Kowalski, B.R. (1988). *J. Chemom.* **2**, 67.

186. Low, K.H., Zain, S.Md., Abas, M.R. and Khan, R.A. (2009). *Sens. & Instrumen. Food Qual.* **3,** 203.

187. Madsen, R., Lundstedt, T. and Trygg, J. (2010). *Anal. Chim. Acta* **659(1-2)**, 23.

188. Mandal, B.K. and Suzuki, K.T. (2002). *Talanta* **58**, 201.

189. Manutsewee, N., Aeungmaitrepirom, W., Varanusupakul, P. and Imyim, A. (2007). *Food Chem.* **101**, 817.

190. Mars, J.C. and Crowley, J.K. (2003). *Remote Sens. Environ.* **84(3)**, 422.

191. Martins, C.I.M., Eding, E.H. and Verreth, J.A.J. (2010). *Food Chem*. DOI: 10.1016/j.foodchem.2010.11.108.

192. Mas, S., de Juan, A., Tauler, R., Olivieri A.C., and Escandar, G.M. (2010). *Talanta* **80(3)**, 1052.

193. Matlock, M.M., Howerton, B.S. and Atwood, D.A. (2003). *Adv. Environ. Res.* **7(2)**, 495.

194. Matoso, E., Kubota, L.T. and Cadore, S. (2003). *Talanta* **60(6)**, 1105.

195. Mc. Curdy, E. and Potter, D. (2001). *Spectros. Eur*. **13(3)**, 14.

196. Mehta, S.K., Malik, A.K., Gupta, U. and Rao, A.L.J. (2004) *E-J. Environ. Agric. Food Chem.* **3(6)**, 784.

197. Mendil, D. and Uluözlü, Ö.D. (2007). *Food Chem.* **101(2)**, 739.

198. Mendil, D., Demirci, Z., Tuzen, M. and Soylak, M. (2010). *Food Chem. Toxicol.* **48(3)**, 865.

199. Mester, Z. and Sturgeon, R. (2003). *Sample Preparation for Trace Element Analysis, Vol. XLI*. Amsterdam: Elsevier B.V.

200. Meyer, P.A., Brown, M.J. and Falk, H. (2008). *Mutat. Res.* **659**, 166.

201. Milton, A.H., Hasan, Z., Rahman, A. and Rahman, M. (2001). *J. Occup. Health* **43**, 136.

202. Mohan, D. and Pittman Jr., C.U. (2007). *J. Hazard. Mater.* **142(1-2)**, 1.

203. Mokhtar, M., Aris, A.Z., Munusamy, V. and Praveena, S.M. (2009). *Eur. J. Sci. Res.* **30(3)**, 348.

204. Momen, A.A., Zachariadis, G.A., Anthemidis, A.N. and Stratis, J.A. (2007). *Talanta* **71**, 443.

205. Moneeb, M.S. (2006). *Talanta* **70(5)**, 1035.

206. Munck, L., Nørgaard, L., Engelsen, S.B., Bro, R. and Andersson, C.A. (1998). *Chemometr. Intell. Lab. Syst.* **44**, 31.

207. Nachman, K.E., Graham, J.P., Price, L.B. and Silbergeld, E.K. (2005). *Environ. Health Perspect.* **113(9)**, 1123.

208. Nakagawa, H., Tabata, M., Morikawa, Y., Senma, M., Kitagawa, Y., Kawano, S. and Kido, T. (1990). *Arch. Environ. Health* **45**, 283.

209. Nam, S.H., Chung, H., Kim, J.J. and Lee, Y.I. (2008). *Bull. Korean Chem. Soc.* **29(11)**, 2237.

210. Nandlal, S. and Pickering, T. (2004). *Tilapia fish farming in Pacific Island countries. Volume 1. Tilapia hatchery operation.* Noumea, New Caledonia: Secretariat of the Pacific Community.

211. Navarro-Alarcon, M. and Cabrera-Vique, C. (2008). *Sci. Total Environ.* **400(1-3)**, 115.

212. Nelms, S. (2005). *Inductively Coupled Plasma Mass Spectrometry Handbook.* Oxford: Blackwell.

213. Ni, Y.N. (1993). *Anal. Chim. Acta* **284(1)**, 199.

214. Ni, Y.N., Chen, S.H. and Kokot, S. (2002). *Anal. Chim. Acta* **463(2)**, 305.

215. Ni, Y.N., Zhang, G.W. and Kokot, S. (2005). *Food Chem.* **89(3)**, 465.

216. Niazi, A. and Yazdanipour, A. (2008). *Chin. Chem. Lett.* **19**, 860.

217. Niazi, A., Yazdanipour, A. and Ramezani, M. (2007). *Chin. Chem. Lett.* **18**, 989.

218. Nickson, R.T., McArthur, J.M., Ravenscroft, P., Burgess, W.G. and Ahmed, K.M. (2000). *Appl. Geochem.* **15**, 403.

219. Nielsen, S.S. (2010). *Food Analysis 4th ed.* Springer: New York.

220. Nogami, E.M., Kimura, C.C.M., Rodrigues, C., Malagutti, A.R., Lenzi, E. and Nozaki, J. (2000). *Ecotoxicol. Environ. Safe.* **45**, 291.

221. Olivieri, A.C., Faber, N.(K.)M., Ferré, J., Boqué, R., Kaliva, J.H. and Mark, H. (2004). *Pure Appl. Chem.* **78(3)**, 633.

222. Omar, M.M. and Mohamed, G.G. (2005) *Spectrochim. Acta A* **61**, 929.

223. Otto, M. (2007). *Chemometric: Statistical and Computer Application in Analytical Chemistry, 2ed*. Darmstadt: Wiley-VCH.

224. Palaniappan, PL.RM., Sabhanayakam, S., Krishnakumar, N. and Vadivelu, M. (2008). *Food Chem. Toxicol.* **46(7)**, 2440.

225. Paneque, P., Álvarez-Sotomayor, M.T., Clavijo, A. and Gómez, I.A. (2010) *Microchem. J.* **94(2)**, 175.

226. Park, K.S., Seo, Y.C., Lee, S.J. and Lee J.H. (2008). *Powder Technol.* **180(1-2)**, 151.

227. Parker, J.L. and Bloom, N.S. (2005). *Sci. Total Environ.* **337(1-3)**, 253.

228. Paul, B.K. (2004). *Soc. Sci. Med.* **58(8)**, 1741.

229. Paul, S.O. (2009) *Chemometr. Intell. Lab. Syst.* **97(1)**, 104.

230. Pedlar, R.M. and Klaverkamp, J.F. (2002). *Aquat.Toxicol.* **57**, 153.

231. Peré-Trepat, E., Ginebreda, A. and Tauler, R. (2007). *Chemometr. Intell. Lab. Syst.* **88(1)**, 69.

232. Pérez Cid, B., Boia, C., Pombo, L. and Rebelo, E. (2001). *Food Chem.* **75(1)**, 93.

233. Peters, G.M., Maher, W.A., Krikowa, F., Roach, A.C., Jeswani, H.K., Barford, J.P., Gomes, V.G. and Reible, D.D. (1999). *Mar. Environ. Res.* **47(5)**, 491.

234. Pettas, I.A. and Karayannis, M.I. (2003). *Anal. Chim. Acta* **491(2)**, 219.

235. Pizzol, M., Thomsen, M. and Andersen, M.S. (2010). *Sci. Total Environ.* **408(22)**, 5478.

236. Plackett, R.L. and Burman, J.P. (1946). *Biometrika* **33,** 305.

237. Qiu, Y.W., Lin, D., Liu, J.Q. and Zeng, E.Y. (2010). *Ecotoxicol. Environ. Safe.* DOI: 10.1016/j.ecoenv.2010.10.008.

238. Qu, N., Zhu, M., Mi,H., Dou, Y. and Ren, Y. (2008). *Spectrochim. Acta A* **70(5)**, 1146.

239. Raghunath, R., Tripathi, R.M., Suseela, B., Bhalke, S., Shukla, V.K. and Puranik, V.D. (2006). *Sci. Total Environ.* **356(1-3)**, 62.

240. Raimundo Jr., I.M. and Narayanaswamy, R. (2003). *Senor. Actuat. B* **90**, 189.

241. Reilly, C. (2002). *Metal Contamination in Food: Significance for Food Quality and Human Health.* Oxford: Blackwell Science Ltd.

242. Reis, P.A., Valente, L.M.P. and Almeida, C.M.R. (2008). *Food Chem.* **108(3)**, 1094.

243. Retief, N.R., Avenant-Oldewage, A. and du Preez, H. (2006). *Phys. Chem. Earth* **31(15-16)**, 840.

244. Rio Segade, S., Dieguez Albor, M.C., Fernandez Gomez, E. and Falque Lopez, E. (2003). *Int. J. Environ. Anal. Chem.* **83**, 343.

245. Roa, E.C., Capangpangan, M.B. and Schultz. M. (2010). *J. Environ. Chem. Ecotox.* **2(9)**, 141.

246. Rodriguez, A.M.G., de Torres, A.G., Pavon, J.M.C. and Ojeda, C.B. (1998). *Talanta* **47(2)**, 463.

247. Rodriguez-Nogales, J.M. (2006). *Food Chem.* **98**, 782.

248. Rojas, F.S. and Ojeda, C.B. (2009). *Anal. Chim. Acta* **635(1)**, 22.

249. Roychowdhury, T., Uchino, T., Tokunaga, H. and Ando, M. (2002). *Chemosphere* **49**, 605.

250. Saavedra, Y., González, A., Fernández, P. and Blanco, J. (2004). *Spectrochim. Acta B* **59**, 533.

251. Samadi-Maybodi, A and Darzi S.K.H.N. (2008). *Spectrochim. Acta A* **70(5)**, 1167.

252. Samecka-Cymerman, A. and Kempers, A.J. (2004). *Ecotox. Environ. Safe.* **59**, 64.

253. Santelli, R.E., de Almeida Bezerra, M. de SantAna, O.D., Cassella, R.J. and Ferreira, S.L.C. (2006). *Talanta* **68**, 1083.

254. Sanz, M.B., Sarabia, L.A., Herrero, A. and Ortiz, M.C. (2003). *Anal. Chim. Acta* **489**, 85.

255. Sapkota, A., Sapkota, A.R., Kucharski, M., Burke, J., McKenzie, S., Walker, P. and Lawrence, R. (2008). *Environ. Int.* **34(8)**, 1215.

256. Satarug, S., Baker, J.R., Reilly, P.E.B., Moore, M.R. and Williams, D.J. (2002). *Arch. Environ. Health* **57**, 69.

257. Scancar, J., Stibilj, V. and Milacic, R. (2004). *Food Chem.* **85(1)**, 151.

258. Schmitt, C.J., and Brumbaugh, W.G. (1990). *Arch. Environ. Contam. Toxicol.* **19**, 731.

259. Selim Reza, A.H.M., Jean, J.S., Yang, H.J., Lee, M.K., Woodall, B., Liu, C.C., Lee, J.F. and Luo, S.D. (2010). *Water Res.* **44(6)**, 2021.

260. Shiomi, K. (1994). Arsenic in marine organisms: chemical forms and toxicology aspects. In: Nriagu JO. (ed) Arsenic, In: Environment. Part II: Human Health and Ecosystem Effect. John Wiley & Sons, New York, pp. 261-282.

261. Silvestre, M.D., Lagarda, M.J., Farré, R., Martínez-Costa, C. and Brines, J. (2000). *Food Chem.* **68**, 95.

262. Sim, S.F., Devagi, K. and Sung, C.L. (2006). *Malays. J. Chem*. **8(1)**, 10.

263. Singh, K.P., Warsono, Bartolucci, A.A. and Bae, S. (2001). *Math. Comput. Model.* **33(6-7)**, 793.

264. Sivaperumal, P., Sankar, T.V. and Viswanathan Nair P.G (2007) *Food Chem.* **102(3)**, 612.

265. Smith, A.H., Lopipero, P.A., Bates, M.N. and Steinmaus, C.M. (2002). *Science* **296**, 2145.

266. Smith, F.R. and Arsenault, E.A. (1996). *Talanta* **43**, 1207.

267. Smith, R.L. (1994). *Risk Anal.* **14(4)**, 433.

268. Smuda, J., Dold, B., Friese, K., Morgenstern, P. and Glaesser, W. (2007). *J. Geochem. Explor.* **92(2-3)**, 97.

269. Soeroes, C., Goessler, W., Francesconi, K.A., Kienzl, N., Shaeffer, R., Fodor, P. and Kuehnelt, K. (2005). *J. Agric. Food Chem.* **53**, 9238.

270. Southworth, G.R., Lindberg, S.E, Zhang, H. and Anscombe, F.R. (2004). *Atmos. Environ.* **38(4)**, 597.

271. Soylak, M., Tuzen, M., Souza, A.S., Korn, M.d.G.A. and Ferreira, S.L.C. (2007). *J. Hazard. Mater.* **149**, 264.

272. Stagg, R.M. and Shuttleworth, T.J. (1982). *J. Comp. Physiol.* **149B**, 83.

273. Stalikas, C., Fiamegos, Y., Sakkas, V. and Albanis, T. (2009). *J. Chromatogr., A* **1216**, 175.

274. Storelli, M.M. (2008). *Food Chem. Toxicol.* **46(8)**, 2782.

275. Suadicani, P., Hein, H.O. and Gyntelberg, F. (1992). *Atherosclerosis* **96(1)**, 33.

276. Sun, Y.S. and Ko, C.J. (2004). *Microchem. J.* **78**, 163.

277. Sures, B., Steiner, W., Rydlo, M. and Taraschewski, H. (1999). *Environ. Toxicol. Chem.* **18**, 2574.

278. Sures, B., Taraschewski, H. and Haug, C. (1995). *Anal. Chim. Acta.* **311(2)**, 135.

279. Svensson, B.G., Schütz, A., Nilsson, A., Åkesson, I., Åkesson, B. and Skerfving, S. (1992). *Sci. Total Environ.* **126,** 61.

280. Şxahin, S., Demir, C. and Güçer, Ş. (2007) *Dyes Pigments* **73**, 368.

281. Tangen, A. and Lund, W. (1999). *Spectrochim. Acta B* **54**, 1831.

282. Tanner, S.D. and Baranov V.I. (1999*). J. Am. Soc. Mass Spectrom.* **10(11)**, 1083.

283. Tanner, S.D., Baranov, V.I. and Bandura, D.R. (2002). *Spectrochim. Acta B* **57(9)**, 1361.

284. Teixeira, L.S.G. and Rocha, F.R.P. (2007). *Talanta* **71**, 1507.

285. Torres, D.P., Frescura, V.L.A. and Curtius, A.J. (2009). *Michrochim. J.* **93(2)**, 206.

286. Tsai, S.M., Wang, T.N. and Ko, Y.C. (1998). *J. Toxicol. Environ. Health A* **55**, 389.

287. Tsai, S.M., Wang, T.N. and Ko, Y.C. (1999). *Arch. Environ. Health* **54**,186.

288. Tseng, C.H. (2002). *Angiology* **53(5)**, 529.

289. Tseng, C.H. (2005). *J. Environ. Sci. Health. C* **23(1)**, 55.

290. Tseng, C.H., Chong, C.K., Tseng, C.P., Hsueh, Y.M., Chiou, H.Y., Tseng, C.C. and Chen, C.J. (2003). *Toxicol. Lett.* **137**, 15.

291. Tseng, C.H., Tai, T.Y., Chong, C.K., Tseng, C.P., Lai, M.S., Lin, B.J., Chiou, H.Y., Hsueh, Y.M., Hsu, K.H. and Chen, C.J. (2000). *Environ. Health Perspect.* **108**, 847.

292. Türkmen M. and Ciminli, C. (2007). *Food Chem.* **103**, 670.

293. Türkmen, A., Türkmen, M., Tepe, Y. and Akyurt, I. (2005). *Food Chem.* **91(1)**, 167.

294. Türkmen, M., Türkmen, A., Tepe, Y., Töre, Y. and Ateş, A. (2009). *Food Chem.* **113**, 233.

295. Tüzen, M. (2003). *Food Chem.* **80(1)**, 119.

296. Tüzen, M. (2009). *Food Chem. Toxicol.* **47**, 1785.

297. Uluözlü, Ö.D., Tüzen, M., Mendil, D. and Soylak, M. (2007). *Food Chem.* **104(2)**, 835.

298. Ureña, R., Peri, S., del Ramo, J. and Torreblanca, A. (2007). *Environ. Int.* **33(4)**, 532.

299. Uriu, K., Morimoto, I., Kai, K., Okazaki, Y., Okada, Y., Qie, Y.L., Okimoto, N., Kaizu, K., Nakamura, T. and Eto, S. (2000). *Toxicol. Appl. Pharmacol.* **164**, 264.

300. USEPA (1975). *Interim Primary Drinking Water Standards*, Fed. Reg. 40, 11,990.

301. USEPA (1994a). *Method 200.8*, USEPA, Cincinnati, Ohio.

302. USEPA (1994b). *Method 3015*, USEPA, Washington, DC.

303. USEPA (1996). *Method 3052*, USEPA, Washington, DC.

304. USEPA (1998). *Method 6020A*, Washington, DC.

305. USEPA (1999). *Surface Water Sampling. Field Sampling Guidance Document #1225*, USEPA, California.

306. USEPA (2000a). *Guidance for Assessing Chemical Contaminant Data for Use in Fish Advisories. Vol. 1: Fish Sampling and Analysis*, USEPA, Washington, DC.

307. USEPA (2000b). *Guidance for Assessing Chemical Contaminant Data for Use in Fish Advisories. Vol. 2: Risk Assessment and Fish Consumption Limits*, USEPA, Washington, DC.

308. USEPA (2007). *Method 3051A*, USEPA, Washington, DC.

309. USEPA (2010). *Risk-based concentration table*, USEPA, Philadelphia, PA.

310. Usero, J., Gonzalez-Regalado, E. and Gracia, I. (1996). *Mar, Pollut. Bull.* **32(3)**, 305.

311. Usero, J., Izquierdo, C., Morillo, J. and Gracia, I. (2004). *Environ. Int.* **29(7),** 949.

312. USFDA (1993a). *Guidance Document for Arsenic in Shellfish*, FDA, Washington, DC.

313. USFDA (1993b). *Guidance Document for Cadmium in Shellfish*, Center for Food Safety and Applied Nutrition, Rockville, MD.

314. USNAS (2000). *Dietary Reference Intakes for Vitamin C, Vitamin E, Selenium, and Caroteroids*, Food and Nutrition Board, Washington, DC.

315. Uysal, K., Köse, E., Bülbül, M., Dönmez, M., Erdoğan, Y., Koyun, M., Ömeroğlu, C. and Özmal, F. (2009). *Environ. Monit. Assess*. **157**, 355.

316. Van der Oost, R., Beyer, J. and Vermeulen, N.P.E. (2003). *Environ. Toxicol. Pharmacol.* **13(2)**, 57.

317. Venkatesh, G. and Singh, A.K. (2005). *Talanta* **67(1)**, 187.

318. Vicente-Martorel, J.J., Galindo-Riaño, M.D., García-Vargas, M. and Granado-Castro, M.D. (2009). *J. Hazard. Mater.* **162(2-3)**, 823.

319. Visser, A.E., Griffin, S.T., Hartman, D.H. and Rogers, R.D. (2000). *J. Chromatogr. B* **743**, 107.

320. Wagner, A. and Boman, J. (2003). *Spectrochim. Acta B* **58(12)**, 2215.

321. Wang, Q.R., Kim, D.K., Dionysiou, D.D., Sorial, G.A. and Timberlake, D. (2004). *Environ. Pollut.* **131(2)**, 323.

322. Wang, R, Wong, M.H. and Wang, W.X (2010). *Environ.Pollut.* **158(8)**, 2694.

323. Wang, S.L. and Mulligan, C.N. (2006). *Sci. Total Environ.* **366 (2-3)**, 701.

324. Wang, S.W., Lin, K.H., Hsueh, Y.M. and Liu, C.W. (2007). *Bull. Environ. Contam. Toxicol.* **78**, 137.

325. Wang, X.L., Sato, T., Xing, B.S., Tao, S. (2005). *Sci. Total Environ.* **350(1-3)**, 28.

326. Watanabe, H. and Matsunaga, H. (1976). *Japan analyst* **25(1)**, (1976), 35.

327. Wcisło, E., Ioven, D., Kucharski, R. and Szdzuj, J. (2002). *Chemosphere* **47(5)**, 507.

328. Wells, G. (1996). *Hazard Identification and Risk Assessment*. Warwickshare: Institution of Chemical Engineers.

329. WHO (1986). *Environmental Health Criteria 58, Selenium*, IPCS, Geneva.

330. WHO (1990). *Environmental Health Criteria 101, Methylmercury*, IPCS, Geneva.

331. WHO (1992). *Environmental Health Criteria 134, Cadmium*, IPCS, Geneva.

332. WHO (1995). *Environmental Health Criteria 165, Inorganic Lead*, IPCS, Geneva.

333. WHO (2001). *Environmental Health Criteria 224, Arsenic Compounds, 2nd ed.*, IPCS, Geneva.

334. WHO (2008). The Global Health Observatory (GHO) database, Available from: http://apps.who.int/ghodata/

335. Williams. J.E. (2000). Chapter 13: Coefficient of Condition of Fish. In: Schneider, J.C. ed. *Manual of fisheries survey methods II: with periodic updates.* Michigan Department of Natural Resources, Fisheries Special Report 25: Ann Arbor.

336. Wong, C.S.C., Duzgoren-Aydin, N.S., Aydin, A. and Wong, M.H. (2006). *Sci. Total Environ.* **368(2-3)**, 649.

337. Workman JR., J.J., Mobley, P.R., Kowalski, B.R. and Broc, R. (1996). *Appl. Spectrosc. Rev.* **31(1)**, 73.

338. Wu, M.M., Kuo, T.L., Hwang, Y.H. and Chen, C.J. (1989). *Am. J. Epidemiol.* **130**, 1123.

339. Wu, S.M. Shih, M.J. and Ho, Y.C. (2007). *Comp. Biochem. Physiol. C* **145(2)**, 218.

340. Xie, R.K. Seip, H.M., Wibetoe, G., Nori, S. and McLeod, C. W. (2006). *Sci. Total Environ.* **370(2-3)**, 409.

341. Xie, S.F. and Yan, X.B. (2005). *Foreign Med. Sci.* **32,** 240.

342. Yang, C.Y., Chiu, H.F., Chang, C.C., Ho, S.C. and Wu, T.N. (2005). *Environ. Res.* **98**, 127.

343. Yang, G.Q., Wang, S., Zhou, R. and Sun, S. (1983). *Am. J. Clin. Nutr.* **37**, 872.

344. Yang, K.X. and Swami, K. (2007). *Spectrochim. Acta B* **62(10)**, 1177.

345. Ybañez, N., Cervera, M.L. and Montoro, R. (1992). *Anal. Chim. Acta* **258(1)**, 61.

346. Yoshida, T., Yamauchi, H. and Sun, G.F. (2004). *Toxicol. Appl. Pharmacol.* **198(3)**, 243.

347. Yudovich, Ya.E. and Ketris M.P. (2005). *Int. J. Coal Geol.* **62(3)**, 107.

348. Yun, J.S. and Choi, H.S. (2000). *Talanta* **52(5)**, 893.

349. Zahir, F., Rizwi, S.J., Haq, S.K. and Khan, R.H. (2005). *Environ. Toxicol. Pharmacol.* 20(2), 351.

350. Zaporozhets, O., Petruniock, N., Bessarabova, O. and Sukhan, V. (1999). *Talanta* **49**, 899.

351. Zarei, K. Atabati, M. and Malekshabani, Z. (2006). *Anal. Chim. Acta* **556(1)**, 247.

352. Zhang, C.J., Miura, J. and Nagaosa, Y. (2005). *Anal. Sci*. **21**, 1105.

353. Zhang, G.H., Hu, M.H., Huang, Y.P. and Harrison, P.J., (1990). *Mar. Environ. Res.* **25**, 179.

354. Zhang, G.W. and Pan J.H. (2011). *Spectrochim. Acta Part A* **78(1)**, 238.

355. Zhang, L. and Wong, M.H. (2007). *Environ. Int.* **33(1)**, 108.

356. Zheng, Y., van Geen, A., Gavrieli, A., Dhar, R., Simpson, J. and Ahmed, K.M. (2004). *Appl. Geochem.* **19**, 201.

357. Zhou, H.Y. and Wong, M.H. (2000). *Water Res.* **34(17)**, 4234.

358. Zhou, S., Belzile, N. and Chen, W.W. (1998). *Int. J. Environ. Anal. Chem.* **72(3)**, 205.

359. Zirong, X. and Shijun, B. (2007). *Ecotox. Environ. Safe.* **67(1)**, 89.